Unravelling the molecular bases of carotenoid biosynthesis in maize

Judit Berman Quintana

Unravelling the molecular bases of carotenoid biosynthesis in maize

by Judit Berman Quintana

Doctoral Dissertation

January 2016

Universitat de Lleida

Escola Tècnica i Superior
d'Enginyeria Agrària

Departament de Producció Vegetal i
Ciència Forestal

The photo on the cover of the thesis appeared as a covered page on an issue of Plant Molecular Biology in which the article Berman et al., 2013 was featured. The full reference is: Berman J, Zhu C, Pérez-Massot E, Arjó G, Zorrilla-López U, Masip G, et al. (2013) Can the world afford to ignore biotechnology solutions that address food insecurity? Plant Mol Biol. 83:5–19.

Supervisor: Dr Paul Christou

Departament de Producció Vegetal i Ciència Forestal

Escola Tècnica i Superior d'Enginyeria Agrària

Universitat de Lleida

Co-Supervisor: Dr Changfu Zhu

Departament de Producció Vegetal i Ciència Forestal

Escola Tècnica i Superior d'Enginyeria Agrària

Universitat de Lleida

TABLE OF CONTENTS

INDEX OF FIGURES

GENERAL INTRODUCTION

CHAPTER 1: CLONING AND FUNCTIONAL CHARACTERIZATION OF MAIZE (*Zea mays* L.) CAROTENOID EPSILON HYDROXYLASE

CHAPTER 2: THE ROLE OF THE ARABIDOPSIS ORANGE GENE ON CAROTENOID AND KETOCAROTENOID ACCUMULATION IN MAIZE HYBRIDS

CHAPTER 3: INCREASED β-CAROTENE CONTENT IN MAIZE ENDOSPERM THROUGH RNAI-MEDIATED SILENCING OF CAROTENOID β-HYDROXYLASE (*Zmbch1* AND *Zmbch2*) IN DIFFERENT GENOTYPES

CHAPTER 4: IMPACT OF INCREASED CAROTENOID CONTENT ON STARCH ACCUMULATION IN TRANSGENIC MAIZE

CHAPTER 5: DEVELOPMENT OF HIGH CAROTENOID TRANSGENIC MAIZE HYBRIDS WITH AGRONOMIC PERFORMANCE SIMILAR TO COMMERCIAL HYBRIDS

INDEX OF TABLES

GENERAL INTRODUCTION

CHAPTER 1: CLONING AND FUNCTIONAL CHARACTERIZATION OF MAIZE (*Zea mays* L.) CAROTENOID EPSILON HYDROXYLASE

CHAPTER 2: THE ROLE OF THE ARABIDOPSIS OR GENE ON CAROTENOID AND KETOCAROTENOID ACCUMULATION IN MAIZE HYBRIDS

CHAPTER 3: INCREASED β-CAROTENE CONTENT IN MAIZE ENDOSPERM THROUGH RNAI-MEDIATED SILENCING OF CAROTENOID β-HYDROXYLASE (*Zmbch1* AND *Zmbch2*) IN DIFFERENT GENOTYPES

CHAPTER 4: IMPACT OF INCREASED CAROTENOID CONTENT ON STARCH ACCUMULATION IN TRANSGENIC MAIZE

CHAPTER 5: DEVELOPMENT OF HIGH CAROTENOID TRANSGENIC MAIZE HYBRIDS WITH AGRONOMIC PERFORMANCE SIMILAR TO COMMERCIAL HYBRIDS

ACKNOWLEDGEMENTS

I would like to express my gratitude to my supervisor Paul Christou for his valuable and patient guidance, enthusiastic encouragement and excellent advice in science and beyond. I would have not achieved this success without his endless support during my PhD. I am grateful to acknowledge Teresa Capell for her constant feedback and her energetic personality and enthusiasm on disseminating our scientific work all around the world.

I also would like to express my great appreciation to my co-supervisor Changfu Zhu, who was always ready to help me with constructive suggestions and useful advice. I would like to offer my special thanks to Ludovic Bassie for useful discussions; his in depth knowledge in analytical procedures was invaluable to me.

My PhD work was immeasurable aided by the friendly atmosphere and continuous technical and emotional support during the last four years. It is a pleasure to convey my gratitude to all the people who helped me in reaching this important goal. I wish you lot of luck and success in your work and personal life.

I would like to thank my very good lab mate Gemma Farré for helping me getting started in the lab with good tutoring and useful scientific advice. Thank you for developing the basis I used for my experiments.

To all my good friends and ex-colleagues: Bruna Miralpeix, Maite Sabalza, Georgina Sanahuja, Evangelia Vamvaka, Chao Bai and Raviraj Banakar; all the moments we shared in and out of the lab helped me to become the scientist I am right now.

To Eduard Pérez, Uxue Zorrilla, Gemma Massip, Gemma Arjó and Daniela Zanga, we shared many fun moments during our PhD research together and in the future we will have more lovely time together. I value our friendship very much.

A en Jaume Capell, per ensenyar-me a estimar la feina i les plantes, pels consells de vida i per aconseguir que a l'hivernacle no hi hagi lloc per a les preocupacions.

I am thankful to Núria Cabernet for dealing with administrative work and for always being kind and helpful.

I also would like to acknowledge many professors and PAS whose contribution enriched my work professionally. To Paquita Vilaró, for her technical support in HPLC analysis; Ramon

Canela, for his help in the interpretation of the results as well as Gerhard Sandmann, Biosynthesis Group, Molecular Biosciences, J.W. Goethe Universitaet; Albert Tomas, for facilitating the equipment management for carotenoid extraction, and to the other members of the chemistry department; Xavier Calomarde, for his technical support in microscopy and Vicente Medina and Pilar Muñoz for their support in microscopy analysis and passion for this technique; Antonio Michelena and Jaume Lloveres, for their advice on field experiments.

To Ana Pelacho, thank you for introducing me to Paul and Teresa; and thanks to the Universitat de Lleida for giving me the opportunity to develop myself during the degree, the master and finally the PhD.

My PhD thesis could never have been fulfilled without the full support of my family and friends. I am deeply and forever indebted to them.

Vull agrair als meus pares i tiets el suport, l'amor i l'educació que he rebut des de sempre. Sense vosaltres hagués ensopegat més de dos cops amb la mateixa pedra. Als avis, la seva comprensió incondicional. Gràcies a la meva germana Alba per cedir-me el seu caràcter perfeccionista durant la redacció i per seguir el fil de les explicacions. Finalment, moltes gràcies, Santiago Chauvell, pel suport moral i la passió que em demostres cada dia.

SUMMARY

My research program focused on the elucidation of the mechanisms of carotenoid accumulation in maize (*Zea mays*). I amplified a putative carotenoid ε-hydroxylase, named CYP97C19, from the yellow maize variety B73. Metabolic profiling of the carotenoid pathway in Arabidopsis *lut1* mutant (lacking lutein) overexpressing maize CYP97C19 confirmed the accumulation of lutein in transgenic lines at the expense of zeinoxanthin. This allowed me to conclude that maize CYP97C19 is a functional ε-hydroxylase. In a separate experiment, I characterized two transgenic lines overexpressing the Arabidopsis *ORANGE* gene (*AtOR*). Both lines exhibited an increase in carotenoid content without any concomitant upregulation of endogenous carotenogenic gene expression. The highest carotenoid accumulating line was crossed with different transgenic lines with diverse carotenoid profiles. In cases in which the original transgenic parent that was crossed with the *AtOR* line accumulated low levels of total carotenoids, resulting hybrid exhibited a substantial increase of total carotenoid content without any changes in the qualitative carotenoid composition. No changes at the metabolite and transcript profiles were observed in the hybrids when the carotenoid content in the original parents used to cross with the *AtOR* line was high. Results from these experiments suggest that one of the functions of the *ORANGE* gene in maize endosperm is to generate a metabolic sink for carotenoids because of the increase of carotenoid content. Results from experiments in which carotenoid β-hydroxylase (BCH1 and BCH2) was silenced in genotypes able to accumulate high lutein and high zeaxanthin levels indicated that these genes are determinants of β-carotene and zeaxanthin accumulation. I also investigated the interactions between the carotenoid and starch biosynthetic pathways as they share common precursors. I analyzed total starch content in four transgenic maize lines: one line overexpressing *AtOR* (L1) and three lines expressing different carotenogenic gene combinations (L2, L3 and L4, expressing *Zmpsy1; Zmpsy1, PacrtI* and *ParacrtW;* and *Zmpsy1; PacrtI* and *Gllycb,* respectively). In transgenic lines with a high carotenoid content total starch content was lower by approximately 8%. I established that this effect was due to downregulation of starch-related biosynthetic genes. Finally, a transgenic line (HC) overexpressing *Zmpsy1* and *PacrtI* was crossed with different inbred lines belonging to well-known heterotic groups in order to obtain high-yielding hybrids accumulating carotenoids. I assessed the performance of the hybrids (agronomic and ear morphologic traits) in two different locations in one growing season. Results indicated that field performance of high

carotenoid maize hybrids was similar or on occasion superior to commercial hybrids commonly grown in the area.

RESUMEN

Mi programa de investigación se ha centrado en el estudio de los mecanismos de acumulación de carotenoides en maíz (*Zea mays*). Inicialmente, cloné de la variedad de maíz B73 un gen candidato para la enzima ε-hidroxilasa de carotenoides (CYP97C19). Basándome en los resultados del perfil metabólico de la ruta de los carotenoides en líneas transgénicas del mutante de Arabidopsis *lut1* (carente de luteína) que sobre expresaban CYP97C de maíz (la acumulación de luteína en las líneas transgénicas se producía a expensas de una reducción de zeinoxantina), concluí que el gen CYP97C19 de maíz era una ε-hidroxilasa de carotenoides funcional. En un proyecto independiente, caractericé dos líneas transgénicas de maíz que sobreexpresaban el gen *ORANGE* de Arabidopsis (*AtOR*). Las dos líneas mostraron un incremento del contenido de carotenoides sin variar la expresión de genes carotenogénicos endógenos. Posteriormente, crucé la línea que acumulaba más carotenoides con líneas transgénicas con perfiles de carotenoides distintos. En los casos en que el parental transgénico acumulaba pocos carotenoides, el híbrido resultante mostró un incremento sustancial del contenido de carotenoides sin cambios aparentes en la composición de éstos. En cambio, ningún efecto se observó en los niveles metabólicos y transcriptómicos de los híbridos cuando el contenido de carotenoides de los parentales era elevado. Los resultados de estos experimentos indican que una de las funciones del gen *ORANGE* de Arabidopsis en endospermo de maíz es generar un sumidero metabólico para la acumulación de carotenoides debido al incremento del contenido de carotenoides provocados por éste. Paralelamente, silencié las enzimas β-hidroxilasa de carotenoides, la BCH1 y la BCH2, mediante RNAi en cultivares de maíz que acumulan elevadas cantidades de luteína y zeaxantina. Los resultados me permitieron concluir que estas dos enzimas son clave para la determinación del contenido de β-caroteno y zexantina en maíz. También analicé la interacción entre la ruta metabólica de los carotenoides y la del almidón ya que comparten precursores comunes. El análisis del contenido total de almidón en cuatro líneas transgénicas (L1: sobreexpresión de *AtOR*; L2, sobreexpresión de *Zmpsy1*; L3, sobreexpresión de *Zmpsy1, PacrtI* y *ParacrtW;* L4, sobreexpresión de *Zmpsy1*, *PacrtI* y *Gllycb*) demostró que se producía una disminución de hasta el 8%. Confirmé que este efecto se debía a la reducción de la capacidad biosintética de formación de almidón a distintos niveles. Finalmente, crucé una línea transgénica (HC) que sobreexpresaba *Zmpsy1* y *PacrtI* con diferentes líneas puras pertenecientes a grupos heteróticos conocidos para obtener híbridos de maíz de alta producción y acumulación de

carotenoides. Evalué el desarrollo de los híbridos (caracteres agronómicos y morfológicos) en dos localidades distintas durante una estación de cultivo. Los resultados indicaron que el comportamiento en campo de los híbridos con alto contenido de carotenoides fue similar y en ocasiones superior a los híbridos comerciales que se cultivan en la zona.

RESUM

El programa de recerca que he desenvolupat s'ha centrat en l'estudi dels mecanismes d'acumulació de carotenoides en blat de moro (*Zea mays*). Inicialment, vaig clonar de la varietat de blat de moro B73 un gen candidat a ε-hidroxilasa de la ruta biocinètica dels carotenoides (CYP97C19). En base als resultats obtinguts en línies transgèniques derivades del mutant d'Arabidopsis *lut1* (mancat de luteïna) en les quals es va sobreexpressar el gen CYP9719 de blat de moro, que confirmaven l'acumulació de luteïna a expenses de zeinoxantina, vaig concloure que CYP97C19 és una ε-hidroxilasa de carotenoides funcional. En un segon projecte, vaig generar i caracteritzar dues línies transgèniques de blat de moro que sobreexpressaven el gen *ORANGE* d'Arabidopsis (*AtOR*). Les dues línies mostraren un increment en el contingut de carotenoides sense augmentar l'expressió de gens carotenogènics endògens. Posteriorment vaig creuar la línia que acumulava més carotenoides amb línies transgèniques que presentaven perfils de carotenoides diferents. En els casos en què el parental transgènic original creuat amb *AtOR* tenia poca concentració de carotenoides, l'híbrid resultant va mostrar un increment substancial del contingut de carotenoides, sense canvis aparents en la composició d'aquests. En canvi, quan el contingut de carotenoides dels parentals era elevat no es van observar canvis a nivell de metabòlits i transcripts en els híbrids. Els resultats d'aquests experiments suggereixen que una de les funcions del gen *ORANGE* d'Arabidopsis en l'endosperma de blat de moro és generar un depòsit metabòlic per a carotenoides arran de l'increment de carotenoides que provoca la seva sobreexpressió. Paral·lelament, vaig silenciar els enzims β-hidroxilasa de carotenoides, el BCH1 i el BCH2, a través de RNAi en diferents cultivars de blat de moro que acumulaven elevades quantitats de luteïna i zeaxantina. Els resultats que vaig obtenir em van permetre concloure que aquestes dos enzims eren clau per a modular el contingut de β-carotè en blat de moro. També vaig investigar la interacció entre la ruta metabòlica dels carotenoides i la del midó, ja que comparteixen precursors comuns. L'anàlisi del contingut total de midó en quatre línies transgèniques (L1: sobreexpressió de AtOR; L2, sobreexpressió de *Zmpsy1*; L3, sobreexpressió de *Zmpsy1*, *PacrtI* i *ParacrtW;* L4, sobreexpressió de *Zmpsy1*, *PacrtI* i *Gllycb*) va mostrar fins a una disminució del 8%. A més, vaig establir que aquest efecte era degut a la reducció de la capacitat biosintètica per formar midó a diferents nivells. Finalment, vaig creuar una línia transgènica (HC) que sobreexpressa *Zmpsy1* i *PacrtI* amb diferents línies pures representants de grups heteròtics coneguts per tal d'obtenir híbrids de blat de moro

d’altra producció i acumulació de carotenoides. Vaig avaluar el desenvolupament dels híbrids (caràcters agronòmics i morfològics) en dos localitats diferents durant una estació de cultiu. Els resultats indicaren que el comportament en el camp dels híbrids amb alt contingut de carotenoides era semblant, i en ocasions superior, als híbrids comercials que es cultiven a la zona.

LIST OF ABREVIATIONS

ADGPP: ADP-glucose pyrophosphorylase

AFLPs: amplified fragment length polymorphisms (AFLPs)

AGPase: ADP-glucose pyrophosphorylase

ANOVA: Analysis of variance

ATP: adenosine triphosphate

BCH: carotenoid β-hydroxylase

BKT: β-carotene ketolase

CaMV 35S: Cauliflower Mosaic Virus 35S

CCD: Capsanthin and capsorubin synthase

cDNA: complementary DNA

CRTB: bacterial phytoene synthase

CRTI: bacterial β-carotene desaturase

CRTISO: carotenoid isomerase

CRTW: bacterial β-carotene ketolase

CRTY: bacterial lycopene cyclase

CRTZ: bacterial β-carotene hydroxylase

CSPD:Disodium3-(4-methoxyspiro{1,2-dioxetane-3,2′-(5′-chloro)tricyclo [3.3.1.13,7]decan}-4-yl)phenyl phosphate

CYP97: carotene ε-ring hydroxylase

DAP: days after pollination

DBE: starch debranching enzyme

DMAPP: dimethylallyl diphosphate

DNA: deoxyribonucleic acid

DW: dry weight

DPPH: 2,2-diphenyl-1-picrylhydrazyl

DXP: 1-deoxy-D-xylulose-5-phosphate

DXS: 1-deoxy-D-xylulose 5-phosphate synthase

EST: Expressed Sequence Taq

FW: fresh weigh

G: genotype

GBSS: granule-bound starch synthase

GBSS: tuber-specific granule-bound starch synthase

GGPP: geranylgeranyl diphosphate

GGPPS: geranylgeranyl diphosphate synthase

Gl: *Gentiana lutea*

GOPOD: glucose oxidase/peroxidase

GPI: glucose phosphate isomerase

HC: High Carotenoid

HDR: DXP reductoisomerase

HK: Hexo kinase

Hp: *Haematococcus pluvialis*

HPLC: high performance liquid chromatography

HPT: Hygromycin phosphotransferase

HYDB: carotenoid β-hydroxylase

Ib: *Ipomea batatas*

IZE: Immature zygoti embryos

IPP: isopentenyl diphosphate

IPPI: isopentenyl diphosphate isomerase

L: location

LYCB: lycopene β-cyclase

LYCE: lycopene ε-cyclase

MEP: 2-C-Methyl-D-erythritol 4-phosphate pathway

mRNA: messenger RNA

MS: Murashige and Skoog

MSO: Osmoticum MS media

MSS: Selection MS media

MSR1: Regeneration 1 MS media

MSR1: Regeneration 2 MS media

MVA: mevalonic acid pathway

OR: orange gene

Os: *Oryza sativa*

p326/LMW: wheat low molecular weight glutenin promoter

PCR: Polymerase chain reaction

PDS: phytoene desaturase

PGM: phosphorgluco-mutase

Pho1: plastidial starch phosphorylase

PSY: phytoene synthase

QTL: quantitative trait locus

RNA: ribonucleic acid

RNAi: RNA interference

RT-PCR: reverse transcription PCR

SBE: starch branching enzyme

SD: standard deviation

SE: standard error

SEM: Scanning Electron Microscopy

Sh: *Shrunkengene*

Sl: *Solanum lycopersicon*

SS: soluble starch synthase

TEM: Scanning Electron Microscopy

TPS: Transit Peptide Sequence

UDP: uridine diphosphate

UHPLC: ultra high performance liquid chromatography

VAD: vitamin A deficiency

ZDS: ζ-Carotene desaturase

ZEP: Zeaxanthin epoxidase

ZISO: ζ-carotene isomerase

Zm: *Zea mays*

GENERAL INTRODUCTION

GENERAL INTRODUCTION

Definition and classification of carotenoids

Carotenoids are natural pigments that are synthesized in the plastids of plants and in other photosynthetic organisms such as algae, bacteria and fungi (Zhu et al. 2010). They are essential components of photosynthetic membranes and they can prevent the oxidative disruption of the photosynthetic process (Bartley and Scolnik 1995; Bassi et al. 1993). In addition, they are precursors in the biosynthesis of abscisic acid (Lindgren et al. 2003). Humans and most animals cannot synthesize carotenoids, and must obtain them from dietary sources. Two rare exceptions are the red pea aphid (*Acyrthosiphon pisum*) and the two-spotted spider mite (*Tetranychus urticae*), which have acquired the ability to produce carotenoids from fungi by horizontal gene transfer (Altincicek et al. 2012; Moran and Jarvik 2010).

Carotenoids are divided into two classes. Carotenes are hydrocarbon carotenoids (e.g. α-carotene, β-carotene and lycopene) whereas xanthophylls are molecules containing oxygen, such as lutein and zeaxanthin (hydroxy), echinenone and canthaxanthin (oxo), antheraxanthin (epoxy) and spirilloxanthin (methoxy). Most carotenoids are tetraterpenoids, produced from 8 isoprene molecules and contain 40 carbon atoms. Essentially all carotenoids possess certain common structural features: a polyisoprenoid backbone comprising a long conjugated chain of double bonds in the central portion of the molecule, and near symmetry around the central double bond. This basic structure can be modified in a variety of ways, most frequently by cyclization of the end groups and by the introduction of oxygen functionality, to yield a large family of > 700 compounds, exclusive as *cis* and *trans* isomers (Berman et al. 2015. Because of their structure, carotenoids are efficient free-radical scavengers, and they enhance the vertebrate immune system. Their antioxidant activity is based on their singlet oxygen quenching properties and their ability to trap peroxyl radicals (Krinsky 1998; Rice-Evans et al. 1997).

Natural sources of carotenoids

Carotenoids are present in many fruits and vegetables. For example, β-carotene is present in a wide variety of yellow-orange colored fruits and dark green and orange vegetables such as broccoli, spinach, carrots, squash, sweet potatoes and pumpkin (Farré et al. 2010; Bai et al.

2011). β-Cryptoxanthin is a carotenoid pigment found in peach, papaya, and citrus fruits such as orange and tangerine. Lycopene is the red fruit pigment in tomato, watermelon, pink grapefruit and guava (Bramley 2000). Vietnamese Gac (*Momordica cochinchinensis*) fruit contains the highest known concentration of lycopene (Aoki et al. 2002). Lutein is the most abundant carotenoid in all green vegetables, often representing 50% of the total carotenoid pool. In contrast, zeaxanthin is present in small quantities in most foods (Sommerburg et al. 1998) although some varieties of yellow corn and yellow pepper accumulate high amounts (Minguez-Mosquera and Hornero-Mendez 1994; Quackenbush et al. 1963). Astaxanthin is found in microalgae, yeast, salmon, trout, krill, shrimp, crayfish, crustaceans and the feathers of some birds. It is responsible for the pink color of salmon flesh and the pink-red color of cooked shellfish (Zhu et al. 2009). In *Bixa orellana*, the orange-red apocarotenoid bixin is accumulated in high concentrations, mainly in seeds, and accounts for 80% of the total carotenoids present in the seeds (Rivera-Madrid et al. 2006). Saffron apocarotenoids – crocin, crocetin and picrocrocin – are only found in the red stigma of *Crocus sativus* (Bouvier et al. 2003).

Carotenoid biosynthesis

Terpenoid biosynthesis begins with the condensation of three molecules of isopentenyl diphosphate (IPP) with one molecule of dimethylallyl diphosphate (DMAPP) to produce the C20 compound geranylgeranyl diphosphate (GGPP). In plants, this reaction is catalyzed by GGPP synthase (GGPPS) in the plastids (Chappell 1995) and the equivalent enzyme in bacteria is CRTE (**Figure 1**). The isomeric precursors IPP and DMAPP are derived predominantly from the plastidial methylerythritol 4-phosphate (MEP) pathway although the same precursors are formed by the cytosolic mevalonic acid (MVA) pathway, with which there may be some cross-talk (Rodríguez-Concepción 2006). The first committed step in plant carotenoid biosynthesis is the condensation of two GGPP molecules into 15-*cis*-phytoene by the enzyme phytoene synthase (PSY) (Misawa et al. 1994) and the equivalent enzyme in bacteria is CRTB. This intermediate then undergoes a two-step desaturation reaction in plants catalyzed by phytoene desaturase (PDS) to generate 9,15-*cis*-phytofluene and then 9,15,9'-tri-*cis*-ζ-carotene. This is isomerized by light and/or ζ-carotene isomerase (ZISO) to yield 9,9'-di-*cis*-ζ-carotene, which is converted by ζ-carotene desaturase (ZDS) into 7,9,9'-tri-*cis*-neurosporene and then 7,9,7'9'-tetra-*cis*-lycopene (Chen et al. 2010; Li et al. 2007). The end

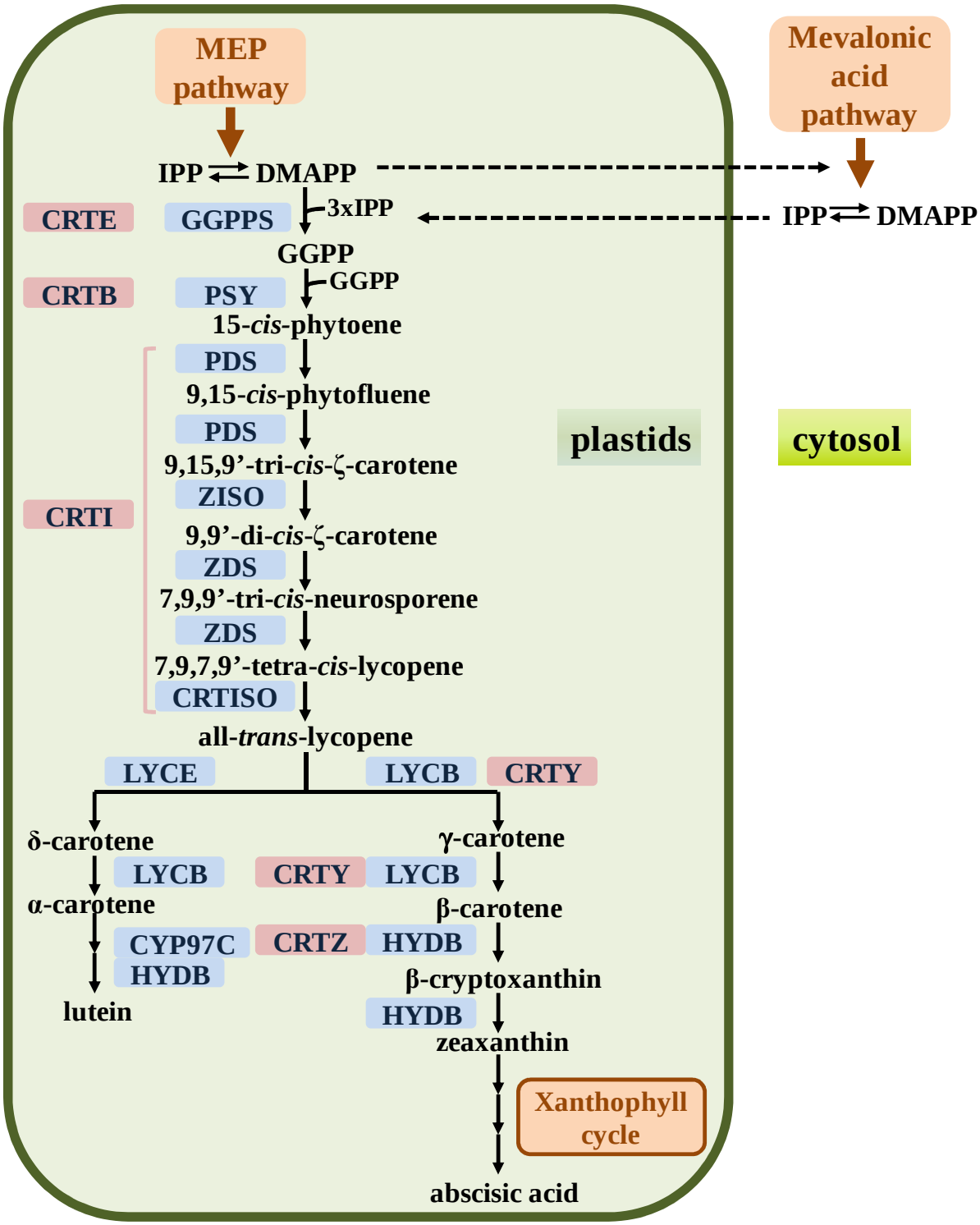

Figure 1 – Carotenoid biosyntethic pathway in plants (blue) and equivalent steps in bacteria (red). Abbreviations: IPP, isopentenyl diphosphate; DMAPP, dimethylallyl diphosphate; GGPP, geranylgeranyl diphosphate; GGPPS, GGPP synthase; PSY, phytoene synthase; PDS, phytoene desaturase; ZISO, ζ-carotene isomerase; ZDS, ζ-carotene desaturase; CRTISO, carotenoid isomerase; LYCB, lycopene β-cyclase; LYCE, lycopene ε-cyclase; CYP97C, carotene ε-ring hydroxylase; HYDB, carotenoid β-hydroxylase; CRTE, bacterial GGPP synthase; CRTB, bacterial phytoene synthase; CRTI, bacterial phytoene desaturase/isomerase; CRTY, bacterial lycopene β-cyclase; CRTZ, bacterial β-carotene hydroxylase (Berman et al. 2015).

product of the desaturation reactions is converted to all-*trans*-lycopene by carotenoid isomerase (CRTISO) in non-green tissue, and by light and chlorophyll (acting as a sensitizer) in green tissue (Breitenbach and Sandmann 2005; Chen et al. 2010; Isaacson et al. 2004).

In non-photosynthetic bacteria, the single enzyme CRTI accomplishes all the above steps and produces all-trans-lycopene directly from 15-*cis*-phytoene (**Figure 1**). Lycopene is an important branch point in the carotenoid pathway because it acts as the substrate for two competing enzymes: lycopene β-cyclase (LYCB), and lycopene ε-cyclase (LYCE) (Cunningham and Gantt 2011). Both enzymes cyclize the linear backbone to generate terminal α- or β-ionone rings, differing by the 4,5- or 5,6-position of the double bond. The addition of one β-ring by LYCB generates γ-carotene, and the addition of a second β-ring to the free end by the same enzyme produces β-carotene. This reaction is rapid, so γ-carotene tends not to accumulate. In bacteria, this reaction is carried out by CRTY. Alternatively, the addition of one ε-ring to lycopene by LYCE generates δ-carotene. This is a poor substrate for LYCE so it is unusual for the second ε-cyclization to take place, but it is a good substrate for LYCB, which adds a β-ring to the free end to produce α-carotene. In the presence of the enzyme carotenoid β-hydroxylase (HYDB), both α-carotene and β-carotene can be converted into more complex downstream carotenoids. In the case of α-carotene, this downstream product is lutein, and in the case of β-carotene the downstream product is zeaxanthin, although the reactions involve the intermediates α-cryptoxanthin and β-cryptoxanthin, respectively (**Figure 1**). A single hydroxylase is required to produce zeaxanthin but two different hydroxylases are essential for the synthesis of lutein (Kim et al. 2009). In bacteria, a functionally similar enzyme is CRTZ. Whereas lutein represents the natural end point of the α-carotene branch, zeaxanthin can be further converted to 5,6-epoxy derivatives, which are part of the xanthophyll cycle. This cycle involves the enzymatic removal of epoxy groups from violaxanthin, antheraxanthin and zeaxanthin which play a critical role in stimulating energy dissipation in photosystem II. At the end of the pathway these products can be converted through a number of additional steps into the important plant hormone abscisic acid (Seo and Koshiba 2002) **(Figure 1**).

Functional characterization of carotenogenic genes

The functional characterization of enzymes in any organism, including plants is essential for the development of targeted metabolic interventions and a better understanding of global

metabolism. Most of the carotenogenic genes were previously functionally characterized through a combination of sequence analysis and complementation in *E. coli*, a non-carotenogenic bacterium. *E. coli* is suitable for this task because the absence of carotenoid synthesis means that recombinant strains can be created to reproduce the target reaction of analysis (Misawa et al. 1990). The products synthesized in *E. coli* can be analyzed by chromatography even thought the colonies exhibit a color phenotype ranging from yellow to red which often provides a quicker means of identification (**Figure 2**). However, the GGPP pool in *E. coli* is not large enough to sustain high levels of carotenoid synthesis. Therefore, prior to heterologous expression of target genes for complementation studies, the amount of GGPP must be increased through the expression of GGPP synthase (encoded by *crtE*), which catalyzes the addition of a C5 isoprenoid unit onto GGPP. The addition of further carotenogenic genes then leads to the production of specific intermediates and downstream carotenoids. For example, the introduction of *crt*E, *crt*B, *crt*I and *crt*Y facilitates the *de novo* synthesis of lycopene, β-carotene and zeaxanthin (Misawa et al. 1990; Hundle et al. 1994) and the further addition of *crtZ* and *crtW* (bacterial carotenoid ketolase) facilitates the synthesis of astaxanthin (Misawa et al. 1995). P450 carotene hydroxylases have been successfully characterized in *E. coli* (Quinlan et al. 2007). Other bacteria suitable for functional characterization of carotenogenic candidate genes include *Zymomonas mobilis*, *Agrobacterium tumefaciens* (Misawa et al. 1991) and *Rhodobacter capsulatus* (Bartley et al. 1991) and the fungus *Mucor circinelloides* (Álvarez et al. 2006).

Figure 2 – The carotenoid biosynthesis in living color. *Escherichia coli* strain TOP 10 was genetically engineered to accumulate different carotenoids as indicated (Cunningham and Grantt 1998).

An alternative system to validate gene function in plants is the use of loss of function mutants and subsequent phenotypic characterization. Mutations in *pds*, *zds*, *crtiso* and *lycbe* in rice produced albinism and viviparity and high accumulation of phytoene, 9,9'-di-cis-ζ-carotene and lycopene, respectively, confirming the function of these genes and their importance in the synthesis of abscisic acid (ABA) (Fang et al. 2008). Similar effects were observed in maize (Matthews et al. 2003; Singh et al. 2003). In pepper, a mutation in the *y* locus (*yellow*) which affects the enzymes capsanthin and capsorubin synthase (CCS) results in yellow fruit (Lefebvre et al, 1998) and in tomato the *wf* (*white flower*) locus was related with HYDB (Galpaz et al. 2006) (**Figure 3**).

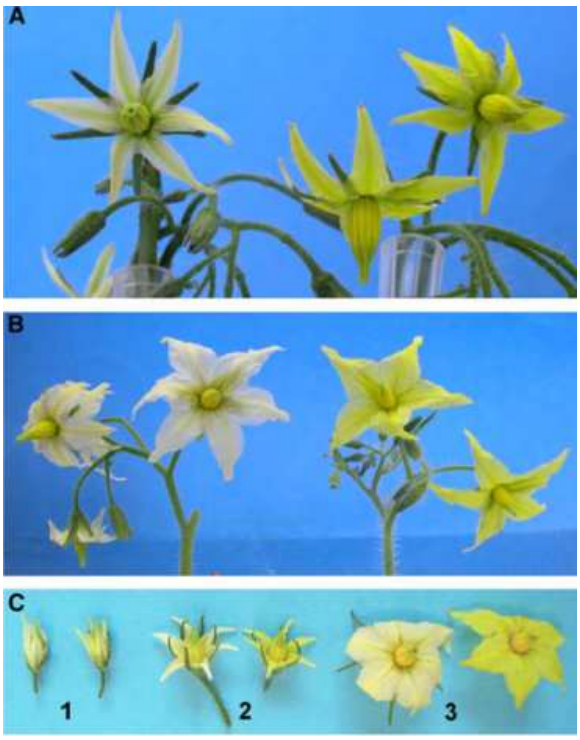

Figure 3 – Flowers of *wf* mutants. (A) *wf1-1* (F2 of a cross LA23703IL3-2) (left) and its nearly isogenic wild-type line (F2 of the same cross). (B) *wf1-2* (e1827) (left) and its isogenic line M82. (C) Flower of *wf1-2* (left) and the wild type (right) in developmental stages 1 to 3 (Galpaz et al. 2006).

A third method for functional gene characterization relies on the use of transgenic plants accumulating higher amounts or new metabolites *in vivo*. In this context, the hemizygous tomato plants overexpressing *cyp97A29* and *cyp97C11* genes encoding the P450 carotenoid β- and ε-hydroxylases, respectively, resulted in an increase of leaf violaxanthin content in the case of *cyp97A29* and an increase of lutein and reduction in the β,β-xanthophylls in *cyp97C11* transgenic plants (Stigliani et al. 2011). Recently, a new method to functionally characterize carotenoid genes based on heterologous gene expression was described in rice callus (Bai et al. 2014). This tissue is white and just accumulates traces levels of carotenoids so the

overexpression of carotenoid genes can be rapidly observed visually if the key genes in the pathway are active and carotenoids accumulate (**Figure 4**). In this case endosperm specific promoters which are also active in rice callus were used. Thus, the rice callus system is a suitable platform to assess gene function without the need to regenerate mature plants and therefore provides a rapid screening platform that avoids the labor-intense process of plant regeneration (Bai et al. 2014; Ahrazem et al. 2015).

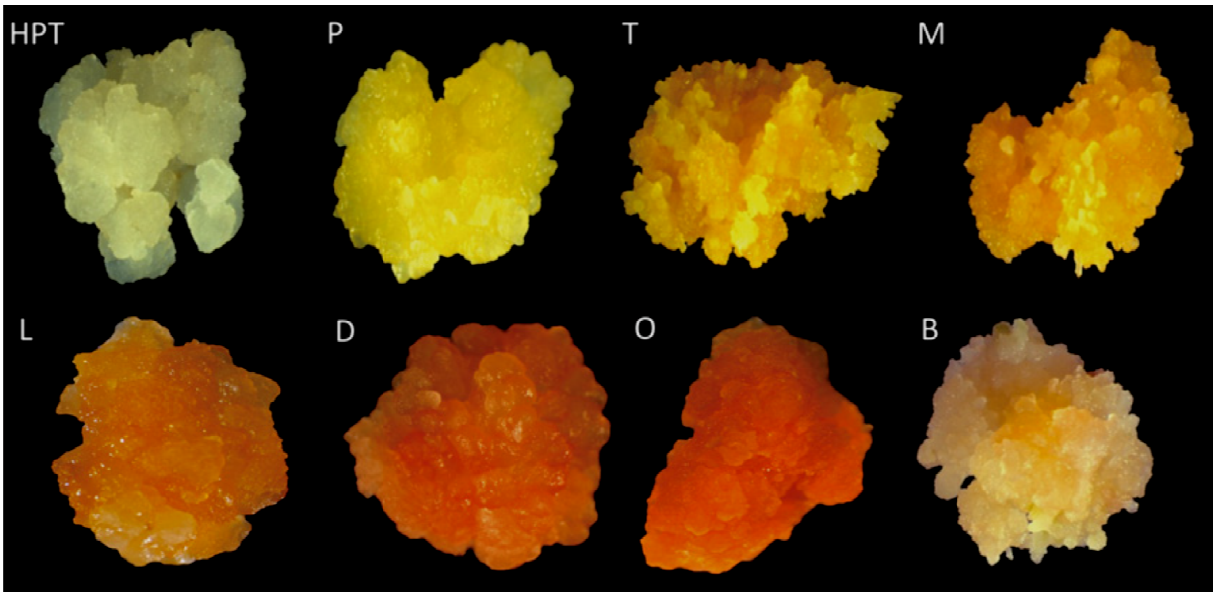

Figure 4 – Phenotypes of eight transgene combinations expressed in rice callus. HPT, callus expressing HPT (white color); P, expression of ZmPSY1 alone results in a pale yellow color; expression of *Zmpsy1* and *AtDXS* in T, *Zmpsy1* and *AtOR* in M, and *Zmpsy1* and *PacrtI* in L, result in a similar yellow color; expression of *AtDXS* in addition to *Zmpsy1* and *PacrtI* in D, or *Zmpsy1*, *PacrtI* and *AtOR* in O, results in a similar orange color; B, expression of *Zmpsy1*, *PacrtI* and *sCrbkt* generates colors ranging from pink to red depending on the accumulation of ketocarotenoids (Bai et al. 2014).

Metabolic engineering strategies to modulate carotenoid levels and composition in plants

Metabolic engineering in plants allows modulation of carotenoid levels and composition. A number of alternative strategies have been used in carotenoid engineering in plants. Upstream MEP pathway precursors are rate-limiting in most of the species and/or tissues lacking carotenoids, e.g. rice endosperm (Rodríguez-Concepción 2010). Thus, increasing precursor supply can provide additional flux into the pathway and increase total carotenoid levels (**Figure 5**). For example this strategy was used in tomato: overexpression of an *E. coli* 1-deoxy-D-xylulose 5-phosphate synthase (DXS) resulted in a 1.6-fold increase in total carotenoids. A second strategy involves the overexpression of carotenogenic genes in order to

release key bottlenecks in the pathway and, consequently, increase total or particular carotenoid levels (**Figure 5**). Golden Rice II (Paine et al. 2005) or high carotenoid maize (Zhu et al. 2008) are good examples of this strategy where the overexpression of maize *psy1* and *Pantoea ananatis crtI* resulted in 26- and 156-fold increase total carotenoids, respectively. The third strategy involves RNAi to down regulate gene expression, thus blocking an entire branch of a particular pathway (e.g. α-branch in the case of carotenoids) or the conversion of a compound to downstream metabolites (**Figure 5)**.

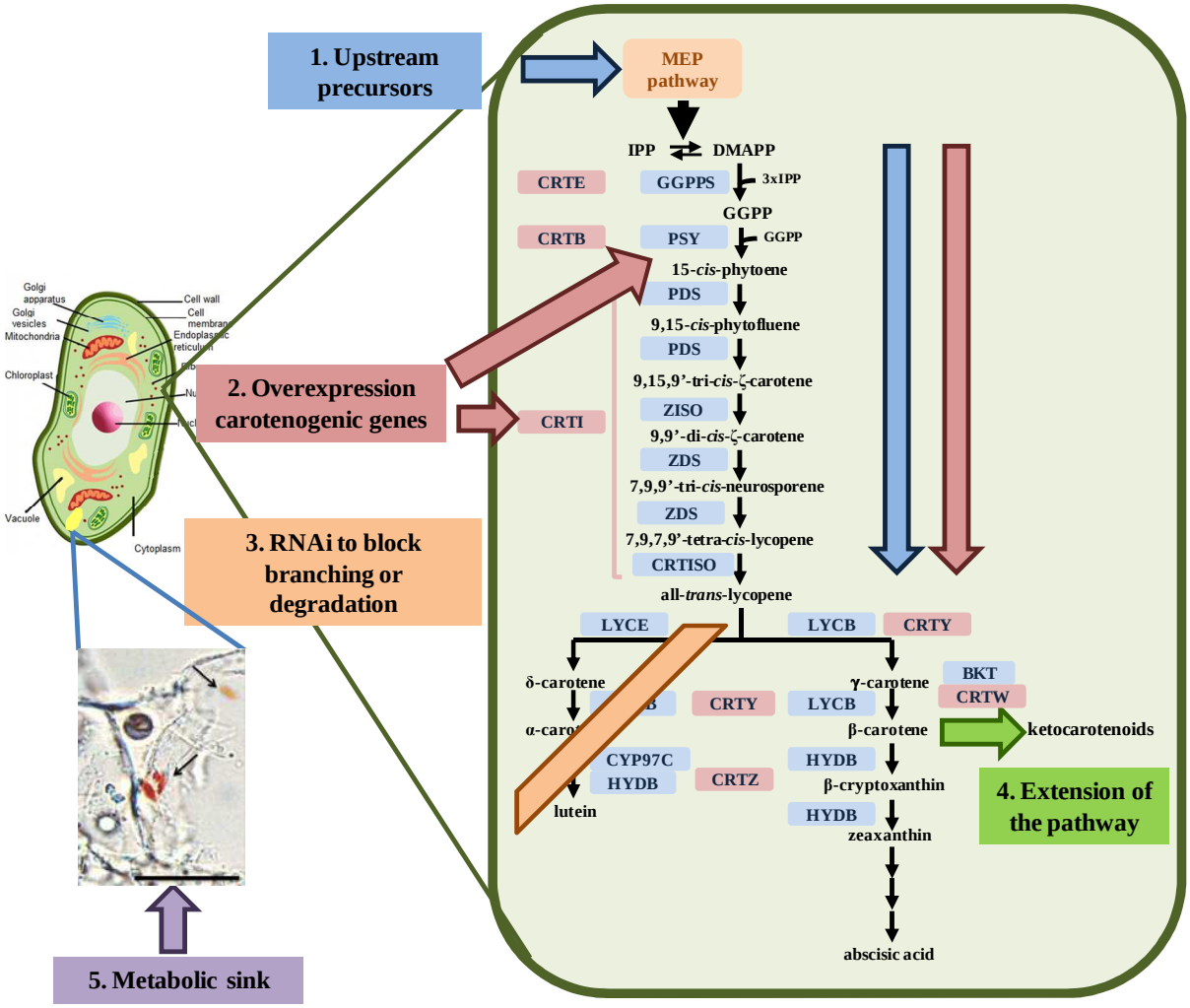

Figure 5 – Strategies to modulate carotenoid levels in plants. Abbreviations as in figure 1. BKT, β-carotene ketolase; CRTW, bacterial β-carotene ketolase (Adapted from Berman et al. 2015; light microscopy from Bai et al., 2014, scale bar 20µm).

Yu et al. (2008) reported down regulation of *lyce* in *Brassica napus* to direct the metabolic flux to the β-branch of the pathway, enhancing seed carotenoid content up to ca: 227 µg/g fresh weight (FW) (45-fold). The β-carotene to lutein ratio increased ca: 8-fold. Blocking HYDB through RNAi resulted in potatoes with β-carotene content of ca: 330µg/g FW compared to trace amounts in wild type (Van Eck et al. 2007). It is also possible to extend the

pathway to produce novel compounds which are not commonly present in plants (**Figure 5**). A good example is accumulation of the valuable ketocarotenoid astaxanthin in carrot, reaching ca: 91µg/g FW by the introduction of β-carotene ketolase from *Haematococcus pluvialis* (HpBKT) (Jayaraj et al. 2008). Carotenoid content in plants can also be modulated through the creation of a metabolic sink by inducing large carotenoid-sequestering organelles and influencing the differentiation of proplastids into chromoplasts. The *orange* gene (*or*) originally discovered in a cauliflower mutant is able to catalyze the transition of proplastids to chromoplasts (Li et al. 2001; Lu et al, 2006; Paolillo et al. 2004). In potato, overexpression of cauliflower *or* resulted in a 10-fold increase in total carotenoids. Carotenoid levels remained stable after long term cold storage (Lopez et al. 2008) (**Figure 5**).

Different strategies can be combined to accumulate even higher levels of carotenoids by influencing metabolism in a more profound manner. In rice endosperm, increasing precursor supply (overexpression of *AtDXS*) simultaneously with overexpressing carotenogenic genes (*Zmpsy1* and *PacrtI*) increased total carotenoid content to ca: 30 µg/g dry weight (DW) compared to plants overexpressing the carotenogenic genes alone (ca: 5.5 µg/g DW; (Bai et al. 2015). In addition, overexpression of Arabidopsis *OR* together with *psy1* and *crtI* resulted in ca: 25 µg/g DW (Bai et al. 2015). In maize, the development of a combinatorial nuclear transformation strategy designed to modify the carotenoid pathway using the elite white-endosperm South African inbred M37W allowed the generation of transgenic plants expressing multiple heterologous enzymes that extended the pathway to ketocarotenoids (Zhu et al. 2008). The pilot study involved the introduction of five genes (*Zmpsy1*, *Gentania lutea llycb* and *bch*, and bacterial *crtI* and *crtW*) under the control of endosperm-specific promoters. This strategy recreated the entire pathway from GGPP to zeaxanthin and also added the enzyme CRTW that converts β-carotene to downstream ketocarotenoids. The recovery of plants carrying random combinations of genes resulted in a metabolically diverse library comprising plants with a range of carotenoid profiles, revealed by easily identifiable endosperm colors ranging from yellow to scarlet. The kernels contained high levels of β-carotene, lycopene, zeaxanthin and lutein, as well as further commercially-relevant ketocarotenoids such as astaxanthin and adonixanthin (Zhu et al. 2008).

Impact of carotenoid enhancement on general metabolism

Genetic engineering of a pathway may have a global effect on global metabolism due to the fact that precursors are consumed at the expense of other resident (Sandmann 2001). One example is dwarfism of transgenic tomato plants with higher levels of carotenoids. In such plants GGPP was diverted away from gibberellins biosynthesis causing the dwarf phenotype. In other cases organ-specific promoters can direct accumulation of newly synthesized compounds to a particular sub-cellular compartment so the impact on plant growth and development is not compromised (reviewed in Peremarti et al. 2010). In addition, not all the collateral effects produced by metabolic engineering are detrimental and there examples in which carotenoid enhancement is positively correlated with stress tolerance (Goo et al. 2015; Kim et al. 2013) or enhancement of other nutrients like oleate and proteins (Schmidt et al. 2015). Recently, a combined transcript, proteome, and metabolite analysis of transgenic maize seeds engineered for enhanced carotenoid synthesis revealed pleotropic effects in core metabolism, mainly in sterol and fatty acid synthesis as well as in soluble sugars (Decourcelle et al. 2015). Little is known regarding the effects of carotenoid-enhanced transgenic plants on global metabolism so it is important to address this aspect as well because of its biochemical and metabolic implications.

Applications of carotenoid lines accumulating specific carotenoids

Reduce Vitamin A Deficiency (VAD)

Vitamin A is an essential nutrient for humans because its reduced form (retinal or retinaldehyde) is required for the production of rhodopsin, an indispensable component for vision and maintenance of epithelial and immune cells. In addition, the acidic form of vitamin A (retinoic acid) is a morphogen in development. Humans can produce retinal and retinoic acid if provided a source of retinol or one of its esters, which are abundant in meat and dietary products. However, retinal can also be synthesized from plant sources, which contain pro-vitamin A carotenoids (β-carotene, α-carotene, γ-carotene, and β-cryptoxanthin), by the enzyme β-carotene 15,15'-monooxygenase (reviewed by Bai et al., 2011; Farré et al., 2011). The dietary reference intake (DRI) for vitamin A is 900 RAE (Retinol Activity Equivalents) for males, 700 RAE for females and 400-500 RAE for children (US Institute of Medicine 2001). One RAE is equivalent to 1 µg of pure retinol, 2 µg of pure β-carotene dissolved in oil,

12 µg of β-carotene in food or 24 µg of other pro-vitamin A carotenoids (US Institute of Medicine 2001).

Most people in the developed world have diets of sufficient diversity to ensure they achieve the DRI for vitamin A, but the situation in developing countries is very different. More than four million children, most from developing countries, exhibit clinical symptoms of severe VAD, including poor immunity, loss of vision in low light conditions (night blindness) and in extreme cases an irreversible form of blindness called xerophthalmia (Sommer 2008). VAD has been addressed by supplementation with an estimated cost of US$ 130 million per year (Berman et al. 2013). Alternative strategies include industrial fortification, biofortification, dietary diversification and the support of public health measures (Stein et al. 2006). In this context, carotenoid enhanced staple crops such as Golden Rice (Paine et al. 2005) and Multivitamin Corn (Naqvi et al. 2009) can cost-effectively reduce VAD (Berman et al. 2013; Stein et al. 2006).

Animal Feed

As animals do not synthesize carotenoids *de novo* these compounds need to be present in sufficient levels as components in animal feed. Feed needs to provide a balanced diet, specific for each animal type in order to achieve high performance. Carotenoids commercially produced for feed can be obtained by chemical synthesis, extracted from natural sources (*Tagetes erecta*, *Capsicum* and tomato) or biosynthesized by microorganisms (*Haematococcus pluvialis*, *Phaffia rhodozyma*, *Blakeslea trispora*) (Berman et al. 2015). The main carotenoids used in animal nutrition include astaxanthin, β-apo-8'-carotenoic acid ethyl ester, lutein, zeaxanthin, canthaxanthin and capsanthin. These are approved feed additives for animal nutrition in the European Union (Regulation (EC) No 1831/2003) (**Table 1**) and in most of the countries around the world. These additives are classified in the EU as 'sensory additives' because they are substances that add or restore color in feedstuff; substances which, when fed to animals, add color to food of animal origin; and/or substances which favorably affect the color of ornamental fish or birds.

For each animal type, industry requires specific carotenoids. For example, in the case of salmonids (e.g. salmon and trout) the orange-pink color of the flesh is normally attained by the addition of astaxanthin which is sometimes combined with canthaxanthin (Breithaupt 2007) (**Table 1**). In crustaceans, carotenoids are used to enhance the pigmentation of the

exoskeleton. Similarly to fish, the carotenoid most commonly used in crustaceans is astaxanthin, but also β-carotene is used, although in some markets it is combined with canthaxanthin (Breithaupt 2007). Feed for ornamental birds, mainly canaries, is supplemented with β-carotene, canthaxanthin and lutein to pigment the plumage. In dogs and cats lycopene, β-carotene, lutein and zeaxanthin are usually used as antioxidant source, to enhance immune status, as well as to prevent age-related macular degeneration (ARMD) (Kim et al. 2000). Egg yolk of laying hens is enhanced by the addition of xanthophylls in feed because nonpolar carotenes do not contribute to its pigmentation (Hencken 1992). To this end, yellow and red pigments alone or in combination are used according to the color desired by the market (**Table 1**).

Table 1 – List of authorized additives in feedingstuffs published in application of article 9t(b) of Council Directive 70/524/EEC concerning additives in feedingstuffs: 1. Carotenoids and xanthopylls (2004).

Additive (EC no)	Source	Species or category of animal	Maximum content (mg/kg) of complete feedingstuff
Capsanthin (E 160c)	*Capsicum*	Poultry	80[a]
β-Apo-8'-carotenal (E 160e)	Synthetic	Poultry	80[a]
β-Apo-8'-carotenoic acid ethyl ester (E 160f)	Synthetic	Poultry	80[a]
Lutein (E 161b)	*Tagetes erecta*	Poultry	80[a]
Cryptoxanthin (E 161c)	*Tagetes erecta*	Poultry	80[a]
Canthaxanthin (E 161g)	Synthetic	Poultry Laying hens Salmon / Trout	25[b] 8[b] 25[c]
Zeaxanthin (E 161h)	*Tagetes erecta* Synthetic	Poultry	80[a]
Citranaxanthin (E 161i)	Synthetic	Laying hens	80[a]
Astaxanthin (E 161j)	Synthetic Biosynthesized	Salmon / Trout	100[c]

a Alone or with other carotenes and xanthophylls.

b Mixtures of canthaxanthin with other carotenes and xanthophylls are premitted provided that the total concentration of the mixture does not exceed 80 mg/kg in the complete feedingstuff.

c Use permitted from the age of six months onwards. The mixture of astaxanthin with canthaxanthin is permitted provided that the total concentration of the mixture does not exceed 100 mg/kg in the complete feedingstuff.

Commercial xanthophyll sources typically used to achieve the desired pigmentation and color include: lutein, zeaxanthin and the β-apo-8'-carotenoic acid ethyl ester as yellow sources and capsanthin, citranaxanthin or canthaxanthin as red sources. Similarly to laying hens, carotenoids are used for broilers and other meat poultry species to confer the desired yellow orange color of skin preferred by some consumers (Breithaupt 2007).

Maize is an important ingredient in poultry feed often representing up to ca: 60% of the total feedingstuff, followed by soybean (15-30%). In this context, the use of engineered maize accumulating specific carotenoids might provide all nutritional requirements and xanthophylls to obtain the desired color in eggs or meat without additional supplements. In addition, most of the feed formulations of poultry and other species such as cows and pigs contain vitamin A as a micronutrient (e.g. 12,000 International Units per ton).

Human food

Most carotenoids are used in the food industry as additives due to their antioxidant and colorant properties (**Table 2**).

Principal processed foods that include carotenoids are cheese, fruit and vegetable preparations and jam, jellies and marmalades. The main carotenoids used as food additives are produced by chemical synthesis or purification from a natural source (e.g. *Bixa orellana, Solanum lycopersicum, Paprika* and *Tagetes erecta*). Biosynthesis by yeast or algae in a reactor is also possible. In Europe, before a new additive can be used in foods it has to be approved by the European Commission which also regulates the maximum level permitted in the final food product (**Table 2**). Similarly to *Paprika* extracts, the generation of new maize lines accumulating specific carotenoids or carotenoid mixtures could allow the possibility of extracting them and further use them as additives in processed foods.

Table 2 – List of carotenoids used in food industry.

Additive (EC no)	Source	Applications in food industry	Maximum limit (mg/kg)	Regulation
β-carotene (E 160a)	Synthetic Biosynthesized	fats and oils, cheese products, processed meat and fish, jam, jellies and marmalades, fruit and vegetable preparations, butters, breakfast cereals	*quantum satis*	(EU)No 129/2011 (EU) No 738/2013
Annato, bixin, norbixin (E 160b)	*Bixa orellana*	drinks, desserts, edible ices, fats and oils, bakery, batters, cheese products, breakfast cereals, decorations and coatings, snacks, milk products, processed fish and nuts	10-50	(EU)No 129/2011
Paprika extract, capsanthin, capsorubin (E 160c)	*Paprika*	cheese products, processed meat and fish, jam, jellies and marmalades, fruit and vegetable preparations, breakfast cereals	*quantum satis*	(EU) No 129/2011 (EC) No 738/2013 (EC) No 601/2014 (EC)No 093/2014
Lycopene (E 160d)	*Solanum lycopersicum* Synthetic	drinks, desserts, edible ices, milk products, protein products, food supplements, fruits and vegetables, chewing gum, cheese products, seasonings and condiments, jam, jellies and marmalades, coatings and decorations for meat, dietary foods for weight control diets, dietary foods for special medical purposes, soups, bakery, batters, sauces, snacks, processed fish and nuts	5-500	(EU)No 129/2011 (EU) No 232/2012
β-Apo-8'-carotenal (E 160e)	Synthetic	processed cheese, fruit and vegetable preparations, processed fish	100-250	(EU) No 232/2012
Lutein (E 161b)	*Tagetes erecta* Biosynthesized	processed cheese, fruit and vegetable preparations, jam, jellies and marmalades, processed fish	100-250	(EU) No 232/2012

References

Ahrazem O, Rubio-Moraga A, Berman J, Capell T, Christou P, Zhu C, Gómez-Gómez L (2015) The carotenoid cleavage dioxygenase CCD2 catalysing the synthesis of crocetin in spring crocuses and saffron is a plastidial enzyme. New phytologist (in press). doi: 10.1111/nph.13609

Altincicek B, Kovacs JL, Gerardo NM (2012) Horizontally transferred fungal carotenoid genes in the two-spotted spider mite Tetranychus urticae. Biol Lett. 8:253–257.

Álvarez V, Rodríguez-Sáiz M, de la Fuente JL, Gudiña EJ, Godio RP, Martín JF, et al. (2006) The crtS gene of Xanthophyllomyces dendrorhous encodes a novel cytochrome-P450

hydroxylase involved in the conversion of β-carotene into astaxanthin and other xanthophylls. Fungal Genet Biol. 43:261–272.

Aoki H, Kieu NTM, Kuze N, Tomisaka K, Van Chuyen N (2002) Carotenoid pigments in GAC fruit (Momordica cochinchinensis SPRENG). Biosci Biotechnol Biochem. 66:2479–2482.

Bai C, Capell T, Berman J, Medina V, Sandmann G, Christou P, et al. (2015) Bottlenecks in carotenoid biosynthesis and accumulation in rice endosperm are influenced by the precursor-product balance. Plant Biotechnol J. (in press) doi: 10.1111/pbi.12373

Bai C, Rivera SM, Medina V, Alves R, Vilaprinyo E, Sorribas A, et al. (2014) An in vitro system for the rapid functional characterization of genes involved in carotenoid biosynthesis and accumulation. Plant J. 77:464–475.

Bai C, Twyman RM, Farré G, Sanahuja G, Christou P, Capell T, et al. (2011) A golden era-pro-vitamin A enhancement in diverse crops. Vitr Cell Dev Biol - Plant. 47:205–221.

Bartley GE, Scolnik PA (1995) Plant carotenoids: pigments for photoprotection, visual attraction, and human health. Plant Cell. 1995;7:1027–1038.

Bartley GE, Viitanen P V, Pecker I, Chamovitz D, Hirschberg J, Scolnik PA (1991) Molecular cloning and expression in photosynthetic bacteria of a soybean cDNA coding for phytoene desaturase, an enzyme of the carotenoid biosynthesis pathway. Proc Natl Acad Sci U S A. 88:6532–6536.

Bassi R, Pineau B, Dainese P, Marquardt J (1993) Carotenoid-binding proteins of photosystem II. Eur J Biochem. 212:297–303.

Berman J, Zhu C, Pérez-Massot E, Arjó G, Zorrilla-López U, Masip G, et al. (2013) Can the world afford to ignore biotechnology solutions that address food insecurity? Plant Mol Biol. 83:5–19.

Berman J, Zorrilla-López U, Farré G, Zhu C, Sandmann G, Twyman RM, et al. (2015) Nutritionally important carotenoids as consumer products. Phytochem Rev. 14:727-743.

Bouvier F, Suire C, Mutterer J, Camara B (2003) Oxidative remodeling of chromoplast carotenoids: identification of the carotenoid dioxygenase CsCCD and CsZCD genes involved in Crocus secondary metabolite biogenesis. Plant Cell. 15:47–62.

Bramley PM (2000) Is lycopene beneficial to human health? Phytochemistry. 54:233–236.

Breitenbach J, Sandmann G (2005) ζ-Carotene cis isomers as products and substrates in the plant poly-cis carotenoid biosynthetic pathway to lycopene. Planta. 220:785–793.

Breithaupt DE (2007) Modern application of xanthophylls in animal feeding - a review. Trends Food Scie Tech. 18:501–506.

Chappell J (1995) Biochemistry and Molecular Biology of the Isoprenoid Biosynthetic Pathway in Plants. Annu. Rev. Plant Physiol. Plant Mol. Biol. 46:521–547.

Chen Y, Li F, Wurtzel ET (2010) Isolation and characterization of the Z-ISO gene encoding a missing component of carotenoid biosynthesis in plants. Plant Physiol. 153:66–79.

Chow J, Klein EY, Laxminarayan R (2010) Cost-effectiveness of "golden mustard" for treating vitamin a deficiency in India. PLoS One. 5:e12046.

Cunningham FX, Gantt E (1998) Genes and enzymes of carotenoid biosynthesis in plants. Annu. Rev. Plant Physiol. Plant Mol. Biol. 49:557-583.

Cunningham FX, Gantt E (2011) Elucidation of the Pathway to Astaxanthin in the Flowers of Adonis aestivalis. Plant Cell. 23:3055–3069.

Decourcelle M, Perez-Fons L, Baulande S, Steiger S, Couvelard L, Hem S, et al. (2015) Combined transcript, proteome, and metabolite analysis of transgenic maize seeds engineered for enhanced carotenoid synthesis reveals pleotropic effects in core metabolism. J Exp Bot. (in press). DOI: 10.1093/jxb/erv120

Fang J, Chai C, Qian Q, Li C, Tang J, Sun L, et al. (2008) Mutations of genes in synthesis of the carotenoid precursors of ABA lead to pre-harvest sprouting and photo-oxidation in rice. Plant J. 54:177–189.

Farré G, Bai C, Twyman RM, Capell T, Christou P, Zhu C (2011) Nutritious crops producing multiple carotenoids - a metabolic balancing act. Trends Plant Sci. 16:532–540.

Farré G, Sanahuja G, Naqvi S, Bai C, Capell T, Zhu C, et al. (2010) Travel advice on the road to carotenoids in plants. Plant Sci. 179:28–48.

Galpaz N, Ronen G, Khalfa Z, Zamir D, Hirschberg J (2006) A Chromoplast-Specific Carotenoid Biosynthesis Pathway Is Revealed by Cloning of the Tomato white- flower Locus. Plant Cell. 18:1–14.

Goo Y-M, Han E-H, Jeong JC, Kwak S-S, Yu J, Kim Y-H, et al. (2015) Overexpression of the sweet potato IbOr gene results in the increased accumulation of carotenoid and confers tolerance to environmental stresses in transgenic potato. C R Biol. 338:12–20.

Hencken H (1992) Chemical and physiological behavior of feed carotenoids and their effects on pigmentation. Poult Sci. 71:711–717.

Hundle B, Alberti M, Nievelstein V, Beyer P, Kleinig H, Armstrong GA, et al. (1994) Functional assignment of Erwinia herbicola Eho10 carotenoid genes expressed in Escherichia coli. Mol Gen Genet. 245:406–416.

Isaacson T (2004) Analysis in Vitro of the Enzyme CRTISO Establishes a Poly-cis-Carotenoid Biosynthesis Pathway in Plants. Plant Physiol. 136:4246–4255.

Jayaraj J, Devlin R, Punja Z (2008) Metabolic engineering of novel ketocarotenoid production in carrot plants. Transgenic Res. 17:489–501.

Kim HW, Chew, BP, Wong, TS, Park, JS, Weng, BB, Byme KM, et al. (2000) Dietary lutein stimulates immune response in the canine. Vet Immunol Immunopathol. 74:315–327.

Kim J, Smith JJ, Tian L, DellaPenna D (2009) The evolution and function of carotenoid hydroxylases in Arabidopsis. Plant Cell Physiol. 50:463–479.

Kim SH, Ahn YO, Ahn MJ, Jeong JC, Lee HS, Kwak SS (2013) Cloning and characterization of an Orange gene that increases carotenoid accumulation and salt stress tolerance in transgenic sweetpotato cultures. Plant Physiol Biochem. 70:445–454.

Krinsky NI (1998) Overview of lycopene, carotenoids, and disease prevention. Proc Soc Exp Biol Med. 218:95–97.

Lefebvre V, Kuntz M, Camara B, Palloix A (1998) The capsanthin-capsorubin synthase gene: A candidate gene for the y locus controlling the red fruit colour in pepper. Plant Mol Biol. 36:785–789.

Li F, Murillo C, Wurtzel ET (2007) Maize Y9 encodes a product essential for 15-cis-zeta-carotene isomerization. Plant Physiol. 144:1181–1189.

Li L, Paolillo DJ, Parthasarathy MV, Dimuzio EM GD (2001) A novel gene mutation that confers abnormal patterns of betacarotene accumulation in cauliflower (Brassica oleracea var. botrytis). Plant J. 26:59–67.

Lindgren LO, Stålberg KG, Höglund A-S (2003) Seed-specific overexpression of an endogenous Arabidopsis phytoene synthase gene results in delayed germination and increased levels of carotenoids, chlorophyll, and abscisic acid. Plant Physiol. 132:779–785.

Lopez AB, Van Eck J, Conlin BJ, Paolillo DJ, O'Neill J LL (2008) Effect of the cauliflower Or transgene on carotenoid accumulation and chromoplast formation in transgenic potato tubers. J Exp Bot. 59:213–223.

Lu S, Van Eck J, Zhou X, Lopez AB, O'Halloran DM, et al. (2006) The cauliflower Or gene encodes a DnaJ cysteine-rich domain-containing protein that mediates high levels of beta-carotene accumulation. Plant Cell. 18:3594–3605.

Matthews PD, Luo R, Wurtzel ET (2003) Maize phytoene desaturase and ζ-carotene desaturase catalyse a poly-Z desaturation pathway: Implications for genetic engineering of carotenoid content among cereal crops. J Exp Bot. 54:2215–2230.

Minguez-Mosquera MI, Hornero-Mendez D (1994) Comparative Study of the Effect of Paprika Processing on the Carotenoids in Peppers (Capsicum annuum) of the Bola and Agridulce Varieties. J Agric Food Chem. 42:1555–1560.

Misawa N, Nakagawa M, Kobayashi K, Yamano S, Izawa Y, Nakamura K, et al. (1990) Elucidation of the Erwinia uredovora carotenoid biosynthetic pathway by functional analysis of gene products expressed in Escherichia coli. J Bacteriol. 172:6704–6712.

Misawa N, Satomi Y, Kondo K, Yokoyama A, Kajiwara S, Saito T, et al. (1995) Structure and functional analysis of a marine bacterial carotenoid biosynthesis gene cluster and astaxanthin biosynthetic pathway proposed at the gene level. J Bacteriol. 177:6575–6584.

Misawa N, Truesdale MR, Sandmann G, Fraser PD, Bird C, Schuch W, et al. (1994) Expression of a tomato cDNA coding for phytoene synthase in Escherichia coli, phytoene formation in vivo and in vitro, and functional analysis of the various truncated gene products. J Biochem. 116:980–985.

Misawa N, Yamano S, Ikenaga H (1991) Production of β-carotene in Zymomonas mobilis and Agrobacterium tumefaciens by introduction of the biosynthesis genes from Erwinia uredovora. Appl Environ Microbiol. 57:1847–1849.

Moran N, Jarvik T (2010) Lateral transfer of genes from fungi underlies carotenoid production in aphids. Science. 328:624–627.

Naqvi S, Zhu C, Farre G, Ramessar K, Bassie L, Breitenbach J, et al. (2009) Transgenic multivitamin corn through biofortification of endosperm with three vitamins representing three distinct metabolic pathways. Proc Natl Acad Sci U S A. 106:7762–7767.

Paine J, Shipton C, Chaggar S, Howells RM, Kennedy MJ, Vernon G, et al. (2005) Improving the nutritional value of Golden Rice through increased pro-vitamin A content. Nat Biotechnol. 23:482–487.

Paolillo DJ, Garvin DF, Parthasarathy MV (2004) The chromoplasts of Or mutants of cauliflower (Brassica oleracea L. var. botrytis). Protoplasma. 224:245–253.

Peremarti A, Twyman RM, Gómez-Galera S, Naqvi S, Farré G, Sabalza M, et al. (2010) Promoter diversity in multigene transformation. Plant Mol Biol. 73:363–378.

Quackenbush, FW, Firch, JG, Brunson, AM, House L (1963) Carotenoid, oil, and tocopherol content of corn inbreds. Cereal Chem. 40:250–253.

Quinlan RF, Jaradat TT, Wurtzel ET (2007) Escherichia coli as a platform for functional expression of plant P450 carotene hydroxylases. Arch Biochem Biophys. 458:146–157.

Rice-Evans CA, Sampson J, Bramley PM, Holloway DE (1997) Why do we expect carotenoids to be antioxidants in vivo? Free Radic Res. 26:381–398.

Rivera-Madrid R, Escobedo-GM RM, Balam-Galera E, Vera-Ku M, Harries H. (2006) Preliminary studies toward genetic improvement of annatto (Bixa orellana L.). Sci Hortic. 109:165–172.

Rodríguez-Concepción M (2006) Early steps in isoprenoid biosynthesis: Multilevel regulation of the supply of common precursors in plant cells. Phytochem Rev. 5:1–15.

Rodríguez-Concepción M (2010) Supply of precursors for carotenoid biosynthesis in plants. Arch. Biochem. Biophys. 504:118–122.

Sandmann G (2001) Genetic manipulation of carotenoid biosynthesis: strategies, problems and achievements. Trends Plant Sci. 6:14–17.

Schmidt M, Parrott W, Hildebrand DF, Berg RH, Cooksey A, Pendarvis K, et al. (2015) Transgenic soya bean seeds accumulating β-carotene exhibit the collateral enhancements of oleate and protein content traits. Plant Biotechnol J. 13:590–600.

Seo M, Koshiba T (2002) Complex regulation of ABA biosynthesis in plants. Trends Plant Sci. 7:41–48.

Singh M, Lewis PE, Hardeman K, Bai L, Rose JKC, Mazourek M, et al. (2003) Activator mutagenesis of the pink scutellum1/viviparous7 locus of maize. Plant Cell. 15:874–884.

Sommer A (2008) Vitamin a deficiency and clinical disease: an historical overview. J Nutr. 138:1835–1839.

Sommerburg O, Keunen J, Bird A, van Kuijk FJ (1998) Fruits and vegetables that are sources for lutein and zeaxanthin: the macular pigment in human eyes. Br J Ophthalmol. 82:907-910.

Stein AJ, Sachdev HPS, Qaim M (2006) Potential impact and cost-effectiveness of Golden Rice. Nat Biotechnol. 24:1200–1201.

Stigliani AL, Giorio G, D'Ambrosio C (2011) Characterization of P450 Carotenoid beta- and epsilon-hydroxylases of tomato and transcriptional regulation of xanthophyll biosynthesis in root, leaf, petal and fruit. Plant Cell Physiol. 52:851–865.

US Institute of Medicine (2001) Dietary Reference Intakes for Vitamin A, Vitamin K, Arsenic, Boron, Chromium, Copper, Iodine, Iron, Manganese, Molybdenum, Nickel, Silicon, Vanadium, and Zinc.

Van Eck J, Conlin B, Garvin DF, Mason H, Navarre D, Brown CR (2007) Enhancing beta-carotene content in potato by rnai-mediated silencing of the beta-carotene hydroxylase gene. Am J Potato Res. 84:331–342.

Yu B, Lydiate DJ, Young LW, Schäfer UA, Hannoufa A (2008) Enhancing the carotenoid content of Brassica napus seeds by downregulating lycopene epsilon cyclase. Transgenic Res. 17:573–585.

Zhu C, Bai C, Sanahuja G, Yuan D, Farré G, Naqvi S, et al. (2010) The regulation of carotenoid pigmentation in flowers. Arch. Biochem. Biophys. 132–141.

Zhu C, Naqvi S, Breitenbach J, Sandmann G, Christou P, Capell T (2008) Combinatorial genetic transformation generates a library of metabolic phenotypes for the carotenoid pathway in maize. Proc Natl Acad Sci U S A. 105:18232–18237.

Zhu C, Naqvi S, Capell T, Christou P (2009) Metabolic engineering of ketocarotenoid biosynthesis in higher plants. Arch Biochem Biophys. 483:182–190.

AIMS AND OBJECTIVES

AIMS AND OBJECTIVES

The overarching aim of my dissertation has been to develop a mechanistic understanding of carotenoid accumulation, especially β-carotene, in maize endosperm by using different approaches and to evaluate the impact of high carotenoid transgenic lines on starch metabolism. A further aim was to generate transgenic maize hybrids with high carotenoid content and investigate their agronomic properties.

My specific objectives were to:

1. Analyze the effects of *Zmcyp97C* on carotenoid metabolism in an Arabidopsis mutant lacking lutein.

2. Generate different transgenic M37W maize lines with downregulated β-hydroxylase genes and evaluate the impact of this downregulation in different genetic backgrounds generated through crossing with inbred lines and transgenic lines with specific lutein and zeaxanthin content.

3. Unravel the mechanism(s) of carotenoid accumulation in maize as a result of creating a carotenoid sink in endosperm.

4. Investigate the interaction between the carotenoid and starch biosynthetic pathways as they share common precursors.

5. Investigate the agronomic performance of transgenic maize hybrids by crossing a high carotenoid accumulating transgenic line with different inbred lines belonging to well-known heterotic groups.

CHAPTER 1

Cloning and functional characterization of maize (*Zea mays* L.) carotenoid epsilon hydroxylase

CHAPTER 1: CLONING AND FUNCTIONAL CHARACTERIZATION OF MAIZE (*Zea mays* L.) CAROTENOID EPSILON HYDROXYLASE

1.1 Abstract

The assignment of functions to genes in the carotenoid biosynthesis pathway is necessary to understand how the pathway is regulated and to obtain the basic information required for metabolic engineering. Few carotenoid ε-hydroxylases have been functionally characterized in plants although this would provide insight into the hydroxylation steps in the pathway. I therefore isolated mRNA from the endosperm of maize (*Zea mays* L., inbred line B73) and cloned a full-length cDNA encoding CYP97C19, a putative heme-containing carotenoid ε hydroxylase and member of the cytochrome P450 family. The corresponding *cyp97C19* genomic locus on chromosome 1 was found to comprise a single-copy gene with nine introns. We expressed *cyp97C19* cDNA under the control of the constitutive CaMV 35S promoter in the *Arabidopsis thaliana lut1* knockout mutant, which lacks a functional *cyp97C (lut1*) gene. The analysis of carotenoid levels and composition showed that lutein accumulated to high levels in the rosette leaves of the transgenic lines but not in the untransformed *lut1* mutants. These results allowed the unambiguous functional annotation of maize CYP97C19 as an enzyme with strong zeinoxanthin ε-ring hydroxylation activity.

1.2 Introduction

Gene functional characterization is important to elucidate the regulatory mechanism of a biosynthetic pathway and to acquire fundamental information for pathway engineering. Non-heme di-iron carotenoid β-hydroxylases (BCH) and heme-containing cytochrome P450 hydroxylases, (CYP)-type hydroxylases are primarily responsible for β- hydroxylation of β,β-carotenoids and α-hydroxylation of ε,β-carotenoids, respectively, but exhibit some overlapping activities, most notably in hydroxylation of the β-ring of α-carotene (Kim et al. 2009). To date, multiple BCH-type hydroxylases from plants and bacteria have been cloned and functionally characterized (Farré et al. 2010; Li et al. 2010; Zhu et al. 2009) but only a few carotenoid ε-hydroxylases, which are indispensable for e.g. lutein synthesis, have been functionally characterized in plants (**Figure 1.1)**.

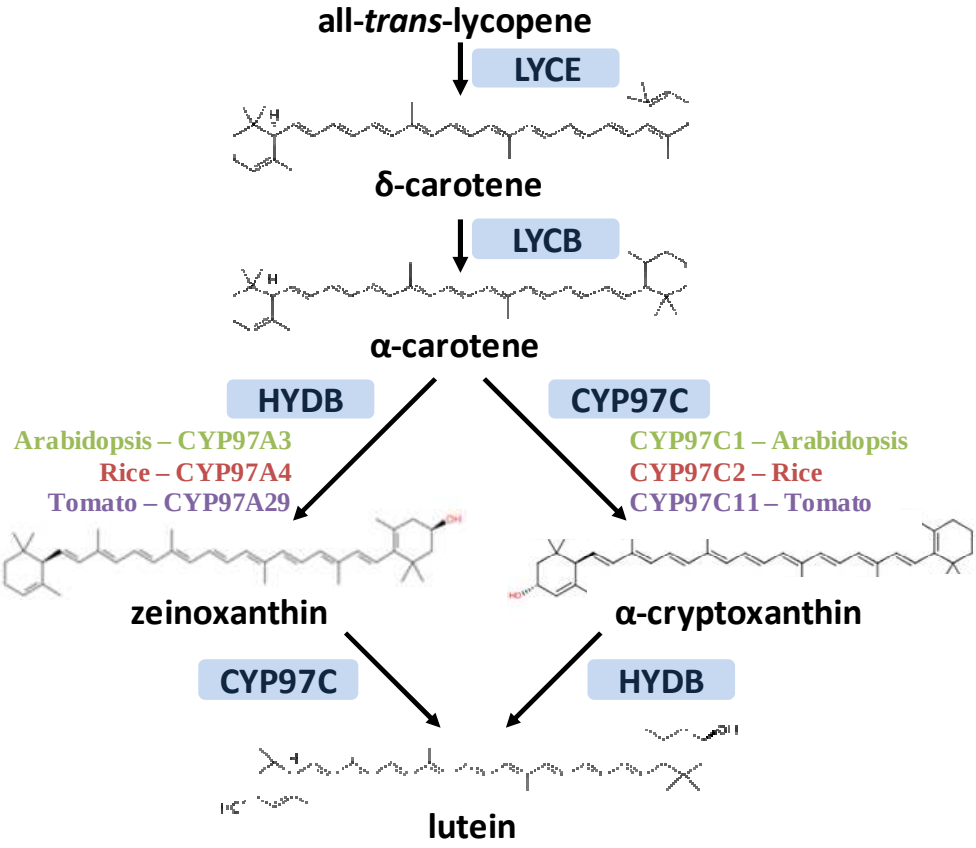

Figure 1.1 – Biosynthesis pathway from lycopene to lutein and the characterized CYP-type hydroxylases for lutein synthesis. Abbreviations: LYCB, lycopene β-cyclase; LYCE, lycopene ε-cyclase; CYP97C, carotene ε-ring hydroxylase; HYDB, β-carotene hydroxylase (Adapted from Kim et al. 2009).

In *Arabidopsis thaliana*, two genes encode BCH (BCH1 and BCH2) and two genes code for CYP-type (carotenoid β-hydroxylase CYP97A3 and carotenoid ε-hydroxylase CYP97C1) (Kim and DellaPenna 2006; Kim et al. 2009; Sun et al. 1996; Tian and Dellapenna 2001). These genes were successfully characterized by the identification of *lut1* and *lut5* locus mutants (lacking lutein). CYP97C1 catalyzes hydroxylation of the ε-ring of α-carotene to produce α-cryptoxanthin or ε-ring of zeinoxanthin to yield lutein, whereas CYP97A3 is responsible mainly for the hydroxylation of the β-ring of α-carotene to produce zeinoxanthin or β-ring of α-cryptoxanthin to yield lutein (Kim and DellaPenna 2006; Tian et al. 2003) (**Figure 1.1**).

Rice *CYP97C2* and *CYP97A4*, the orthologs of *A. thaliana CYP97C1* and *CYP97A3*, have been isolated and characterized through *in vitro* functional complementation in *E. coli* (Quinlan et al. 2007). Rice CYP97A4 is highly active towards the β-ring of both α-carotene and β-carotene, but it is inactive towards the ε-ring of α-carotene. Conversely, rice CYP97C2 shows high activity towards the ε-ring and a moderate activity toward the β-ring of α-

carotene, but a very low activity toward the β-rings of β-carotene in an *E. coli* functional complementation system (Quinlan et al. 2007). Rice carotenoid β-ring hydroxylase CYP97A4 was demonstrated to play an important role in α-carotene hydroxylation through the analysis of rice *CYP97A4* mutants (Lv et al. 2012) (**Figure 1.1**).

Tomato *CYP97C11* and *CYP97A29* genes were isolated and characterized by *in planta* analysis using transgenic tomato plants (Stigliani et al. 2011). The constitutive overexpression of the tomato carotenoid ε-hydroxylase *cyp97C11* in transgenic tobacco significantly increased the amount of lutein in the leaves and was found to have an important function in alleviating chilling stress-induced photoinhibition and photooxidation (Zhou et al. 2013) (**Figure 1.1**). In addition to CYP97 P450 type carotenoid hydroxylases in higher plants, cytochrome P450 type β-carotene hydroxylases CYP175 are exclusively present in the thermostable bacterium *Thermus thermophilus* HB27 and *Asy* the yeast *Xanthophyllomyces dendrorhous* shows β-carotene hydroxylase activity in the conversion of β-carotene to zeaxanthin (Blasco et al. 2004; Ojima et al. 2006). Recently the cytochrome P450-type *PuCHY1* belonging to the CYP97B subfamily from red algae *Porphyra umbilicalis* was found to encode functional β-carotene hydroxylase (Yang et al. 2014).

To date, only carotenoid ε-hydroxylases from *A. thaliana*, rice and tomato have been functionally characterized (Kim et al. 2009; Lv et al. 2012; Quinlan et al. 2007; Stigliani et al. 2011; Tian et al. 2003) (**Figure 1.1**) by using different strategies described in the general introduction. In maize, the P450-type carotenoid hydroxylase *cyp97C19* gene represents the ortholog of *A. thaliana CYP97C1*. However, the gene has not been functionally characterized. Here I describe the isolation of the maize *cyp97C19* gene and the elucidation of its genomic structure, followed by a functional characterization in transgenic *Arabidopsis thaliana* mutant *lut1* (lacking CYP97C).

1.3 Materials and methods

1.3.1. Plant materials

Maize plants (*Zea mays* L. cv B73) were grown in the greenhouse and growth chamber at 28/20°C day/night temperature with a 10 h photoperiod and 60–90% relative humidity for the first 50 days, followed by maintenance at 21/18°C day/night temperature with a 16-h

photoperiod thereafter. Plants were self-pollinated to obtain seeds. Mature leaf and endosperm tissues were frozen rapidly in liquid nitrogen and stored at –80°C.

Control *A. thaliana* plants (wild-type Col-0 or *lut1* mutant; Tian et al. 2004) and transgenic plants derived from these, were grown in a growth chamber or greenhouse with a 16h photoperiod at 23°C. Harvested dry *A. thaliana* seeds were stored for 2 weeks at 4°C before planting in soil or on agar.

1.3.2 Nucleic acid isolation and cDNA synthesis

Genomic DNA was extracted from leaf tissue as described by Edwards et al. (1991). Total RNA was isolated using the RNeasy Plant Mini Kit (Qiagen, Valencia, CA, USA) and DNA was removed with DNase I (RNase-free DNase Set, Qiagen). Total RNA was quantified using a Nanodrop 1000 spectrophotometer (Thermo Scientific, Vernon Hills, Illinois, USA), and 2 µg total RNA was used as template for first strand cDNA synthesis with Ominiscript reverse transcriptase (Qiagen) in a 20 µl total reaction volume, following the manufacturer's recommendations.

1.3.3 Cloning and sequencing of the putative maize CYP97C cDNA

The rice *cyp97C2* cDNA (GenBank: AK065689) was used as a query to search the maize expressed sequence tag (EST) database, and matches were used to design primers for full-length cDNA cloning. EST sequences (GenBank: CF244398 and CF245241) from inbred line B73 were found with high sequence identity to the ends of the rice *cyp97C2* cDNA. The full-length cDNA was amplified using 1 µl cDNA prepared as above from the endosperm of maize inbred line B73, 25 days after pollination (DAP), primers forward 5′-CAC ACG GCG ATG CCT GCC ACG GTC TTC-3′ and reverse 5′-TCT ATT TCG ATT CGC TCA GCG CTA ACT C-3′, and the GoTaq DNA Polymerase Kit (Promega, Madison, WI, USA) in a 50 µl reaction volume. The samples were heated to 95°C for 3 min, followed by 30 cycles at 94°C for 45 s, 60°C for 45 s and 72°C for 2 min. After the last amplification cycle, the samples were incubated at 72°C for 10 min. The products were purified from a 0.8% w/v agarose gel using the Geneclean II Kit (BIO 101 Systems, Solon, OH, USA) and cloned into the PCR II TOPO vector (TA Cloning Kit, Invitrogen, Carlsbad, CA, USA) for sequencing using the Big Dye Terminator v3.1 Cycle Sequencing Kit on a 3130x1 Genetic Analyzer (Applied Biosystems, Foster City, CA, USA).

1.3.4 Bioinformatic analysis

The Maize Genetics and Genomic Database (http://www.maizegdb.org/), the GRAMENE database (http://www.gramene.org/) and GenBank (http://blast.ncbi.nlm.nih.gov/Blast.cgi) were searched for homologous sequences using BLAST, and multiple sequences were aligned using ClustalW2 (http://www.ebi.ac.uk/Tools/msa/clustalw2/). Protein sequences were screened for chloroplast signal peptides using the ChloroP 1.1 server at http://www.cbs.dtu.dk/services/ChloroP/ (Emanuelsson et al. 1999). Gene structures were predicted by aligning mRNA to genomic DNA using Spidey (http://www.ncbi.nlm.nih.gov/spidey/).

1.3.5 Construction of maize CYP97C gene expression vector for *A. thaliana* transformation

Gene-specific primers, with a *Nco*I restriction site (underlined) in the forward primer 5′-CCA TGG ATT AGA TGC CTG CCA CGG TCT TCG CCT CC-3′ and a *Bst*EII restriction site in the reverse primer 5′ GGT CAC CTA TTT CGA TTC GCT CAG CGC TAA CT-3′ were used to amplify the full-length maize *CYP97C19* coding sequence, which was then inserted into binary vector pCAMBIA1302, linearized with the same enzymes to yield pCAMBIA-ZmCYP97C19.

1.3.6 Transformation and selection of *A. thaliana*

The pCAMBIA-ZmCYP97C19 plasmids were introduced into *Agrobacterium tumefaciens* strain GV3101 by electroporation (Mattanovich et al. 1989) and the recombinant bacteria were grown at 28°C overnight before the *A. thaliana lut1* mutant was transformed using the floral dip method (Clough and Bent 1998). *A. thaliana* seeds were wetted with 75% ethanol for 1 min, washed once with sterile water, surface sterilized with a 50% bleach containing 0.05% Tween-20 for 10 min, and rinsed with sterile water five times. *A. thaliana* T1 seeds obtained after floral dip transformation were selected on 0.7% agar plates containing half-strength Murashige and Skoog (MS) medium (Murashige and Skoog 1962) containing 1% sucrose, supplemented with 50 mg/l hygromycin B (Roche, Mannheim, Germany) for 10 days in a growth chamber, before transfer to standard horticultural soil in the greenhouse. *A. thaliana* transformation was performed in School of Life Sciences, Changchun Normal University, Changchun, China. T2 seeds were harvested and germinated seedlings were selected on half-strength MS medium containing 1% sucrose, 0.7% agar and 50 mg/l

hygromycin B for 7 days in a growth chamber. Five hygromycin-resistant plants were transferred to individual glass pots (7 cm diameter x 11 cm) filled with MS medium containing 2% sucrose and 0.7% agar for 2 weeks in the growth chamber. *A. thaliana* (Col-0 and *lut1* mutant) plants were cultured on the same MS medium without hygromycin B as controls. For each line and control, the rosette leaves from at least 50 plants were pooled in three biological replicates for HPLC analysis, DNA and RNA extraction.

1.3.7 DNA and RNA analyses

Leaf genomic DNA (10 µg for *A. thaliana*) was digested with appropriate restriction enzymes and fractionated by 0.8% (w/v) agarose gel electrophoresis before blotting onto a positively-charged nylon membrane (Roche) according to the manufacturer's instructions. Nucleic acids were fixed by UV crosslinking. The transferred DNA fragments were hybridized with appropriate digoxigenin-labeled probes at 42°C overnight using DIG Easy Hyb buffer (Roche). The membrane was washed twice for 10 min in 2x SSC, 0.1% SDS at room temperature, twice for 30 min in 0.5x SSC, 0.1% SDS at 68°C, once for 20 min in 0.2x SSC, 0.1% SDS at 68ºC and then once for 10 min in 0.1x SSC, 0.1% SDS at 68°C. After immunological detection with anti-DIG-AP (Roche) chemiluminescence generated by disodium 3-(4-methoxyspiro(1,2-dioxetane-3,2′-(5′-chloro)tricyclo[3.3.1.1^{3,7}]decan)-4-yl)phenyl phosphate (CSPD) (Roche) was detected on Kodak BioMax light film (Sigma-Aldrich, St. Louis, USA) according to the manufacturer's instructions. The 1228-bp maize *CYP97C19* probe for DNA blot analysis was prepared by PCR under the conditions described above using primers forward 5′-GTC TCC GAG TTC CTC TTC GGC TCC GGC T-3′ and reverse 5′-CTA TTT CGA TTC GCT CAG CGC TAA CTC A-3′.

Total RNA (20 µg) extracted from *A. thaliana* leaves was fractionated on a denaturing 1.2% (w/v) agarose gel containing formaldehyde prior to blotting. The membrane was probed with digoxigenin-labeled partial cDNAs prepared as above using the PCR-DIG Probe Synthesis Kit (Roche), with hybridization carried out at 50°C overnight using DIG Easy Hyb buffer and the same probe as described above. Washing, immunological detection and CSPD chemiluminescence were also carried out as described above.

1.3.8 Carotenoid extraction and quantification

Carotenoids were extracted from *A. thaliana* freeze-dried leaves by heating in methanol containing 6% KOH for 20 min at 60°C. The extract was partitioned into 10% ether in petroleum ether (bp 40-60°C), the upper phase was collected and the solvent evaporated. After re-dissolving in acetone, the carotenoids were analyzed by HPLC on a 15 cm Nucleosil C18 column at 20°C with a mobile phase of acetonitrile/methanol /2-propanol (85:10:5). Absorbance at 450 nm and individual peaks were recorded with a Kontron DAD 440 photodiode array detector. Individual carotenoids were identified by comparing with authentic standards, their retention times, and absorbance spectra. Carotenoid extraction and quantification was performed in Biosynthesis Group, Molecular Biosciences, Goethe University Frankfurt, Frankfurt, Germany.

1.4 Results

1.4.1 Cloning and characterization of the maize cyp97C19 gene

The maize *cyp97C19* cDNA encoding a full-length putative carotenoid ε-hydroxylase was amplified from the 25-DAP endosperm mRNA of maize inbred line B73 by RT-PCR (GenBank: GU130217). The full-length *Zmcyp97C19* cDNA encoded a 556-residue protein with a predicted molecular weight of 61.9 kDa. The chloroplast transit peptide prediction software ChloroP v1.1 indicated the presence of a putative 53-residue transit peptide. The *Zm*CYP97C19 amino acid sequence showed 88.6% similarity and 82.6% identity to rice CYP97C2, 80.8% similarity and 69.9% identity to *A. thaliana* CYP97C1, and 78.4% similarity and 68.7% identity to tomato CYP97C11 (**Figure 1.2**).

The *Zmcyp97C19* cDNA sequence was used to screen MaizeGDB maize genomic resources to identify the corresponding gene. A single genomic sequence from chromosome 1 of the maize B73 genome matched the *Zmcyp97C19* cDNA sequence with 100% identity, suggesting that *Zmcyp97C19* is a single-copy gene (GenBank: AC177851). The *Zmcyp97C19* gene was found to have nine introns and ten exons (**Figure 1.3**) which is the same structure as the homologous rice gene *cyp97C2* (Quinlan et al. 2007). In contrast, the homologous genes in *A. thaliana* (*CYP97C1*) and tomato (*cyp97C11*) have eight introns and nine exons (Tian et al. 2004; Stigliani et al. 2011).

Figure 1.2 – Multiple alignments of CYP97C protein sequences from maize (Zm, *Zea mays*; GenBank: GU130217), rice (Os, *Oryza sativa*; GenBank: AK065689), Arabidopsis (At, *Arabidopsis thaliana*; GenBank: NM_115173) and tomato (Sl, *Solanum lycopersicon*; GenBank: EU849604).

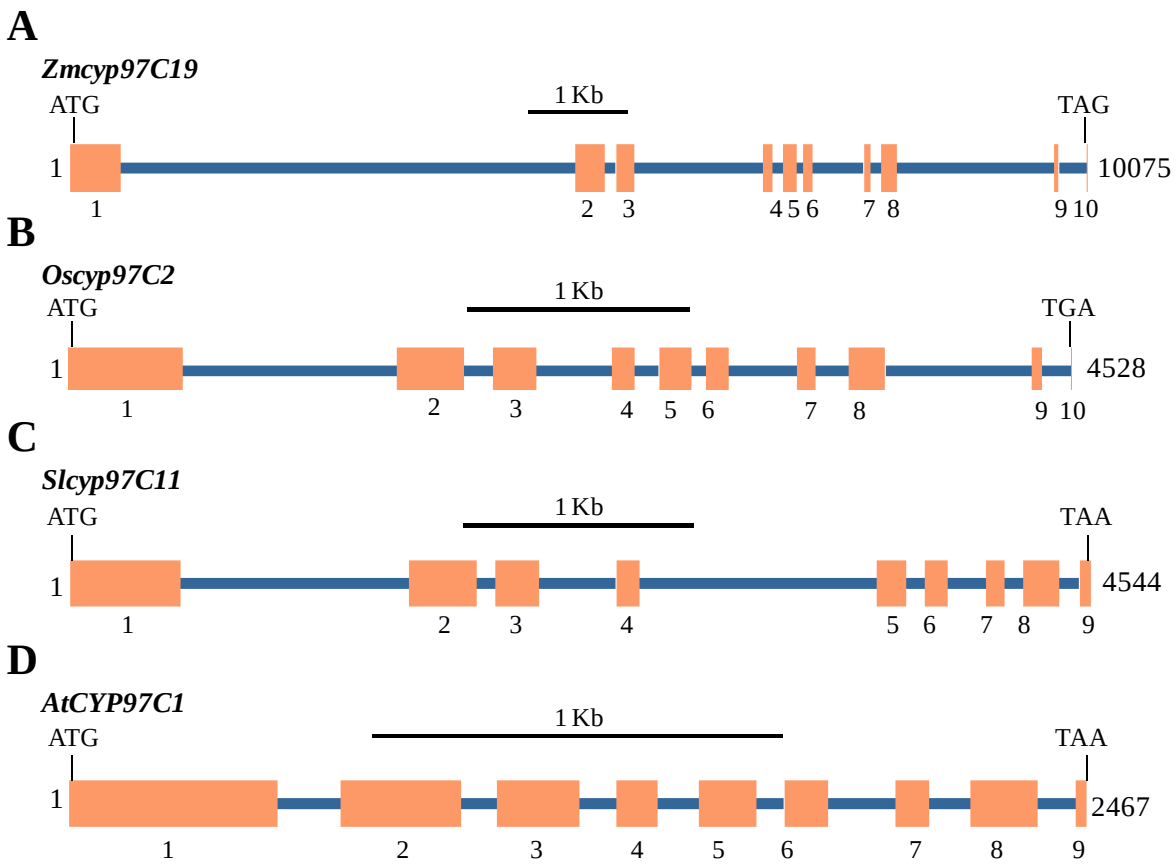

Figure 1.3 – Gene structures for maize, rice, tomato and A. thaliana CYP97C homologs. Orange boxes represent exons. Blue lines represent introns. The lengths of DNA sequences are indicated on the above. *Zm*, *Zea mays* cDNA; GenBank: GU130217), rice (*Os*, *Oryza sativa* cDNA; GenBank: AK065689), Arabidopsis (*At*, *Arabidopsis thaliana* cDNA; GenBank: NM_115173), tomato (*Sl*, *Solanum lycopersicon* cDNA and genomic DNA; GenBank: EU849604 and EU849603).

1.4.2 Screening and selection of transgenic A. thaliana plants

A. thaliana lut1 mutant plants were transformed with the maize *CYP97C19* gene controlled by the constitutive CaMV 35S promoter, and self-pollination gave rise to T1 seeds that yielded hygromycin-resistant T1 plants. These plants were analyzed by genomic PCR to confirm the integrity of the *ZmCYP97C19* transgene using primers that annealed to the CaMV 35S promoter and *ZmCYP97C19* sequences. The complete *ZmCYP97C19* transgene was present in 15 T1 lines and leaves from these lines were used to determine carotenoid profiles by HPLC analysis. Three lines that accumulated the highest levels of lutein in the leaves were used for in depth analysis. T2 seedlings from these three self-pollinated T1 lines were selected on hygromycin, and rosette leaves were taken from these transgenic T2 plants as well as *lut1* mutant and wild-type controls. The leaves were used for HPLC analysis to determine the carotenoid profiles and DNA and RNA extraction for molecular characterization.

1.4.3 Analysis of transgene integration

The three transgenic T2 lines were compared by DNA blot analysis with wild-type and *lut1* mutant controls. The DNA was digested with *Eco*RI and *Xba*I and the blots were probed under high stringency conditions with a 1228-bp *ZmCYP97C19* DNA sequence lacking *Eco*RI and *Xba*I restriction sites.

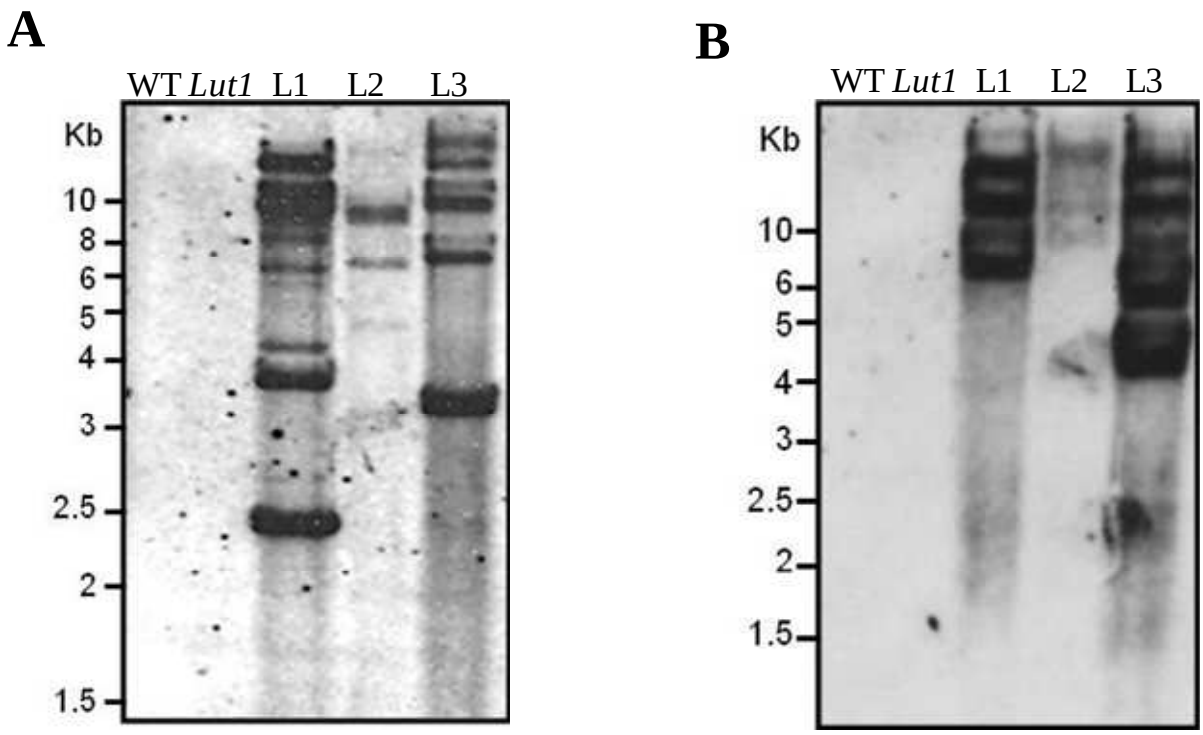

Figure 1.4 – DNA blot analysis of *Zmcyp97C19* transgene in *A. thaliana* wild type, *lut1* mutant and three different transgenic lines transformed with *Zmcyp97C19* driven by the CaMV 35S promoter. Genomic DNA (10 µg) from rosette leaves was separately digested with *Eco*RI (A) and *Xba*I (B). The DNA blot was hybridized with a *Zmcyp97C19* gene probe. WT, wild-type (Col-0); Lut1, *lut1* mutant; L1, line 1; L2, line 2; L3, line 3.

The results showed that the three transgenic lines had different hybridization band patterns indicating they were independent transformants, whereas the wild-type and *lut1* mutant controls did not show any hybridizing bands as expected (**Figure 1.4**). Multiple bands were visible on the DNA blots representing lines 1 and 3 regardless of which enzyme was used, indicating multiple copies of the transgene were present in the genome, whereas line 2 presented three bands with each of the enzymes, suggesting the presence of three transgene integration sites (**Figure 1.4**).

1.4.4 Analysis of transgene expression

Transgene expression was analyzed by mRNA blot, revealing that *Zmcyp97C19* mRNA was present in the rosette leaves of all three transgenic lines, whereas no mRNA was present in the controls (**Figure 1.5**). This confirmed that the transgene was intact and strongly expressed in all three transgenic lines.

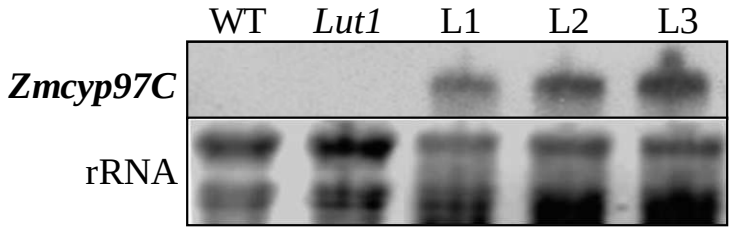

Figure 1.5 – RNA blot analysis of maize *cyp97C19* transgene expression in *A. thaliana* wild-type, *lut1* mutant and three different transgenic lines transformed with *Zmcyp97C19* driven by the CaMV 35S promoter. Each lane was loaded with 20 μg total RNA from rosette leaves. Ribosomal RNA stained with ethidium bromide is shown as a loading control. The blot was hybridized with a *Zmcyp97C19* probe. WT, wild type (Col-0); *Lut1*, *lut1* mutant; L1, line 1; L2, line 2; L3, line 3.

1.4.5 Analysis of carotenoid profiles

The carotenoid composition of rosette leaves from the transgenic lines, wild-type plants and *lut1* mutants was determined by HPLC, and the results are summarized in **Table 1.1**. Lutein and β-carotene were the predominant carotenoids in wild-type leaves, whereas zeinoxanthin and β-carotene were the major carotenoids in the leaves of *lut1* mutant plants, but lutein was only present in trace amounts (**Figure 1.6**). In contrast, the expression of *Zmcyp97C19* in the *lut1* mutant background caused a significant increase in the lutein content (to 26.5%, 32.2% and 49.6% of total carotenoids in transgenic lines 1, 2 and 3, respectively). The lutein appeared to be derived from zeinoxanthin, because the abundance of this carotenoid was reduced from 36.5% in the *lut1* mutant to 15.5%, 14.7% and 7.3% in transgenic lines 1, 2 and 3, respectively (**Figure 1.6** and **Table 1**). *Zmcyp97C19* therefore appears to encode a functional carotenoid ε-hydroxylase, which catalyzes the conversion of zeinoxanthin to lutein by adding a hydroxyl group at the 3′ position of the ε-ring (**Figure 1.1**). The transgenic lines also accumulated higher levels of violaxanthin than the *lut1* mutant, this being the major β,β-xanthophyll, but lower levels of β-carotene, zeaxanthin and antheraxanthin (**Table 1.1**).

Table 1.1 – Abundance of individual carotenoids in *Arabidopsis thaliana* leaves (%) and the total carotenoid content (µg/g dry weight).

	Nx	Viox	Anx	Lut	Zeax	HOaC	aCar	bCar	Total Car
WT	1.1±0.4	5.7±2.6	1.6±1.0	54.9±5.4	tr	nd	tr	35.8±8.3	1271.3±385.5
lut1	1.1±0.3	7.5±0.8	10.1±1.1	tr	3.8±0.3	36.5±2.8	tr	41.0±3.1	719.3±208.9
Line 1	1.6±0.8	17.2±4.6	6.1±1.4	26.5±8.3	tr	15.7±5.3	tr	29.1±2.5	1251.7±116.2
Line 2	1.2±0.3	20.0±4.2	4.8±0.9	32.2±4.3	2.6±2.0	14.1±0.8	tr	25.2±2.3	923.7±96.5
Line 3	1.3±0.5	13.4±1.1	4.0±0.4	49.6±2.6	tr	7.3±1.0	tr	22.6±2.3	913.0±202.7

Values are mean ± standard deviation of at least three replicates. Abbreviations: Nx, neoxanthin; Viox, violaxanthin; Anx, antheraxanthin; Lut, lutein; Zeax, zeaxanthin; HOaC, zeinoxanthin; aCar, α-carotene; bCar, β-carotene; Total Car, total carotenoids; nd, not detected; tr, trace, less than 0.1%; WT, wild type.

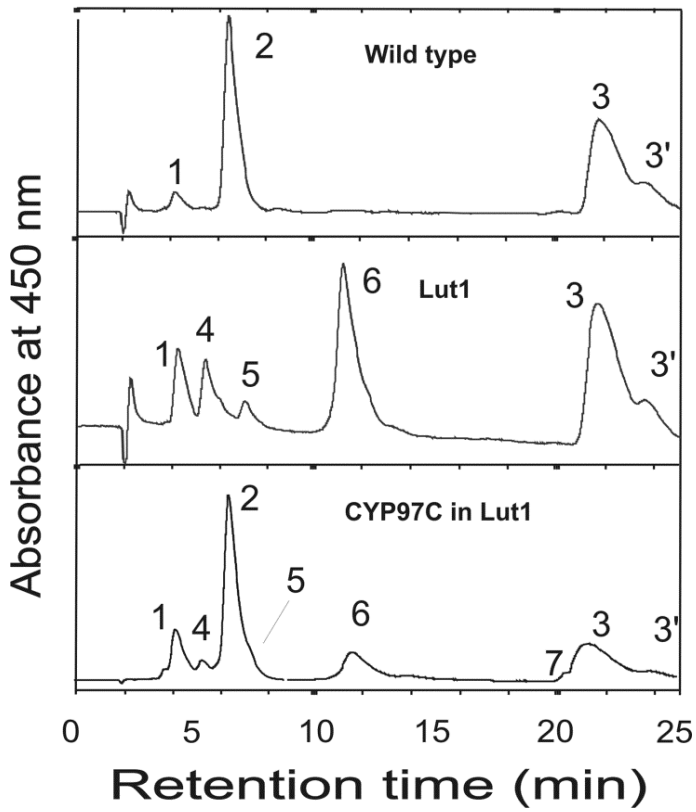

Figure 1. 6 – HPLC analysis of carotenoids in rosette leaves of *A. thaliana* wild-type, *lut1* mutant and transgenic lines transformed with *ZmCYP97C19* driven by the CaMV 35S promoter. Peak 1, violaxanthin; peak 2, lutein, peak 3, β-carotene; peak 3', β-carotene *cis* isomer; peak 4, antheraxanthin; peak 5, zeaxanthin; peak 6, zeinoxanthin; peak 7, α-carotene. Wild type, Col-0; Lut1, *lut1* mutant; CYP97C19 in *Lut1*, transgenic lines.

1.5 Discussion

The catalytic activities of different carotenogenic enzymes determine the abundance and composition of carotenoids in maize endosperm. Phytoene synthase (PSY) is a major rate-limiting step in the carotenoid biosynthesis pathway. Multiple isozymes of PSY regulate carotenogenesis in a tissue-specific manner in maize and rice (Li et al. 2008; Welsch et al. 2008) and fluctuating levels of the enzymes exert quantitative effects on the carotenoid content, as demonstrated in transgenic canola (Shewmaker et al. 1999), tomato (Fraser et al. 2002) and maize (Zhu et al. 2008). Other enzymes are responsible for the carotenoid profile. For example, lycopene ε-cyclase (LYCE) plays a key role by competing with lycopene β-cyclase (LYCB) to regulate the formation of α-carotene and its derivatives in maize endosperm (Harjes et al. 2008).

Two classes of structurally-unrelated enzymes catalyze the hydroxylation of α- and β- ionone rings in higher plants. These are the CYP97-type heme-containing cytochrome P450 hydroxylases (Tian et al. 2004; Kim and DellaPenna, 2006) and the ferredoxin-dependent BCH-type non-heme di-iron hydroxylases (Sun et al. 1996, Tian and DellaPenna, 2001; Tian et al. 2003). These enzyme classes have overlapping substrate specificities but *in vivo* analysis has shown that BCH isozymes are predominantly responsible for the synthesis of β,β-xanthophylls, i.e. they have limited activity towards the ε-ring of α-carotene but significant activity towards the β-ring with exception of the maize *crtRB3* (also known as BCH1) that affects the accumulation of α-carotene (Zhou et al. 2012). In contrast, the CYP97 enzymes have evolved to function preferentially the synthesis of α-xanthophylls and show substantial divergence in their preferences for *in vivo* substrates. Maize BCH2 (also known as *hyd3* and *CrtRB1*) is developmentally regulated but preferentially expressed in the endosperm, where it governs the critical steps in the conversion of β-carotene to zeaxanthin via β-cryptoxanthin (Vallabhaneni et al. 2009; Li et al. 2010; Babu et al. 2012, Yan et al. 2010; Naqvi et al. 2011). Hypomorphic alleles therefore cause the accumulation of β-carotene (Vallabheneni et al. 2009; Yan et al. 2010).

Many BCH-type β-carotene hydroxylases from higher plants have been extensively characterized, allowing their use in rational metabolic engineering strategies (Farré et al. 2010; 2014; 2015). However, only the Arabidopsis, rice and tomato CYP P450 carotenoid ε-hydroxylases have received similar attention (Tian et al. 2004; Kim et al 2009; Quinlan et al. 2007; Stigliani et al. 2011). *A. thaliana* CYP97C1 shows high activity towards the α-carotene

ε-ring and moderate activity toward the β-ring, but minimal activity toward the β-rings of β-carotene (Tian et al. 2004; Kim et al. 2009). In contrast, rice CYP97C2 shows weak ε-ring hydroxylase activity and no β-ring hydroxylase activity in *E. coli* cells accumulating α-carotene (not an *in vivo* substrate) or β-carotene (Quinlan et al. 2007). Tomato CYP97C11 only shows activity towards the ε-ring of α-carotene (Stigliani et al. 2011). The preferred pathway for lutein synthesis in Arabidopsis, rice and tomato is through the sequential action of CYP97A and CYP97C (Kim et al. 2009; Stigliani et al. 2011; Quinlan et al. 2012). CYP97A converts α-carotene to zeinoxanthin, which is in turn hydroxylated by CYP97C to form lutein. In tomato, hydroxylation of the ε-ring of zeinoxanthin by CYP97C11 appears to be the most critical step in lutein synthesis because the activity of this enzyme cannot be replaced by CYP97A29 or by either of the tomato BCH-type carotenoid hydroxylases. The hydroxylation of α-carotene to lutein in tomato is therefore mediated by the β-hydroxylation of α-carotene to zeinoxanthin catalyzed by CYP97A29 followed by the ε-ring hydroxylation of zeinoxanthin to lutein by CYP97C11 (Stigliani et al. 2011). The first step can be partially complemented by CRTR-B1 (BCH1), CRTR-B2 (BCH2) or CYP97C11, but the ε-ring of zeinoxanthin can only be hydroxylated by CYP97C11 (Stigliani et al. 2011). The constitutive overexpression of the tomato carotenoid ε-hydroxylase CYP97C11 in transgenic tobacco significantly increased the amount of lutein in the leaves and alleviated the photo-inhibition and photo-oxidation caused by chilling stress (Zhou et al. 2013).

The cDNA encoding the putative carotenoid ε-hydroxylase CYP97C19 was isolated from maize endosperm and constitutively overexpressed in the *A. thaliana lut1* knockout mutant, which has the low-lutein *cyp97C1* mutant phenotype. This was confirmed by the analysis of carotenoid pigments in wild-type and *lut1* mutant plants, which showed carotenoid profiles consistent with previous results (Kim et al. 2009). The lutein levels in transgenic *A. thaliana* plants overexpressing *Zmcyp97C19* were much higher than in the untransformed *lut1* mutant although not as high as wild-type levels (**Table 1.1**). Furthermore, the high levels of zeinoxanthin in the *lut1* mutant were reduced in the transgenic lines, confirming that ZmCYP97C19 is an ε-hydroxylase that can use zeinoxanthin as a substrate. However, we did not detect α-cryptoxanthin, the α-carotene derivative hydroxylated at position 3 of the ε-ring, in either the *lut1* mutant or the transgenic lines, whereas trace amounts were present in wild-type leaves (**Table 1.1** and **Figure 1.6**). This suggests that α-carotene may not be a preferred substrate for *Zm*CYP97C19, or that any α-cryptoxanthin thus formed is efficiently converted to lutein by the endogenous β-ionone ring hydroxylase.

The carotenoid content and composition of maize endosperm varies substantially between varieties reflecting different patterns of carotenogenic gene expression (Harjes et al. 2008; Messias et al. 2014). The expression of *psy1*, *hyd3* (*bch2*) and *cyp97C* has recently been evaluated in 22 different maize landraces (Messias et al. 2014). High levels of *Zmcyp97C* expression levels or a low *hyd3/cyp97C* expression ratio correlated positively with high lutein levels, which is consistent with our finding that *Zm*CYP97C is needed to produce lutein. In contrast, high levels of *hyd3* expression or a high *hyd3/cyp97C* expression ratio correlated positively with high zeaxanthin levels (Messias et al. 2014). The *Zmcyp97C19* mRNA levels remained constant throughout endosperm development in the white maize inbred variety M37W (Farre et al. 2013).

The functional analysis of enzymes in crops is necessary for the development of targeted metabolic interventions. In this context, *Zm*CYP97C19 appears to be important because of its key role in lutein biosynthesis and therefore its potential application in cereals for lutein biofortification. Lutein is increasingly regarded as an essential nutrient because of its proposed role in maintaining vision and preventing age-related maculopathy (Farre et al. 2013). Lutein is also valuable in the food, feed and nutraceutical markets as an additive and health-promoting natural product (Giorio et al. 2013; Berman et al. 2014). A better understanding of the regulation of lutein synthesis in plants is therefore likely to be valuable for human and animal health and in the commercial development of carotenoid-based supplements.

1.6 Conclusions

A putative carotenoid ε-hydroxylase, named CYP97C19, was correctly amplified from B73 maize. An in depth bioinformatic analysis revealed that CYP97C19 sequence has high similarity and identity of those CYP97C previously functional characterized in rice, Arabidopsis and tomato and that it is single copy in maize. Overexpression of maize CYP97C19 in Arabidopsis *lut1* mutant (lacking of lutein) is a good system to functional characterize the gene. Up to 15 independent transgenic lines were regenerated and 3 of them were analyzed in detail. Nucleic acid blots confirmed multiple transgene integration sites and high transgene expression. Metabolic profile of the carotenoid pathway confirmed the presence of lutein in transgenic lines at expenses of zeinoxanthin which allows getting the conclusion that maize CYP97C19 is a functional ε-hydroxylase.

1.7 References

Babu R, Rojas NP, Gao S, Yan J, Pixley K (2012) Validation of the effects of molecular marker polymorphisms in LcyE and CrtRB1 on provitamin A concentrations for 26 tropical maize populations. Theor Appl Genet. 126:389-399.

Bai C, Twyman RM, Farre G, Sanahuja G, Christou P, Capell T, et al. (2011) A golden era—pro-vitamin A enhancement in diverse crops. In Vitro Cell Dev Biol—Plant. 47: 205-221.

Berman J, Zorrilla-López U, Farré G, Zhu C, Sandmann G, Twyman RM, et al. (2015) Nutritionally important carotenoids as consumer products. Phytochem Rev. 14:727-743.

Blasco F, Kauffmann I, Schmid RD (2004) CYP175A1 from *Thermus thermophilus* HB27, the first β-carotene hydroxylase of the P450 superfamily. Appl Microbiol Biotechnol. 64:671–674.

Clough SJ, Bent AF (1998) Floral dip: a simplified method for Agrobacterium-mediated transformation of Arabidopsis thaliana. Plant J. 16:735–743.

Da Silva Messias R, Galli V, Dos Anjos E Silva SD, Rombaldi CV (2014) Carotenoid biosynthetic and catabolic pathways: gene expression and carotenoid content in grains of maize landraces. Nutrients. 6:546-563.

Edwards K, Johnstone C, Thompson C (1991) A simple and rapid method for the preparation of plant genomic DNA for PCR analysis. Nucleic Acids Res. 19:1349.

Emanuelsson O, Nielsen H, von Heijne G (1999) ChloroP, a neural network-based method for predicting chloroplast transit peptides and their cleavage sites. Protein Sci. 8:978–984.

Farre G, Bai C, Twyman RM, Capell T Christou P, Zhu C (2011) Nutritious crops producing multiple carotenoids — a metabolic balancing act. Trends Plant Sci. 16:532-540.

Farre G, Blancquaert D, Capell T, Van Der Straeten D, Christou P, Zhu C (2014) Engineering complex metabolic pathways in plants. Ann Rev Plant Biol. 65:187-223.

Farre G, Capell T, Twyman RM, Christou P, Zhu C (2015) Knowledge-driven approaches for engineering complex metabolic pathways in plants. Curr Opin Biotechnol. 32: 54-60.

Farre G, Rivera SM, Alves R, Vilaprinyo E, Sorribas A, Canela R, et al. (2013) Targeted transcriptomics and metabolic profiling reveals temporal bottlenecks in the maize carotenoid pathway that can be addressed by multigene engineering. Plant J. 75:441-455.

Farré G, Sanahuja G, Naqvi S, Bai C, Capell T, Zhu C, et al. (2010) Travel advice on the road to carotenoids in plants. Plant Sci. 179:28–48.

Fraser PD, Bramley PM (2004) The biosynthesis and nutritional uses of carotenoids. Prog Lipid Res. 43:228-265.

Fraser PD, Romer S, Shipton CA, Mills PB, Kiano JW, Misawa N, et al. (2002) Evaluation of transgenic tomato plants expressing an additional phytoene synthase in a fruit-specific manner. Proc Natl Acad Sci USA. 99:1092-1097.

Giorio G, Yildirim Arzu, Stigliani AL, D'Ambrosio C (2013) Elevation of lutein content in tomato: A biochemical tug-of-war between lycopene cyclases. Metab Eng. 20:167-176.

Harjes CE, Rocheford TR, Bai L, Brutnell TP, Kandianis CB, Sowinski SG, et al. (2008) Natural genetic variation in lycopene epsilon cyclase tapped for maize biofortification. Science. 319:330-333.

Kim J, DellaPenna D (2006) Defining the primary route for lutein synthesis in plants: the role of Arabidopsis carotenoid beta-ring hydroxylase CYP97A3. Proc Natl Acad Sci U S A. 103:3474–3479.

Kim J, Smith JJ, Tian L, DellaPenna D (2009) The evolution and function of carotenoid hydroxylases in Arabidopsis. Plant Cell Physiol. 50:463–479.

Li F, Vallabhaneni R, Yu J, Rocheford T, Wurtzel ET (2008) The maize phytoene synthase gene family: overlapping roles for carotenogenesis in endosperm, photomorphogenesis, and thermal stress tolerance. Plant Physiol. 147:1334-1346.

Li Q, Farre G, Naqvi S, Breitenbach J, Sanahuja G, Bai C, et al. (2010) Cloning and functional characterization of the maize carotenoid isomerase and β-carotene hydroxylase genes and their regulation during endosperm maturation. Transgenic Res. 19:1053-1068.

Lv MZ, Chao DY, Shan JX, Zhu MZ, Shi M, Gao JP, et al. (2012) Rice carotenoid β-ring hydroxylase CYP97A4 is involved in lutein biosynthesis. Plant Cell Physiol. 53:987–1002.

Mattanovich D, Rüker F, Machado AC, Laimer M, Regner F, Steinkellner H, et al. (1989) Efficient transformation of Agrobacterium spp. by electroporation. Nucleic Acids Res. 17:6747

Murashige T, Skoog F (1962) A Revised Medium for Rapid Growth and Bio Assays with Tobacco Tissue Cultures. Physiol Plant. 15:473–497.

Naqvi S, Zhu C, Farre G, Sandmann G, Capell T, Christou P (2011) Synergistic metabolism in hybrid corn indicates bottlenecks in the carotenoid pathway and leads to the accumulation of extraordinary levels of the nutritionally important carotenoid zeaxanthin. Plant Biotechnol J. 9:384-393.

Ojima K, Breitenbach J, Visser H, Setoguchi Y, Tabata K, Hoshino T, et al. (2006) Cloning of the astaxanthin synthase gene from *Xanthophyllomyces dendrorhous* (*Phaffia rhodozyma*) and its assignment as a β-carotene 3-hydroxylase/4-ketolase. Mol Genet Genomics. 275:148–158.

Quinlan RF, Jaradat TT, Wurtzel ET (2007) *Escherichia coli* as a platform for functional expression of plant P450 carotene hydroxylases. Arch Biochem Biophys. 458:146–157.

Quinlan RF, Shumskaya M, Bradbury LM, Beltrán J, Ma C, Kennelly EJ, et al. (2012) Synergistic interactions between carotene ring hydroxylases drive lutein formation in plant carotenoid biosynthesis. Plant Physiol. 160:204-214.

Shewmaker CK, Sheehy JA, Daley M, Colburn S, Ke DY (1999) Seed-specific overexpression of phytoene synthase: increase in carotenoids and other metabolic effects. Plant J. 20:401-412.

Stigliani AL, Giorio G, D´Ambrosio C (2011) Characterization of P450 carotenoid β- and ε-hydroxylases of tomato and transcriptional regulation of xanthophyll biosynthesis in root, leaf, petal and fruit. Plant Cell Physiol. 52:851-865.

Sun Z, Gantt E, Cunningham FX (1996) Cloning and functional analysis of the β-carotene hydroxylase of *Arabidopsis thaliana*. J Biol Chem 271:24349–24352.

Tian L, Dellapenna D (2001) Characterization of a second carotenoid β-hydroxylase gene from Arabidopsis and its relationship to the LUT1 locus. Plant Mol Biol. 47:379–388.

Tian L, Magallanes-Lundback M, Musetti V, DellaPenna D (2003) Functional analysis of β- and ε-ring carotenoid hydroxylases in Arabidopsis. Plant Cell. 15:1320-1332.

Tian L, Musetti V, Kim J, Magallanes-Lundback M, DellaPenna D (2004) The Arabidopsis LUT1 locus encodes a member of the cytochrome p450 family that is required for carotenoid ε-ring hydroxylation activity. Proc Natl Acad Sci U S A. 101:402–407.

Vallabhaneni R, Gallagher CE, Licciardello N, Cuttriss AJ, Quinlan RF, Wurtzel ET (2009) Metabolite sorting of a germplasm collection reveals the *hydroxylase3* locus as a new target for maize provitamin A biofortification. Plant Physiol. 151:1635-1645.

Welsch R, Wust F, Bar C, Al-Babili S, Beyer P (2008) A third phytoene synthase is devoted to abiotic stress-induced abscisic acid formation in rice and defines functional diversification of phytoene synthase genes. Plant Physiol. 147:367-380.

Wurtzel ET, Cuttriss A, Vallabhaneni R (2012) Maize provitamin A carotenoids, current resources, and future metabolic engineering challenges. Front Plant Sci. 3:29.

Yan J, Kandianis CB, Harjes CE, Bai L, Kim EH, Yang X, et al. (2010) Rare genetic variation at *Zea mays* crtRB1 increases β-carotene in maize grain. Nat Genet. 42: 322-327.

Yang LE, Huang XQ, Hang Y, Deng YY, Lu QQ, Lu S (2014) The P450-type carotene hydroxylase PuCHY1 from Porphyra suggests the evolution of carotenoid metabolism in red algae. J Integr Plant Biol. 56:902-915.

Zhou B, Deng YS, Kong FY, Li B, Meng QW (2013) Overexpression of a tomato carotenoid ε-hydroxylase gene alleviates sensitivity to chilling stress in transgenic tobacco. Plant Physiol Biochem. 70:235-245.

Zhou Y, Han Y, Li Z, Fu Y, Fu Z, Xu S, et al. (2012) ZmcrtRB3 encodes a carotenoid hydroxylase that affects the accumulation of α-carotene in maize kernel. J Integr Plant Biol. 54:260-269.

Zhu C, Naqvi S, Breitenbach J, Sandmann G, Christou P, Capell T. (2008) Combinatorial genetic transformation generates a library of metabolic phenotypes for the carotenoid pathway in maize. Proc Natl Acad Sci USA. 105:18232-18237.

Zhu C, Naqvi S, Capell T, Christou P (2009) Metabolic engineering of ketocarotenoid biosynthesis in higher plants. Arch Biochem Biophys. 483:182–190.

CHAPTER 2

The role of the Arabidopsis *OR* gene on carotenoid and ketocarotenoid accumulation in maize hybrids

CHAPTER 2: THE ROLE OF THE ARABIDOPSIS *ORANGE* GENE (*OR*) ON CAROTENOID AND KETOCAROTENOID ACCUMULATION IN MAIZE HYBRIDS

2.1 Abstract

The Arabidopsis *ORANGE* gene (*OR*) has been reported to play an important role in carotenoid accumulation in cauliflower, potato and rice. I overexpressed *AtOR* in white maize, which normally accumulates only trace amounts of carotenoids (lutein and zeaxanthin), under the control of the endosperm specific wheat LMW glutenin promoter in order to understand its function and ascertain its impact on carotenoid accumulation. Carotenoid content in OR lines increased up to 17µg/g DW (20-fold increase) compared with wild type. Zeaxanthin and lutein were the predominant carotenoids in OR lines. Transcript analysis of endogenous genes in the carotenoid and MEP pathways and also *pftf* (a transcription factor involved in chromoplasts formation), revealed that only 1–deoxy-D–xylulose 5–phosphate synthase 1 gene (*dxs1*) was upregulated in OR lines compared with wild type, whereas expression of all other genes I analyzed remained unchanged. The highest carotenoid accumulating OR line was crossed with four transgenic lines with different carotenoid and ketocarotenoid content and composition in order to evaluate the role of OR on carotenoid accumulation in different genetic backgrounds. My results indicate that OR increased carotenoid content when the endogenous carotenoid pool in specific lines was low; whereas it had no effect when the native carotenoid pool was high.

2.2 Introduction

Strategies to modulate carotenoid content and composition were described in the general introduction. One of the strategies does not involve modulation of the carotenoid pathway per se; rather it allows increasing carotenoid accumulation by enhancing storage capacity. Chromoplasts accumulate high levels of carotenoid pigments other than chlorophyll in various structures, such as crystalloids (tomato fruits), fibrils (pepper fruits) or membranes (daffodil petals) (Camara et al. 1995). Chromoplasts confer bright yellow, orange or red colors to many flowers (e.g. daffodil, sunflower) and fruits (e.g. tomato, orange, pepper).

Work on chromoplast differentiation in tomato, pepper and cucumber has resulted in the cloning of genes encoding carotenoid biosynthesis enzymes or putative carotenoid-binding proteins (reviewed in Cunningham and Gantt 1998). However, no gene product able to trigger chromoplast differentiation on its own was reported until relatively recently. Chromoplasts are differentiated from proplastids (relatively undifferentiated form of plastids found in meristematic tissues), chloroplasts (photosynthetic plastids in green tissues) or amyloplasts (starch accumulating plastids in storage organs, such as maize endosperm) (**Figure 2.1**).

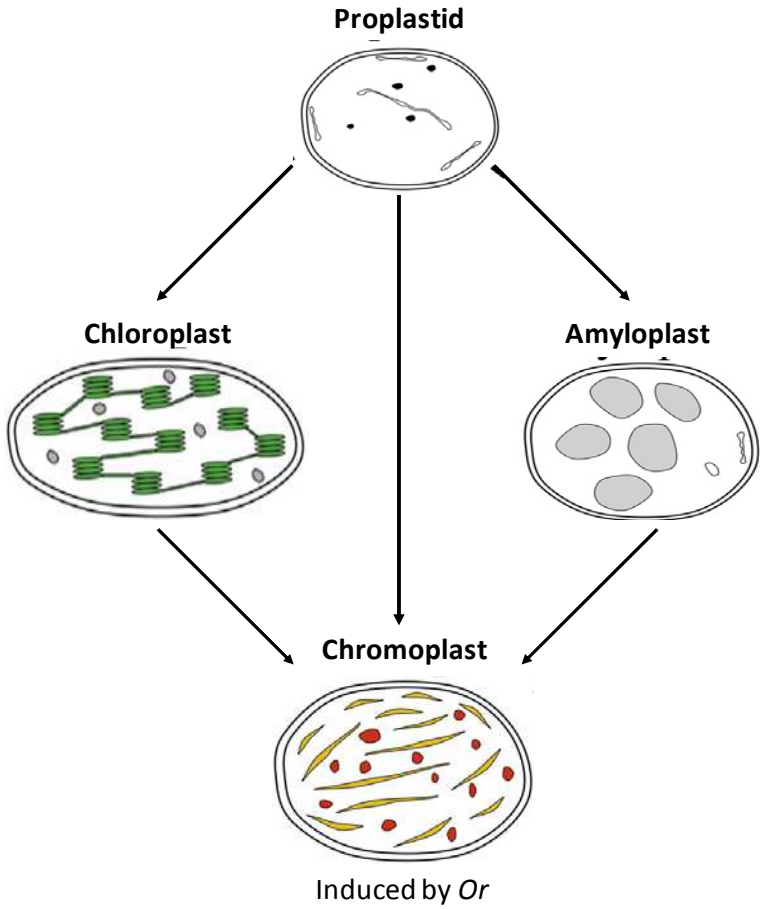

Figure 2.1 – Chromoplast biogenesis from other plastids. Chromoplasts are derived from fully developed chloroplasts or from non-green plastids (proplastids or amyloplasts). (Adapted from Li and Yuan 2013).

A spontaneous mutation of the *orange* (*or*) gene in cauliflower (*Brassica oleracea* var. botrytis) showed a profound effect on carotenoid accumulation (Crisp et al. 1975). Li et al. (2001) reported that *or* did not affect the metabolic flux through the carotenoid pathway and that transcript levels of carotenoid enzymes were unaltered in cauliflower o*r* mutant compared with wild-type. Positive regulation of chromoplast-associated genes such as *pftf* and the fact that *or* encodes a plastid associated protein with a DnaJ cysteine-rich domain involved in chromoplasts differentiation, suggested that the role of *or* might be to sequester carotenoids

into chromoplasts by differentiating them from non-differentiated proplastids (Lu et al. 2006) (**Figure 2.1**). In addition, the *or* mutation limits plastid replication so that a single chromoplast constitutes the plastidome and carotenoid inclusions in *or* chromoplasts resemble those found in carrot root (Paolillo et al. 2004).

The effect of the cauliflower *or* gene was further evaluated in transgenic potatoes, revealing chromoplast differentiation and a 6-fold increase in total carotenoids (Lopez et al. 2008). The only carotenoids present in wild-type tuber were violaxanthin and lutein, but when *or* was overexpressed in the tubers new carotenoids such as phytoene, phytofluene and ζ-carotene accumulated; β-carotene also accumulated (12-17% of total carotenoids) (Lopez et al. 2008). Expression of *or* in transgenic potatoes allowed not only an increase in carotenoid stability for up to 6 months cold storage but also increased carotenoid amounts during this time (18- and 13-fold increase at 5 and 6 months upon storage, respectively; Li et al. 2012; Lopez et al. 2008). Cauliflower *or* has also been used to increase ketocarotenoid content in potato (Campbell et al. 2015).

Orthologs of cauliflower wild-type *or* have been identified in other species, but only the sweet potato and Arabidopsis ortholog have been shown to induce carotenoid accumulation (Kim et al. 2013; Bai et al. 2014, 2015). The *or* gene isolated from orange-fleshed sweet potato (*Ibor*) was implicated in the increased accumulation of carotenoids via upregulating expression of biosynthetic genes as well as the homolog of *pftf*, involved in chromoplasts differentiation, in transgenic sweet potato callus (Kim et al. 2013; Park et al. 2015). Total carotenoid content increased up to 12-fold (Kim et al. 2013). In rice callus, the Arabidopsis *OR* gene (*AtOR*), which was 74.4% identical to its cauliflower wild-type ortholog, increased 2.2-fold total carotenoid content when it was co-expressed with maize *psy1* and *Pantonea Ananatis crtI* compared with just expression of maize *psy1* and *Pantonea Ananatis crtI* (Bai et al. 2014). Orange crystal-like structures were observed in the chromoplasts of orange callus expressing *or*, similarly to those reported in transgenic plants expressing the cauliflower *or* (Li et al. 2006; Lopez et al. 2008). Interestingly, the same structures were observed in transgenic callus co-expressing *AtDXS*, *Zmpsy1* and *PacrtI*, suggesting that chromoplast differentiation may be triggered either by direct expression of a gene involved in the differentiation process (*OR*) or by increasing the flux through the carotenoid pathway to such an extent that the process of chromoplast differentiation is triggered by the abundance of carotenoids (Fraser et al. 2007; Maass et al. 2009). Similarly, plastoglobuli-containing plastids were observed in rice

endosperm overexpressing *AtOR* but in this case expression of the endogenous carotenogenic genes *lyce*, *lycb* and *bch2* was upregulated (Bai et al. 2015).

A number of reports have correlated *or* overexpression with stress tolerance. Carotenoid-enhanced sweet potato callus through overexpression of *Ibor* exhibited increased tolerance to salt-mediated oxidative stress (Kim et al. 2013) and transgenic potato lines overexpressing *Ibor* had a significantly enhanced tolerance to NaCl and Methylviologen-mediated oxidative stress as well as 2,2-diphenyl-1-picrylhydrazyl (DPPH) radical scavenging activity (Goo et al. 2015). These results suggest that *Ibor* may be utilized to develop crops tolerant to salinity and other environmental stresses in addition to improving the nutritional quality by increasing the carotenoid content through the enhancement of sink capacity (Goo et al. 2015).

Transgenic rice plants overexpressing *AtOR* had been generated earlier (Bai et al. 2014, 2015). In maize, the genetic background of the transgenic plants (M37W) provides a blank template for carotenoid biosynthesis because the white endosperm contains only trace amounts of carotenoids due to the very low *Zmpsy1* expression. A representative *AtOR* maize line with increased 32-fold total carotenoid content compared with wild-type without any changes in the qualitative carotenoid profile was crossed with a number of transgenic maize lines expressing different carotenoid- and ketocarotenoid-pathway genes in order to determine the impact of *AtOR* on carotenoid metabolism and accumulation at the mRNA and metabolite levels.

2.3 Materials and methods

2.3.1 Gene cloning and vector construction

The *AtOR* cDNA was cloned directly from *A. thaliana* mRNA by RT–PCR using forward primer (5’-GATGTCATCTTTGGGTAGGATTTTGTCTG-3’) and reverse primer (5’-TGAGATTCTAAGGAAGTAGAATGTGTTGC-3’) based on sequence data in GenBank (accession number NM 203246). The cDNA was transferred to the pGEM-T Easy vector (Promega), and the resulting plasmid pGEM-AtOR was digested with *Eco*RI. *AtOR* was introduced into vector p326 (Stoger et al., 1999), between the wheat low-molecular weight (LMW) glutenin gene promoter and the *nos* terminator (**Figure 2.2**). The right orientation of *AtOR* driven by LMW promoter was selected by PCR with the forward primer from LMW

promoter and reverse primer from *AtOR*, and the final plasmid of p326-AtOR was further confirmed by sequencing the whole plasmid.

A truncated β–carotene ketolase gene (*bkt)* from *C. reinhardtii* (Zhong et al. 2011) was chemically synthesized by a commercial vendor (MWG eurofins, Ebersberg, Germany) and optimized for maize codon usage. The modified gene (*sCrbkt*) was fused with the transit peptide sequence (TPS) from the *Phaseolus vulgaris* small subunit of ribulose bisphosphate carboxylase (Schreier et al. 1985) and the 5'-untranslated region of the rice alcohol dehydrogenase gene (OsADH-UTR) (Sugio et al. 2008) under the control of the maize γ–zein promoter. The TPS was also optimized for maize codon usage (**Figure 2.2**).

The *CrtZ* gene encoding β-carotene hydroxylase (*sBrCrtZ*) from *Brevundimonas* sp. Strain SD212 (MBIC 03018) was chemically synthesized according to the codon usage of *Brassica napus* (accession number AB377272) (provided by Dr. Norihiko Misawa, Japan). The *sBrcrtZ* gene fused with the pea small subunit of Rubisco as TPS and OsADH-UTR was digested with *Bam*HI and *Sac*I and the digested fragments were cloned into the *Bam*HI and *Sac*I site of plasmid pGZ63 containing the maize γ-zein gene promoter, OsADH-UTR-TPS and the *nos* terminator (**Figure 2.2**).

The β-carotene ketolase *sBrcrtW* from *Brevundimonas* sp. Strain SD212 (Nishida et al. 2005) was chemically synthesized according to the codon usage of *Brassica napus* (provided by Dr. Norihiko Misawa, Japan) and fused to the full-length OsADH-UTR (Sugio et al., 2008) and to the transit peptide sequence from pea ribulose 1, 5-bisphospate carboxylase small subunit (Schreier et al. 1985). These DNA fragments were inserted into plasmid GZ63 containing the maize γ-zein gene promoter and the *nos* terminator (**Figure 2.2**).

Zea mays lycopene ε-cyclase *lyce* cDNA fragment was amplified by RT-PCR using forward (5'-GGAATTCTCTAGACGATCTCGGCGCCGCTCGGCTGCT-3') and reverse primers (5'-GACTAGTGGATCCCAATGAGACCTACAGTGAGACCT-3') based on sequence information in GenBank (accession numbers EF622043) and suitable restriction sites were incorporated subsequently by PCR. The amplified *lyce g*enes were sub-cloned into the pHorP vector containing the Barley D-hordein promoter, a 300 bp-long *gusA* gene fragment and the ADP-glucose pyrophosphorylase (ADGPP) terminator. To incorporate the target gene fragments into pHorP, the vector was digested with *Xba*I and *Bam*HI to introduce a sense *lyce* fragment between the barley D-hordein promoter and the *gusA* gene fragment, resulting in

pHorP-ZmLYCE sense. In the second step, the pHorP-ZmLYCE sense plasmid was digested with *Spe*I and *Eco*RI, to introduce the antisense *lyce* fragment between the *gusA* gene fragment and ADGPP terminator, resulting in pHorP-RNAi-ZmLYCE (**Figure 2.2**).

Transgene expression vectors for *Zmpsy1*, *Gllycb* and *PacrtI* were previously described (Zhu et al. 2008) (**Figure 2.2**).

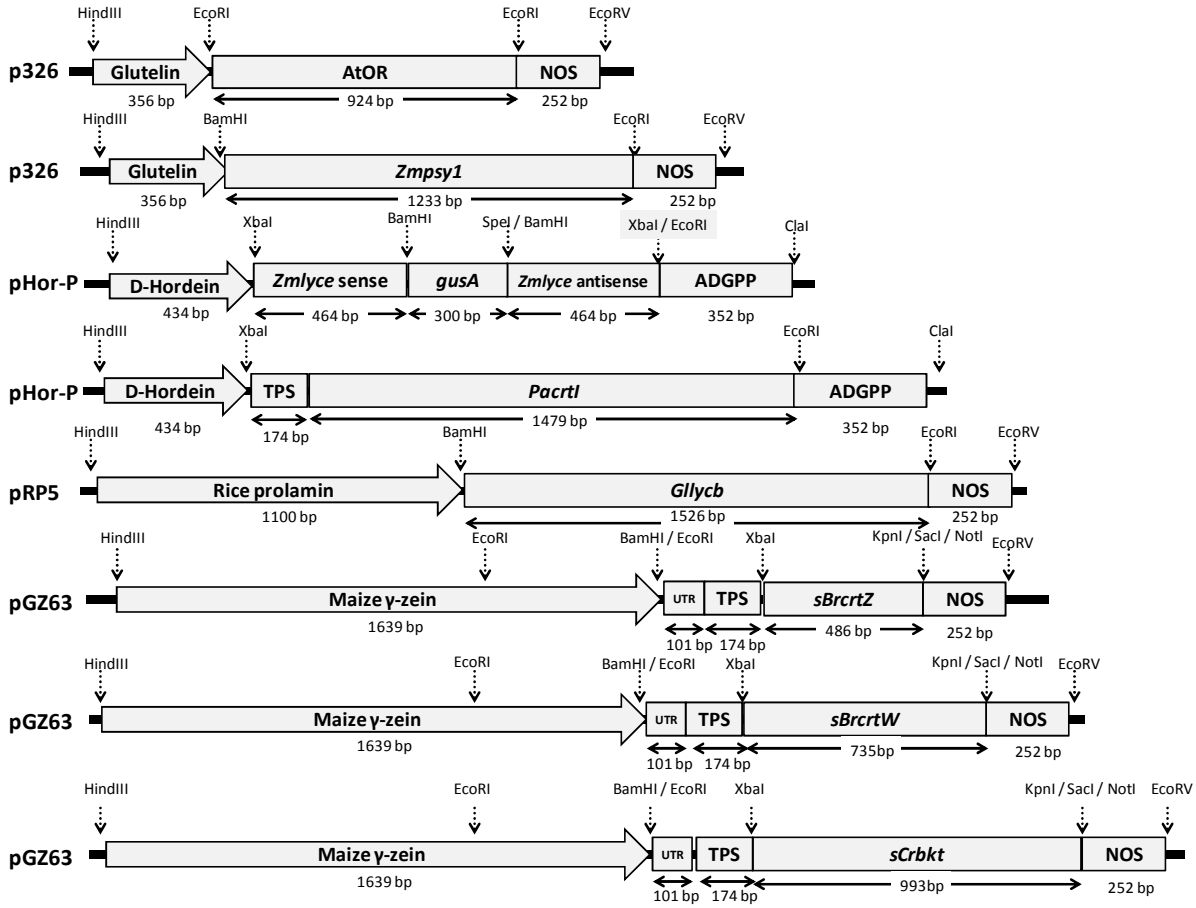

Figure 2.2 – Schematic representation of transgenes used in this experiment.

2.3.2 Maize transformation and plant growth

To obtain transgenic maize plants expressing *AtOR* (OR line), *Zmpsy1* (CARO1 line), *sBrcrtZ*, *sBrcrtW* and *sCrbkt* (KETO1 line) and *Zmpsy1*, *PacrtI*, RNAiLYCE and *sCrbkt* (KETO2 line), wild type maize plants (*Zea mays* L., cv. M37W) were grown in the greenhouse or growth room with a 10 h photoperiod (28/20°C day/night temperature) and 60–90% relative humidity for 50 days, followed by a 16 h photoperiod (21/18°C day/night temperature) thereafter. Fourteen-day-old immature zygotic embryos (IZEs) were excised aseptically and cultured on N6 medium (MSP, **Table 2.1**).

Table 2.1. – Media composition (amounts listed to prepare 1l).

ÍTEM	CALLUS INDUCTION (MSP)	OSMOTICUM MEDIUM (MSO)	SELECTION MEDIUM (MSS)	SHOOTING MEDIUM (MSR1)	ROOTING MEDIUM (MSR2)
Dark / light	Dark	Dark	Dark	Light	Light
Approx. time in culture	4 days 2 days after bombardment	4 h before and 16 h after bombardment	4-6 weeks (two subcultures)	2-3 weeks	Until plantlets have sufficient roots
N6 macro-nutrients[1]	50 ml	50 ml	50 ml	--	--
N6 micro-nutrients[2]	5 ml	5 ml	5 ml	--	--
Fe-EDTA[3]	5 ml	5 ml	5 ml	5 ml	5 ml
MS Powder (Duchefa, Haarlem, Nederland)	--	--	--	4.4 g	4.4g
Casein Hydrolysate (Duchefa)	0.1 g	0.1 g	0.1 g	--	--
L-Proline (Sigma)	2.8 g	2.8 g	2.8 g	--	--
Sucrose (Sigma)	20 g	20 g	20 g	30g	30g
Mannitol (Sigma)	--	36.4 g	--	--	--
Sorbitol (Sigma)	--	36.4 g	--	--	--
2,4-D[4] (Duchefa)	200µl	200µl	200µl	50µl	--
	Adjusted pH to 5.8 with KOH				
Gelrite (Sigma)	4 g	--	4 g	4 g	4 g
Agarose (Sigma)	--	4 g	--	--	--
	Autoclaved at 121ºC for 20 min				
BAP[5]	--	--	--	10ml	--
PPT[6]	--	--	300µl	300µl	300µl
N6 Vitamins[7]	5 ml	5 ml	5 ml	5 ml	5 ml
$AgNO_3$[8]	1ml	1ml	1ml	85ul	85ul

[1] N6-macronutrients (1L, 20x): 9.26 g $(NH_4)_2 \cdot SO_4$, 56.6 g KNO_3, 3.32 g $CaCl_2 \cdot 2H_2O$, 3.7 g $MgSO_4 \cdot 7H_2O$ and 8g KH_2PO_4.

[2] N6-micronutrients (500 mL, 200x): 250 mg $MnS_4 \cdot H_2O$, 150 mg $ZnSO_4 \cdot 7H_2O$, 160 mg H_3BO_3, 80 mg KI, 2 5mg $Na_2MoO_4 \cdot H_2O$ and 2.5 mg $CuSO_4 \cdot 5H_2O$.

[3] Fe-EDTA: 1.112 g $FeSO_4 \cdot 7H_2O$ and 1.49 g EDTA-$Na_2 \cdot 2H_2O$.

[4] 2,4-D (2,4-Dichlorophenoxyacetic acid) 4 mg/mL: 0.04 g to 10 mL 100% EtOH.

[5] BAP (benzylaminopurine) 1 mg/mL: 0.01g to 10 mL dH_2O.

[6] PPT (phosphinothricin) 10 mg/mL: 0.1g to 10 mL dH_2O.

[7] N6 Vitamins (200 mL, 200x): 20mg nicotinic acid, 20 mg pyridoxine HCL, 40 mg Thiamine HCL and 80 mg Glycine.

[8] $AgNO_3$ 10 mg/mL: 0.3g $AgNO_3$ to 30 mL dH_2O.

After 4 days, IZEs were placed on osmoticum media (MSO, **Table 2.1**) four hours before bombardment with 10 mg of gold particles coated with the constructs and the selectable

marker *bar* (Christensen and Quail 1996) at a molar ratio of 3:1 as reported (Christou et al. 1991) and returned to MSO for 16 h before selection. Bombarded callus were selected on phosphinothricin-supplemented medium (MSS, **Table 2.1**) and transgenic plantlets were regenerated on regeneration media (MSR1 and MSR2, **Table 2.1**) and hardened off in soil (**Figure 2.3**). Two independent lines for OR and 1 line for the other combinations (CARO1, KETO1 and KETO2, respectively) were selected for further analysis.

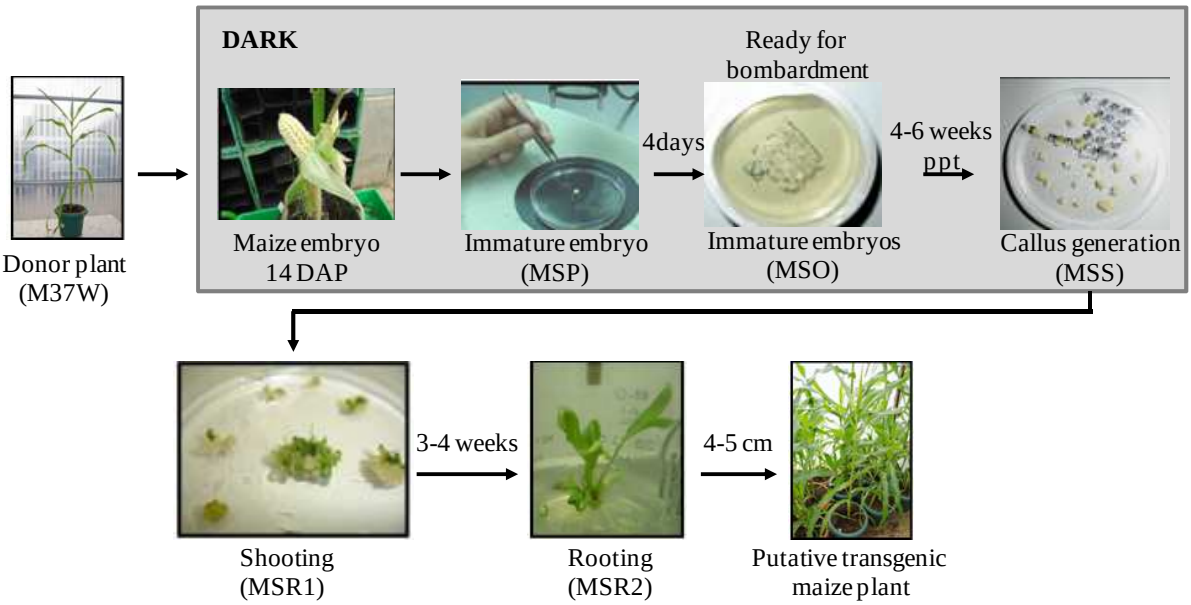

Figure 2.3 – Maize transformation process.

The highest-expressing line for each transgene combination was selected by mRNA blot analysis and was self-pollinated to homozygosity. Homozygous OR, CARO1, KETO1, KETO2, one already available transgenic line carrying *Zmpsy1+PaCrtI+Gllycb* (Ph4, named here CARO2; Zhu et al. 2008) (**Table 2.2**) and wild type M37W plants were grown in the greenhouse at 28/20°C day/night temperature with a 10 h photoperiod and 60%–90% humidity during the first 50 days, followed by maintenance at 28/20°C day/night temperature with a 16 h photoperiod and 60%–90% humidity thereafter. All lines were self-pollinated to be used as controls and out-crossed with an OR line (pollen donor) to obtain ORxCARO1, ORxCARO2, ORxKETO1 and ORxKETO2. For further analysis endosperm samples were taken from immature seeds at 30 days after pollination (DAP), frozen in liquid nitrogen and stored at -80°C until analysis.

Table 2.2. – Transgenic lines used in this experiment to generate hybrids with *AtOR* transgenic line.

Transgenic line	Foreign genes
CARO1	*Zmpsy1*
CARO2	*Zmpsy1, PacrtI, Gllycb*
KETO1	*sCrbkt, sBrcrtW, sBrcrtZ*
KETO2	*Zmpsy1, RNAiLYCE, sCrbkt, sBrcrtZ*

2.3.3 RNA extraction and cDNA synthesis

The protocols are described in detail in Chapter 1, section 1.2.2.

2.3.4 Real-time qRT-PCR

Real-time RT-PCR was performed on a BioRad CFX96^{TM} system using 25µl mixtures containing 10 ng of synthesized cDNA, 1x iQ SYBR green supermix (BioRad, Hercules, CA, USA) and 0.2 µM forward and reverse primers (**Table 2.3**).

Cyp97A (carotenoid β-hydroxylase) and *cyp97C* (carotenoid ε-hydroxylase) gene primer information was obtained from Naqvi et al., 2011. Serial dilutions of cDNA (125–0.2 ng) were used to generate standard curves for each gene. PCR was performed in triplicate using 96-well optical reaction plates. Cycling conditions consisted of a single incubation step at 98ºC for 2 min followed by 35 cycles of 98ºC for 5 s and 59.4ºC for 30 s. Specificity was confirmed by product melt curve analysis over the temperature range 65–95ºC with fluorescence acquired after every 0.5ºC increase, and the fluorescence threshold value and gene expression data were calculated with BioRad CFX96^{TM} software. Values represent the mean of three biological replicates ± SE. Amplification efficiencies were compared by plotting the ΔCt values of different primer combinations of serial dilutions against the log of starting template concentrations using the CFX96^{TM} software.

Table 2.3 – Oligonucleotide sequences of maize actin, endogenous carotenogenic genes and transgenes for Real-Time PCR analysis.

Gene	Forward	Reverse
Zmactin	5'-CGATTGAGCATGGCATTGT-3'	5'-CCCACTAGCGTACAACGAA-3'
Zmbch1	5'-CCACGACCAGAACCTCCAGA-3'	5'-CATGGCACCAGACATCTCCA-3'
Zmbch2	5'-GCTTGTTAGCAGTCCGGT-3'	5'-GAAAGGAGGATGGCGATAGAT-3'
Zmlycb	5'-GACGCCATCGTAAGGTTCCTC-3'	5'-TCGAGGTCCAGCTTGAGCAG-3'
Zmlyce	5'-AGTCCATCAATGCTTGCATGG-3'	5'-CATCTCGGCACCCTGAAAAAG-3'
Zmcyp97A	5'-CTGGAGCGTCTGAAAGTCA-3'	5'-GGACCAAATCCAAACGAGAT-3'
Zmcyp97B	5'-CTGAGGAGAAGGACTTGA-3'	5'-TCCACTGGTCTGTCTGCGAT-3'
Zmcyp97C	5'-GTTGACATTGGATGTGATTGG-3'	5'-AACCAACCTTCCAGTATGGC-3'
Zmdxs1	5'-AGGTCGGCAAGGCAGGAT-3'	5'-TCCAGCGGCTTGCAGAACCT-3'
Zmdxs2	5'-GCTGAACTACTTCCAGAAGCG-3'	5'-CTGCAGGAACGACGAGTAGA-3'
Zmdxs3	5'-GGCACGCTTCAGTTCTATCCA-3'	5'-CTCTTAGGGCGTCATCGTG-3'
Zmdxr	5'-TCCATTGTCACGCTTCTAGC-3'	5'-TGGCGAGCAACTTCTATGAC-3'
Zmpftf	5'-CATTGAGAAGGAGACACTGGC-3'	5'-TTGACTTTAGGCAGGGAGGG-3'
Zmpsy1	5'-CATCTTCAAAGGGGTCGTCA-3'	5'-CAGGATCTGCCTGTACAACA-3'
Zmpsy2	5'-TCACCCATCTCGACTCTGCTA-3'	5'-GATGTGATCTACGGATGGTTCAT-3'
PacrtI	5'-GTGGCGCAAGATGATCGTCAA-3'	5'-GCCAGAAGACCACGTACATCCA-3'
sCrbkt	5'-CCACCATCACACAGGGGAA-3'	5'-AGGTTCGGATTGCCCCTATG-3'
Gllycb	5'-TAAGGCTGGAAGTAGCAGTGC-3'	5'-GCAGGACCACCACCAACAAT-3'
sBrcrtz	5'-GAGGGATGCGTTTCTTTCG-3'	5'-AGCCAACTCAGCCTCCAAA-3'
sBrcrtw	5'-TCTCTTGTTATCGTGCCAGC -3'	5'-GCCACAATGAAAAGTCCCA -3'
AtOR	5'- TTCTCTATCACCGCCCAAAAC -3'	5'- GCCATAGCCATTCCTGTGC -3'

2.3.5 Carotenoid extraction and UPLC analysis

Maize endosperm was excised by removing the seed coat and embryo. Samples were freeze-dried before extraction and 3-5 seeds per sample were ground to a fine powder. Carotenoids in 50-100mg samples were extracted in 15 ml methanol:ethyl acetate (6:4 v/v) at 58ºC for 20 min. The mixture was filtered, transferred to a separatory funnel, 15 ml hexane:diethyl ether (9:1 v/v) were added and agitated gently for 1 min. The organic phase was washed twice with saturated NaCl water and the aqueous phase was removed. The samples were dried under N_2 and stored at -80ºC until injection.

The extracts were dissolved in 210-600 µl injection solvent [ACN/MeOH 7:3, v/v]/acetone 3:2, v/v. UHPLC analysis was carried out at SCT-DATCEM, University of Lleida, Spain, using an Acquity Ultra Performance LC system linked to a PDA 2996 detector (Waters, Milford, USA). Mass detection was carried out using an Acquity TQD tandem-quadrupole MS equipped with a Zspray electrospray interface (Waters). MassLynx software version 4.1 (Waters) was used to control the instruments and also for data acquisition and processing. UHPLC separations were performed on a reversed-phase column Acquity UPLC C18 BEH 130 Å, 1.7 µm, 2.1 × 150 mm (Waters). The mobile phase consisted of solvent A, ACN/MeOH 7:3, v/v, and solvent B, water 100%. Carotenoids in samples were quantified using a PDA detector through the external standard method. Identification of carotenoids was carried out as previously described (Rivera et al. 2013). MS analyses were conducted by atmospheric pressure chemical ionization (APCI), and the conditions used are the same as those described by Rivera et al. 2011. Authentic standards used for quantification were β-carotene, lutein, β-cryptoxanthin and astaxanthin (Sigma), zeaxanthin (Fluka, Buchs SG, Switzerland), phytoene and antheraxanthin (Carotenature, Lupsingen, Switzerland).

2.3.6 TEM microscopy analysis

Maize 30 DAP endosperm pieces (0.5 x 2.0 mm) were fixed in 2.5% v/v glutaraldehyde in 0.1 M phosphate buffer (pH 7.2) overnight at 4°C. Samples were washed twice for 10 minutes with 0.1 M sodium phosphate buffer (pH 7.2) at 4ºC and then fixed in 1% w/v osmium tetroxide in water for 2 h. After washing twice with sodium acetate (0.1M for 2 minutes) they were incubated in uranyl acetate (0.5% in water) for 30 minutes and washed twice with sodium acetate (0.1M) for 2 min). Samples were then dehydrated in an acetonitrile (Panreac Química SLU, Barcelona, Spain) series (30–100%) before embedding in epoxy resin Araldite® Embed 812 (Epon-812) (Aname Electron Microscopy Sciences, Madrid, Spain) and polymerized at 60°C for 48 h. Ultra-thin sections (75-80 nm) were prepared with a diamond knife using a Reichert Jung Ultramicrotome Ultracut E (Leica Nova Scotia, Dartmouth, Canada), mounted on SPI-ChemTM Formvar film/carbon-coated copper grids, and stained with uranyl acetate and Reynold's lead citrate prior to examination using an EM 910 (80 kV) transmission electron microscope (Zeiss, *Oberkochen*, Germany). TEM microscopy was performed in SCT – Electron microscopy, Universitat de Lleida, Spain.

2.4 Results

2.4.1 Transgenic lines overexpressing the Arabidopsis Orange (AtOR) gene exhibit an increase in carotenoid content without concomitant upregulation of carotenogenic gene expression

Two *AtOR*-expressing lines (OR1 and OR2) were previously obtained following direct DNA transfer of the *AtOR* into M37W immature maize embryos in earlier experiments in the laboratory. T_0 plants were self-pollinated to obtain T_1 plants that were used for further analysis. T_2 seeds from T_1 plants obtained by self-pollination were by mRNA blot to monitor *AtOR* transcript levels (**Figure 2.4**).

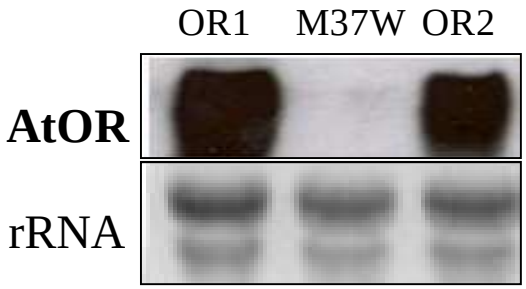

Figure 2.4 –mRNA blot analysis of AtOR in wild type (M37W) and two different transgenic lines (OR1 and OR2) transformed with AtOR gene driven by the wheat LMW-glutelin promoter. Each lane was loaded with 25 μg total RNA isolated from endosperm tissue. Ribosomal RNA stained with ethidium bromide is shown as a loading control.

Carotenoid quantification revealed that M37W (wild-type) endosperm accumulated traces of zeaxanthin, lutein, violaxanthin and antheraxanthin. Total carotenoids were ca: 1 μg/g DW. Line OR1 accumulated high amounts of zeaxanthin (ca: 10 μg/g DW) followed by lutein (ca: 2 μg/g DW), antheraxanthin (ca: 2 μg/g DW), β-cryptoxanthin (ca: 1 μg/g DW) and traces of violaxanthin in the endosperm. Line OR2 accumulated high amounts of zeaxanthin (ca: 6 μg/g DW) followed by lutein (ca: 2 μg/g DW) and traces of β-cryptoxanthin, antheraxanthin and violaxanthin in the endosperm. Total carotenoid content in lines OR1 and OR2 was ca: 17 μg/g DW and 9 μg/g DW, respectively (**Figure 2.5**).

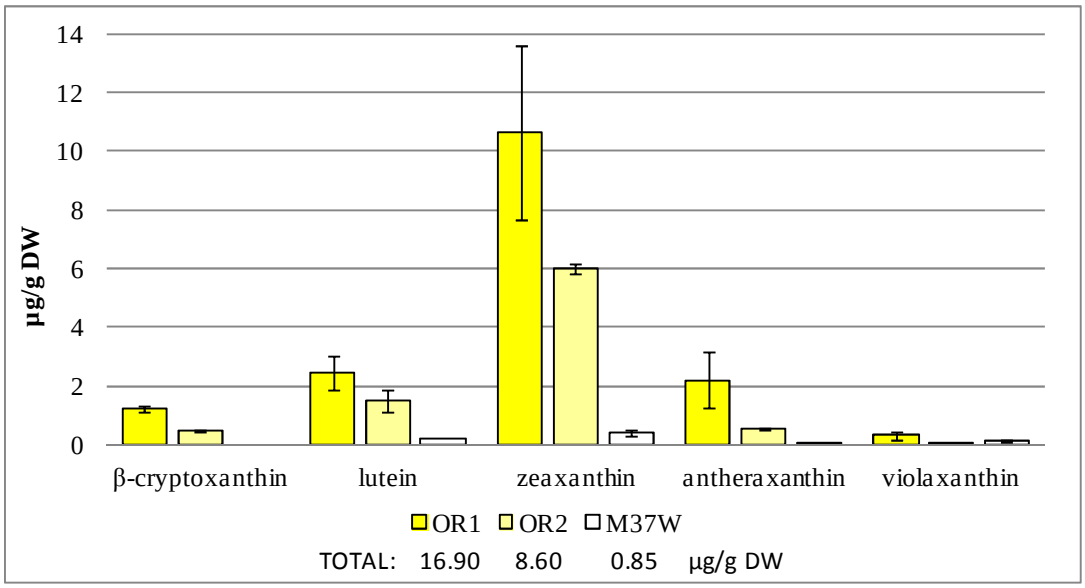

Figure 2.5 – Carotenoid content and composition in wild-type M37W and transgenic lines OR1 and OR2 T_2 at 30 DAP (µg/g DW±SE) (n= 3-5 seeds).

Quantitative real-time RT-PCR was used to compare relative transcript levels of endogenous genes in the carotenoid pathway, MEP pathway and *pftf*, a transcription factor involved in chromoplast formation in OR1, OR2 and M37W (**Figure 2.6**). The following endogenous carotenogenic genes were analyzed at the mRNA level: *phytoene synthase 1* and *2* (*Zmpsy1/2*), *lycopene ε-cyclase* (*Zmlyce*), *lycopene β-cyclase* (*Zmlycb*), *carotenoid β-hydroxylases* (*Zmbch1*, *Zmbch2*, *Zmcyp97A* and *Zmcyp97B*) and *carotenoid ε-hydroxylase* (*Zmcyp97C*). Transcript levels of all the endogenous genes analyzed were similar in OR1 and OR2 compared with M37W, with the exception of *Zmlyce* transcript levels which were downregulated in the transgenic lines compared to M37W (**Figure 2.6A**). *1-Deoxy-D-xylulose-5-phosphate synthase 1*, *2* and *3* (*Zmdxs1/2/3*), *1-deoxy-D-xylulose-5-phosphate reductase* (*Zmdxr*) and *methylbut-2-enyl-diphosphate reductase* (*Zmhdr*), endogenous genes in the MEP pathway were analyzed at the mRNA level. Transcript levels of the endogenous genes described above were similar in OR1 and OR2 compared with M37W wild-type, with the exception of *dxs1* transcript levels which were upregulated (ca: 2-fold) in transgenic lines compared with wild-type (**Figure 2.6B**). Transcript levels of plastid fusion/translocation factor (*Zmpftf*) implicated in chromoplasts formation were not significantly different in OR1 and OR2 transgenic lines compared with M37W (**Figure 2.6C**).

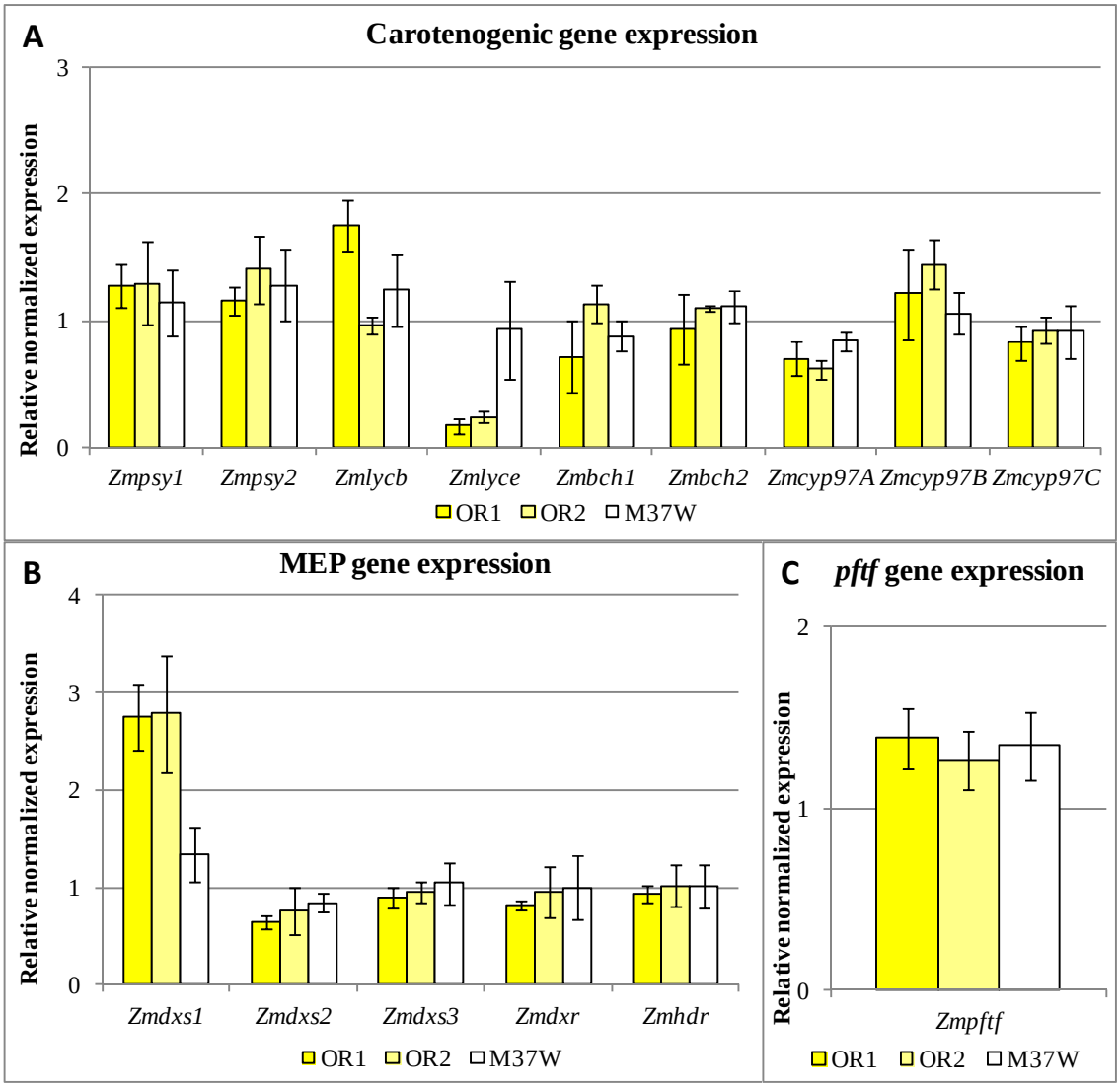

Figure 2.6 – Relative mRNA expression of endogenous carotenogenic genes (A), MEP pathway-related genes (B) and *pftf* (C) in 30 DAP maize endosperm, normalized against actin mRNA and presented as the mean of three biological replicates ± SE. Abbreviations: *Zmpsy1*, *phytoene synthase 1*; *Zmpsy2*, *phytoene synthase 2*; *Zmlyce*, l*ycopene ε-cyclase*; *Zmlycb*, *lycopene β-cyclase*; *Zmbch1*, *carotenoid β-hydroxylase 1*; *Zmbch2*, *carotenoid β-hydroxylase 2*; *Zmcyp97A/B*, *carotene β-hydroxylase*; *Zmcyp97C*, *carotene ε-hydroxylase*, *Zmdxs1/2/3*, *1-Deoxy-D-xylulose-5-phosphate synthase*; *Zmdxr*, *1-Deoxy-D-xylulose-5-phosphate reductase*; *Zmhdr*, *methylbut-2-enyl-diphosphate reductase*; *Zmpftf*, plastid fusion/translocation factor.

2.4.2 Genetic background influences seed color phenotype in hybrids between *AtOR* transgenic lines and different parents but only when the carotenoid content of the parents is low

In order to evaluate the role of the Arabidopsis OR in carotenoid and ketocarotenoid accumulation I crossed OR line with transgenic lines having different genetic backgrounds: two different transgenic lines accumulating medium (CARO1) or high (CARO2) levels of carotenoids and two different transgenic lines accumulating low (KETO1) or high (KETO2)

levels of ketocarotenoids. CARO1 (transgenic line expressing *Zmpsy1*), KETO1 (transgenic line expressing a combination of hydroxylase (*sBrcrtZ)* and two ketolases: *sCrbkt* and *sBrcrtW*) and KETO2 line (transgenic line expressing *Zmpsy1*, *sCrbkt*, *sBrcrtZ* and RNAi construct to block endogenous *lyce*) were obtained by using the same procedure employed to generate the original OR lines, whereas CARO2 (transgenic line expressing *Zmpsy1*, *PacrtI* and *Gllycb*) was described previously (Zhu et al. 2008) (**Table 2.2, see section 2.3**). The highest carotenoid accumulating OR line (OR1) was used as pollen donor to pollinate CARO1, CARO2, KETO1 and KETO2 to obtain ORxCARO1, ORxCARO2, ORxKETO1 and ORxKETO2 lines (**Figure 2.7**).

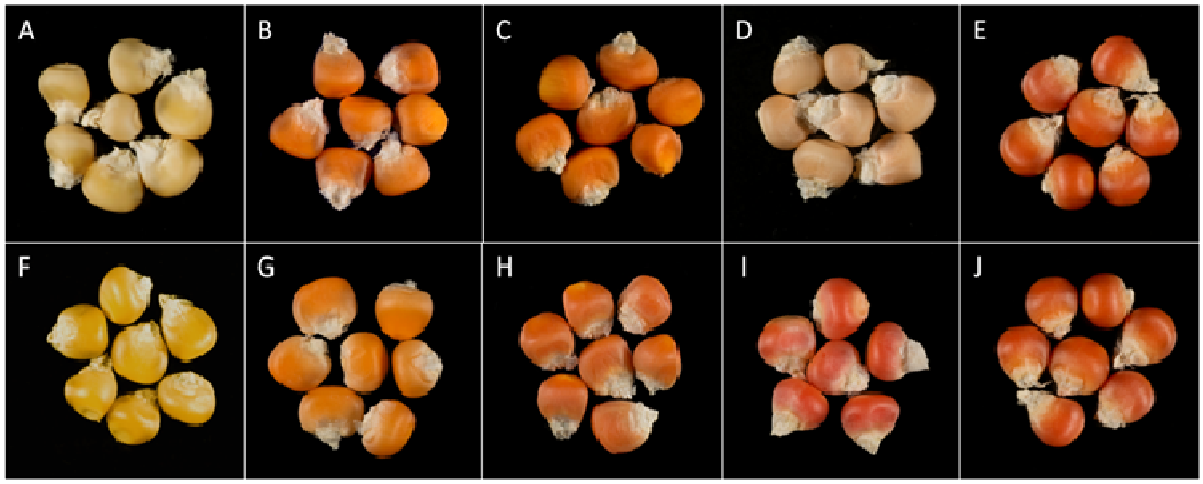

Figure 2.7 – Phenotype of wild-type (A) and transgenic seeds with different carotenoid and ketocarotenoid profiles: CARO1 (B), CARO2 (C), KETO1 (D) and KETO2 (E) and the resulting seeds from the cross with OR; (F): ORxCARO1 (G), ORxCARO2 (H), ORxKETO1 (I) and ORxKETO2 (J). A substantial change in seed color phenotype resulted when *AtOR* was expressed in M37W background (white to yellow) and in low-ketocarotenoid (KETO1) background (light pink to redish-pink) suggesting that *AtOR* plays an important role in carotenoid and ketocarotenoid accumulation when the amounts of carotenoids were low in the original (parent) line (KETO1). No changes in color phenotype were observed when the amounts of carotenoids were high in the parents (CARO1, CARO2 and KETO2).

When *AtOR* was expressed in white maize, the phenotype of resulting seeds was yellow in color, suggesting a substantial increase in carotenoids (e.g. lutein and/or zeaxanthin) in the transgenic seeds. Seeds from CARO1 and CARO2 lines were orange and intense orange, respectively, due to the accumulation of β-carotene, lutein and zeaxanthin, whereas seeds from KETO1 and KETO2 lines were pink and red, respectively, as a result of accumulation of different amount of ketocarotenoids. T_1 seeds from the crosses referred to above exhibited similar phenotypes in the case of ORxCARO1, ORxCARO2 and ORxKETO2 compared with the corresponding parents. Seeds from ORxKETO1 exhibited a substantial change in color

from pale pink (KETO1) to deep red-pink (ORxKETO1) suggesting a substantial increase in the accumulation of ketocarotenoids (**Figure 2.7**).

At 30 DAP endosperm samples were frozen in liquid nitrogen and stored at -80ºC until RNA extraction was performed to measure transgene expression by qRT-PCR (**Figure 2.8**).

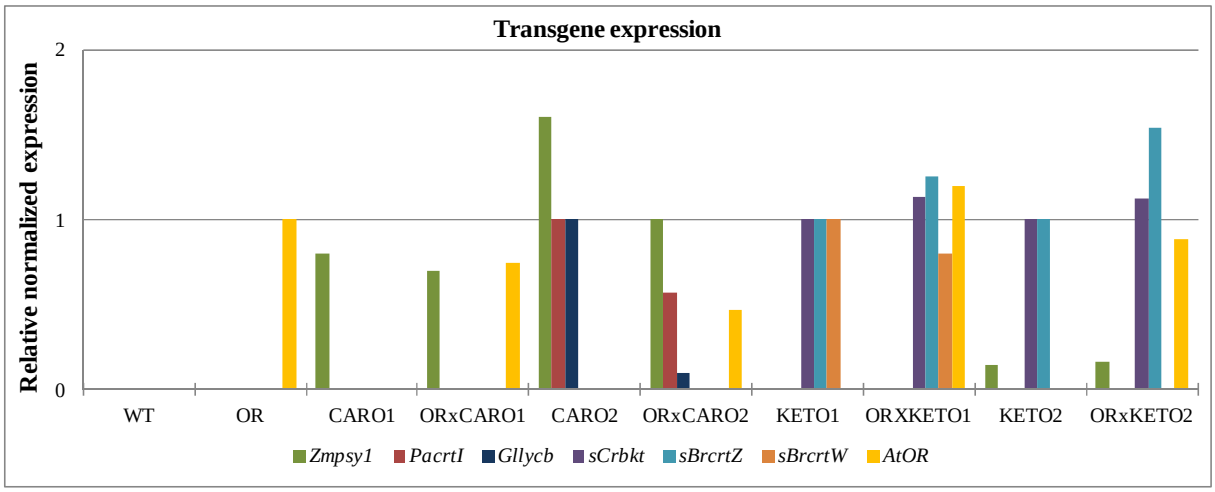

Figure 2.8 –Transcript accumulation normalized against actin in wild-type and transgenic lines presented as mean of three technical replicates. Standard error bars were not included because of the use of technical replicates rather than biological replicates. The aim was to show expression of the introduced transgenes rather than compare different transcript profiles.

As expected, WT seeds did not express any of the transgenes; OR expressed only AtOR, as expected; CARO1 expressed only *Zmpsy1*; CARO2 expressed *Zmpsy1*, *PacrtI* and *Gllycb*; KETO1 expressed *sBrcrtZ, sCrbkt* and *sBrcrtW*; KETO2 expressed *Zmpsy1*, *sCrbkt* and *sBrcrtZ*; the corresponding crosses expressed *AtOR* in addition to the transgenes present in their respective parents.

2.4.3 Introgression of *AtOR* reveals an increase in carotenoid content and composition of transgenic hybrids but only when the carotenoid content of the parents is low

Carotenoid content of wild-type, transgenic lines (OR, CARO1, CARO2, KETO1 and KETO2) and the crosses generated with OR (ORxCARO1, ORxCARO2, ORxKETO1 and ORxKETO2) was evaluated at 30 and 60 DAP in order to measure differences in carotenoid content and composition at two different developmental stages: middle stage of grain filling and completely developed seeds.

In the 2013 growing season, M37W accumulated low levels of zeaxanthin (ca: 0.4 µg/g DW), lutein (ca: 0.2 µg/g DW) and violaxanthin (0.1 µg/g DW) and traces of antheraxanthin at

30DAP. At 60DAP, M37W accumulated low amounts of zeaxanthin (ca: 0.3 µg/g DW) and lutein (ca: 0.2 µg/g DW) but violaxanthin was not detected. When *AtOR* was overexpressed into M37W the carotenoid composition in the endosperm remained the same, although the quantity of each compound increased drastically at 30 DAP from ca: 1 µg/g DW in M37W to ca: 25 µg/g DW (35-fold increase) in OR line: zeaxanthin (ca: 12 µg/g DW; 30-fold increase), antheraxanthin (ca: 7 µg/g DW; 170-fold increase), lutein (ca: 5 µg/g DW; 23-fold increase) and violaxanthin (ca: 2 µg/g DW; 15-fold increase). At 60 DAP total carotenoid content in OR was ca: 20 µg/g DW. Downstream compounds, violaxanthin and antheraxanthin did not accumulate but β-cryptoxanthin was detectable (ca: 1 µg/g DW). Zeaxanthin (ca: 11 µg/g DW; 38-fold increase over WT) and lutein (ca: 8 µg/g DW; 39-fold increase over WT) were the main carotenoids in OR transgenic line (**Table 2.4**).

CARO1 accumulated ca: 66 µg/g DW (94-fold increase over WT) total carotenoids at 30 DAP and ca: 91 µg/g DW (181-fold increase over WT) at 60 DAP. At 30 DAP zeaxanthin (ca: 23 µg/g DW; 58-fold increase over WT), antheraxanthin (ca: 14 µg/g DW; 350-fold increase over WT), lutein (ca: 9 µg/g DW; 47-fold increase over WT) and phytoene (ca: 8 µg/g DW) were the main carotenoids, followed by violaxanthin (ca: 4 µg/g DW; 39-fold increase over WT), β-carotene (ca: 3 µg/g DW), lycopene (ca: 3 µg/g DW) and β-cryptoxanthin (ca: 1 µg/g DW). When seeds were completely dry there was a shift in the carotenoid composition towards a reduction of downstream compounds and a concomitant increase in the first precursor in the pathway, phytoene (ca: 61 µg/g DW). At 60 DAP zeaxanthin (ca: 12 µg/g DW; 39-fold increase over WT), lutein (ca: 6 µg/g DW; 32-fold increase over WT) and antheraxanthin (ca: 6 µg/g DW) were the main carotenoids followed by β-carotene (ca: 2 µg/g DW), violaxanthin (ca: 2 µg/g DW), β-cryptoxanthin (ca: 1 µg/g DW) and lycopene (ca: 1 µg/g DW) (**Table 2.4**). When OR was crossed with CARO1 transgenic line to generate ORxCARO1 hybrid, carotenoid content and composition did not change substantially in the hybrid compared with CARO1. ORxCARO1 accumulated ca: 68 µg/g DW total carotenoids. Unfortunately, the analysis of ORxCARO1 at 60 DAP was not possible due to technical problems (**Table 2.4**).

Table 2.4 – Carotenoid content and composition in wild-type M37W, transgenic lines OR, CARO1, CARO2, KETO1 and KETO2; and hybrids ORxCARO1, ORxCARO2, ORxKETO1 and ORxKETO2 T_1 at 30 (*) and 60 DAP (**) (µg/g DW±SE) (n= 3-5 seeds). Abbreviations: Phyt, phytoene; Lyco, lycopene; βcryp, β-cryptoxanthin; βcaro, β-carotene; Lut, lutein; Zea, zeaxanthin; Anthe, antheraxanthin; Viola, violaxanthin; CAROT, carotenoids.

Sample	Phyt	Lyco	βcryp	βcaro	Lut	Zea	Anthe	Viola	TOTAL CAROT
M37W *	0.0±0.0	0.0±0.0	0.0±0.0	0.0±0.0	0.2±0.0	0.4±0.1	0.0±0.0	0.1±0.0	0.7
M37W**	0.0±0.0	0.0±0.0	0.0±0.0	0.0±0.0	0.2±0.0	0.3±0.0	0.0±0.0	0.0±0.0	0.5
OR *	0.0±0.0	0.0±0.0	0.0±0.0	0.0±0.0	4.5±0.2	12.1±1.8	6.8±0.4	1.5±0.3	24.9
OR**	0.0±0.0	0.0±0.0	1.2±0.0	0.0±0.0	7.8±0.8	11.4±1.5	0.0±0.0	0.0±0.0	20.4
CARO1*	7.8±0.2	2.6±0.4	1.4±0.1	3.4±0.7	9.4±0.4	23.2±2.8	14.0±1.1	3.9±0.0	65.7
CARO1**	60.7±0.7	0.8±0.1	0.9±0.0	2.3±0.1	6.4±0.3	11.8±0.8	5.8±0.4	2.1±0.0	90.8
CARO2*	17.5±0.6	0.0±0.0	2.0±0.0	11.3±0.4	9.4±0.1	23.3±2.5	13.2±0.5	2.4±0.1	79.1
CARO2**	117.0±1.0	0.0±0.0	1.5±0.0	8.2±0.2	8.8±0.3	18.1±0.9	1.8±0.2	0.0±0.0	155.4
KETO1*	0.0±0.0	0.0±0.0	0.0±0.0	0.0±0.0	0.0±0.0	0.0±0.0	0.0±0.0	0.0±0.0	0.0
KETO1**	0.0±0.0	0.0±0.0	0.0±0.0	0.0±0.0	0.0±0.0	0.0±0.0	0.0±0.0	0.0±0.0	0.0
KETO2*	4.1±0.2	5.2±0.4	2.8±0.7	6.9±0.3	1.2±0.0	7.5±0.3	4.5±0.1	0.8±0.1	33
KETO2**	53.7±1.0	5.0±0.5	0.0±0.0	11.8±0.6	0.7±0.1	6.4±0.4	1.3±0.0	0.0±0.0	78.9
ORx CARO1*	8.8±0.3	1.9±0.2	1.4±0.2	3.7±0.2	8.7±0.3	23.9±1.6	15.1±0.8	4.2±0.1	67.7
ORx CARO2*	20.0±0.8	0.0±0.0	1.9±0.1	9.0±0.3	9.9±0.3	23.1±0.6	12.6±1.6	2.5±0.1	79.0
ORx CARO2**	102.2±2.8	0.0±0.0	0.8±0.7	5.9±0.2	9.8±0.6	14.6±1.7	1.6±0.1	0.0±0.0	134.9
ORx KETO1*	0.0±0.0	0.0±0.0	0.0±0.0	0.0±0.0	0.0±0.0	0.0±0.0	0.0±0.0	0.0±0.0	0.0
ORx KETO1**	0.0±0.0	0.0±0.0	0.0±0.0	0.0±0.0	0.0±0.0	0.0±0.0	0.0±0.0	0.0±0.0	0.0
ORx KETO2*	11.7±0.4	6.6±0.4	0.0±0.0	4.2±0.1	1.0±0.1	3.3±0.9	2.8±0.1	0.8±0.0	30.4
ORx KETO2**	61.3±2.0	4.2±0.0	0.0±0.0	5.2±0.1	0.5±0.0	1.6±0.2	0.9±0.1	0.0±0.0	73.7

CARO2 had a higher carotenoid content compared to CARO1 [ca: 79 µg/g DW at 30 DAP (113-fold increase over WT) and ca: 155 µg/g DW (311-fold increase over WT) at 60 DAP]. At 30 DAP CARO2 accumulated mainly zeaxanthin (ca: 23 µg/g DW; 58-fold increase over WT), phytoene (ca: 18 µg/g DW), antheraxanthin (ca: 13 µg/g DW; 330-fold increase over

WT), β-carotene (ca: 11 µg/g DW) and lutein (ca: 9 µg/g DW; 47-fold increase over WT) followed by violaxanthin (ca: 2 µg/g DW; 24-fold increase over WT) and β-cryptoxanthin (ca: 2 µg/g DW). Similarly to CARO1, phytoene accumulation increased (ca: 117 µg/g DW) at the expense of downstream carotenoids at 60 DAP. Zeaxanthin (ca: 18 µg/g DW; 60-fold increase over WT), lutein (ca: 6 µg/g DW; 44-fold increase over WT) and β-carotene (ca: 8 µg/g DW) were the prevalent carotenoids followed by antheraxanthin (ca: 2 µg/g DW) and β-cryptoxanthin (ca: 2 µg/g DW) in mature seeds at 60DAP (**Table 2.4**). When OR was crossed with CARO2 to generate ORxCARO2, the carotenoid content and composition in the hybrid did not change substantially compared to CARO2 which already accumulated high amounts of carotenoids at 30 and 60 DAP. Total carotenoid conent in ORxCARO2 was ca: 79 µg/g DW and ca: 135 µg/g DW at 30 DAP and 60 DAP, respectively (**Table 2.4**).

Table 2.5 – Ketocarotenoid content and composition of wild-type (M37W) and transgenic lines OR, CARO1, CARO2, KETO1 and KETO2; and hybrids ORxCARO1, ORxCARO2, ORxKETO1 and ORxKETO2 T1 at 30 (*) and 60 DAP (**) (µg/g DW±SE) (n= 3-5 seeds). Abbreviations: Asta, astaxanthin; Cantha, canthaxanthin; Adonir, adonirubin; Adonix, adonixanthin; 3OH.echi, 3-OH-echinenone; KETO, ketocarotenoids.

Sample	Astax	Cantha	Adonir	Adonix	3OH.echi	TOTAL KETO
M37W*	0.0±0.0	0.0±0.0	0.0±0.0	0.0±0.0	0.0±0.0	0.0
M37W**	0.0±0.0	0.0±0.0	0.0±0.0	0.0±0.0	0.0±0.0	0.0
OR *	0.0±0.0	0.0±0.0	0.0±0.0	0.0±0.0	0.0±0.0	0.0
OR**	0.0±0.0	0.0±0.0	0.0±0.0	0.0±0.0	0.0±0.0	0.0
CARO1*	0.0±0.0	0.0±0.0	0.0±0.0	0.0±0.0	0.0±0.0	0.0
CARO1**	0.0±0.0	0.0±0.0	0.0±0.0	0.0±0.0	0.0±0.0	0.0
CARO2*	0.0±0.0	0.0±0.0	0.0±0.0	0.0±0.0	0.0±0.0	0.0
CARO2**	0.0±0.0	0.0±0.0	0.0±0.0	0.0±0.0	0.0±0.0	0.0
KETO1*	0.4±0.0	0.0±0.0	0.0±0.0	0.0±0.0	0.0±0.0	0.4
KETO1**	0.6±0.1	0.0±0.0	0.0±0.0	0.0±0.0	0.0±0.0	0.6
KETO2*	22.1±0.3	1.9±0.1	3.0±0.1	1.7±0.6	2.8±0.0	31.5
KETO2**	16.0±0.5	2.9±0.1	4.0±0.1	1.1±0.4	1.7±0.0	25.7
ORxCARO1*	0.0±0.0	0.0±0.0	0.0±0.0	0.0±0.0	0.0±0.0	0.0
ORxCARO2*	0.0±0.0	0.0±0.0	0.0±0.0	0.0±0.0	0.0±0.0	0.0
ORxCARO2**	0.0±0.0	0.0±0.0	0.0±0.0	0.0±0.0	0.0±0.0	0.0
ORxKETO1*	8.6±0.6	0.0±0.0	0.0±0.0	0.0±0.0	0.0±0.0	8.6
ORxKETO1**	8.1±0.3	0.0±0.0	0.0±0.0	0.0±0.0	0.0±0.0	8.1
ORxKETO2*	19.9±0.6	1.5±0.0	2.7±0.1	0.9±0.5	2.9±0.1	27.9
ORxKETO2**	9.4±0.4	2.0±0.0	2.6±0.1	0.6±0.2	1.5±0.0	16.1

KETO1 accumulated relatively low amounts of ketocarotenoids (ca: 0.4 µg/g DW at 30 DAP and ca: 0.6 µg/g DW at 60 DAP) and accumulated astaxanthin as the only carotenoid at both time points (ca: 0.4 and 0.6 µg/g DW at 30 and 60 DAP, respectively). Thus, the small amount of carotenoids present at basal levels in M37W was converted to ketocarotenoids as a result of the expression of the heterologous carotenoid β-hydroxylase (*sBrcrtZ*) and β-carotene ketolases (*sCrbkt* and *sBrcrtW*) (**Table 2.5**). In the case of ORxKETO1, the carotenoid profile was similar to the KETO1 parent but the total amount of carotenoids increased up to ca: 9 µg/g DW (22-fold increase over KETO1) at 30 DAP and ca: 8 µg/g DW (14-fold increase over KETO1) at 60 DAP. The only ketocarotenoid in ORxKETO1 was astaxanthin (ca: 9 µg/g DW; 22-fold increase over KETO1). At 60 DAP astaxanthin was the only ketocarotenoid (ca: 8 µg/g DW; 14-fold increase over KETO1) (**Table 2.4; Table 2.5**).

KETO2 accumulated high levels of ketocarotenoids compared to KETO1 [ca: 32 µg/g DW (80-fold increase over KETO1) and ca: 26 µg/g DW (17-fold increase over KETO1) at 30 and 60 DAP, respectively]. In addition, KETO2 accumulated ca: 33 µg/g DW and ca: 79 µg/g DW total carotenoids at 30 and 60 DAP, respectively. At 30 DAP it accumulated high amounts of astaxanthin (ca: 22 µg/g DW) and low amounts of other ketocarotenoids such as adonirubin (ca: 3 µg/g DW), 3-OH-echinenone (ca: 3 µg/g DW), canthaxanthin (ca: 2 µg/g DW) and adonixanthin (ca: 2 µg/g DW). It also accumulated small amounts of lutein (ca: 1 µg/g DW; 6-fold increase over WT) and other β,β-carotenes and xanthophylls compared to WT, including zeaxanthin (ca: 8 µg/g DW; 19-fold increase over WT), β-carotene (ca: 7 µg/g DW), antheraxanthin (ca: 5 µg/g DW; 113-fold increase over WT), β-cryptoxanthin (ca: 3 µg/g DW) and violaxanthin (ca: 1 µg/g DW; 8-fold over WT). In addition, it accumulated upstream precursors including lycopene (ca: 5 µg/g DW) and phytoene (ca: 4 µg/g DW). Similarly to CARO1 and CARO2, dry seeds from KETO2 accumulated higher amounts of the upstream precursor phytoene (ca: 54 µg/g DW) whereas downstream metabolites decreased. Astaxanthin was still the predominant ketocarotenoid at 60 DAP (ca: 16 µg/g DW), followed by adonirubin (ca: 4 µg/g DW), canthaxanthin (ca: 3 µg/g DW), 3-OH-equinenone (ca: 2 µg/g DW) and adonixanthin (ca: 1 µg/g DW) (**Table 2.5**). β-Carotene (ca: 12 µg/g DW) was the predominant carotene and zeaxanthin (ca: 6 µg/g DW; 21-fold increase over WT) was the predominant xanthophyll at 60 DAP. Levels of lutein were very low compared to CARO1 and CARO2 (ca: 1 µg/g DW) (**Table 2.4)**. When OR was crossed with KETO2 to generate

ORxKETO2 the carotenoid profile in the endosperm did not change substantially compared to KETO2 parent which accumulated high amounts of carotenoids and ketocarotenoids. ORxKETO2 accumulated ca: 30 µg/g DW and ca: 74 µg/g DW total carotenoids at 30 and 60 DAP, respectively, and ca: 28 µg/g DW and ca: 16 µg/g DW total ketocarotenoids at 30 and 60 DAP, respectively (**Table 2.4; Table 2.5**).

2.4.4 Transcript analysis of endogenous carotenoid and MEP pathway genes and *pftf* indicates no obvious changes in the levels of accumulation of these endogenous genes in hybrids and their respective parents

Quantitative real-time RT-PCR was used to compare relative transcript levels of endogenous carotenogenic genes, MEP pathway genes and *Zmpftf*, as described in section 2.3.1. Transcript levels of each gene in the WT were taken as reference (value 1.00). Levels of expression of each gene in transgenic lines CARO2 and KETO2 and their corresponding crosses ORxCARO2 and ORxKETO2 were compared relatively to the WT (**Figure 2.9**).

In CARO2, transcript levels of *Zmpsy2, Zmlyce, Zmbch2, Zmcyp97B, Zmcyp97C* in the carotenoid pathway, *Zmdxs1, Zmdxs3, Zmdxr* and *Zmhd* in the MEP pathway and *Zmpftf* remained the same as in the WT. Transcript levels of *Zmcyp97A, Zmbch1, Zmlycb* in the carotenoid pathway and *Zmdxs2* in the MEP pathway were higher in CARO2 compared with WT (ca: 2-, 3-, 6- and 11-fold increase over WT, respectively) and transcript levels of *psy1* increased substantially due to the expression of the transgene (ca: 10,000 fold increase over WT). In ORxCARO2, transcript analysis indicated that transcript levels of *Zmpsy2*, *Zmlyce*, *Zmcyp97B* and *Zmcyp97C* in the carotenoid pathway, *Zmdxs1, Zmdxs3* and *Zmhdr* in the MEP pathway and *Zmpftf* remained similar to WT. *Zmcyp97A* transcript levels were similar to WT and lower than in the CARO2 parent, whereas transcript levels of *Zmbch1* were higher than WT and similar to CARO2 in the hybrid. Transcript levels of *Zmpsy1* (ca: 5,600 fold increase over WT), *Zmlycb* (ca: 2-fold increase over WT) and *Zmdxs2* (ca: 7 fold-increase over WT) were higher than WT and lower than CARO2. Transcript levels of *Zmbch2* (ca: 3-fold increase over WT) and *Zmdxr* (ca: 2-fold increase over WT) were higher in ORxCARO2 than in WT and CARO2 parents.

In KETO2, transcript levels of *Zmpsy2*, *Zmlyce*, *Zmbch2* in the carotenoid pathway, *Zmdxs1, Zmdx3, Zmdxr* and *Zmhdr* in the MEP pathway and *Zmpftf* did not changed compared with WT. Transcript levels of *Zmlycb, Zmbch1, Zmcyp97A, Zmcyp97B, Zmcyp97C* and *Zmdxs2*

were higher (ca: maximum 4-fold) in KETO2 compared to WT. Levels of *psy1* increased substantially due to the expression of the transgene (ca: 1,000 fold increase over WT). In ORxKETO2 transcript levels of *Zmlyce*, *Zmbch2*, *Zmdxs1*, *Zmdxs3*, *Zmdxr* and *Zmpftf* were similar to WT. Transcript levels of *Zmcyp97A* and *Zmcyp97B* remained similar in ORxKETO2 line compared with WT but lower than KETO2 parent. However, transcript levels of *Zmpsy1*, *Zmpsy2*, *Zmlycb*, *Zmbch2*, *Zmhdr* and *Zmdxs2* were similar to KETO2 parent and higher than WT. Transcript levels of *Zmcyp97C* were similar to WT and KETO2.

GENES	WT	CARO2	ORxCARO2	KETO2	ORxKETO2	KETO1	ORxKETO1
***Zm*psy1**	1.00 d	9940 a	5585 b	1027 c	927 c	1.08 d	1.10 d
***Zm*psy2**	1.00 b	0.79 b	1.20 b	1.48 ab	2.34 a	1.03 b	1.05 b
***Zm*lyce**	1.00 ab	1.23 ab	1.91 a	0.83 b	1.06 ab	0.35 c	0.45 c
***Zm*lycb**	1.00 c	5.94 a	2.35 b	3.21 ab	2.34 b	0.85 c	0. 77 c
***Zm*bch1**	1.00 c	2.95 b	2.11 b	4.34 a	4.51 a	0.52 d	0.64 d
***Zm*bch2**	1.00 b	1.53 b	2.55 a	1.86 ab	1.75 ab	1.43 b	1.38 b
***Zm*cyp97A**	1.00 b	1.60 a	1.10 b	1.61 a	1.09 b	1.24 b	1.16 b
***Zm*cyp97B**	1.00 b	1.34 b	2.16 ab	3.25 a	2.17 ab	1.15 b	1.28 b
***Zm*cyp97C**	1.00 b	1.26 b	1.37 ab	2.20 a	1.51 ab	1.09 b	1.16 b
***Zm*dxs1**	1.00 b	1.01 b	0.68 b	0.81 b	0.67 b	0.83 b	1.40 a
***Zm*dxs2**	1.00 c	11.13 a	6.74 b	3.79 b	4.35 b	0.72 c	0.86 c
***Zm*dxs3**	1.00 a	0.90 a	1.21 a	0.94 a	1.80 a	0.69 a	0.75 a
***Zm*dxr**	1.00 b	1.06 b	1.64 a	1.05 b	0.83 b	0.42 c	1.08 b
***Zm*hdr**	1.00 b	1.80 ab	2.27 ab	2.92 ab	3.22 a	1.13 b	1.06 b
***Zm*pftf**	1.00 a	0.90 a	1.08 a	1.02 a	1.28 a	1.35 b	1.10 b

Figure 2.9 – Relative mRNA expression for endogenous carotenogenic genes, MEP pathway-related genes and Zmpftf in 30 DAP maize endosperm, normalized against actin mRNA and presented as the mean of three biological replicates. Transcript levels in WT (M37W) were taken as reference and given the value 1.00. Down-regulated and up-regulated gene expression compared with WT, shown in different intensity red and green color, respectively, corresponding to lower or higher values. Abbreviations: *Zmpsy1*, *phytoene synthase 1*; *Zmpsy2*, *phytoene synthase 2*; *Zmlyce*, *lycopene ε-cyclase*; *Zmlycb*, *lycopene β-cyclase*; *Zmbch1*, *carotenoid β-hydroxylase 1*; *Zmbch2*, *carotenoid β-hydroxylase 2*; *Zmcyp97A/B*, P450-*carotenoid β-hydroxylase*; *Zmcyp97C*, P450-*carotenoid ε-hydroxylase*, *Zmdxs1/2/3*, *1-Deoxy-D-xylulose-5-phosphate synthase*; *Zmdxr*, *1-Deoxy-D-xylulose-5-phosphate reductase*; *Zmhdr*, *methylbut-2-enyl-diphosphate reductase*; *Zmpftf*, plastid fusion/translocation factor. Different letters correspond to statistical significant different groups at P>0.01. Means not sharing the same letter are significantly different (Tukey HSD, $P < 0.05$).

In KETO1 transcript levels of *Zmpsy1*, *Zmpsy2*, *Zmbch2*, *Zmlycb*, *Zmcyp97A*, *Zmcyp97B*, *Zmcyp97C* in the carotenoid pathway, *Zmdxs1*, *Zmdxs2*, *Zmdxs3* and *Zmhdr* in the MEP pathway and *Zmpftf* remained similar to WT. Transcript levels of *Zmlyce* and *Zmbch1* were downregulated ca: maximum 3-fold in KETO1 over WT. Finally, transcript profile of carotenogenic genes, MEP pathway-related genes and *Zmpftf* in ORxKETO1 were similar to KETO1 with the exception of *Zmdxs1* which accumulated at statistically significant higher levels than in the WT. *Zmdxr* levels remained similar to the WT but were statistically significantly higher compared to KETO1 (**Figure 2.9**).

2.4.5. Increase of carotenoid content in diverse genetic backgrounds leads to the creation of a metabolic sink

Endosperm transmission electron microscopy (TEM) analysis of the first layer of cells under the epithelium of WT, OR, CARO1, CARO2, KETO1, KETO2 and ORxKETO1 at 30 DAP revealed electron-dense plastoglobuli inside plastids. Analysis of ORxCARO1, ORxCARO2 and ORxKETO2 were not performed due to the fact that no differences were observed in seed color phenotype, carotenoid content and endogenous gene expression amongst hybrids and their corresponding parents CARO1, CARO2 and KETO2. Plastoglobuli inside plastids of WT and KETO1 were present in very few plastids, whereas lines accumulating higher amounts of total carotenoids, CARO1, CARO2 and KETO2, contained many plastids with plastoglobuli. The number of plastoglobuli in OR and ORxKETO1 was higher compared to WT and KETO1, respectively (**Figure 2.10**).

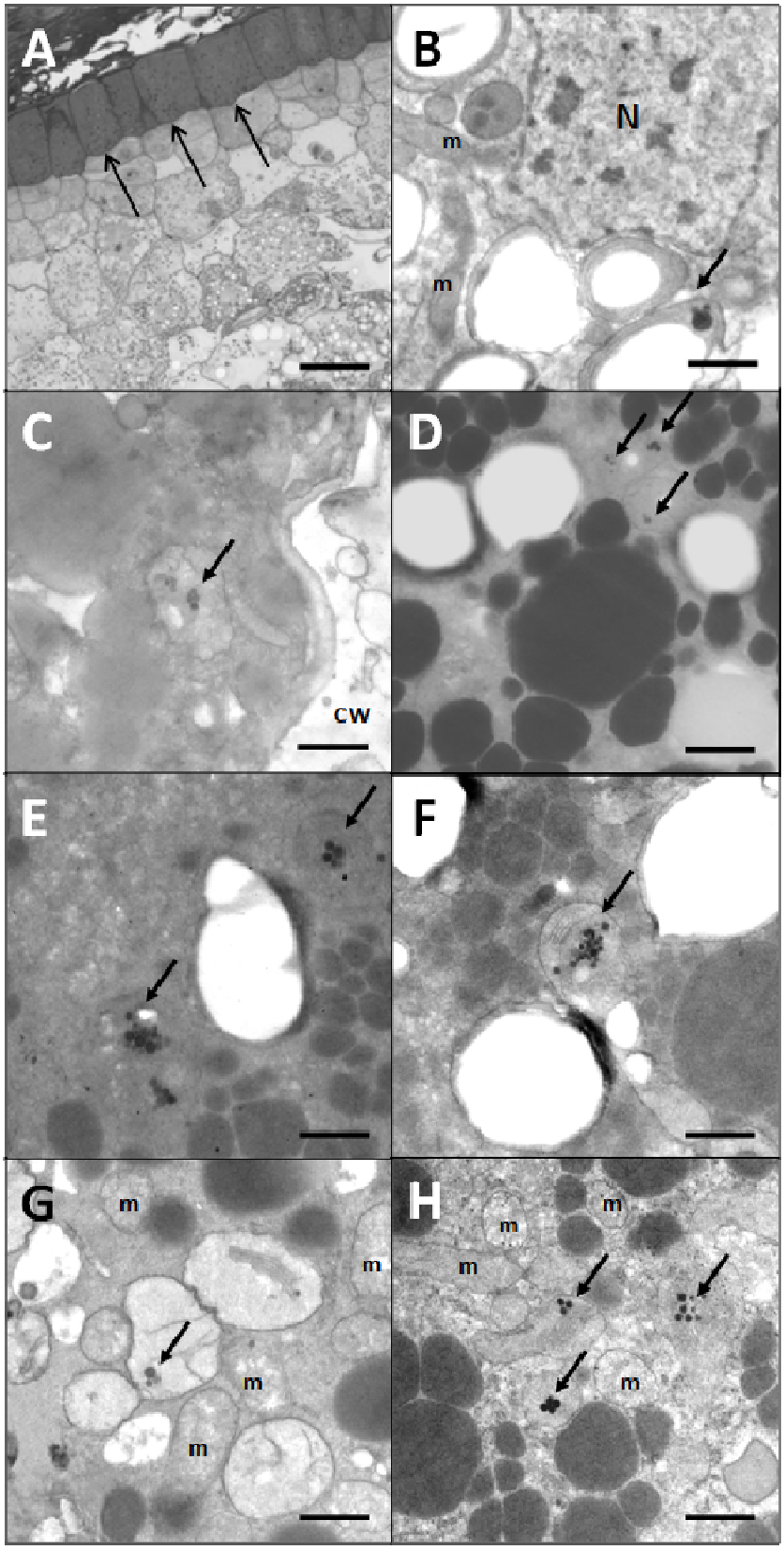

Figure 2.10 – Micrographs of 30 DAP endosperm from WT and transgenic maize lines OR, CARO1, CARO2, KETO1, KETO2 and ORxKETO1. A. Light micrograph of WT endosperm; arrows indicate aleurone cell layer. B-H Transmission electron microscopy of WT (B), OR (C), CARO1 (D), CARO2 (E), KETO2 (F), KETO1 (G) and ORxKETO1 (H). Arrows indicate plastoglobuli inside plastids. Abbreviations: m, mitochondria; cw, cell wall; N, nucleus. Scale bar: 30µm (A), 0.7 µm (B-H).

2.5 Discussion

2.5.1 The *AtOR* transgene enhances total carotenoid content without altering composition in the endosperm of hybrids only when the pre-existing carotenoid pool in the parents is low

The identification of a splicing mutation of the *orange* (*or*) gene (which is not a carotenoid pathway gene) increases carotenoid accumulation, especially β-carotene, via induction of chromoplast differentiation in cauliflower (Li et al. 2001). Thus, the generation of metabolic sink due to overexpression of *or* has been used as a strategy to increase carotenoid content in different plant species. In potato tubers cv. Desiree, overexpression of cauliflower *or* increased the carotenoid content, specially β-carotene, which continuously increased under cold storage (Lopez et al. 2008; Li et al. 2012). However, in potato tubers cv. Phureja no increase on cold storage was observed and carotenoid increased ca. 60%, mainly because of zeaxanthin, antheraxanthin, violaxanthin and lutein (Campbell et al. 2015). Different behavior in terms of carotenoid accumulation in different potato cultivars (cv. Desiree vs cv. Phureja) suggests that endogenous carotenoid profiles might influence the manner through which expression of the *or* gene affects carotenoid accumulation. In rice, the overexpression of Arabidopsis *OR* (*AtOR*) increases the carotenoid content of callus (Bai et al. 2014) and seeds (Bai et al. 2015) when it is overexpressed in combination with carotenogenic genes *Zmpsy1* and *PacrtI*. However, no increase of carotenoid content was observed when *AtOR* was overexpressed alone which suggest that chromoplast differentiation is primarily triggered by carotenoid accumulation above a certain threshold and that the presence of orange protein may augment or potentiate this process but is not sufficient without other drivers of carotenoid accumulation (Bai et al. 2014, 2015). Overexpression of sweetpotato *or* (*Ibor*) not only increases the β-carotene content in transgenic *Ibor* calli, but also significantly increases the α-carotene, lutein, β-crytoxanthin and zeaxanthin content suggesting that *Ibor* influences carotenogenic gene expression. The transgenic *Ibor* calli also exhibit increased antioxidant activity and tolerance to salt stress most likely because of the increase in carotenoid content (Kim et al. 2013). Furthermore, overexpression of *Ibor* in sweet potato resulted in ca: 3-fold increase of total carotenoid content although the composition was not influenced by the overexpression of *Ibor* since only pre-existing carotenoids in the non-transgenic control were elevated (Goo et al. 2015). Introduction of *IbOr-Ins* into purple-fleshed sweetpotato plants

enhanced both anthocyanin and carotenoid accumulation in their storage roots suggesting the generation of metabolic sink for pigments (Park et al. 2015).

In maize, I observed two distinct situations concerning the role of *AtOR* in increasing total carotenoid accumulation in the endosperm. In the first scenario, when pre-existing total carotenoids were low in the parent used to cross with OR (e.g. KETO1), introgression of *AtOR* increased the total carotenoid content up to 22-fold at 30 DAP in the corresponding hybrid (**Table 2.3**). Interestingly, carotenoid composition did not change suggesting that *AtOR* enhances carotenoid accumulation rather than modifying the endogenous carotenoid pathway. Carotenoid composition of KETO1 did not change substantially at 60 DAP compared to 30 DAP and the behavior of the hybrid (ORxKETO1) was similar to the parent (KETO1) revealing that carotenoid levels remain relatively constant throughout seed development in this line (**Figure 2.10**).

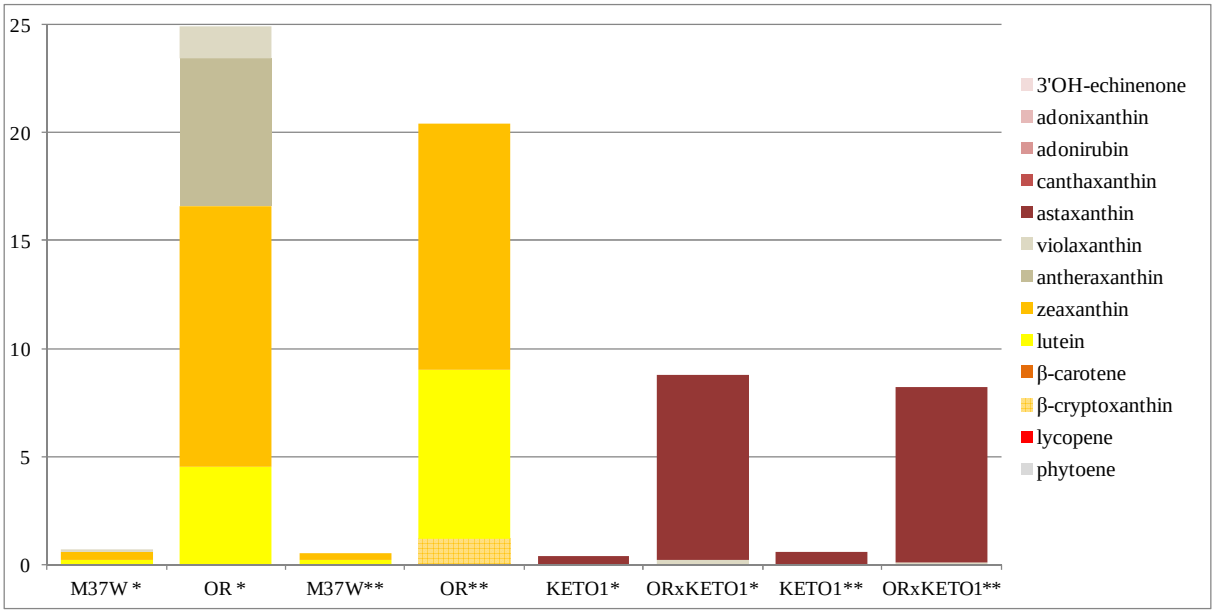

Figure 2.11 – Total carotenoid content and composition in wild-type M37W, transgenic lines OR and KETO1 and hybrid ORxKETO1 ORxKETO2 in T_1 generation at 30 DAP (*) and 60 DAP (**) (n=3-5 seeds).

The second situation is defined when the pre-existing total carotenoid content was high in the parent used to cross with OR (e.g. CARO1, CARO2 and KETO2). In this scenario *AtOR* did not influence carotenoid content and composition at 30 or 60 DAP in the resulting hybrids. Carotenoid composition of CARO1, CARO2 and KETO2 changed slightly at 60 DAP compared to 30 DAP mainly because of the increase of phytoene and reduction of other carotenoids such as lutein, zeaxanthin and antheraxanthin. The behavior of the hybrid was similar to the corresponding parent. Novel compounds accumulated in hybrids that were only

detected at trace amounts in the corresponding parents confirmed that AtOR increased the amount of pre-existing carotenoids (**Figure 2.11**).

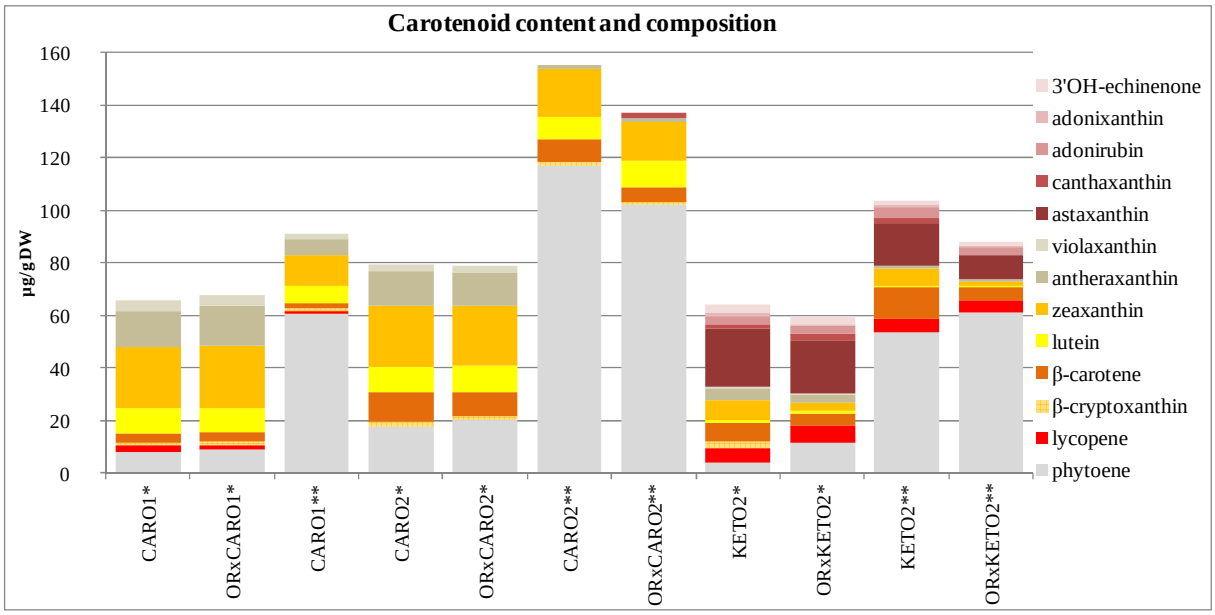

Figure 2. 12 – Carotenoid content and composition in CARO1, CARO2 and KETO 2; and hybrids ORxCARO1, ORxCARO2 and ORxKETO2 in T_1 generation at 30 DAP (*) and 60 DAP (**) (n=3-5 seeds).

2.5.2 Endogenous carotenoid biosynthetic genes, MEP pathway genes, and the *pftf* transcriptor factor are not upregulated in hybrids harboring the *AtOR* gene despite increases in total endosperm carotenoid content

In previous reports, there was no indication that the cauliflower *or* induced carotenoid biosynthesis gene expression (Li et al. 2001, 2006; Lu et al. 2006). However, it has been shown in potato that cauliflower *or* regulated stability of PSY protein, which provided higher enzyme activity for continuous biosynthesis of carotenoids during storage (Li et al. 2012). In addition, cauliflower OR protein may function in association with the molecular chaperone system to stabilize protein folding (Li et al. 2012). Furthermore, a recent report revealed that Arabidopsis OR proteins function as the major regulators of PSY protein and activity and that OR modulates carotenoid biosynthesis by means of post-transcriptional regulation of PSY (Zhou et al. 2015). In contrast, in sweet potato callus overexpression of *Ibor* revealed that increased carotenoid accumulation was via an upregulation of carotenoid biosynthetic genes *Ibpsy*, *Ibcrtiso*, *Iblycb* and *Ibbch* (Kim et al. 2013). Similarly, the overexpression of *Ibor* in an anthocyanin-rich purple-fleshed cultivar resulted in upregulation of carotenogenic genes *Ibpds*, *Ibzds*, *Iblycb*, *Ibbch* and *Ibzep*. Interestingly, *Iblyce* was downregulated and carotenoid

cleavage dioxygenases *Ibccd1*, *Ibccd4* and 9-cis-epoxycarotenoid dioxygenases (*nced*) were also upregulated (Goo et al. 2015; Park et al. 2015). In transgenic rice endosperm overexpressing *AtOR* resulted in upregulation of the endogenous carotenogenic genes *Oslyce*, *Oslycb* and *Osbch2* (Bai et al. 2015). These results suggested that *OR* might increase carotenoid content because of the upregulation of endogenous carotenoid biosynthetic pathway genes.

In maize, a detailed transcript analysis of carotenogenic genes revealed no dramatic changes in transcript accumulation in OR lines compared to wild-type, with the exception of ca: 2-fold downregulation of *Zmlyce*, which correlates with high zeaxanthin content in the OR lines because the metabolic flux was directed through β-branch of the pathway (**Figure 2.5**). Lower transcript levels of *Zmlyce* were also measured in KETO1 compared to WT (3-fold decrease), suggesting that extension of the carotenoid pathway to ketocarotenoids directs flux to the β-branch of the pathway. Lower transcript levels of *Zmlyce* compared to WT were also measured when OR was introgressed into a more complex transgenic maize line with a combination of a β-carotenoid hydroxylase gene (*sBrcrtZ*) and two carotenoid ketolase genes (*sCrbkt* and *sBrcrtW*) (ORxKETO1) even transcript levels were similar to OR and KETO1 parents (**Figures 2.6** and **2.8**). Thus, no synergistic effect was observed in transcript levels of *Zmlyce* in the ORxKETO1 hybrid. However, downregulation of *Zmlyce* transcript levels compared to WT was not observed in transgenic lines overexpressing carotenogenic genes (CARO1, CARO2 and KETO2) or their corresponding hybrids with OR (ORxCARO1, ORxCARO2 and ORxKETO2), suggesting that *AtOR* does not affect endogenous gene expression in this lines. Furthermore, transgenic lines overexpressing carotenogenic genes (CARO1, CARO2 and KETO2) and their corresponding hybrids with OR (ORxCARO1, ORxCARO2 and ORxKETO2) showed a significant increase of *Zmlycb* transcript levels suggesting that overexpression of carotenogenic genes directs the flux through the β-branch of the carotenoid pathway in the M37W background.

In order to assess the potential influence of *AtOR* on early precursors of the carotenoid pathway, *Zmdxs1*, *Zmdxs2*, *Zmdxs3*, *Zmdxr* and *Zmhdr* gene expression involved in the MEP pathway was evaluated. No changes in transcript levels of MEP pathway genes were measured in transgenic line overexpressing *AtOR* with the exception of ca: 2-fold upregulation of *Zmdxs1*, which might suggest slight flux increase in the carotenoid pathway resulting in increase of accumulation of carotenoids (**Figure 2.5**). Similar results were obtained when OR was introgressed into a more complex transgenic maize line with a

combination of a β-carotenoid hydroxylase gene (*sBrcrtZ*) and two carotenoid ketolase genes (*Crbkt* and *sBrcrtW*) (ORxKETO1). However, upregulation of *Zmdxs1* transcript levels compared to WT was not observed in transgenic lines overexpressing carotenogenic genes (CARO1, CARO2 and KETO2) and their corresponding hybrids with OR (ORxCARO1, ORxCARO2 and ORxKETO2) (**Figure 2.8**). Furthermore, transgenic lines overexpressing carotenogenic genes (CARO1, CARO2 and KETO2) and their corresponding hybrids with OR (ORxCARO1, ORxCARO2 and ORxKETO2) exhibited a significant increase of *Zmdxs2* transcript levels compared to WT, suggesting that overexpression of carotenogenic genes produces a positive feedback regulation and increases the metabolic flux through the carotenoid pathway in M37W background. In Arabidopsis callus, the effect of *AtOR* in the expression of two MEP pathway genes (*AtDXS* and *AtDXR*) was evaluated, resulting in up to 1.2- and 1.3-fold increase over WT, respectively (Yuan et al. 2015). However, authors concluded that expression of carotenoid biosynthetic genes were not greatly affected in *AtOR* callus (Yuan et al. 2015).

The plastid fusion/translocation factor *pftf* is known to be involved in chromoplast differentiation in red pepper (Hugueney et al. 1995). Overexpression of *Ibor* resulted in increase of *pftf* transcript levels in sweet potato callus and tubers, suggesting that chromoplast formation is triggered (Kim et al. 2013; Goo et al. 2015; Park et al. 2015). No changes in the Zm*pftf* transcript levels were observed in transgenic maize hybrids in which *AtOR* was introgressed compared to WT (**Figure 2.8**), suggesting that *AtOR* does not trigger chromoplast formation by itself.

2.5.3 Formation of carotenoid-rich plastoglobuli in endosperm tissues is due to high levels of newly synthesized carotenoids rather than a direct effect of *AtOR* gene expression

The cauliflower *or* gene is the only known gene that acts as a *bona fide* molecular switch to trigger chromoplasts differentiation of non-colored plastids into chromoplasts (Li et al. 2006; Lu et al. 2006; Li et al. 2012). In addition, *or* induced the formation of chromoplasts containing carotenoid sequestering structures in potato, which were not observed in tubers of potato cultivars that accumulate high levels of carotenoids (Lopez et al. 2008). Recently, alteration of a single amino acid in a wild-type OR greatly enhanced its ability to promote carotenoid accumulation by triggering biogenesis of membranous chromoplasts in

Arabidopsis callus without altering carotenogenic gene expression (Yuan et al. 2015). However, morphological changes in plastids have been observed in tomato fruits and canola endosperm expressing PSY (Shewmaker et al. 1999; Fraser et al. 2007; Nogueira et al. 2013). These observations suggest that plastids are modified to accommodate increased levels of carotenoids produced in them. Overexpression of PSY can also induce crystalline-type carotenoid sequestering structures in Arabidopsis callus, suggesting that the chromoplast differentiation program may be a response to the accumulation of carotenoids above a certain threshold unless differentiation is triggered by OR before this threshold is reached (Maass et al. 2009). In transgenic rice, *AtOR* expression might influence carotenoid levels both directly and indirectly. Chromoplast differentiation is primarily triggered by carotenoid accumulation above a certain threshold and the presence of *AtOR* protein may augment and potentiate this process. However, expression of *AtOR* alone is not sufficient to trigger chromoplast differentiation as no evidence that AtOR triggers chromoplast differentiation in the absence of carotenogenic transgenes (*Zmpsy1* and *PacrtI*) (Bai et al. 2014, 2015). Storage organs of many species synthesize and deposit carotenoids primarily in amyloplast membranes (Li et al. 2012). Amyloplasts serve as a crystalline-type β-carotene sequestering sink (Cao et al. 2012). These carotenoid sequestering structures have 2 roles: (1) sequester excess carotenoid away from plastid membranes, thus stimulating their continuous biosynthesis and (2) are a stable deposition sink that protects carotenoids from degradation (Li et al. 2012). Amyloplasts in maize contain carotenoids (Wurtzel 2004). In maize, I observed amyloplasts and other plastids containing electron-dense plastoglobuli that might contain low amounts of carotenoids in a low carotenoid genetic background (M37W and KETO1). More plastoglobuli were observed in high carotenoid maize backgrounds (CARO1, CARO2 and KETO2). In addition, overexpression of AtOR in OR line and in ORxKETO1, the hybrid resulting from OR and KETO1 cross, resulted in a substantial increase in the amount of plastoglobuli containing plastids, as well as in the number of plastoglobuli inside the plastids. These observations suggest that plastoglobuli are formed as a result of the increase in the carotenoid content in transgenic lines. Recently, it has been reported in Arabidopsis callus that *AtOR* that did not change the appearance of the plastids *per se* but alteration of a single amino acid in *AtOR* results in generation of plastids containing larger and electron-dense plastoglobuli. *AtOR* mutant rather than *AtOR* appears to be a unique protein able to mediate chromoplast biogenesis (Yuan et al. 2015).

2.6 Conclusions

The Arabidopsis *ORANGE* gene (*AtOR*) has been overexpressed in the white endosperm M37W inbred line. I characterized two independent transgenic lines overexpressing AtOR. Both lines exhibited an increase in carotenoid content without any concomitant upregulation of endogenous carotenogenic, or MEP pathway genes, with the exception of *Zmdxs1*. I conclude that the increased carotenoid content by overexpression of *AtOR* is not due to upregulation of endogenous transcript levels. The highest carotenoid accumulating line was crossed with different transgenic lines with diverse carotenoid profiles. In cases in which the original transgenic parent crossed with the OR line accumulated low levels of total carotenoids, resulting hybrids exhibited a substantial increase of carotenoid content without any changes in the qualitative carotenoid composition. No changes at the metabolite and transcript profile levels were observed in the hybrids when the carotenoid content in the original parents used to cross with the OR line was high. Overexpression of *Zmpsy1* alone or in combination with other carotenogenic genes in maize endosperm resulted in the formation of plastoglobuli structures that are known to act as a metabolic sink for carotenoids inside plastids. These structures were also observed in the original OR line and also in the resulting hybrids derived from parent with a low carotenoid content suggesting that a metabolic sink inside plastids can also be generated as a result of substantial increases in carotenoid content.

2.7 References

Bai C, Capell T, Berman J, Medina V, Sandmann G, Christou P, et al. (2015) Bottlenecks in carotenoid biosynthesis and accumulation in rice endosperm are influenced by the precursor-product balance. Plant Biotechnol J. (in press) DOI: 10.1111/pbi.12373.

Bai C, Rivera SM, Medina V, Alves R, Vilaprinyo E, Sorribas A, et al. (2014) An in vitro system for the rapid functional characterization of genes involved in carotenoid biosynthesis and accumulation. Plant J. 77:464–475.

Camara B, Hugueney P, Bouvier F, Kuntz M, Monéger R (1995) Biochemistry and molecular biology of chromoplast development. Int Rev Cytol. 163:175–247.

Campbell R, Morris WL, Mortimer CL, Misawa N, Ducreux LJM, Morris JA, et al. (2015) Optimising ketocarotenoid production in potato tubers: Effect of genetic background, transgene combinations and environment. Plant Sci. 234:27–37.

Cao H, Zhang J, Xu J, Ye J, Yun Z, Xu Q, et al. (2012) Comprehending crystalline β-carotene accumulation by comparing engineered cell models and the natural carotenoid-rich system of cytrus. J Exp Bot. 63:4403–4417.

Christensen AH, Quail PH (1996) Ubiquitin promoter-based vectors for high-level expression of selectable and/or screenable marker genes in monocotyledonous plants. Transgenic Res. 5:213–218.

Christou P, Ford TL, Kofron M (1991) Production of Transgenic Rice (Oryza Sativa L.) Plants from Agronomically Important Indica and Japonica Varieties via Electric Discharge Particle Acceleration of Exogenous DNA into Immature Zygotic Embryos. Nature 9:957–962.

Crisp P, Walkey DGA, Bellman E, Roberts E (1975) A mutation affecting curd colour in cauliflower (*Brassica oleracea* L. var. Botrytis DC). Euphytica. 24:173–176.

Cunningham FX, Gantt E (1998) Genes and enzymes of carotenoid biosynthesis in plants. Annu Rev Plant Physiol Plant Mol Biol. 49:557–583.

Fraser PD, Enfissi EMA, Halket JM, Truesdale MR, Yu D, Gerrish C, et al. (2007) Manipulation of Phytoene Levels in Tomato Fruit : Effects on Isoprenoids, Plastids, and Intermediary Metabolism. Plant Cell. 19:3194–3211.

Goo Y-M, Han E-H, Jeong JC, Kwak S-S, Yu J, Kim Y-H, et al. (2015) Overexpression of the sweet potato *IbOr* gene results in the increased accumulation of carotenoid and confers tolerance to environmental stresses in transgenic potato. C R Biol. 338:12–20.

Hugueney P, Bouvier F, Badillo A, D'Harlingue A, Kuntz M, Camara B (1995) Identification of a plastid protein involved in vesicle fusion and/or membrane protein translocation. Proc Natl Acad Sci U S A. 92:5630–5634.

Kim SH, Ahn YO, Ahn MJ, Jeong JC, Lee HS, Kwak SS (2013) Cloning and characterization of an *Orange* gene that increases carotenoid accumulation and salt stress tolerance in transgenic sweetpotato cultures. Plant Physiol Biochem. 70:445–454.

Li L, Lu S, Cosman KM, Earle ED, Garvin DF, O'Neill J (2006) β-Carotene accumulation induced by the cauliflower *Or* gene is not due to an increased capacity of biosynthesis. Phytochemistry. 67:1177–1184.

Li L, Paolillo DJ, Parthasarathy M V, Dimuzio EM, Garvin DF, Plant US, et al. (2001) A novel gene mutation that confers abnormal patterns of β-carotene accumulation in cauliflower (Brassica oleracea var. botrytis). Plant J. 26:59–67.

Li L, Yang Y, Xu Q, Owsiany K, Welsch R, Chitchumroonchokchai C, et al. (2012) The or gene enhances carotenoid accumulation and stability during post-harvest storage of potato tubers. Mol Plant. 5:339–352.

Li L, Yuan H (2013) Chromoplast biogenesis and carotenoid accumulation. Arch Biochem Biophys. 539:102–109.

Lopez AB, Van Eck J, Conlin BJ, Paolillo DJ, O'Neill J LL (2008) Effect of the cauliflower Or transgene on carotenoid accumulation and chromoplast formation in transgenic potato tubers. J Exp Bot. 59:213–223.

Lu S, Van Eck J, Zhou X, Lopez AB, O'Halloran DM, Cosman KM et al. (2006) The cauliflower *Or* gene encodes a DnaJ cysteine-rich domain-containing protein that mediates high levels of beta-carotene accumulation. Plant Cell. 18:3594–3605.

Maass D, Arango J, Wüst F, Beyer P, Welsch R (2009) Carotenoid crystal formation in Arabidopsis and carrot roots caused by increased phytoene synthase protein levels. PLoS One. 4:e6373.

Nishida Y, Adachi K, Kasai H, Shizuri Y, Shindo K, Sawabe A, et al. (2005) Elucidation of a carotenoid biosynthesis gene cluster encoding a novel enzyme, 2,2'-beta-hydroxylase, from *Brevundimonas* sp. strain SD212 and combinatorial biosynthesis of new or rare xanthophylls. Appl Environ Microbiol. 71:4286–4296.

Nogueira M, Mora L, En EMA, Bramley PM, Fraser PD (2013) Subchromoplast Sequestration of Carotenoids Affects Regulatory Mechanisms in Tomato Lines Expressing Different Carotenoid Gene Combinations. Plant Cell. 25:1–20.

Paolillo DJ, Garvin DF, Parthasarathy MV (2004) The chromoplasts of Or mutants of cauliflower (*Brassica oleracea* L. var. botrytis). Protoplasma. 224:245–253.

Park SC, Kim SH, Park S, Lee HU, Lee JS, Park WS, et al. (2015) Enhanced accumulation of carotenoids in sweetpotato plants overexpressing IbOr-Ins gene in purple-fleshed sweetpotato cultivar. Plant Physiol Biochem. 86:82–90.

Schreier PH, Seftor EA, Schell J, Bohnert HJ (1985) The use of nuclear-encoded sequences to direct the light-regulated synthesis and transport of a foreign protein into plant chloroplasts. EMBO J 4:25–32.

Shewmaker CK, Sheehy JA, Daley M, Colburn S, Ke DY (1999) Seed-specific overexpression of phytoene synthase: Increase in carotenoids and other metabolic effects. Plant J. 20:401–412.

Sugio T, Satoh J, Matsuura H, Shinmyo A, Kato K (2008) The 5'-untranslated region of the *Oryza sativa* alcohol dehydrogenase gene functions as a translational enhancer in monocotyledonous plant cells. J Biosci Bioeng. 105(3):300–302.

Wurtzel ET (2004) Chapter five Genomics, genetics, and biochemistry of maize carotenoid biosynthesis. Recent Adv Phytochem. 38:85–110.

Yuan H, Owsiany K, Sheeja TE, Zhou X, Rodriguez C, Li Y, et al. (2015) A Single Amino Acid Substitution in an ORANGE Protein Promotes Carotenoid Overaccumulation in Arabidopsis. Plant Physiol. 169:421–431.

Zhong Y-J, Huang J-C, Liu J, Li Y, Jiang Y, Xu Z-F, et al. (2011) Functional characterization of various algal carotenoid ketolases reveals that ketolating zeaxanthin efficiently is essential for high production of astaxanthin in transgenic Arabidopsis. J Exp Bot. 62:3659–3669.

Zhou X, Welsch R, Yang Y, Álvarez D, Riediger M, Yuan H, et al. (2015) Arabidopsis OR proteins are the major posttranscriptional regulators of phytoene synthase in controlling carotenoid biosynthesis. Proc Natl Acad Sci. 112:3558–3563.

Zhu C, Naqvi S, Breitenbach J, Sandmann G, Christou P, Capell T (2009) Combinatorial genetic transformation generates a library of metabolic phenotypes for the carotenoid pathway in maize. Proc Natl Acad Sci U S A. 105:18232–18237.

CHAPTER 3

Increased β-carotene content in maize endosperm through RNAi-mediated silencing of carotenoid β-hydroxylase (*Zmbch1* and *Zmbch2*) in different genetic backgrounds

CHAPTER 3: INCREASED β-CAROTENE CONTENT IN MAIZE ENDOSPERM THROUGH RNAi-MEDIATED SILENCING OF CAROTENOID β-HYDROXYLASES IN DIFFERENT GENETIC BACKGROUNDS

3.1 Abstract

I generated independent transgenic maize lines in which the carotenoid β-hydroxylases *Zmbch1* and *Zmbch2* were downregulated. A RNAi-cassette was introgressed into different maize genetic backgrounds selected on the basis of their carotenoid profile in order to evaluate the effect of silencing the two hydroxylases on carotenoid content and composition in the resulting hybrids. β-Carotene content increases substantially in all hybrids in which *Zmbch1* and *Zmbch2* was silenced confirming that carotenoid β-hydroxylases play a key role in the conversion of β-carotene to zeaxanthin. I also investigated carotenoid accumulation of the α-branch of the pathway because *Zmbch1* is the only non-heme di-iron carotenoid β-hydroxylase involved in lutein synthesis. Interestingly, transcript accumulation of carotenoid ε-hydroxylase (*Zmcyp97C*) decreased in hybrids compared to the highest expressing parents.

3.2 Introduction

Non-heme di-iron carotenoid β-hydroxylases (BCH) and heme-containing cytochrome P450 hydroxylases (CYP-type hydroxylases) are primarily responsible carotenoid hydroxylation. They exhibit overlapping activities, most notably in the hydroxylation of the β-ring of α-carotene (Kim et al. 2009). Studies involving mutants suggested that CYP97A and CYP97C are responsible for catalyzing the hydroxylation of the β- and ε-rings of α-carotene, respectively, while BCH1 and BCH2 catalyze the two β-ring hydroxylations of β-carotene (Kim and DellaPenna 2006; Sun et al. 1996; Tian and Dellapenna 2001; Tian et al. 2003) (**Figure 3.1**).

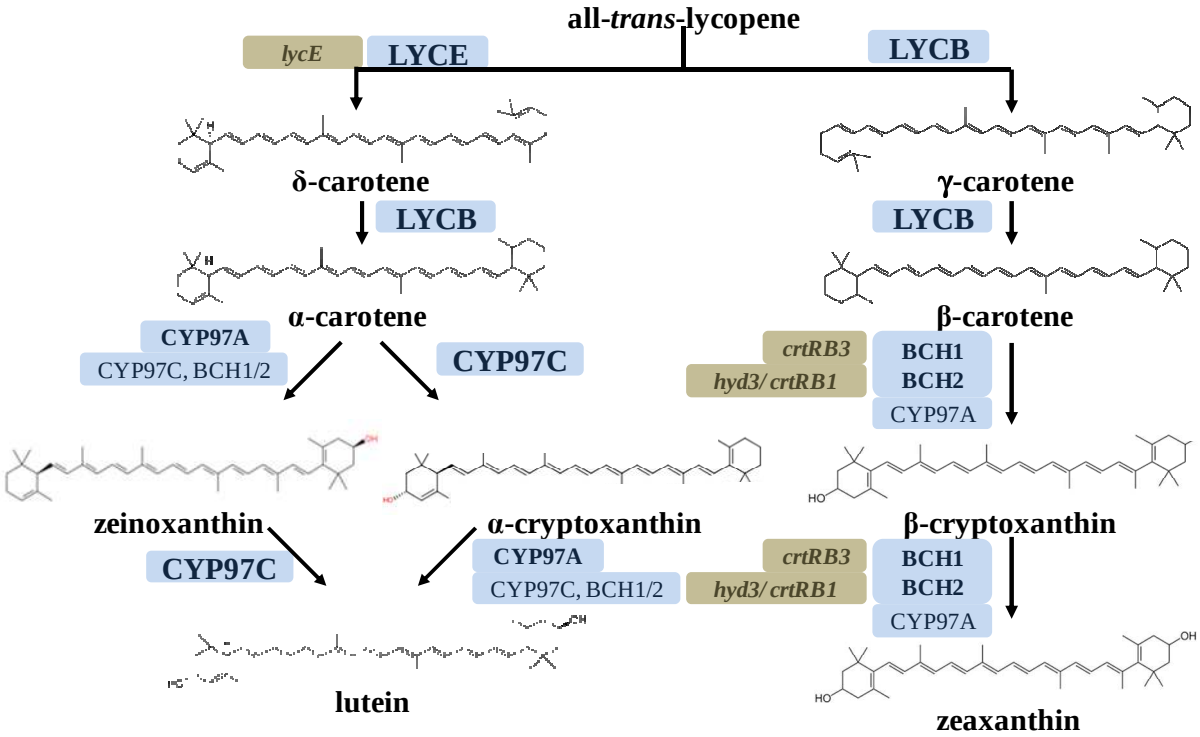

Figure 3.1 – Xanthophyll biosynthetic pathway. The gene(s) encoding the major activity at each step are shown in bold (blue). Identified maize locus name corresponding to each enzyme is shown in brown. Abbreviations: LYCB, lycopene β-cyclase; LYCE, lycopene ε-cyclase; CYP97C, heme-containing cytochrome P450 carotene ε-ring hydroxylase; CYP97A, heme-containing cytochrome P450 carotene β-ring hydroxylase; BCH1/2, Non-heme di-iron β-carotene hydroxylases (Adapted from Kim et al. 2009).

In maize, the natural genetic diversity allowed identification of hydroxylation genes associated with reduced β-carotene content in the endosperm (Vallabhaneni et al. 2009). *Hyd3* locus in chromosome 10, also named *crtRB1*, encodes for BCH2 (Vallabhaneni et al. 2009; Yan et al. 2010; Babu et al. 2013) (Figure 3.1). Alleles associated with reduced transcript accumulation correlate with higher β-carotene concentrations and decreased β-cryptoxanthin and zeaxanthin content, revealing its importance in the hydroxylation of the β-ring of β-carotene and β-cryptoxanthin (Yan et al. 2010). Maize hybrids with higher β-carotene content were generated by introgression of reduced transcript accumulation of *crtRB1* (Muthusamy et al. 2014). The gene encoding BCH1 is *crtRB3*, and acts as a β-hydroxylase (Zhou et al. 2012). An additional locus with allelic variation that correlates with high β-carotene content is *lycE*. This allele directs flux into the α-branch of the pathway reducing levels of β,β-carotenoids (Harjes et al. 2008). Carotenoid cleavage dioxygenase 1 (*ccd1*) that produces apocarotenoids mainly from lycopene, β-carotene and zeaxanthin, also has alleles associated with reduced transcript that correlate with higher β-carotene amounts (Messias et al. 2014).

In order to develop a better understanding of the roles of BCH1 and BCH2 in carotenoid biosynthesis in maize endosperm, a combination of conventional breeding and metabolic engineering approaches can be helpful. First, conventional breeding allowed identification of *bch1* and *bch2* as key genes for β-carotene enhancement (Vallabhnaneni et al. 2009; Zhou et al. 2012). *CrtRB1* alleles have been correlated with high β-carotene content and the introgression of these alleles has been carried out in elite inbred lines resulting in up to 12-fold increase of β-carotene content over the recurrent parent (Muthusamy et al. 2014). However, introgression of specific *crtRB1* alleles to the recurrent parent requires extensive field trials and it is time-consuming. Thus, down-regulation of *bch1* and *bch2* through metabolic engineering can facilitate the generation of novel lines with low expression of these enzymes and high β-carotene content.

Very few commercial maize lines are amenable to genetic transformation. Transformation of the elite South African M37W inbred line with a RNA interference (RNAi) construct that down regulates expression of *bch1* and *bch2* allowed the generation of maize lines in which lower transcript levels of *bch1* and *bch2*. A number of studies using RNAi gene silencing in plants have been reported. For example down-regulation of the endogenous photomorphogenesis regulatory gene, *det1*, under the control of a fruit-specific promoter in tomato increased carotenoid and flavonoid contents, whereas other parameters of fruit quality were largely unchanged (Davuluri et al. 2005). Similarly, *det1* was down regulated in *Brassica napus* seeds to increase the levels of carotenoids and reduce the levels of sinapate esters (Wei et al. 2009). Down-regulation of 9-cis e-epoxycarotenoid dioxygenase (*nced*), which catalyzes epoxidation of zeaxanthin to antheraxanthin and violaxanthin resulted in tomato fruit with increased accumulation of upstream carotenoids such as lycopene [1.6-fold; 220 µg/g fresh weight (FW)] and β-carotene (2-fold; 40 µg/g FW) (Sun et al. 2012). In potato, the introduction of an antisense fragment to block the expression of *lyce* resulted in 14-fold increased β-carotene accumulation (ca: 43 µg/g DW) (Diretto et al. 2006). Silencing of *bch* increased β-carotene levels from trace amounts in wild type potato tubers up to 331µg/100 g FW in transgenic tubers (Van Eck et al. 2007). In transgenic sweet potato callus (*Ipomoea batatas*), the β-carotene content was approximately 21-fold higher than in controls, whereas the lutein content was reduced to undetectable levels when *lyce* was down regulated (Kim et al. 2013). Sweet orange plants (cv. Pineapple) have also been targeted to block *bch* through RNAi resulting in oranges with a deep orange phenotype and significant increases (up to 36-fold; ca: 114ng/g FW) in β-carotene content in the pulp (Pons et al. 2014).

After identification of transgenic maize lines with down regulated *bch1* and *bch2* expression, self-pollination was performed to homozygosis. These lines were subsequently used as donors to pollinate different lines with specific carotenoid composition in order to evaluate the effect of silencing *bch* in different maize genetic backgrounds (**Table 3.1**).

3.3 Materials and methods

3.3.1 Gene cloning and vector construction

Zmbch2 cDNA fragment of *Zea mays* was cloned by RT-PCR using forward primer 5´-ggaattctctagactatcgcttcagctggcaaatggag-3´ (*Eco*RI and *Xba*I sites are underlined) and reverse primer 5´-gactagtggatccaacttgtccatgtggtgtatcttg-3´ (*Bam*HI and *Spe*I sites are underlined) based on sequence information in GenBank (accession number: AY844958) and suitable restriction sites were incorporated subsequently by PCR. Genes were sub-cloned into the pHorP vector containing the barley D-hordein promoter, a 300 bp-long *gusA* gene fragment and the ADP-glucose pyrophosphorylase terminator (ADGPP). To incorporate the target gene fragments into pHorP the vector was digested with *Xba*I and *Bam*HI to introduce the sense *bch* fragment between the barley D-hordein promoter and the *gusA* gene fragment, resulting in pHorP-*bch* sense. In the second step, the plasmid was digested with *Spe*I and *Eco*RI, to introduce the antisense *bch* fragment between the *gusA* gene fragment and ADGPP terminator, resulting in pHorP-RNAi-*bch* (**Figure 3.2**).

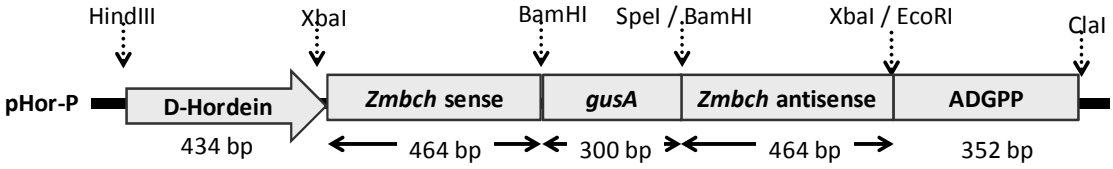

Figure 3.2 – Schematic representation of pHorP-RNAi-*Zmbch*.

3.3.2. Maize transformation and plant growth

The maize transformation protocol is described in detail in Chapter 2 section 2.2.2. Homozygous lines listed in **Table 3.1** were grown under the conditions described in Chapter 2 section 2.2.2.

Table 3.1 – Maize lines with specific carotenoid accumulation used in this study to evaluate the effect of BCH downregulation by RNAi.

Line	Genotype	Source	Carotenoid profile	References
B73	Inbred	USDA	High lutein Very low β/ε ratio	(Harjes et al. 2008) (Vallabhaneni and Wurtzel 2009)
C17	Inbred	USDA	High β-carotene High β/ε ratio	(Yan et al. 2010)
NC356	Inbred	USDA	High zeaxanthin Very high β/ε ratio	(Yan et al. 2010)
Psy1	Transgenic Zmpsy1	Applied plant biotechnology, Universitat de Lleida, Spain	High zeaxanthin and β-carotene High β/ε ratio	See chapter 2
O1-3	Transgenic AtOR	Applied plant biotechnology, Universitat de Lleida, Spain	High zeaxanthin Medium β/ε ratio	See chapter 2
O2-9	Transgenic AtOR	Applied plant biotechnology, Universitat de Lleida, Spain	High zeaxanthin Medium β/ε ratio	See chapter 2

USDA: United States Department of Agriculture
CSIC: Consejo Superior de Investigaciones Científicas

3.3.3 RNA extraction and cDNA synthesis

The protocols are described in detail in Chapter 1, section 1.2.2.

3.3.4. RNA blot analysis

The protocol is described in detail in Chapter 1, section 1.2.7.

3.3.5. Real-time qRT-PCR

The protocol is described in detail in Chapter 2 section 2.2.5.

3.3.6. Carotenoid extraction and UPLC analysis

This protocol is described in detail in section 2.2.6.

3.4 Results

3.4.1 Transgenic maize lines with RNAi-mediated gene silencing of *Zmbch1* and *Zmbch2*

I transformed fourteen-day-old immature zygotic embryos of South African elite white maize inbred M37W by bombarding them with gold particles coated with a RNAi construct specifically designed to downregulate endogenous β-carotene hydroxylase 2 (*Zmbch2*) in the endosperm under selection with the *bar* gene. Because of the high homology (96.4%) at the DNA level between *Zmbch1* and *Zmbch2*, the same RNAi construct was expected to also downregulate *Zmbch1*. This was confirmed by the results as described subsequently. Regenerated plants were self-pollinated to homozygosity (T_3). mRNA blot analysis of T_3 endosperm at 30 DAP revealed that endogenous *Zmbch2* was totally silenced in two of the transgenic lines (B1 and B7) and substantially but not completely in two additional lines (B9 and B13) (**Figure 3.3**).

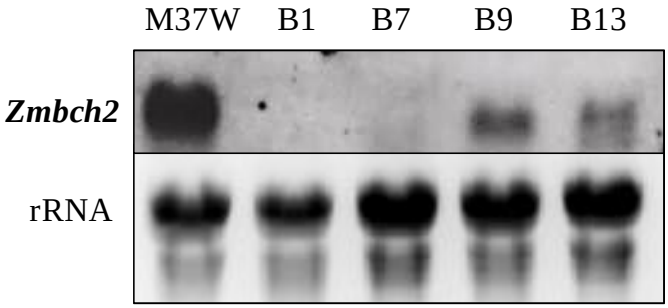

Figure 3.3 – mRNA blot analysis (25 µg of total RNA per lane) was used to monitor *Zmbch2* mRNA accumulation in the endosperm at 30 DAP of wild type (M37W) and independent transgenic lines B1, B7, B9 and B13

Zmbch1 transcript levels were not detectable by mRNA blot so quantitative RT-PCR was used to determine transcript accumulation for this gene in M37W and the transgenic lines. *Zmbch1* was downregulated in all transgenic lines ca: 3-fold compared to M37W (**Figure 3.4**).

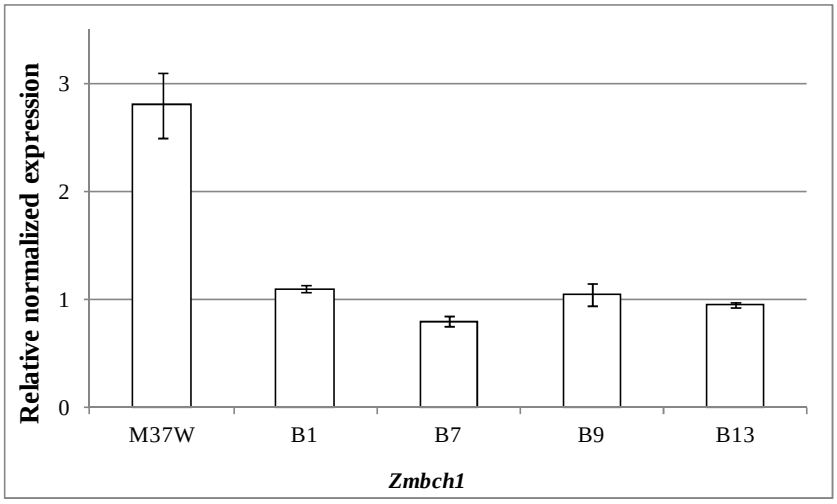

Figure 3. 4 – Transcript levels of endogenous *Zmbch1* gene in wild-type (M37W) and transgenic lines B1, B7, B9 and B13 presented as mean of three technical replicates ± SD (n=3-5 seeds)

3.4.2 Carotenoid composition in inbred lines used as parents to introgress RNAi*bch*

Transgenic lines B7 and B13 in which *Zmbch1* transcript levels were silenced at similar levels, and simultaneously *Zmbch2* transcript levels were silenced totally or partially, respectively, in the same two lines, were used to generate hybrids with different inbred lines. The wild type inbred parents had diverse carotenoid profiles. The purpose of these experiments was to investigate the impact of the different degrees of silencing of carotene β-hydroxylases (BCH) introgressed into the hybrids, on carotenoid accumulation in immature maize endosperm. Inbred lines B73 and C17 accumulated lutein as the predominant carotenoid and lines NC356, O1-3, O2-9 and psy1 accumulated zeaxanthin as the predominant carotenoid (**Figure 3.5**).

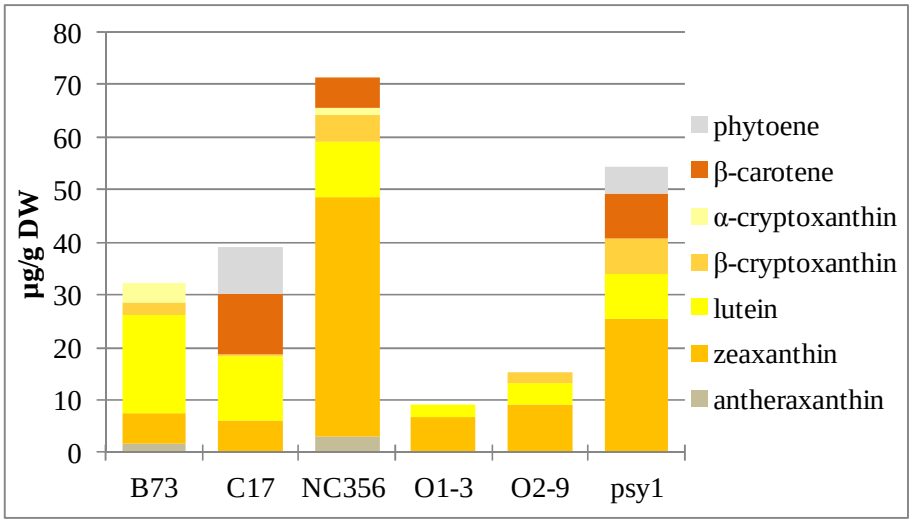

Figure 3. 5 – Carotenoid composition of lines used to cross with B7 and B13.

Different parents, selected on the basis of their endosperm carotenoid content and composition, were crossed with B7 and B13 to generate the corresponding hybrids following the scheme shown in **Figure 3.6**. T_1 hybrid seeds were collected at 30 DAP and kept at -80ºC until further analysis to determine carotenoid content and composition, and transcriptomic analysis of endogenous β-carotene hydroxylases. Crosses B7xO1-3, B7xO2-9 could not be obtained due to technical problems so they were not included in further analysis.

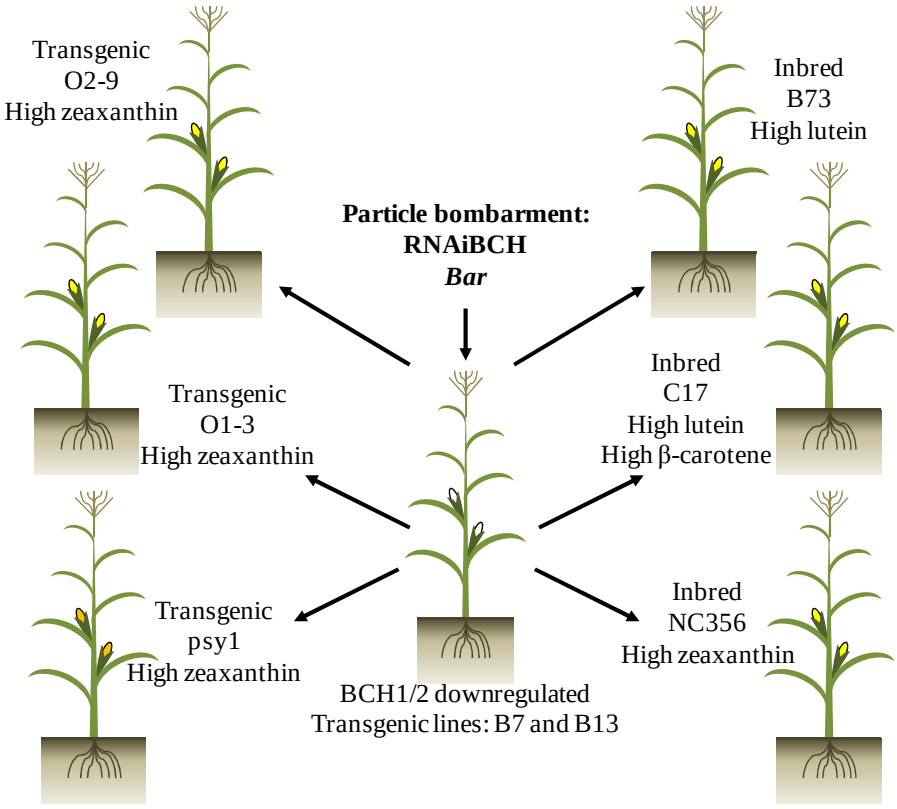

Figure 3. 6 - Schematic representation indicating how the hybrids were generated. Transgenic lines B7 and B13 in which *Zmbch1* and *Zmbch2* were silenced were used to pollinate B73 and C17 (accumulating lutein as the predominant carotenoid), NC356, O1-3, O2-9 and psy1 (accumulating zeaxanthin as the predominant carotenoid).

3.4.3 Carotenoid content and composition of hybrids derived from parents with diverse carotenoid profiles and transgenic line in which endogenous *Zmbch1* and *Zmbch2* were silenced

Endosperm carotenoid content and composition of M37W, B7, B13, B73, C17, NC356, O1-3, O2-9 and psy1 and the corresponding hybrids (B7xB73, B13xB73, B7xC17, B13xC17, B7xNC356, B13xNC356, B13xO1-3, B13xO2-9, B7xpsy1 and B13xpsy1) was evaluated at 30 DAP (**Table 3.2**).

Table 3. 2 – Carotenoid content and composition of wild-type (M37W), B7, B13, B73, C17, NC356, O1-3, O2-9 and psy1 parents and the corresponding hybrids at 30 DAP (µg/g DW±SE) (n= 3-5 seeds). The percentage of individual carotenoids in the endosperm is shown in brackets. Abbreviations: anthera, antheraxanthin; zea, zeaxanthin; lut, lutein; β-crypto, β-cryptoxanthin; α-crypto, α-cryptoxanthin; β-caro, β-carotene; phyto, phytoene; total caro, total carotenoids

Plant line	anthera µg/g DW (%)	zea µg/g DW (%)	lut µg/g DW (%)	β-crypto µg/g DW (%)	α-crypto µg/g DW (%)	β-caro µg/g DW (%)	phyto µg/g DW (%)	Total caro µg/g DW
WT	0.0±0.00 (0)	2.0±0.10 (59)	1.1±0.00 (32)	0.0±0.00 (0)	0.0±0.00 (0)	0.0±0.00 (0)	0.3±0.00 (9)	3.4
B7	0.0±0.00 (0)	2.8±0.27 (60)	1.9±0.19 (40)	0.0±0.00 (0)	0.0±0.00 (0)	0.0±0.00 (0)	0.0±0.00 (0)	4.7
B13	0.3±0.02 (6)	2.5±0.19 (57)	1.7±0.14 (37)	0.0±0.0 (0)	0.0±0.00 (0)	0.0±0.00 (0)	0.0±0.00 (0)	4.5
B73	1.5±0.09 (5)	6.1±0.38 (19)	18.6±0.93 (57)	2.8±0.23 (8)	3.6±0.18 (11)	0.0±0.00 (0)	0.0±0.00 (0)	32.6
B7x B73	1.2±0.04 (3)	7.4±0.23 (17)	18.1±0.18 (43)	3.3±0.24 (8)	3.5±0.20 (8)	7.1±0.45 (17)	1.8±0.12 (4)	42.4
B13x B73	0.9±0.05 (3)	4.6±0.06 (13)	18.5±0.04 (54)	1.8±0.24 (5)	1.8±0.05 (5)	5.8±0.21 (17)	0.7±0.02 (2)	34.1
C17	0.0±0.00 (0)	6.2±0.20 (16)	12.0±0.30 (31)	0.6±0.03 (1)	0.0±0.00 (0)	11.4±0.90 (29)	8.7±0.02 (22)	38.9
B7x C17	0.8±0.01 (2)	7.3±0.20 (19)	9.0±0.21 (24)	2.6±0.15 (7)	1.0±0.01 (3)	12.6±0.17 (33)	4.8±0.13 (13)	38.1
B13x C17	0.4±0.01 (1)	11.2±0.22 (25)	8.5±0.18 (19)	2.8±0.03 (6)	1.2±0.01 (3)	14.9±0.51 (34)	5.4±0.11 (12)	44.4
NC356	3.0±0.19 (4)	45.5±0.78 (62)	10.8±0.17 (15)	5.0±0.25 (7)	3.7±0.16 (5)	5.9±0.41 (8)	0.0±0.00 (0)	73.9
B7x NC356	3.0±0.04 (3)	23.7±0.04 (23)	22.7±0.5 (22)	10.5±0.19 (10)	11.9±0.28 (12)	26.0±1.00 (25)	4.9±0.15 (5)	102.7
B13x NC356	2.2±0.00 (3)	13.2±0.17 (19)	20.2±0.10 (29)	3.0±0.19 (4)	5.2±0.16 (7)	25.3±1.40 (36)	0.4±0.00 (1)	69.5
O1-3	0.2±0.02 (2)	6.5±0.38 (61)	2.6±0.08 (25)	1.3±0.01 (12)	0.0±0.00 (0)	0.0±0.00 (0)	0.0±0.00 (0)	10.6
B13x O1-3	0.5±0.03 (7)	3.4±0.36 (45)	1.1±0.1 (14)	0.9±0.05 (12)	0.5±0.02 (6)	1.2±0.03 (15)	0.0±0.00 (0)	7.6
O2-9	0.0±0.00 (0)	9.3±2.02 (62)	3.9±0.35 (26)	1.9±0.40 (13)	0.0±0.00 (0)	0.0±0.00 (0)	0.0±0.00 (0)	15.1
B13x OR2-9	0.8±0.06 (7)	6.5±0.04 (53)	2.2±0.08 (18)	1.2±0.01 (9)	0.6±0.05 (5)	1.8±0.04 (15)	0.0±0.00 (0)	13.1
psy1	0.0±0.00 (0)	25.5±2.14 (47)	8.5±0.35 (16)	6.6±0.29 (12)	0.0±0.00 (0)	8.7±0.75 (16)	5.0±0.18 (9)	54.3
B7x psy1	4.5±0.05 (4)	23.8±0.19 (22)	12.3±0.17 (12)	10.5±0.25 (10)	9.3±0.09 (9)	29.9±0.49 (28)	15.7±0.10 (15)	106.0
B13x psy1	4.2±0.3 (5)	19.2±0.25 (23)	7.3±0.15 (9)	5.9±0.12 (7)	4.6±0.03 (5)	20.7±0.09 (25)	23.0±0.18 (27)	84.9

B7 and B13 transgenic lines accumulated similar amounts of total carotenoids (ca: 4.5 µg/g DW) as M37W (ca: 3 µg/g DW). In both lines zeaxanthin (ca: 2.5 µg/g DW) predominated over lutein (ca: 2 µg/g DW). Traces of antheraxanthin accumulated in B13 but not in B7 transgenic lines (**Table 3.2; Figure 3.7**).

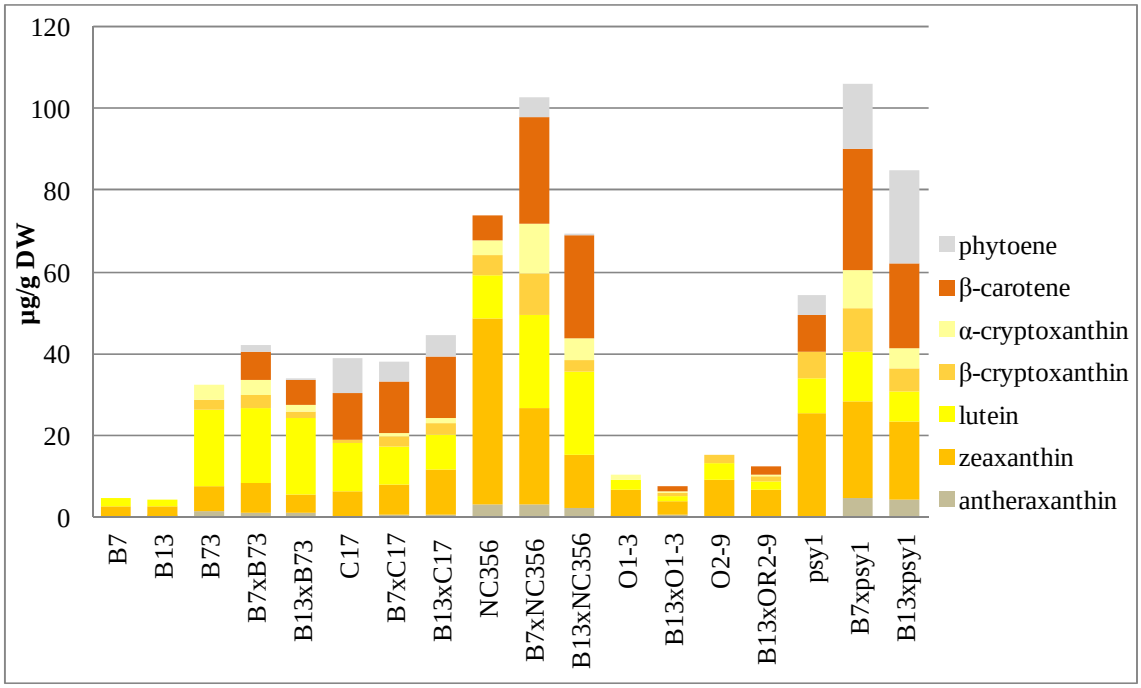

Figure 3. 7 – Carotenoid composition of B7, B13, B73, C17, NC356, O1-3, O2-9, psy1 and the corresponding hybrids with B7 and B13 at 30 DAP.

3.4.3.1 Carotenoid content and composition in hybrids and corresponding parents accumulating higher amounts of ε-carotenoids relatively to β-carotenoids

B73 accumulated high amounts of ε-carotenoids relatively to β-carotenoids. Lutein (ca: 19 µg/g DW) was the predominant carotenoid followed by zeaxanthin (ca: 6 µg/g DW), α-cryptoxanthin (ca: 4 µg/g DW), β-cryptoxanthin (ca: 3 µg/g DW) and antheraxanthin (ca: 2 µg/g DW). Total carotenoid content in B73 was ca: 33 µg/g DW. Total carotenoids in B7xB73 increased 1.3-fold to ca: 42 µg/g DW. Lutein (ca: 18 µg/g DW; no changes compared to B73) and zeaxanthin (ca: 7 µg/g DW; 1.2-fold increase compared to B73) were the predominant carotenoids in the hybrid, whereas β-cryptoxanthin (ca: 3 µg/g DW; 1.3-fold decrease compared to B73), α-cryptoxanthin (ca: 3 µg/g DW; no changes compared to B73) and antheraxanthin (ca: 1 µg/g DW; 1.3-fold decrease compared to B73) accounted for the rest of carotenoids. Interestingly, β-carotene (ca: 7 µg/g DW) and phytoene (ca: 2 µg/g DW) which were absent in B73, accumulated in the hybrid. Total carotenoid content in B13xB73 was ca: 34 µg/g DW, which was not significantly different from B73 parent. Lutein was the predominant carotenoid in the hybrid (ca: 19 µg/g DW; no changes compared to B73) followed by zeaxanthin (ca: 5 µg/g DW; 1.3-fold decrease compared to B73), β-cryptoxanthin (ca: 2 µg/g DW; 1.4-fold decrease compared to B73), α-cryptoxanthin (ca: 2 µg/g DW; 2-fold decrease compared to B73) and traces of antheraxanthin. Interestingly, β-carotene (ca: 6 µg/g

DW) and traces of phytoene (ca: 1 µg/g DW) which were absent in B73, accumulated in the hybrid (**Table 3.2; Figure 3.7**).

C17 accumulates high amounts of ε-carotenoids relative to β-carotenoids. Lutein (ca: 12 µg/g DW) and β-carotene (ca: 11 µg/g DW) were the predominant carotenoids followed by phytoene (ca: 9 µg/g DW) and zeaxanthin (ca: 6 µg/g DW) whereas traces of β-cryptoxanthin (ca: 1 µg/g DW) accounted for the remaining carotenoids in this line. The total carotenoid content in C17 was ca: 39 µg/g DW. Total carotenoid content in B7xC17 was ca: 38 µg/g DW, which was not significantly different from C17 parent. β-carotene (ca: 13 µg/g DW; 1.1-fold increase compared to C17) was the predominant carotenoid followed by lutein (ca: 9 µg/g DW; 1.3-fold decrease compared to C17), zeaxanthin (ca: 7 µg/g DW; 1.2-fold increase compared to C17), phytoene (ca: 5 µg/g DW; 1.8-fold decrease compared to C17) and β-cryptoxanthin (ca: 3 µg/g DW; 4.4-fold increase compared to C17). Traces of α-cryptoxanthin (ca: 1 µg/g DW) and antheraxanthin (ca: 1 µg/g DW), which were absent in C17, accumulated in the hybrid. Total carotenoids in B13xC17 hybrid increased by 1.1-fold to ca: 44 µg/g DW. β-carotene (ca: 15 µg/g DW; 1.2-fold increase compared to C17) was the predominant carotenoid followed by zeaxanthin (ca: 11 µg/g DW; 1.8-fold increase compared to C17), lutein (ca: 8 µg/g DW; 1.4-fold decrease compared to C17), phytoene (ca: 5 µg/g DW; 1.6-fold decrease compared to C17) and β-cryptoxanthin (ca: 3 µg/g DW; 4.9-fold increase compared to C17). Traces of α-cryptoxanthin (ca: 1 µg/g DW) and antheraxanthin (ca: 0.5 µg/g DW), which were absent in C17, accumulated in the hybrid (**Table 3.2; Figure 3.7**).

3.4.3.2 Carotenoid content and composition in hybrids and corresponding parents accumulating higher amounts of β-carotenoids relatively to ε-carotenoids

NC356 accumulates the highest amount of total carotenoids among all lines (ca: 74 µg/g DW). Zeaxanthin (ca: 46 µg/g DW) and lutein (ca: 11 µg/g DW) were the predominant carotenoids. β-Carotene (ca: 6 µg/g DW), β-cryptoxanthin (ca: 5 µg/g DW), α-cryptoxanthin (ca: 4 µg/g DW) and antheraxanthin (ca: 3 µg/g DW) accounted for the remaining carotenoids in this line). Total carotenoids in B7xNC356 increased by 1.4-fold to ca: 103 µg/g DW. β-carotene (ca: 26 µg/g DW; 4.4-fold increase compared to NC356) was the predominant carotenoid followed by zeaxanthin (ca: 24 µg/g DW; 1.9-fold decrease compared to NC356), lutein (ca: 23 µg/g DW; 2.1-fold increase compared to NC356), α-cryptoxanthin (ca: 12 µg/g DW; 3.2-fold increase compared to NC356) and β-cryptoxanthin (ca: 11 µg/g DW; 2.1-fold increase compared to NC356). Phytoene (ca: 5 µg/g DW), which was absent in NC356,

accumulated in the hybrid and antheraxanthin (ca: 3 µg/g DW; no changes compared to NC356) accounted for the rest of carotenoids. Total carotenoid content in B13xNC356 decreased was ca: 68 µg/g DW, which was not significantly different from NC356. β-carotene (ca: 25 µg/g DW) was the predominant carotenoid followed by lutein (ca: 20 µg/g DW; 1.9-fold increase compared to NC356), zeaxanthin (ca: 13 µg/g DW; 3.4-fold decrease compared to NC356), α-cryptoxanthin (ca: 5 µg/g DW; 1.4-fold increase compared to NC356), β-cryptoxanthin (ca: 3 µg/g DW; 1.7-fold decrease compared to NC356) and antheraxanthin (ca: 2 µg/g DW; 1.4-fold decrease). Traces of phytoene, which were absent in NC356, accumulated in the hybrid (**Table 3.2; Figure 3.7**).

O1-3 accumulated high amounts of β-carotenoids relative to ε-carotenoids. Zeaxanthin (ca: 6 µg/g DW) was the predominant carotenoid followed by lutein (ca: 3 µg/g DW). β-cryptoxanthin (ca: 1 µg/g DW) and traces of antheraxanthin accounted for the rest of carotenoids (ca: 11 µg/g DW). Total carotenoids in B13xO1-3 decreased by 1.4-fold to ca: 8 µg/g DW. Zeaxanthin (ca: 3 µg/g DW; 1.9-fold decrease compared to O1-3) was the predominant carotenoid followed by lutein (ca: 1 µg/g DW; 2.4-fold decrease compared to O1-3), β-cryptoxanthin (ca: 1 µg/g DW; 1.4-fold decrease compared to O1-3) and traces of antheraxanthin. Interestingly, β-carotene (ca: 1 µg/g DW) and traces of α-cryptoxanthin, which were absent in O1-3 accumulated in the hybrid. Unfortunately, the cross B7xO1-3 was not possible due to technical problems (**Table 3.2; Figure 3.7**).

O2-9 accumulated high amounts of β-carotenoids relative to ε-carotenoids. Zeaxanthin (ca: 9 µg/g DW) was the predominant carotenoid followed by lutein (ca: 4 µg/g DW). β-cryptoxanthin (ca: 2 µg/g DW) accounted for the rest of carotenoids (ca: 15 µg/g DW). Total carotenoids in B13xO2-9 decreased by 1.2-fold to ca: 13 µg/g DW. Zeaxanthin (ca: 7 µg/g DW; 1.4-fold decrease compared to O2-9) was the predominant carotenoid followed by lutein (ca: 2 µg/g DW; 1.8-fold decrease compared to O2-9) and β-cryptoxanthin (ca: 1 µg/g DW; 1.6-fold decrease compared to O2-9). Interestingly, β-carotene (ca: 2 µg/g DW) and traces of α-cryptoxanthin and antheraxanthin, which were absent in O2-9 accumulated in the hybrid. Unfortunately, the cross B7xO2-9 was not possible due to technical problems (**Table 3.2; Figure 3.7**).

Psy1 accumulated high amounts of β-carotenoids relative to ε-carotenoids. Zeaxanthin (ca: 26 µg/g DW), β-carotene (ca: 9 µg/g DW), lutein (ca: 9 µg/g DW), β-cryptoxanthin (ca: 7 µg/g DW) and phytoene (ca: 5 µg/g DW) accounted for ca: 54 µg/g DW total carotenoids. Total

carotenoids in B7xpsy1 increased by 2-fold to ca: 106 µg/g DW. β-carotene (ca: 30 µg/g DW; 3.4-fold increase compared to psy1), zeaxanthin (ca: 24 µg/g DW; no changes compared to psy1) and phytoene (ca: 16 µg/g DW; 3.1-fold increase compared to psy1) were the predominant carotenoids followed by lutein (ca: 12 µg/g DW; 1.4-fold increase compared to psy1) and β-cryptoxanthin (ca: 11 µg/g DW; 1.6-fold increase compared to psy1). α-Cryptoxanthin (ca: 9 µg/g DW) and antheraxanthin (ca: 5 µg/g DW) which were absent in psy1, accumulated in the hybrid. Total carotenoids in B13xpsy1 increased by 1.6-fold to ca: 85 µg/g DW. β-carotene (ca: 21 µg/g DW; 2.4-fold increase compared to psy1), phytoene (ca: 23 µg/g DW; 4.6-fold increase compared to psy1) and zeaxanthin (ca: 19 µg/g DW; 1.3-fold decrease compared to psy1) were the predominant carotenoids followed by lutein (ca: 7 µg/g DW; 1.2-fold decrease compared to psy1) and β-cryptoxanthin (ca: 6 µg/g DW; 1.1.-fold decrease compared to psy1). α-Cryptoxanthin (ca: 5 µg/g DW) and antheraxanthin (ca: 4 µg/g DW) which were absent in psy1, accumulated in the hybrid (**Table 3.2; Figure 3.7**).

3.4.5 Transcriptomic analysis of transgenes and endogenous carotene β- and ε-hydroxylase genes in maize hybrids reveals different expression profiles amongst hybrids due to the effect of RNAi-mediated gene silencing

Endosperm samples (30 DAP) were frozen in liquid nitrogen and stored at -80ºC until RNA extraction was performed to measure transgene expression by qRT-PCR (**Figure 3.8**). As expected, transgene transcript levels were not detected in M37W, B7 and B13 endosperm; *AtOR* transcripts were detected in O1-3, O2-9 and the corresponding hybrids B13xO1-3 and B13xO2-9; *Zmpsy1* transcripts were detected in psy1 line and the corresponding hybrids B7xpsy1 and B13xpsy1 (**Figure 3.8**).

A comparison amongst hydroxylase transcript accumulation in M37W relatively to *Zmbch1* revealed that *Zmbch1* and *Zmcyp97C* transcripts accumulated at similar levels in the wild type. Transcript levels of *Zmcyp97A* and *Zmcyp97B* in the wild type were 18- and 9-fold higher, respectively, than *Zmbch1* levels whereas transcript levels of *Zmbch2* were 150-fold higher than *Zmbch1* (**Figure 3.9**).

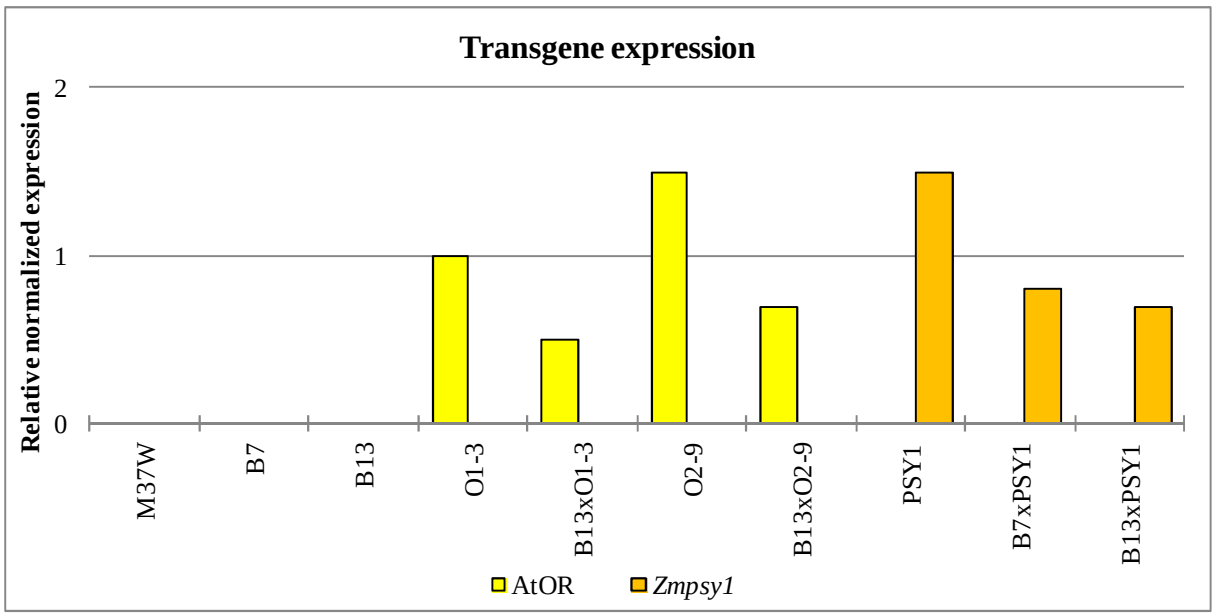

Figure 3. 8 – Transgene expression normalized against actin in the wild-type (M37W) and transgenic lines presented as mean of three technical replicates. Standard error bars were not included because of the use of technical replicates rather than biological replicates. The aim was to show expression of the introduced transgenes rather than compare different transcript profiles.

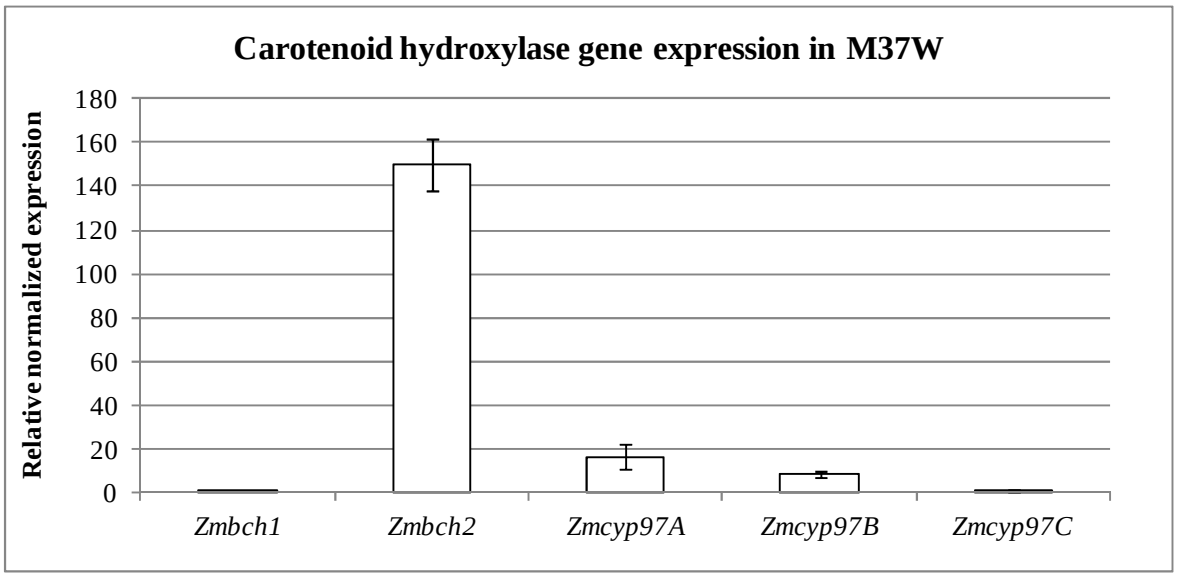

Figure 3. 9 – Relative mRNA accumulation of endogenous hydroxylase genes in wild type (M37W); *Zmbch1*, *Zmbch2*, *Zmcyp97A*, *Zmcyp97B* and *Zmcyp97C* in 30 DAP maize endosperm, normalized against actin mRNA, relative to *Zmbch1* and presented as the mean of three technical replicates ± SE. Abbreviations: *Zmbch1*, *carotenoid β-hydroxylase 1*; *Zmbch2*, *carotenoid β-hydroxylase 2*; *Zmcyp97A/B, carotene ε-hydroxylase*; *Zmcyp97C*.

In addition to transgenes, endogenous hydroxylases *Zmbch1*, *Zmbch2*, *Zmcyp97A*, *Zmcyp97B* and *Zmcyp97C* were analyzed at 30 DAP in M37W, B73, C17, NC356, O1-3, O2-9 and psy1 and the hybrids generated with B7 and B13 (B7xB73, B13xB17, B7xC17, B13xC17, B7xNC356, B13xNC356, B13xO1-3, B13xO2-9, B7xpsy1 and B13xpsy1 (**Figure 3.10**). Transcript levels of *Zmbch1* and *Zmbch2* were downregulated in both transgenic lines (B7

and B13) ca: 1.5 and ca: 2-fold, respectively compared to wild type. mRNA accumulation of *Zmcyp97A* and *Zmcyp97B* were similar in B7 and B13 lines over M37W. However, *Zmcyp97C* was ca: 3.5-fold decreased compared to M37W (**Figure 3.10**).

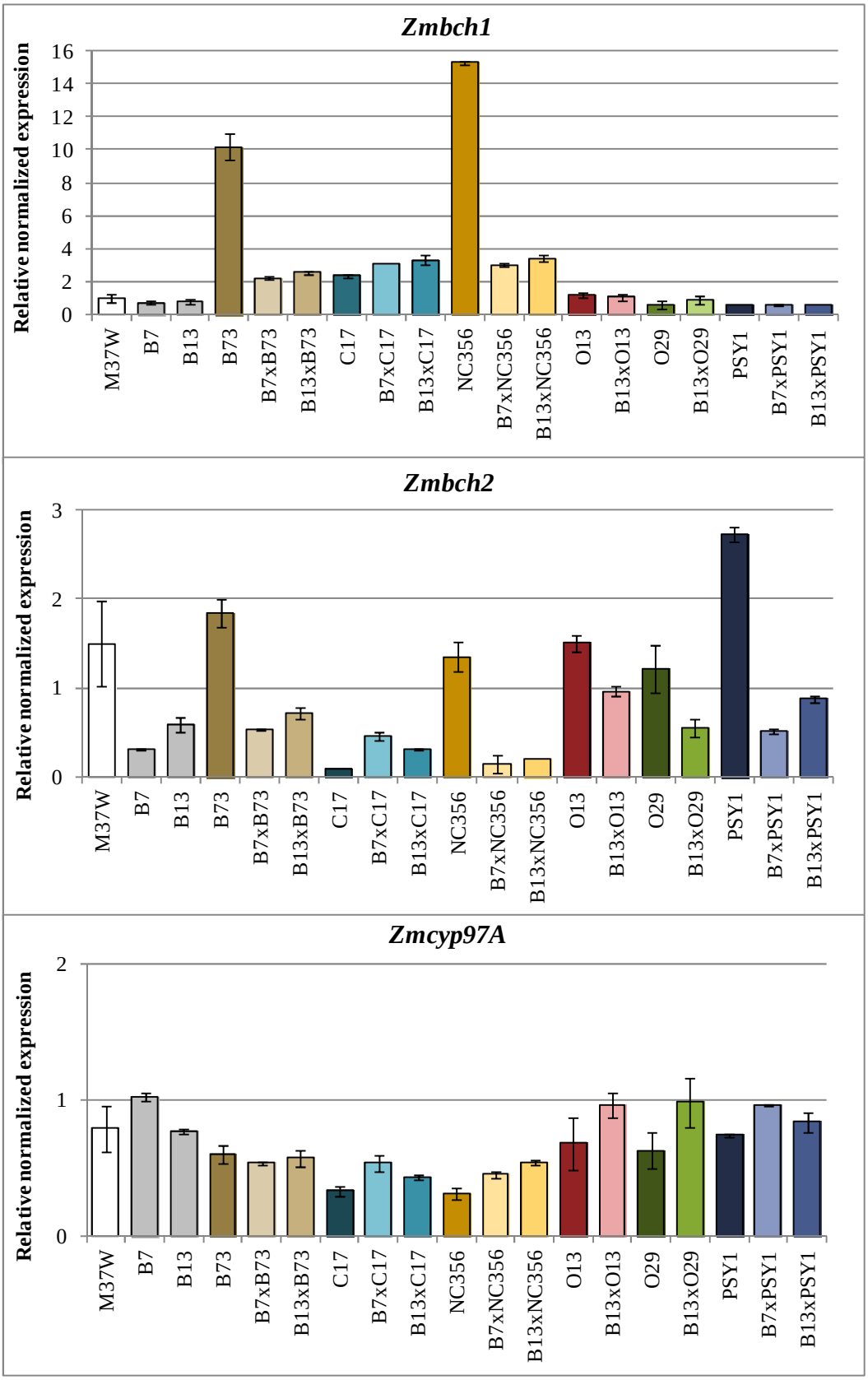

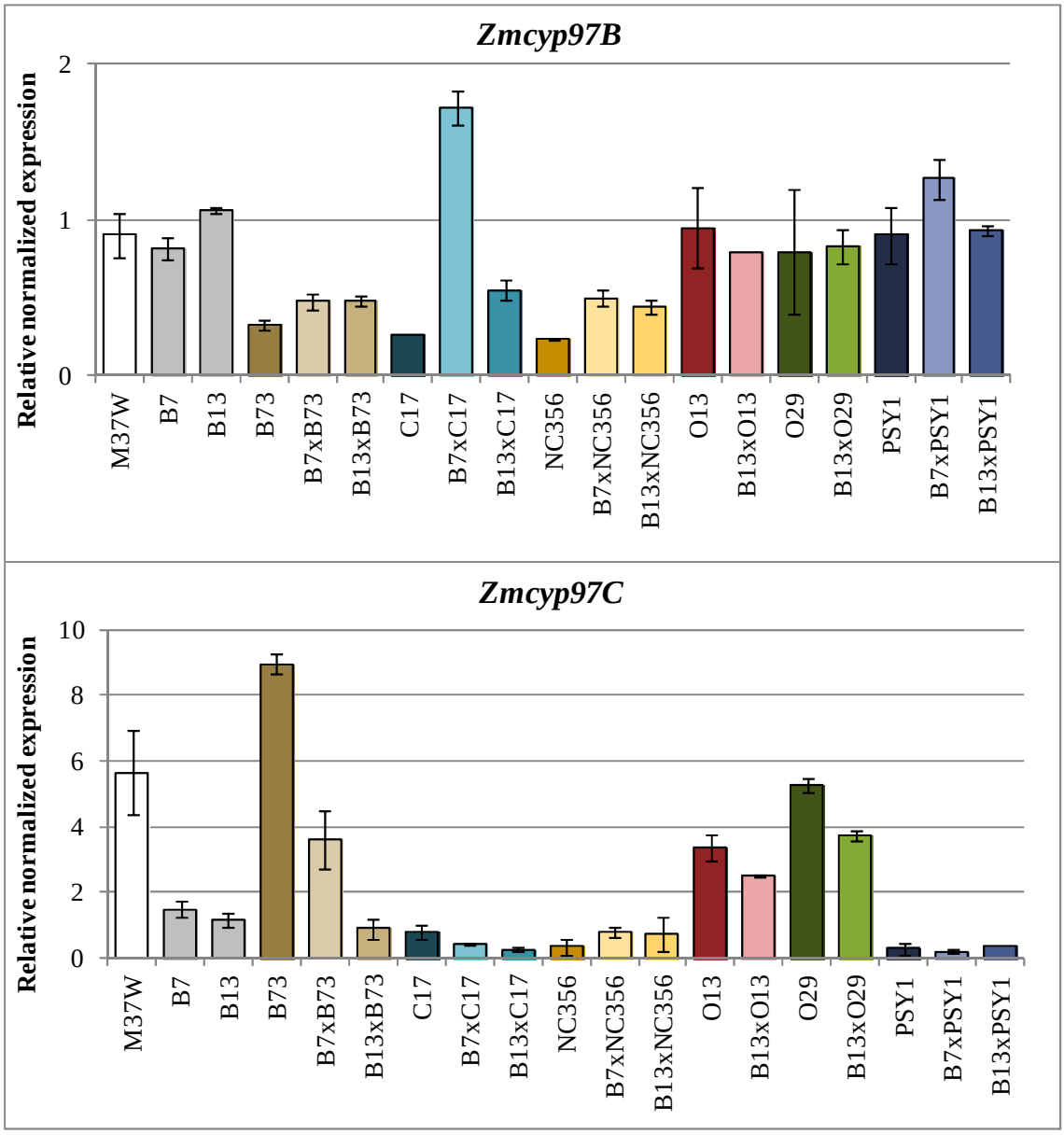

Figure 3. 10 – mRNA accumulation of endogenous hydroxylases: *Zmbch1*, *Zmbch2*, *Zmcyp97A*, *Zmcyp97B* and *Zmcyp97C* in 30 DAP maize endosperm, normalized against actin and relative to M37W mRNA and presented as the mean of three technical replicates ± SE. Abbreviations: *Zmbch1, carotenoid β-hydroxylase 1*; *Zmbch2, carotenoid β-hydroxylase 2*; *Zmcyp97A/B, carotene β-hydroxylase*; *Zmcyp97C, carotene ε-hydroxylase*.

3.4.5.1 mRNA accumulation of endogenous hydroxylase genes in hybrids and corresponding parents accumulating higher amounts of ε-carotenoids relatively to β-carotenoids

Transcript levels of *Zmbch1* and *Zmcyp97C* were higher in B73 over M37W (ca: 10- and 1.5-fold, respectively), whereas transcript levels of *Zmbch2* and *Zmcyp97A* were similar to M37W and transcript levels of *Zmcyp97B* were 2-fold downregulated in B73 over M37W. Transcript levels of endogenous *Zmbch1* and *Zmbch2* in B7xB73 and B13xB73 were downregulated (ca: 5- and 4-fold, respectively) in both hybrids compared to B73. Transcript levels of *Zmcyp97A*

were similar in B7xB73 and B13xB73 hybrids than B73. Transcript levels of *Zmcyp97B* were upregulated (ca: 1.5-fold) in B7xB73 and B13xB73 hybrids compared to B73 and transcript levels of *Zmcyp97C* were decreased (ca: 2-fold and 9-fold, respectively) in B7xB73 and B13xB73 hybrids compared to B73 (**Figure 3.10**).

Transcript levels of *Zmbch1* were higher in C17 compared to M37W (ca: 2-fold), whereas transcript levels of *Zmbch2, Zmcyp97A, Zmcyp97B* and *Zmcyp97C* were downregulated (ca: 15-, 2-, 3- and 12-fold, respectively), compared to M37W. In B7xC17 and B13xC17 hybrids, transcript levels of endogenous *Zmbch1* did not change compared to parents. However, transcript levels of *Zmbch2* were downregulated (ca: 5- fold) in both hybrids compared to M73W although they were slightly higher than C17. Transcript levels of *Zmcyp97A* were decreased (ca: 1.5- fold) in both hybrids compared to M37W parent although they were slightly higher than C17. Transcript levels of *Zmcyp97B* were upregulated (ca: 7- and 2-fold, respectively), in B7xC17 and B13xC17 compared to C17 and transcript levels of *Zmcyp97C* were downregulated (ca: 2-fold) over C17 (**Figure 3.10**).

3.4.5.2 mRNA accumulation of endogenous hydroxylase genes in hybrids and corresponding parents accumulating higher amounts of β-carotenoids relatively to ε-carotenoids

Transcript levels of *Zmbch1* were higher (ca: 15-fold) in NC356 compared to M37W, whereas transcript levels of *Zmbch2* were similar and transcript levels of *Zmcyp97A, Zmcyp97B* and *Zmcyp97C* were downregulated (ca: 2-, 5- and 12-fold, respectively), compared to M37W. In B7xNC356 and B13xNC356 hybrids, transcript levels of endogenous *Zmbch1* and *Zmbch2* were downregulated (ca: 5- and 7-fold, respectively), in both hybrids compared to NC356. Transcript levels of *Zmcyp97A* and *Zmcyp97C* did not change in both hybrids compared to NC356, whereas transcript levels of *Zmcyp97B* were upregulated (ca: 2- fold) in hybrids compared to NC356 (**Figure 3.10**).

Transcript levels of *Zmbch1, Zmbch2, Zmcyp97A, Zmcyp97B* and *Zmcyp97C* did not change in O2-9 compared to M37W. In B13xO1-3 hybrid, transcript levels of endogenous *Zmbch1* did not change, whereas transcript levels of *Zmbch2* were downregulated (ca: 3- fold) compared to O1-3. Transcript levels of *Zmcyp97A, Zmcyp97B* and *Zmcyp97C* did not change in B13xO1-3 hybrid compared to O1-3 parent (**Figure 3.10**).

Transcript levels of *Zmbch1, Zmbch2, Zmcyp97A, Zmcyp97B* and *Zmcyp97C* were similar in O2-9 compared to M37W. In B13xO2-9 hybrid, transcript levels of endogenous *Zmbch1,*

Zmcyp97A and *Zmcyp97B* were similar to WT, whereas transcript levels of *Zmbch2* and *Zmcyp97C* were downregulated (ca: 2- and 1.2-fold, respectively), in hybrid compared to O2-9 parent (**Figure 3.10**).

Transcript levels of *Zmbch1*, *Zmcyp97A* and *Zmcyp97B* were similar in psy1 compared to M37W, whereas transcript levels of *Zmbch2* were upregulated (ca: 2-fold) and transcript levels of *Zmcyp97C* were downregulated (ca: 12-fold) in psy1 line compared to M37W. In B7xpsy1 and B13xpsy1, transcript levels of endogenous *Zmbch2* were downregulated (ca: 5- and 3-fold, respectively), in both hybrids compared to psy1 line. Transcript levels of *Zmbch1*, *Zmcyp97A, Zmcyp97B* and *Zmcyp97C* were similar in hybrids than psy1 line (**Figure 3.10**).

3.5 Discussion

3.5.1 RNAi-mediated silencing of endogenous *Zmbch1* and *Zmbch2* genes leads to a significant increase of β-carotene accumulation in the endosperm of hybrids derived from parents with diverse carotenoid profiles

Two classes of structurally-unrelated enzymes catalyze the hydroxylation of α- and β- ionone rings in higher plants: CYP97-type heme-containing cytochrome P450 hydroxylases and BCH-type non-heme di-iron hydroxylases. Maize *bch2* (also known as *hyd3* and *crtRB1*) is developmentally regulated but preferentially expressed in the endosperm, where it governs the critical steps in the conversion of β-carotene to zeaxanthin via β-cryptoxanthin (Vallabhaneni et al. 2009; Li et al. 2010; Babu et al. 2012, Yan et al. 2010; Naqvi et al. 2011). *Zmbch2* is the only carotenoid hydroxylase expressed at high enough levels to be detected by mRNA blot (Li et al. 2010). Hypomorphic alleles cause the accumulation of β-carotene in maize endosperm (Vallabheneni et al. 2009; Yan et al. 2010). *Zmbch2* alleles have been correlated with high β-carotene content and the introgression of these alleles has been carried out into elite inbred lines resulting in up to 12-fold increase of β-carotene content over the recurrent parent (Muthusamy et al. 2014). In contrast, candidate-gene association analysis identified 18 polymorphic sites in *ZmcrtRB3* (BCH1) significantly associated with one or more carotenoid-related traits in 126 diverse yellow maize inbred lines. These results indicate that *bch1* plays a role in hydrolyzing both α- and β-carotenes. Polymorphisms in *bch1* had higher influence on variation of α-carotene than β-carotene levels (Zhou et al. 2012).

Zmbch1 and *Zmbch2* cDNAs in maize endosperm are highly homologous (96.4%) at the DNA level. They map to different chromosomes but encode very similar proteins (76.6% identity, with highly conserved motifs typical of an iron-containing monooxygenase) (Li et al. 2010). Previous reports indicated that in bacteria producing β-carotene and expressing the *Zmbch2* cDNA, more than half of the β-carotene was converted into downstream products, approximately 80% β-cryptoxanthin and 20% zeaxanthin. In contrast, bacteria expressing *Zmbch1* cDNA were only able to convert less than 5% of the available β-carotene to β-cryptoxanthin as the sole product. This functional difference might indicate that the two genes diverged during evolution to fulfill different roles in carotenoid biosynthesis (Li et al. 2010).

I generated transgenic plants in which *Zmbch1* and *Zmbch2* were downregulated simultaneously as the RNAi cassette was targeted to a high homology region of the two genes (**Figures 3.3** and **3.4**). *Zmbch2* gene silencing varied amongst transgenic lines as indicated by mRNA blot analysis: Transgenic lines B1 and B7 exhibited total silencing of *Zmbch2* whereas in lines B9 and B13, *Zmbch2* was only partially silenced. The extent of *Zmbch1* silencing could only be determined by qPCR because of the low levels of *Zmbch1* transcripts which accumulated in the endosperm of these lines. I measured a relatively uniform decrease in the levels of *Zmbch1* transcript accumulation in all the transgenic lines (ca: 3-fold). This suggests that the insertion of the RNAi cassette into the maize genome might affect the effectiveness of the RNAi construct because the effects observed in independent lines were different. The M37W inbred line used for transformation only accumulates traces of carotenoids as *Zmpsy1* expresses at very low level in the endosperm of this line (Zhu et al. 2008; Naqvi et al. 2009). Consequently, primary transformants in a M37W genetic background are not suitable to evaluate the effects of the silencing of these two β-carotene hydroxylases in the endosperm. For this reason I introgressed the RNAi cassette resident in the M37W transformants B7 and B13) into different maize lines, selected on the basis of their endosperm carotenoid content and composition (**Figure 3.5**). I chose lines B7 and B13 as introgression parents in order to assess whether complete or partial silencing of *Zmbch2* might have an effect on carotenoid accumulation.

Carotenoid composition analysis of hybrids generated with transgenic lines B7 and B13 in which *Zmbch1* transcript levels were downregulated at similar levels and *Zmbch2* transcript levels were downregulated at high and intermediate levels, respectively, revealed a variation in carotenoid composition (**Table 3.2**; **Figure 3.7**). The effect of silencing of *Zmbch1* and *Zmbch2* appears to be more pronounced in the β-branch of the pathway. β-Carotene was

absent in the endosperm of B73, O1-3 and O2-9. However, the corresponding hybrids accumulated up to ca: 5µg/g DW of total carotenoids in the endosperm. NC356 and psy1 hybrids accumulated β-carotene at levels up to 3.4-fold higher than their corresponding parents (ca: 30 µg/g DW). However, no significant changes were observed in β-carotene levels of C17 hybrids because *Zmbch2* transcript levels were already low in the C17 parent (**Figure 3.9**). β-Cryptoxanthin levels increased in C17 hybrids and decreased in O1-3 and O2-9 hybrids. β-Cryptoxanthin levels increased in hybrids between B7 and B73, NC356 and psy1. In contrast β-cryptoxanthin levels decreased in the corresponding hybrids with B13. The higher degrees of *Zmbch2* silencing in the B7 parent relative to B13 might explain the different β-cryptoxanthin levels in the two situations. The hydroxylation capacity in the B7 parent is reduced compared to B13, so the monohydroxylated carotenoid β-cryptoxanthin is seen to accumulate at the expense of the dihydroxylated β-carotenoid zeaxanthin. Total zeaxanthin levels decreased in NC356, O1-3 and O2-9 hybrids (with both B7 and B13 parents), and zeaxanthin levels relative to total carotenoids increased also in B73 and psy1 hybrids, suggesting that the increase of β-carotene content correlated with the decrease of zeaxanthin content due to *Zmbch2*. *Zmbch2* polymorphisms based on molecular markers reported by several authors (Vallabhaneni et al. 2009; Li et al. 2010; Babu et al. 2012, Yan et al. 2010) correlated with increase β-carotene content in agreement with my results. In the α-branch of the pathway, β-hydroxylation of α-cryptoxanthin results in the formation of the end-product of the pathway, lutein. α-Cryptoxanthin accumulated in C17, O1-3, O2-9 and psy1 hybrids even though this metabolite was absent in C17, O1-3, O2-9 and psy1. B73 and NC356 hybrids, whose parents accumulated the highest transcript levels of *Zmbch1*, showed an increase of α-cryptoxanthin levels in B7 hybrids compared to the parents and α-cryptoxanthin levels remained the same in B13 hybrids compared to the parents suggesting that an additional β-hydroxylase is required to convert α-cryptoxanthin to lutein. Lutein accumulation was reduced only in C17, O1-3 and O2-9 hybrids but increased in NC356 hybrids and psy1 hybrids and did not change in B73 hybrids, suggesting again that an additional β-hydroxylase is required to convert α-cryptoxanthin to lutein.

3.5.2 RNAi-mediated *Zmbch1* and *Zmbch2* silencing impacts differently the expression of P450-carotene β-hydroxylase and ε-hydroxylase genes

In M37W endosperm *Zmbch2* is highly expressed compared to *Zmbch1*, *Zmcyp97A*, *Zmcyp97B* and *Zmcyp97C* (**Figure 3.9***).* *Zmbch1* has been reported to have a higher impact

on β-hydroxylation of α-carotenoids rather than β-hydroxylation of β-carotenoids as polymorphisms of this gene correlated well with more variation in α- than in β-carotene (Zhou et al. 2012). Transcript levels of *Zmbch1* exhibited the highest variability amongst parents relative to M37W, representing a maximum ca: 15-fold increase. Transcript levels of *Zmbch1* were highly downregulated in B73 and NC356 hybrids compared to their parents, representing a maximum of ca: 5-fold decrease, revealing an efficient downregulation of *Zmbch1* by the RNAi construct in the parent. However, *Zmbch1* transcript downregulation in O1-3, O2-9 and psy1 hybrids was not significant and *Zmbch1* transcript levels in C17 hybrids were higher than in the C17 and M37W parents, suggesting that endogenous *Zmbch1* alleles might influence the effectiveness of the RNAi construct introgressed into these hybrids. Up to ca: 5-fold lower *Zmbch1* transcript levels in hybrids of B73, NC356 compared to their corresponding parents did not correlate with increased α-cryptoxanthin and decreased lutein levels, which suggests that an additional carotenoid β-hydroxylase might be involved in the conversion of α-cryptoxanthin to lutein. In the case of *Zmbch2*, up to 2.5-fold variation was observed amongst all lines (parents and hybrids), revealing low variability in gene expression. However, *crtRB1* (BCH2) locus has been reported to have high impact on β-carotene accumulation (Vallabhaneni et al. 2009), correlating with high expression levels of *Zmbch2* compared to the other β-hydroxylases. *Zmbch2* transcript levels were lower in all hybrids compared to the respective parents with the exception of C17 hybrids in which transcript levels were lower than in the M37W parent (containing the RNAi construct) but higher than the C17 parent. In addition, the different degrees of gene silencing in B7 and B13 also manifested in the hybrids derived from these lines. This indicates that the effectiveness of the RNAi construct is stable over generations. Variation amongst *Zmcyp97A* and *Zmcyp97B* transcript levels in parent lines and hybrids was too low to note significant differences, so differences of transcript levels of *Zmcyp97A* and *Zmcyp97B* might be attributable to natural variation of transcript levels. Low transcript variability suggests that *Zmcyp97A* and *Zmcyp97B* are tightly regulated. Transcript levels of *Zmcyp97A* and *Zmcyp97B* were similar in hybrids compared to their respective parents. In contrast, transcript levels of carotenoid ε-hydroxylase *Zmcyp97C* varied up to 19-fold (increased in B73 relative to C17, which are the two extremes in the variation amongst all the parents). *Zmcyp97C* transcript levels in hybrids were downregulated in B73, C17, O1-3 and O2-9 hybrids, but not in NC356 and psy1 hybrids with respect to their corresponding parents. Interestingly, hybrids which did not have significantly reduced levels of *Zmvyp97C* compared to the parents did not show a reduction in lutein content. This suggests that a downregulation of carotenoid β-hydroxylase transcript

levels might have a collateral effect on downregulation of transcript levels of carotenoid ε-hydroxylase.

3.6 Conclusions

Four independent transgenic lines with RNAi-mediated gene silencing of *Zmbch1* and *Zmbch2* in a M37W genetic background were generated. No differences in carotenoid content and composition of transgenic lines B7 and B13 compared to M37W were measured because of the low pool of carotenoids in the M37W line used for the transformation experiments. Thus, the RNAi*bch* cassette in transgenic lines B7 and B13 lines was introgressed into several lines with different carotenoid profiles. Targeted metabolomics analysis revealed an increase of β-carotene levels at the expense of zeaxanthin in all the hybrids in which *Zmbch1* and *Zmbch2* were downregulated, confirming that the two hydroxylases are crucial for the conversion of β-carotene to zeaxanthin through β-cryptoxanthin. The maximum carotenoid content was in B7xpsy1 hybrid (ca: 30 µg/g DW). Transcript analysis revealed a substantial downregulation of *Zmbch1* in B73 and NC356 hybrids compared to their parents as well as downregulation of *Zmbch2* in all hybrids with the exception of hybrids with C17. A decrease of carotenoid ε-hydroxylase *Zmcyp97C* transcript accumulation in B7 and B13 lines compared to wild-type and in B73, C17, O1-3, O2-9 hybrids compared to their respective parents suggests a pleotropic effect of the downregulation of *Zmbch1* and *Zmbch2*.

3.7 References

Babu R, Palacios Rojas N, Gao S, Yan J, Prixley K (2013) Validation of the effects of molecular marker polymorphisms in LcyE and CrtRB1 on provitamin A concentrations for 26 tropical maize populations. Theor Appl Genet. 126:389–399.

Davuluri GR, van Tuinen A, Fraser PD, Manfredonia A, Newman R, Burgess D, et al. (2005) Fruit-specific RNAi-mediated suppression of DET1 enhances carotenoid and flavonoid content in tomatoes. Nat Biotechnol. 23:890–895.

Diretto G, Tavazza R, Welsch R, Pizzichini D, Mourgues F, Papacchioli V, et al. (2006) Metabolic engineering of potato tuber carotenoids through tuber-specific silencing of lycopene epsilon cyclase. BMC Plant Biol. 6:13-24.

Harjes CE, Rocheford TR, Bai L, Brutnell TP, Kandianis CB, Sowinski SG, et al. (2000) Natural genetic variation in lycopene epsilon cyclase tapped for maize biofortification. Science. 319:330–333.

Kim J, DellaPenna D (2006) Defining the primary route for lutein synthesis in plants: the role of Arabidopsis carotenoid β-ring hydroxylase CYP97A3. Proc Natl Acad Sci U S A. 103:3474–3479.

Kim J, Smith JJ, Tian L, DellaPenna D (2009) The evolution and function of carotenoid hydroxylases in Arabidopsis. Plant Cell Physiol. 50:463–479.

Kim SH, Kim YH, Ahn YO, Ahn MJ, Jeong JC, Lee HS, et al. (2013) Downregulation of the lycopene ε-cyclase gene increases carotenoid synthesis via the β-branch-specific pathway and enhances salt-stress tolerance in sweetpotato transgenic calli. Physiol Plant. 147:432–442.

Li Q, Farre G, Naqvi S, Breitenbach J, Sanahuja G, Bai C, et al. (2010) Cloning and functional characterization of the maize carotenoid isomerase and β-carotene hydroxylase genes and their regulation during endosperm maturation. Transgenic Res. 19:1053–1068.

Messias S, Galli V, Delmar dos Anjos e Silva S, Valmor Rombaldi C (2014) Carotenoid Biosynthetic and Catabolic Pathways: Gene Expression and Carotenoid Content in Grains of Maize Landraces. Nutrients. 6:546–563.

Muthusamy V, Hossain F, Thirunavukkarasu N. (2014) Development of β-Carotene Rich Maize Hybrids through Marker-Assisted Introgression of β-carotene hydroxylase Allele. PLoS One. 9:e113583.

Naqvi S, Zhu C, Farre G, Ramessar K, Bassie L, Breitenbach J, et al. (2009) Transgenic multivitamin corn through biofortification of endosperm with three vitamins representing three distinct metabolic pathways. Proc Natl Acad Sci U S A. 106:7762–7767.

Pons E, Alqu B, Rodr A, Martorell P, Genov S, Ram D, et al. (2014) Metabolic engineering of β-carotene in orange fruit increases its in vivo antioxidant properties. Plant Biotechnol J. 12:17–27.

Sun L, Yuan B, Zhang M, Wang L, Cui M, Wang Q, et al. (2012) Fruit-specific RNAi-mediated suppression of SlNCED1 increases both lycopene and β-carotene contents in tomato fruit. J Exp Bot. 63:3097–2108.

Sun Z, Gantt E, Cunningham FX (1996) Cloning and functional analysis of the β-carotene hydroxylase of Arabidopsis thaliana. J Biol Chem. 271:24349–24352.

Tian L, Dellapenna D (2001) Characterization of a second carotenoid β-hydroxylase gene from Arabidopsis and its relationship to the LUT1 locus. Plant Mol Biol. 47:379–388.

Tian L, Magallanes-Lundback M, Musetti V, DellaPenna D (2003) Functional analysis of β- and ε-ring carotenoid hydroxylases in Arabidopsis. Plant Cell. 15:1320–1332.

Vallabhaneni R, Gallagher CE, Licciardello N, Cuttriss AJ, Quinlan RF, Wurtzel ET. (2009) Metabolite sorting of a germplasm collection reveals the hydroxylase3 locus as a new target for maize provitamin A biofortification. Plant Physiol. 151:1635–1645.

Vallabhaneni R, Wurtzel ET (2009) Timing and biosynthetic potential for carotenoid accumulation in genetically diverse germplasm of maize. Plant Physiol. 150:562–572.

Van Eck J, Conlin B, Garvin DF, Mason H, Navarre D, Brown CR (2007) Enhancing beta-carotene content in potato by rnai-mediated silencing of the beta-carotene hydroxylase gene. Am J Potato Res. 84:331–342.

Wei SHU, Xiang LI, Gruber MY, Rong LI, Zhou R, Zebarjadi A, et al. (2009) RNAi-Mediated suppression of DET1 alters the levels of carotenoids and sinapate esters in seeds of brassica napus. J Agric Food Chem. 57:5326–5333.

Yan J, Kandianis CB, Harjes CE, Bai L, Kim E, Yang X, et al. (2010) Rare genetic variation at Zea mays crtRB1 increases β-carotene in maize grain. Nat Genet. 42:322–327.

Zhou Y, Han Y, Li Z, Fu Y, Fu Z, Xu S, et al. (2012) ZmcrtRB3 Encodes a Carotenoid Hydroxylase that Affects the Accumulation of α-carotene in Maize Kernel. J Integr Plant Biol. 54:260–269.

Zhu C, Naqvi S, Breitenbach J, Sandmann G, Christou P, Capell T (2008) Combinatorial genetic transformation generates a library of metabolic phenotypes for the carotenoid pathway in maize. Proc Natl Acad Sci U S A. 105:18232–18237.

CHAPTER 4

Impact of increased carotenoid content on starch accumulation in transgenic maize

CHAPTER 4: IMPACT OF INCREASED CAROTENOID CONTENT ON STARCH ACCUMULATION IN TRANSGENIC MAIZE

4.1 Abstract

Modulation of a particular biosynthetic pathway may have effects on global metabolism due to the fact that precursors for common pathways may be shared by multiple pathways. Carotenoids are lipid-soluble compounds derived from the condensation of IPP and DMAPP units which are derived from glucose metabolism. Here, I investigated the impact of carotenoid enhancement in transgenic lines on starch metabolism. Total starch decreased up to 8% in transgenic lines compared with wild type, whereas carotenoid content was increased up to 40-fold. Transcriptomic analysis of key endogenous enzymes involved in starch metabolism indicated downregulation of starch synthase 1 (SS1) and starch branching enzyme 1 (SBE1) and upregulation of debranching enzyme (ISA1 and ISA2) in transgenic lines with higher carotenoid content compared with wild type. In addition, phosphoglucomutase (PGM), which catalyzes the production of glucose-1-phosphate from glucose-6-phosphate, was downregulated 2-fold in transgenic lines compared with wild type. Few reports have described the effects of carotenoid enhancement on general metabolism. Consequently these findings provide a starting point to develop a more in depth understanding of the impact of modulating a pathway in the context of global metabolism, particularly if the pathways share common precursors and/or products.

4.2 Introduction

Metabolic engineering to increase particular compounds in plants may have a global effect on the whole metabolism because the novel products synthesized might be produced at the expense of other metabolites (Sandmann 2001). Relatively few studies have reported the impact of carotenoid enhancement in transgenic plants on global metabolism. Microarray analysis in tomato revealed that the constitutive expression of *lycb* affected a number of pathways including the synthesis of fatty acids, flavonoids and phenylpropanoids, the degradation of limonene and pinene, starch and sucrose metabolism and photosynthesis (Guo et al. 2012). A metabolomic analysis of tomato expressing *CrtB* (phytoene synthase) and *CrtI*

(bacterial phytoene desaturase/isomerase), encoding pytoene syntase revealed changes in the steady state levels of metabolites in unrelated pathways, such as amino acid, isoprenoid, lipid, organic acid and sugar metabolism (Nogueira et al. 2013). Transgenic soybean (*Glycine max*) plants overexpressing a seed-specific *CrtB* exhibited a shift in oil composition increasing oleic at the expense of linoleic acid, and a 4% increase in protein content (Schmidt et al. 2015). In maize expressing *Zmpsy1* and *PacrtI* (Zhu et al. 2008), combined transcript, proteome and metabolite analysis revealed pleiotropic effects in core metabolism (Decourcelle et al. 2015). Main changes occurred in sugar metabolism as well as an increase in sterol and fatty acid content (Decourcelle et al. 2015). Carotenoid biosynthesis requires precursors derived from sugars such as pyruvate so it is important that the amount of soluble sugars is adequate to ensure the appropriate amount of precursors for carotenoid biosynthesis. The increase of soluble sugars takes place at the expense of starch (carbohydrate reservoir) (**Figure 4.1**). A decrease of starch content was reported in citrus callus overexpressing *CrtB* where starch level reduction occurred in parallel with significant carotenoid accumulation (Cao et al. 2015b). Alterations of starch in tomato during ripening were also correlated with increased carotenoid accumulation (Tohge et al. 2014).

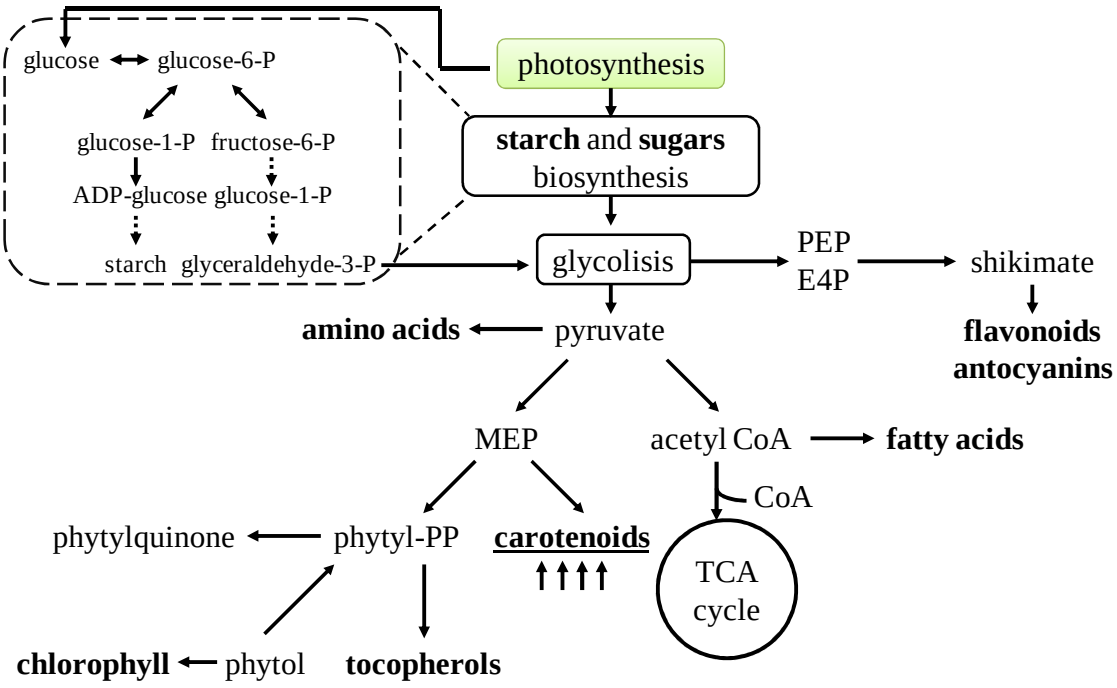

Figure 4. 1 – Overview of general metabolism in maize and relation between products in the different pathways. Metabolites that have been altered as a consequence of increased carotenoid content reported in previous studies are shown in bold. Abbreviations: PEP, phosphoenolpyruvate; E4P, erythrose-4-phosphate; P, phosphate; PP, pyrophosphate. (Adapted from Decourcelle et al. 2015; Tohge et al. 2014; Gallagher et al. 2003).

In order to evaluate the impact of carotenoid enhancement on starch biosynthesis, it is essential to understand starch synthesis in detail. Cereals store energy in the endosperm in the form of starch, which generally consists of two D-glucose homopolymers, the linear polymer amylose and a highly branched glucan (amylopectin) that connects linear chains (James et al. 2003; Jeon et al. 2010). Starch is derived from sucrose, which is the primary form of assimilated carbon in plants. Sucrose is transported from source tissues (leaves) to sink tissues (seeds) where it is converted into uridine diphosphate (UDP)-glucose and -fructose by soluble and membrane-bound forms of the enzyme sucrose synthase. Whereas the latter channels UDP-glucose towards the cellulose synthase complex on the plasma membrane (Hardin et al. 2006), the major soluble form of sucrose synthase in maize seeds, encoded by the *Shrunken1* (*Sh1*) gene (Carlson and Chourey, 1996) provides UDP-glucose as a precursor for starch biosynthesis. UDP-glucose is converted into glucose-1-phosphate by UDP-glucose pyrophosphorylase. Alternatively, fructose derived from sucrose is converted to fructose-6-phosphate by hexose kinase (HI). Fructose-6-phosphate is then converted to glucose-6-phosphate by the action of glucose phosphate isomerise (GPI). Glucose-6-phosphate is in turn converted into glucose-1-phosphate by phosphogluco-mutase (PGM). Glucose-6-phosphate, glucose-1-phosphate and fructose-6-phosphate are key metabolites because they can be directed to both starch synthesis and glycolysis (Gallagher et al. 2003). The committed starch biosynthesis pathway in maize endosperm requires the coordinated activities of multiple enzymes, including ADP-glucose pyrophosphorylase (AGPase), granule-bound starch synthase (GBSS), soluble starch synthase (SS), starch branching enzyme (SBE), starch debranching enzyme (DBE), and plastidial starch phosphorylase (*Pho1*) (James et al. 2003; Jeon et al. 2010) (**Figure 4.2**). The rate-limiting step is the synthesis of ADP-glucose from glucose-1-phosphate and ATP by AGPase (Russell et al. 1993). AGPase is a heterotetramer comprising two large subunits (AGP-L; encoded by *sh2*, *agplemzm*, *agpllzm* or *agpl3*) and two small subunits (AGP-S; encoded by *bt2*, *agpszm* or *agpslzm*) (Hannah et al. 2001; Huang et al. 2014). There are two known GBSS isoforms in maize, with GBSSI playing the major role in the endosperm and GBSSII producing transitory starch in non-storage tissues (Dian et al. 2003; Hirose and Terao, 2004; Vrinten and Nakamura, 2000). Four different SS enzymes have been identified in plants but DU1 and zSSI most likely account for all of the soluble SS activity in developing kernels (Cao et al. 1999; Jeon et al. 2010). SBE generates amylopectin by cleaving the α(1, 4) bonds in polyglucans and reattaching the chain via α(1, 6) bonds. The three major SBE isoforms in developing maize kernels are SBEI, SBEIIa and SBEIIb (Ball and Morell, 2003) and these are encoded by different genes (Ballicora et al. 1995; Beatty et al.

1999; Blauth et al. 2001, 2002). SBEI has no impact on endosperm starch structure, whereas the deficiency of SBEIIb is well known to reduce the branching of starch (Li et al. 2007).

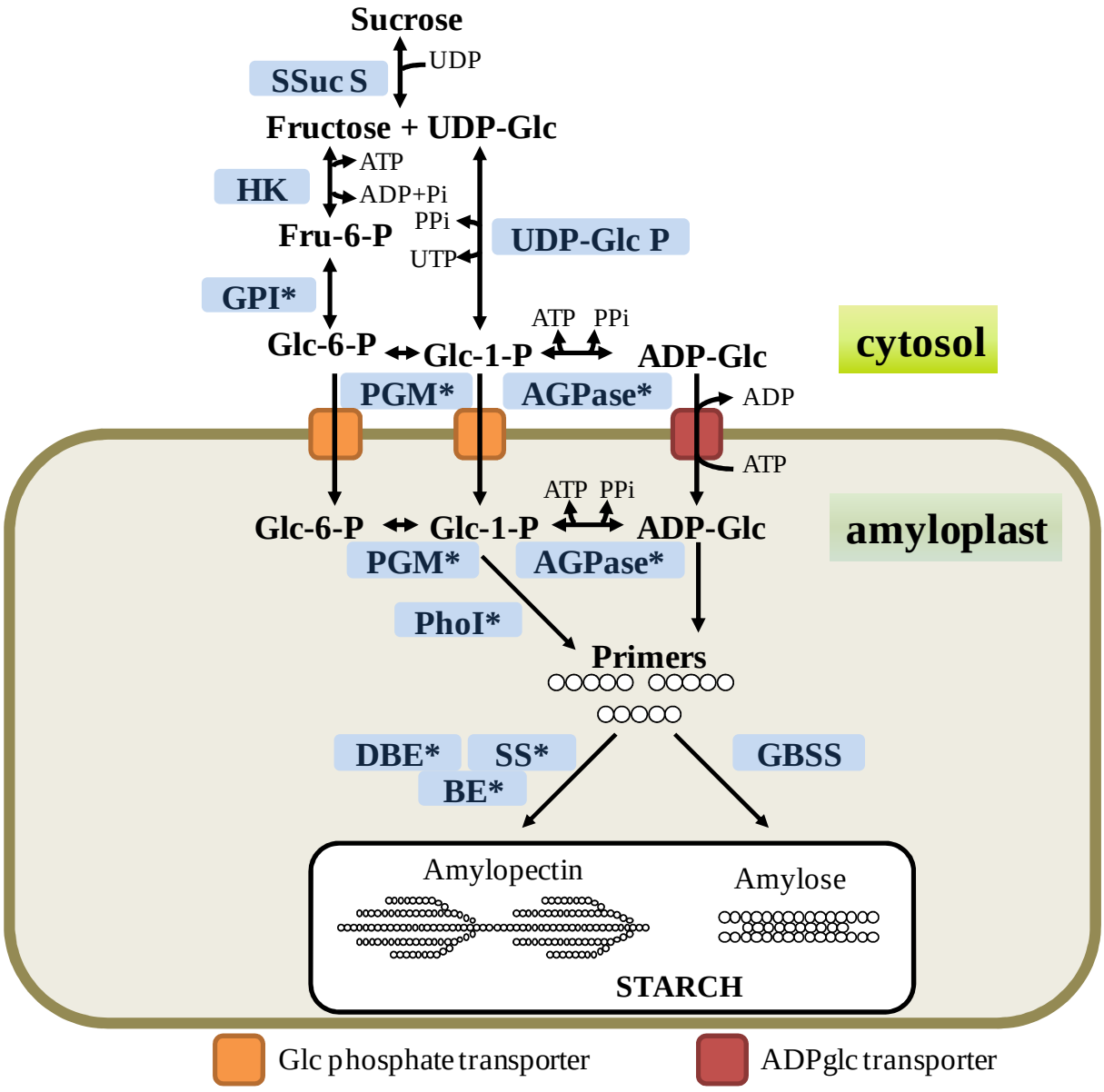

Figure 4.2 – The starch biosynthesis pathway in maize endosperm. Asterisks indicate genes from those transcript levels were evaluated in the experiments reported in this chapter. Metabolite abbreviations: UDP, uridine diphosphate; UDP-Glc, UDP-glucose; Fru-6-P, fructose-6-phosphate; Glc-6-P, glucose-6-phosphate; Glc-1-phosphate, glucose-1-phosphate; ADP-Glc, adenosine diphosphate-glucose. Enzyme abbreviations: SSuc S, soluble sucrose synthase; HK, hexose kinase; GPI, glucose phosphate isomerase; PGM, phosphoglucomutase; AGPase, ADP-Glc pyrophosphorylase, Pho1, plastidial starch phosphorylase; GBSS, granule-bond starch synthase; DBE, debranching enzyme, SS, starch synthase, BE, branching enzyme (Adapted from Jeon et al. 2010; Jiang et al. 2013; Tuncel and Okita 2013).

Two different classes of DBE, isoamylase (ISA) and pullulanase (PUL), directly hydrolyze the α(1, 6) glucosic linkages of polyglucans. In maize endosperm, ISA supports starch synthesis as a heteromeric multi-subunit complex containing both ISA1 and the non-catalytic

protein ISA2 or as a homomeric complex containing only ISA1 (Kubo et al. 2010). Finally, Pho catalyzes the transfer of glucosyl units from glucose-1-phosphate to the non-reducing end of α(1,4)-linked glucan chains. Pho1 and Pho2 are localized in the plastid and cytosol, respectively (Jeon et al. 2010) (**Figure 4.2**). Starch can be degraded in the endosperm of maize seeds by four isozymes of α-amylase (α-amylase-1 to -4) and one isozyme of β-amylase, although this step occurs mainly in germinating seeds (Subbarao et al. 1998).

Wild-type M37W and four different transgenic maize lines overexpressing (L1) *AtOR*, (L2) *Zmpsy1*, (L3) *Zmpsy1*, *PacrtI* and *Gllycb* or (L4) *Zmpsy1*, *PacrtI* and *ParacrtW* were analyzed to determine total carotenoid and total starch content. A targeted transcriptomic analysis of relevant starch biosynthesis genes by qRT-PCR (**Figure 4.2**), transmission electron microscopy (TEM) and scanning electron microscopy (SEM) of endosperm sections revealed a major reduction in the abundance of starch granules in transgenic lines compared to wild-type lines.

4.3 Materials and methods

4.3.1. Plant material

Homozygous lines listed in **Table 4.1** were grown under the conditions described in Chapter 2 section 2.2.2.

Table 4.1 – Maize lines used in this study.

Line	Genotype	Source	References
WT	Inbred	CSIR, Pretoria, South Africa	
L1	Transgenic *AtOR*	Applied plant biotechnology, Universitat de Lleida, Spain	See Chapter 2
L2	Transgenic *Zmpsy1*	Applied plant biotechnology, Universitat de Lleida, Spain	See Chapter 2
L3	Transgenic *Zmpsy1*, *PacrtI*, *ParacrtW*	Applied plant biotechnology, Universitat de Lleida, Spain	(Zhu et al. 2008)
L4	Transgenic *Zmpsy1*, *PacrtI* *Gllycb*	Applied plant biotechnology, Universitat de Lleida, Spain	(Zhu et al. 2008)

4.3.2. RNA extraction and cDNA synthesis

The protocols are described in detail in Chapter 1, section 1.2.2.

4.3.3. Quantitative real-time RT-PCR

The protocol is described in detail in Chapter 2 section 2.2.5. Primer sequences to detect endogenous genes and transgenes are listed in **Table 4.2.**

Table 4.2 – Oligonucleotide sequences for the detection of maize actin, endogenous starch-related genes and transgenes for real-time PCR analysis.

Gene	Forward	Reverse
Zmactin	5'-CGATTGAGCATGGCATTGT-3'	5'-CCCACTAGCGTACAACGAA-3'
Zmpgi	5'-GCACCTGATAACCCTCCACT-3'	5'-AGTAGTTGCCAGTCCAGGTCC-3'
Zmpgm	5'-GGGAGCGTGTTTCTTGTAATC-3'	5'-TCCCTAAACAGCCATCAAAAG-3'
Zmagplem	5'-GATGGGTGCGGATTTGTAT-3'	5'-TTGGAACGCCCTCTTTGT-3'
Zmagpsem	5'-CTCGCAAACGTGCCTTGAT-3'	5'-TCAGGATCAGGCCCAA-3'
ZmphoI	5'-AGGAAATGAAGGTTACGGACG-3'	5'-CCAGCCGTGTTGAGGATAGAC-3'
Zmisa1	5'-TTCGTTGCCTTCACCATGAA-3'	5'-CCGGAAGGTGACTGGTGTTG-3'
Zmisa2	5'-GGCTGTTCGCAATGTTTG-3'	5'-CAGGATCAAATGCTATGGCTTCC-3'
Zmss1	5'-TGAAGGTAGGAAGGGGAGC-3'	5'-TCAGCCCTAACGAGCAAAG-3'
Zmsbe1	5'-AACGGCTGGTGGCAAGAAG-3'	5'-GCCAGTCCAGTCCTCACCAA-3'
Zmpsy1	5'-CATCTTCAAAGGGGTCGTCA-3'	5'-CAGGATCTGCCTGTACAACA-3'
PacrtI	5'-GTGGCGCAAGATGATCGTCAA-3'	5'-GCCAGAAGACCACGTACATCCA-3'
Gllycb	5'-TAAGGCTGGAAGTAGCAGTGC-3'	5'-GCAGGACCACCACCAACAAT-3'
ParacrtW	5'-GTGGCGCAAGATGATCGTCAA-3'	5'-GCCAGACCACGTACATCCA-3'
AtOR	5'- TTCTCTATCACCGCCCAAAAC -3'	5'- GCCATAGCCATTCCTGTGC -3'

4.3.3. Carotenoid extraction and UPLC analysis

This protocol is described in detail in section 2.2.6.

4.3.4. Starch extraction and quantification

Maize endosperm samples were dried at 55ºC overnight and ground into a fine powder. Starch extraction and quantification was performed according to the manufacturer's instructions, using Megazyme total starch kit (Megazyme, Wicklow, Ireland).

4.3.5. TEM and SEM

Maize 30 DAP endosperm pieces (0.5 x 2.0 mm) were fixed in 2.5% v/v glutaraldehyde in 0.1 M phosphate buffer (pH 7.2) overnight at 4°C. TEM samples were prepared as previously described in Chapter 2 section 2.2.7. For SEM DSM 940A (10 kV and 10 mm work distance)

samples were critical-point dried using CPD Emitech K850 (Emitech, Laughton, United Kingdom) and Stub assembled. Finally, they were charcoal coated with Auto 306 (Edwards, Crawley, United Kingdom), gold was evaporated with Balzers SCD 050, Sputter Coated (Leica) and kept at 60ºC until observation.

4.4 Results

4.4.1 Plant growth and transgene expression

Wild-type M37W and transgenic lines L1, L2, L3 and L4 were grown in the greenhouse under controlled conditions to minimize environmental effects. At 30 DAP, endosperm from three independent plants representing each line was excised and stored at -80ºC. The accumulation of *Zmpsy1, PacrtI, Gllycb, ParacrtW* and *AtOR* mRNA was confirmed by qRT-PCR. As expected transcript levels of *Zmpsy1* were detected in at high level in L2, L3 and L4. Low amounts of *Zmpsy1* mRNA accumulated in WT and L1 due to the endogenous *Zmpsy1* gene. Transcript levels of *PacrtI* were detected in L3 and L4, *Gllycb* was detected only in L4, *ParacrtW* was detected only in L3 and *AtOR* was detected only in L1 (**Figure 4.3**).

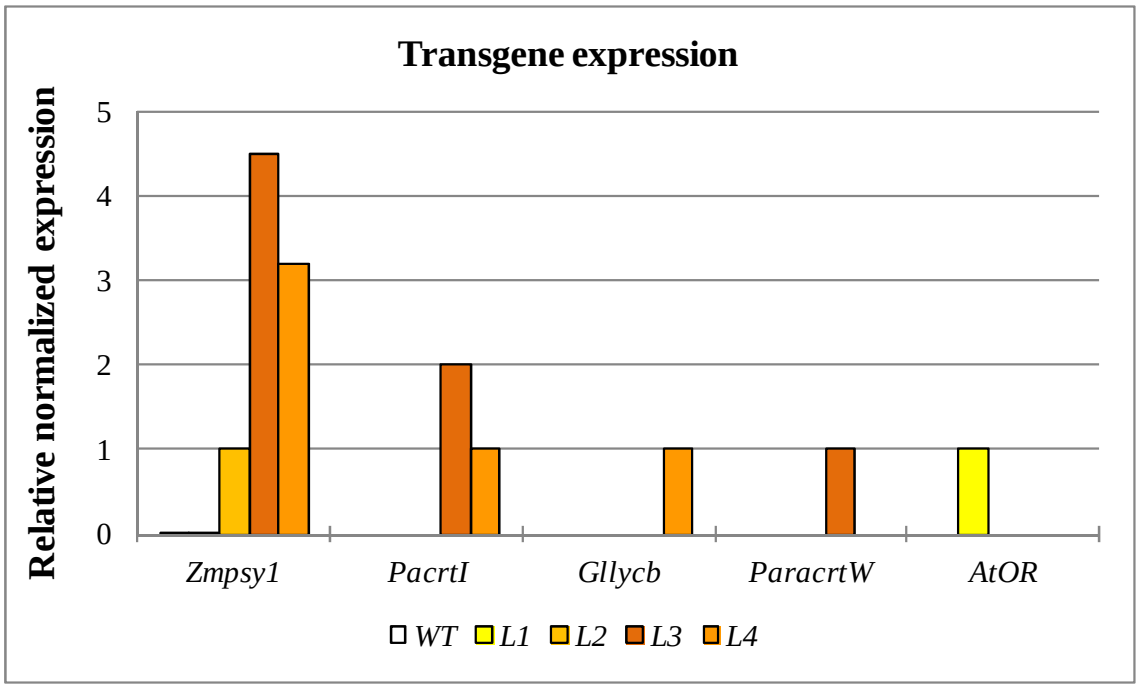

Figure 4.3 – Transgene expression normalized against actin in wild-type and transgenic lines presented as mean of three technical replicates. Transcript levels in the lowest expressing line for each transgene were used as a reference and given the value of 1.0. Color bars represent the different plant lines under investigation.

4.4.2 Total carotenoid content of the transgenic lines

Carotenoid content determined by UHPLC indicated that M37W accumulated low levels of total carotenoids (ca: 3 µg/g DW). L1 accumulated ca: 13 µg/g DW, L2 accumulated ca: 89 µg/g DW, L3 accumulated ca: 127 µg/g DW and L4 accumulated ca: 115 µg/g DW total carotenoids (**Figure 4.4**). The total carotenoid content was determined as the sum of violaxanthin, antheraxanthin, zeaxanthin, lutein, α-cryptoxanthin, β-cryptoxanthin, β-carotene and phytoene.

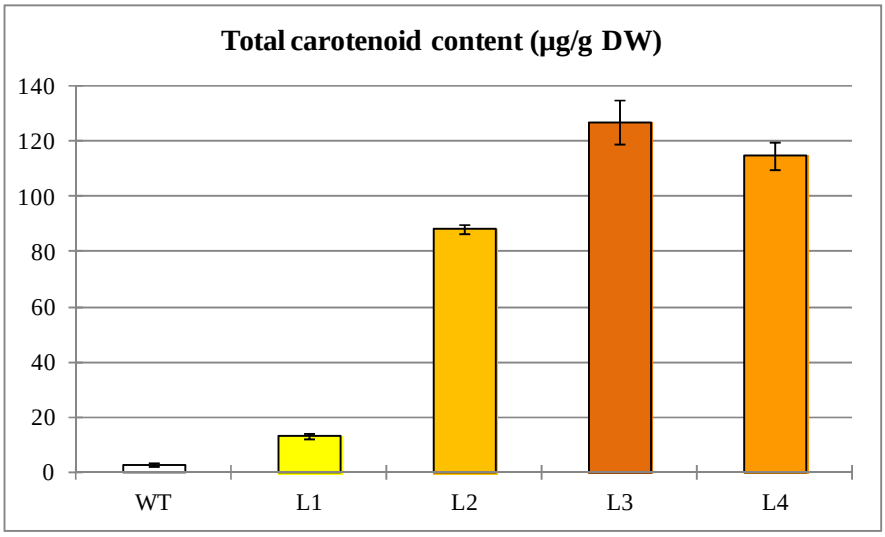

Figure 4.4 – Total endosperm carotenoid content (presented as µg/g dry weight (DW) ± SE (n = 3–5 seeds) of wild-type (WT) and transgenic lines L1, L2, L3 and L4, determined by UHPLC analysis.

4.4.3 Total starch content of the transgenic lines

Total starch from 30 DAP maize endosperm was extracted with ethanol and treated with α-amylase and amyloglucosidase to obtain free glucose which reacts with GOPOD (glucose oxidase/peroxidase) reagent to produce a pink product (quinone imine). Starch was quantified by measuring absorbance produced by the reaction in a spectrophotometer at 510 nm relative to the absorbance of the product with 100 mg/l glucose. Total starch in M37W and L1 represented ca: 65% of the total endosperm weight, whereas total starch in L2, L3 and L4 represented ca: 57%, 61% and 59%, respectively, of the total endosperm weight (**Figure 4.5**).

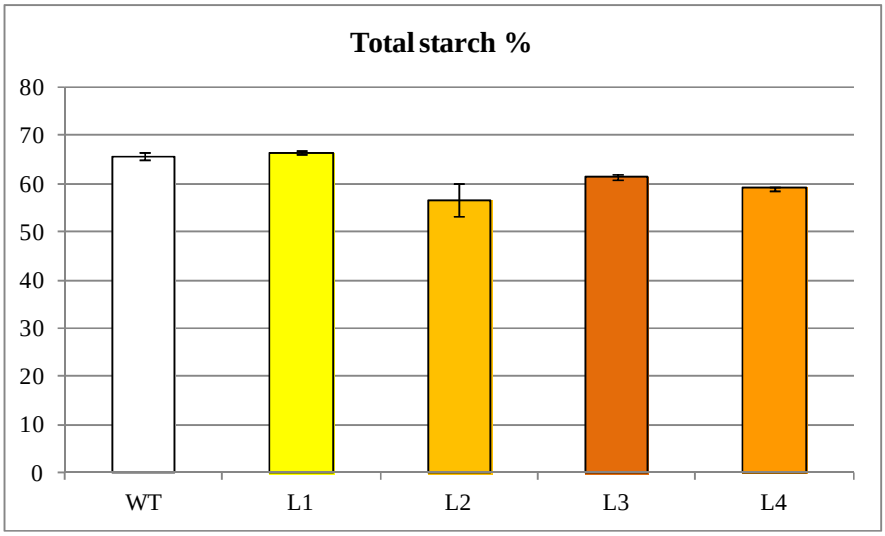

Figure 4.5 – Total endosperm starch content (presented as % ± SE (n = 3–5 seeds) of wild-type (WT) and transgenic lines L1, L2, L3 and L4 determined by spectrophotometry.

4.4.4 TEM and SEM of endosperm tissues in carotenoid-enhanced transgenic lines

SEM analysis of the endosperm from WT plants and the four transgenic lines indicated a reduction in the number of starch granules in the endosperm of transgenic lines L2, L3 and L4 compared with WT and L1 (**Figure 4.6**).

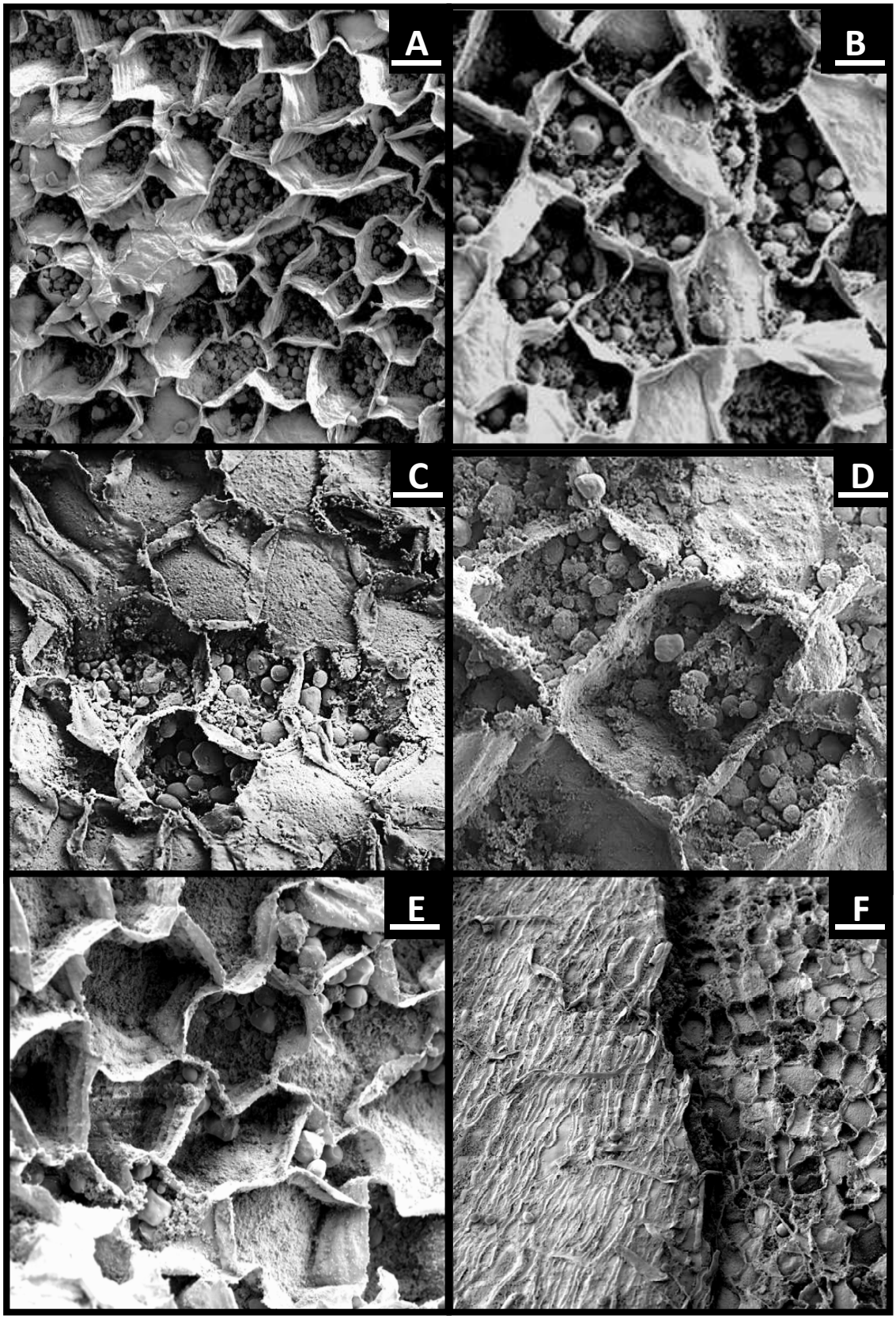

Figure 4.6 – SEM micrographs indicating a reduction in the number of starch granules in the endosperm in L2, L3 and L4 compared with WT. A: WT; B: L1; C: L2; D: L3; E: L4. F: WT endosperm (right) and pericarp epithelium (left). Scale bar A-E: ~ 20µm; F: ~ 50µm.

TEM analysis of the first layer of endosperm cells under the epithelium of WT, L1, L2, L3 and L4 seeds revealed starch deposits in amyloplasts. Even though TEM does not allow the quantification of starch content, WT sections appeared to contain more amyloplasts compared to L2, L3 and L4 (**Figure 4.7**).

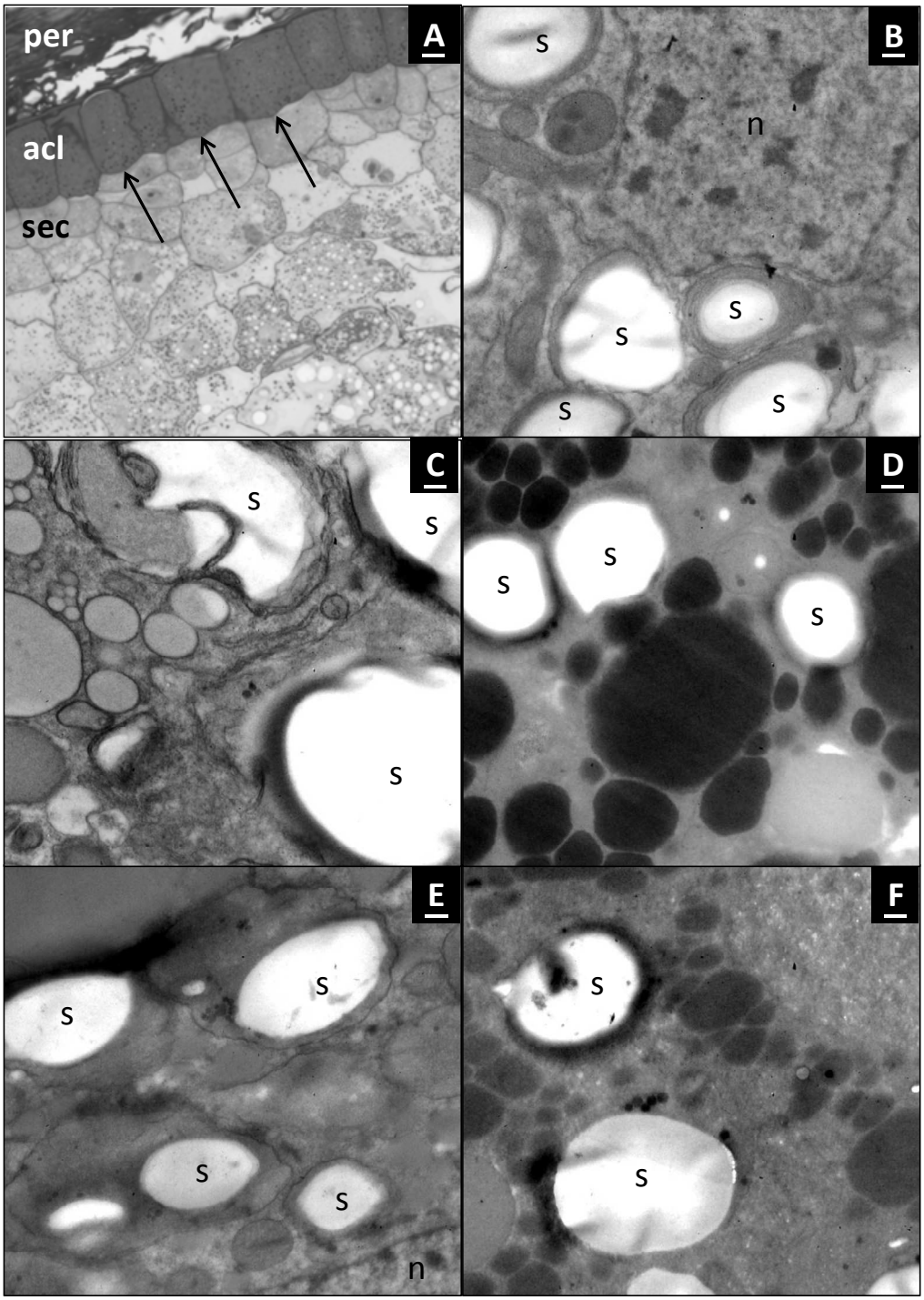

Figure 4.7 – Microscopic analysis of WT and transgenic lines. A. Light micrograph of WT endosperm; arrows indicate aleurone cell layer. B (WT); C (L1); D (L2); E (L3) and F (L4) TEM micrographs of aleurone cell layer indicated a reduction in the number of amyloplasts in transgenic lines L2, L3 and L4, compared with WT. Abbreviations: s, starch deposits; n nucleus; per, pericarp epithelium; acl, aleurone cell layer; sec, starchy endosperm cells. Scale bar: A, 10µm; C-F: 0.19µm.

4.4.5 Transcriptc analysis of starch-related genes in the endosperm of carotenoid-enhanced transgenic lines

Transcript levels of endogenous GPI (glucose 6-phosphate isomerase), PGM (phosphogluco mutase), AGPsem (ADP-glucose pyrophosporylase small subunit isolated from embryo), AGPlem (ADP-glucose pyrophosporylase large subunit isolated from embryo), PHO1 (plastidial starch phosphorylase), ISA1/2 (isoamylase 1/2; debranching enzyme), SS1 (starch synthase 1) and SBE1 (starch branching enzyme 1) were monitored by quantitative real-time RT-PCR in the endosperm at 30 DAP in order to investigate whether endogenous starch-related gene expression was influenced in the carotenoid-enhanced transgenic lines (**Figure 4.8**).

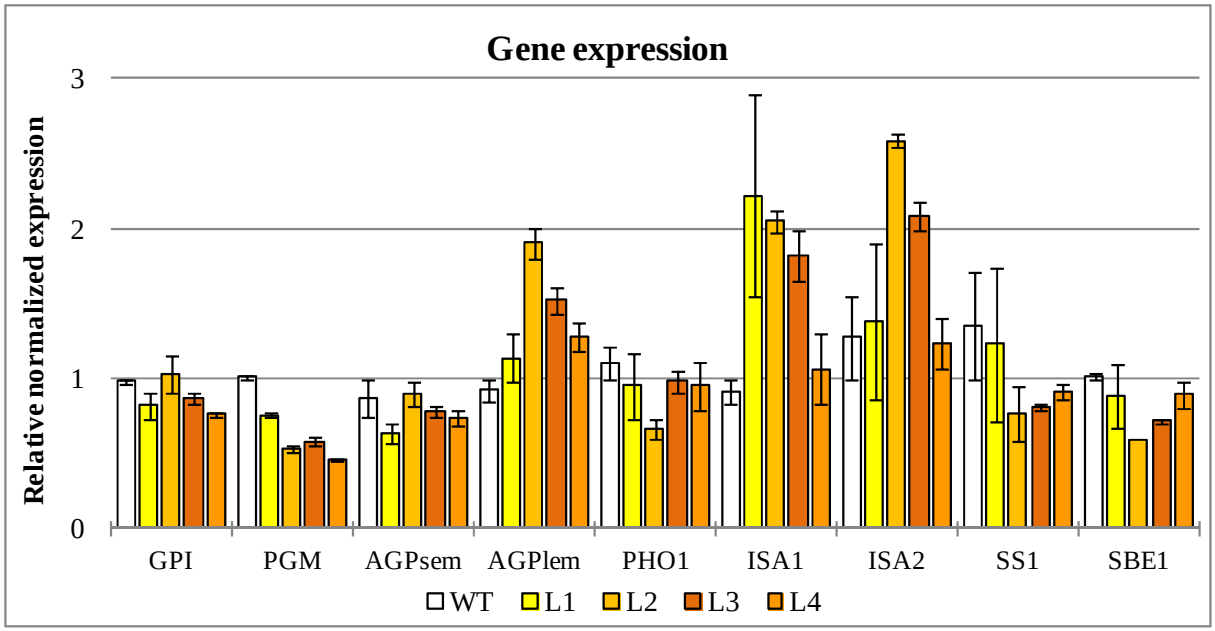

Figure 4.8 – Relative mRNA expression of endogenous starch-related genes in 30 DAP maize endosperm, normalized against actin mRNA and relative to WT and presented as the mean of three biological replicates. Bars represent standard errors. Abbreviations: GPI, glucose 6-phosphate isomerase; PGM, phosphoglucomutase; AGPsem, ADP-glucose pyrophosphorylase small unit isolated from embryo; AGPlem, ADP-glucose pyrophosphorylase large subunit isolated form embryo; PHO1, starch phosphorylase; ISA1/2, isoamylase 1/2 (debranching enzyme); SS1, starch synthase 1; SBE1, starch branching enzyme 1.

GPI transcript levels were similar in the WT, L1, L2 and L3 endosperm, whereas transcript levels in L4 were 1.3-fold lower than WT. PGM mRNA levels were downregulated ca: 2-fold in transgenic lines L2, L3 and L4, and 1.3-fold in transgenic line L1 compared to WT. AGPsem mRNA levels were similar in all lines, whereas AGPlem mRNA levels were up to 2-fold higher in L2, L3 and L4, compared to WT and L1. WT, L1, L3 and L4 seeds contained similar levels of PHO1 mRNA, but there was a 2-fold reduction in L2. ISA1 mRNA accumulation increased by up to 2-fold in L1, L2 and L3 but no changes were observed in L4

compared to WT. ISA2 mRNA levels increased by up to 2-fold in L2 and L3 compared to WT. SS1 mRNA levels reduced by up to 2-fold in L2, L3 and L4, compared to WT and L1. SBE1 mRNA levels were reduced 1.5-fold in L2 and L3 but not in L1 and L4 compared to WT.

4.5 Discussion

4.5.1 Selection of transgenic maize with different endosperm carotenoid contents and compositions to investigate the impact on starch endosperm content

Transgenic lines expressing different transgenes influencing carotenoid metabolism were selected to investigate the impact on starch metabolism in the endosperm. Line L1 expressed only *AtOR*; L2 expressed only *Zmpsy1*; L3 expressed *Zmpsy1*, *PacrtI*, and *ParacrtW*; and L4 expressed *Zmpsy1*, *PacrtI* and *Gllycb*. Lines L2, L3 and L4 accumulated *Zmpsy1* mRNA at different levels (**Figure 4.3**) resulting in different levels of total carotenoids (**Figure 4.4.**). *PacrtI* and *Gllycb* catalyze the synthesis of downstream carotenoids and *ParacrtW* extends the pathway to ketocarotenoids. *AtOR* increases total carotenoid content without altering carotenoid composition in the endosperm (see Chapter 2). The selected lines therefore provide a diverse genetic background with different transgene mRNA levels, resulting in different carotenoid profiles.

4.5.2 Carotenoid accumulation reduces the total starch content in the endosperm

In plant storage organs, carotenoids are synthesized and deposited in amyloplast membranes, which generally have limited capacity for carotenoid production and storage (Wurtzel 2004; Li et al. 2012). Amyloplasts can be converted to chromoplasts when starch breakdown begins, and the starch granules begin to disappear as carotenoid sequestering structures such as plastoglobulis and carotenoid crystals accumulate (Horner et al. 2007). During the ripening of tobacco floral nectarines, a mutually exclusive relationship between carotenoid accumulation and starch deposition has been observed (Horner et al. 2007). The biosynthesis of isoprenoids (carotenoid precursors) in plant cells requires precursors produced in the cytosol by the mevalonate (MVA) pathway and in the plastid by the methylerythritol 4-phosphate (MEP) pathway. A direct correlation between sugar levels and isoprenoid metabolism was observed in an *Arabidopsis thaliana* mutant with increased levels of MEP-derived isoprenoid products

(chlorophylls and carotenoids) without changes in the levels of relevant MEP pathway transcripts, proteins, or enzyme activities (Flores-Pérez et al. 2010). The soluble sugars may therefore accumulate at the expenses of starch, which is a carbohydrate reservoir.

Biochemical analysis revealed that the total starch content fell by up to 8% in the endosperm of carotenoid-enhanced transgenic lines (**Figure 4.5**). This was supported by the cytological analysis of endosperm cells using TEM and SEM (**Figure 4.6** and **4.7**) also revealed no changes in the morphology of starch granules. My data revealed a correlation between carotenoid accumulation and the loss of total starch, suggesting that carotenoid synthesis might occur at the expense of starch-derived carbohydrate metabolism. In citrus callus, the lower starch content reported by (Cao et al. 2015) presumably reflected the plastid modification process induced by significant carotenoid accumulation. Furthermore, declining starch levels during the ripening of tomato fruits were also correlated with increased carotenoid accumulation (Tohge et al. 2014). The carotenoid content of the transgenic lines ranged from ca: 13 µg/g DW in L1 to ca: 127 µg/g DW in L3 (**Figure 4.4**), whereas the starch content was up to 8% lower in L2, L3 and L4, but not in L1. This suggests that an extreme increase in carotenoid accumulation is required to induce collateral effects on starch accumulation.

4.5.3 Endogenous starch pathway gene expression reveals an alternative mechanism to reduce the starch content in carotenoid-enhanced maize lines

Targeted transcript analysis focusing on genes related to starch biosynthesis was carried out to evaluate differences between the wild-type and transgenic lines at key points in the pathway affecting starch accumulation. The evaluation of GPI and PGM, which are early precursors of sugar metabolism that can be directed to either the carotenoid or starch pathways (Gallagher et al. 2003), revealed no differences in GPI expression between WT and transgenic lines, but a 2-fold downregulation of PGM mRNA levels in L2, L3 and L4 compared to WT, and a 1.3-fold decrease in L1 compared to WT. These results suggest that PGM expression plays a key role in the choice between starch and carotenoid biosynthesis because transgenic lines containing less starch (L2, L3 and L4) produced lower levels of PGM mRNA than L1, which accumulated near-wild-type amounts of starch. This hypothesis is supported by the fact that the total starch content was reduced in transgenic plants expressing constitutively an antisense PGM construct. These plants also displayed a reduced rate of photosynthesis, a dramatic

reduction in nucleotide levels, and a general decline in metabolic activity (Lytovchenko et al. 2002).

AGPase, which is the first rate-limiting enzyme in the starch biosynthesis pathway, is a heterotetramer comprising two large subunits (AGP-L, encoded by *sh2*, *agplemzm*, *agpllzm* or *AGPL3*) and two small subunits (AGP-S, encoded by *bt2*, *agpsemzm* or *agpslzm*) (Hannah et al. 2001; Huang et al. 2014). The *agpllzm* and *agpsemzm* genes encode a plastidial AGPase in the maize endosperm and are required for normal levels of starch accumulation even when the cytosolic form of the enzyme is fully functional. The *agplem* gene also functions in the endosperm to generate combinations of subunits that remain functional even when expressed in *Escherichia coli* (Huang et al. 2014). The *agpsemzm* mRNA levels were similar in WT plants and all the transgenic lines, but the *agplem* mRNA levels were higher in L2, L3 and L4 than WT and L1. It therefore appears that the plastidial AGPase activity might not be downregulated and cannot be correlated with the reduced total starch content observed in these lines.

SSI probably accounts for all of the soluble SS activity in developing kernels (Cao et al. 1999; Jeon et al. 2010). The levels of SSI and SBEI mRNA each declined by up to 2-fold in L2, L3 and L4 compared to WT, but there was no difference when comparing WT and L1. In *A. thaliana*, SSI is a plastidial enzyme that is necessary in leaves for the synthesis of normal amylopectin (Delvallé et al. 2005). *A. thaliana* SSI is biochemically related to maize SSI (Commuri and Keeling 2001). However, rice SSI has less impact on starch structure in storage tissues than it does in leaves (Nakamura 2002). The expression of antisense SSI in potato did not affect the synthesis and structure of amylopectin even when SSI activity in potato tubers was no longer detected (Kossmann et al. 1999). The downregulation of SSI may therefore not affect the modification of starch properties but it might have an effect on total starch content. SBE1 generates amylopectin by cleaving the α(1, 4) bonds in polyglucans and reattaching the chain via α(1, 6) bonds (Ball and Morell 2003; Kubo et al. 2010). The observed downregulation of SBEI suggested that the amylopectin content in L2, L3 and L4 may be distinct to that in L1 and WT plants. A direct analysis of amylose/amylopectin profiles was not carried out in the carotenoid-enhanced maize lines, but Blauth et al. (2002) reported that a SBEI-deficient maize mutant produces the same amylopectin profile as wild-type maize. Similarly, the loss of SBEI in the rice *sbe1* mutant did not affect the accumulation of starch or the morphological characteristics of the plant, including the grain – indeed the

starch content in the endosperm of the *sbe1* mutant was comparable to that of wild-type grains (Satoh et al. 2003). However, maize double *sbe1* and *sbeIIb* mutants in a waxy background contained less total starch and altered morphology and physical properties in the endosperm, compared to WT (Li et al. 2007).

Kubo et al. (2010) reported that ISA1 is required for the accumulation of ISA2, which is post-transcriptionally regulated. Transcript analysis showed that ISA1 mRNA is induced in tissues that synthesize starch but returns to low levels during starch degradation, whereas ISA2 mRNA levels remain relatively abundant during periods of both starch biosynthesis and degradation (Kubo et al. 2010). In the carotenoid-enhanced lines, ISA1 mRNA levels increased by up to 2-fold in L1, L2 and L3 but no changes compared to WT were observed in L4, whereas ISA2 mRNA levels increased by up to 2-fold in L2 and L3 compared to WT. The levels of ISA1 and ISA2 mRNA therefore do not correlate with the loss of starch content.

The plastidial isoform of starch phosphorylase (PHO1) has an 80-amino-acid insertion which is not present in PHO2, and binds with high affinity to low-molecular-weight linear malto-oligosaccharides and amylose. In contrast, the cytosolic isoform (PHO2 or PHO-H) binds with high affinity to highly-branched polyglucans such as glycogen (Satoh et al. 2008). Both isoforms catalyze a reversible reaction: in the forward reaction, glucose-1-phosphate donates a glucose unit to the non-reducing end of the α-glucan chain thus releasing inorganic phosphate, whereas the reverse reaction generates glucose-1-phosphate in the presence of inorganic phosphate. Although the enzyme can facilitate both the synthesis and degradation of starch in plants, the degradation role appears to be favored in sink tissues (Satoh et al. 2008). In the carotenoid-enhanced transgenic lines, PHO1 mRNA levels in L1, L3 and L4 were similar to WT plants, but were less abundant in L2.

The transcript analysis of key enzymes in the starch biosynthesis pathway suggests that differences in starch accumulation among the carotenoid-enhanced transgenic maize lines cannot be exclusively attributed to changes in starch biosynthesis. Thus, an alternative mechanism should exist that reduces the starch content in the transgenic lines, such as upregulation of α-amylase and β-amylase, which hydrolyze starch into sugars. Three different mechanisms that modulate the accumulation of metabolites are represented in **Figure 4.9**, i.e. changing the availability of precursors, the capacity for biosynthesis or the capacity for degradation. In carotenoid-enhanced citrus callus, the lower starch content was correlated with the upregulation of α-amylase activity (Cao et al. 2015). However, the upregulation of α-

amylase observed by Cao et al. (2015) appeared to contradict proteomic data reported by Barsan et al. (2012) showing that proteins involved in starch metabolism became less abundant during chromoplastogenesis. In addition, plastid modifications associated with engineered carotenoid accumulation may involve protein dynamics that differ from those reflecting natural chromoplastogenesis in fruit. Despite the strong conservation of the chromoplast proteome between ripening sweet orange and tomato fruits (Zeng et al. 2011), the plastids in the citrus flower petals, roots, embryoids, petioles and callus systems are never involved in natural chromoplastogenesis, and they are distinct from those in the fruits (Cao et al. 2015a).

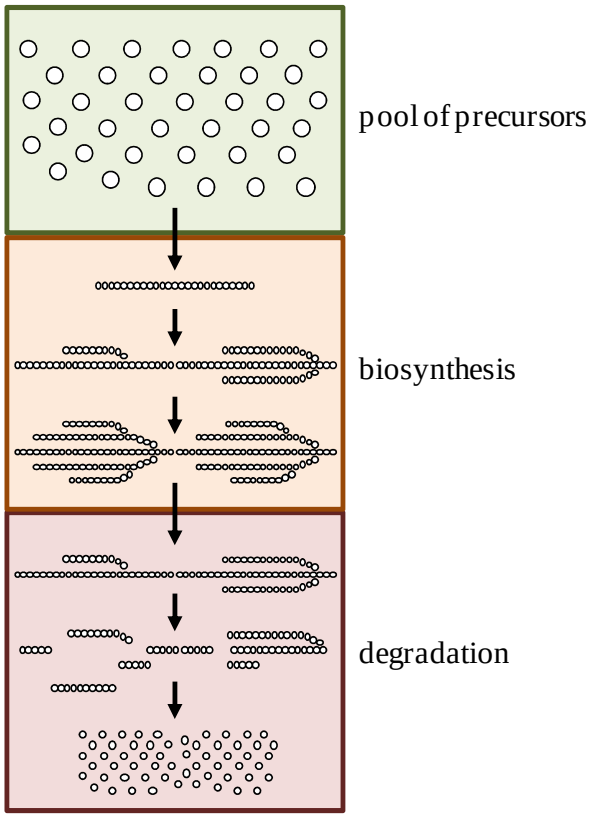

Figure 4.9 – Mechanisms to control the accumulation of specific metabolites.

4.6 Conclusions

The lower total starch content in three transgenic maize lines engineered to accumulate high carotenoid content suggests that carotenoid biosynthesis in maize endosperm may occur at the expense of early precursors that are also required for starch biosynthesis. Lower transcript levels of PGM were detected in high carotenoid accumulating transgenic lines, which might indicate a lower pool of precursors available for starch synthesis. In addition, downregulation of SBE1 and SS1, genes related to starch biosynthesis, suggest that the decrease of starch

content is produced without altering amylopectin structure. A combination of different mechanisms is necessary to reduce the total amount of starch in carotenoid-enhanced maize endosperm.

4.7 References

Ball SG, Morell MK (2003) From bacterial glycogen to starch: understanding the biogenesis of the plant starch granule. Annu Rev Plant Biol. 54:207–233.

Ballicora MA, Laughlin MJ, Fu Y, Okita TW, Barry GF, Preiss J (1995) Adenosine 5'-diphosphate-glucose pyrophosphorylase from potato tuber. Significance of the N terminus of the small subunit for catalytic properties and heat stability. Plant Physiol. 109:245–251.

Beatty MK, Rahman A, Cao H, Woodman W, Lee M, Myers AM, et al. (1999) Purification and molecular genetic characterization of ZPU1, a pullulanase-type starch-debranching enzyme from maize. Plant Physiol. 119:255–266.

Blauth SL, Kim KN, Klucinec J, Shannon JC, Thompson D, Guiltinan M (2002) Identification of Mutator insertional mutants of starch-branching enzyme 1 (*sbe1*) in *Zea mays* L. Plant Mol Biol. 48:287–297.

Blauth SL, Yao Y, Klucinec JD, Shannon JC, Thompson DB, Guilitinan MJ (2001) Identification of Mutator insertional mutants of starch-branching enzyme 2a in corn. Plant Physiol. 125:1396–1405.

Cao H, Wang J, Dong X, Han Y, Ma Q, Ding Y, et al. (2015) Carotenoid accumulation affects redox status, starch metabolism, and flavonoid/anthocyanin accumulation in citrus. BMC Plant Biol. 15:27-33.

Carlson SJ, Chourey PS (1996) Evidence for plasma membrane-associated forms of sucrose synthase in maize. Mol Gen Genet. 252:303–310.

Commuri PD, Keeling PL (2001) Chain-length specificities of maize starch synthase I enzyme: Studies of glucan affinity and catalytic properties. Plant J. 25:475–486.

Decourcelle M, Perez-Fons L, Baulande S, Steiger S, Couvelard L, Hem S, et al. (2015) Combined transcript, proteome, and metabolite analysis of transgenic maize seeds engineered for enhanced carotenoid synthesis reveals pleotropic effects in core metabolism. J Exp Bot. 2015 (in press) DOI: 10.1093/jxb/erv120

Delvallé D, Dumez S, Wattebled F, Roldán I, Planchot V, Berbezy P, et al. (2005) Soluble starch synthase I: A major determinant for the synthesis of amylopectin in *Arabidopsis thaliana* leaves. Plant J.43:398–412.

Dian W, Jiang H, Chen Q, Liu F, Wu P (2003) Cloning and characterization of the granule-bound starch synthase II gene in rice: Gene expression is regulated by the nitrogen level, sugar and circadian rhythm. Planta. 218:261–268.

Flores-Pérez Ú, Pérez-Gil J, Closa M, Wright LP, Botella-Pavía P, Phillips MA, et al. (2001) PLEIOTROPIC REGULATORY LOCUS 1 (PRL1) integrates the regulation of sugar responses with isoprenoid metabolism in Arabidopsis. Mol Plant. 3:101–112.

Gallagher CE, Cervantes-Cervantes M, Wurtzel ET (2003) Surrogate biochemistry: use of Escherichia coli to identify plant cDNAs that impact metabolic engineering of carotenoid accumulation. Appl Microbiol Biotechnol. 60:713-719.

Guo F, Zhou W, Zhang J, Xu Q, Deng X (2012) Effect of the citrus lycopene β-cyclase transgene on carotenoid metabolism in transgenic tomato fruits. PLoS One. 7:e32221.

Hannah LC, Shaw JR, Giroux MJ, Reyss A, Prioul JL, Bae JM, et al. (2001) Maize genes encoding the small subunit of ADP-glucose pyrophosphorylase. Plant Physiol.127:173–183.

Hardin SC, Duncan KA, Huber SC (2006) Determination of structural requirements and probable regulatory effectors for membrane association of maize sucrose synthase 1. Plant Physiol. 141:1106–1119.

Hirose T, Terao T (2004) A comprehensive expression analysis of the starch synthase gene family in rice (*Oryza sativa* L.). Planta. 220:9–16.

Horner HT, Healy R a., Ren G, Fritz D, Klyne a., Seames C, et al. (2007) Amyloplast to chromoplast conversion in developing ornamental tobacco floral nectaries provides sugar for nectar and antioxidants for protection. Am J Bot. 94:12–24.

Huang B, Hennen-bierwagen TA, Myers AM (2014) Functions of Multiple Genes Encoding ADP-Glucose Pyrophosphorylase Subunits in Maize Endosperm. Plant Physiol. 164:596–611.

James MG, Denyer K, Myers AM (2003) Starch synthesis in the cereal endosperm. Curr Opin Plant Biol. 6:215–222.

Jeon J, Ryoo N, Hahn T, Walia H, Nakamura Y (2010) Starch biosynthesis in cereal endosperm. Plant Physiol Biochem. 48:383–392.

Jiang L, Yu X, Qi X, Deng S, Bai B, Li N, et al. (2013) Multigene engineering of starch biosynthesis in maize endosperm increases the total starch content and the proportion of amylose. Transgenic Res. 22:1133–1142.

Kossmann J, Abel GJ, Springer F, Lloyd JR, Willmitzer L (1999) Cloning and functional analysis of a cDNA encoding a starch synthase from potato (Solanum tuberosum L.) that is predominantly expressed in leaf tissue. Planta. 208:503–511.

Kubo A, Colleoni C, Dinges JR, Lin Q, Lappe RR, Rivenbark JG, et al. (2010) Functions of heteromeric and homomeric isoamylase-type starch-debranching enzymes in developing maize endosperm. Plant Physiol.153:956–969.

Li J, Guiltinan MJ, Thompson DB (2007) Mutation of the maize *sbe1a* and *ae* genes alters morphology and physical behavior of wx-type endosperm starch granules. Carbohydrate Res. 342:2619-2627.

Li L, Yang Y, Xu Q, Owsiany K, Welsch R, Chitchumroonchokchai C, et al. The *or* gene enhances carotenoid accumulation and stability during post-harvest storage of potato tubers. Mol Plant. 2012;5(2):339–52.

Nakamura Y (2002) Towards a better understanding of the metabolic system for amylopectin biosynthesis in plants: rice endosperm as a model tissue. Plant Cell Physiol.43:718–725.

Nogueira M, Mora L, En EMA, Bramley PM, Fraser PD (2013) Subchromoplast Sequestration of Carotenoids Affects Regulatory Mechanisms in Tomato Lines Expressing Different Carotenoid Gene Combinations. Plant Cell. 25:1–20.

Russell D, DeBoer D, Stark D, Preiss J, Fromm M (1993) Plastid targeting of *E. coli* β-glucuronidase and ADP-glucose pyrophosphorylase in maize (*Zea mays* L.) cells. Plant Cell Rep. 13:24–27.

Sandmann G (2001) Genetic manipulation of carotenoid biosynthesis: strategies, problems and achievements. Trends Plant Sci. 6:14–17.

Satoh H, Nishi A, Yamashita K, Takemoto Y, Tanaka Y, Hosaka Y, et al. (2003) Starch-branching enzyme I-deficient mutation specifically affects the structure and properties of starch in rice endosperm. Plant Physiol. 133:1111–1121.

Satoh H, Shibahara K, Tokunaga T, Nishi A, Tasaki M, Hwang S-K, et al. (2008) Mutation of the plastidial alpha-glucan phosphorylase gene in rice affects the synthesis and structure of starch in the endosperm. Plant Cell. 20:1833–1849.

Schmidt M, Parrott W, Hildebrand DF, Berg RH, Cooksey A, Pendarvis K, et al. (2015) Transgenic soya bean seeds accumulating β-carotene exhibit the collateral enhancements of oleate and protein content traits. Plant Biotechnol J. 13:590–600.

Subbarao K, Datta R, Sharma R (1998) Amylases synthesis in scutellum and aleurone layer of maize seeds. Phytochemistry. 49:657-666.

Tohge T, Alseekh S, Fernie AR (2014) On the regulation and function of secondary metabolism during fruit development and ripening. J Exp Bot. 65:4599–4611.

Tuncel A, Okita TW (2013) Improving starch yield in cereals by over-expression of ADPglucose pyrophosphorylase: Expectations and unanticipated outcomes. Plant Sci. 211:52–60.

Vrinten PL, Nakamura T (2000) Wheat granule-bound starch synthase I and II are encoded by separate genes that are expressed in different tissues. Plant Physiol. 122:255–264.

Wurtzel ET (2004) Chapter five Genomics, genetics, and biochemistry of maize carotenoid biosynthesis. Recent Adv Phytochem. 38:85–110.

Zeng Y, Pan Z, Ding Y, Zhu A, Cao H, Xu Q, et al. (2011) A proteomic analysis of the chromoplasts isolated from sweet orange fruits [*Citrus sinensis* (L.) Osbeck]. J Exp Bot. 62:5297–5309.

CHAPTER 5

Development of high carotenoid transgenic maize hybrids with agronomic performance similar to commercial hybrids

CHAPTER 5: GENERATION OF HIGH CAROTENOID TRANSGENIC MAIZE HYGRIDS WITH AGRONOMIC PERFORMANCE SIMILAR TO COMMERCIAL HYBRIDS

5.1 Abstract

Transgenic maize hybrids with high carotenoid content were developed by crossing a high carotenoid transgenic maize line (HC), overexpressing *Zmpsy1* and *PartI*, with different tester lines from different heterotic groups. Agronomic traits (days to flower, plant height, ear height and yield) and ear morphological traits (ear length, kernel rows per ear, conicity and ear grain percentage) were evaluated in two different locations in field trials in Spain in inbred lines and the corresponding hybrids. Statistical analysis indicated that most of the parameters were influenced by genotype rather than location. In addition, calculation of heterosis for all the traits was performed in order to determine the performance of hybrids compared with the corresponding parental lines. Higher yields were obtained in hybrids with testers having longer FAO cycles (B73, Mo17 and EZ6), whereas heterosis was higher in hybrids with flint rather than dent kernel types. These experiments resulted in high yielding, carotenoid enriched maize hybrids with agronomic properties equal to or on occasion superior to commercial hybrids commonly grown in the area.

5.2 Introduction

Heterosis or hybrid vigour, describes the superior performance of heterozygous F_1-hybrid plants compared to the average performance of their homozygous inbred parents (Shull 1952; **Figure 5.1**). The most important parameter considered by plant breeders is yield heterosis. However, heterosis can be calculated for increased biomass, size, growth rate and development, resistance to diseases and to insect pests, or to biotic stresses (Shull 1952). Self-pollination of hybrids over several generations leads to a gradual reduction of heterosis and vigor, a phenomenon known as inbreeding depression. Heterosis was first described by Charles Darwin in 1876 after he observed that progeny of cross-pollinated maize were 25% taller than progeny of inbred maize (Darwin 1876). Since then, heterosis has been extensively exploited in plant breeding, particularly in maize because maize can be easily cross-pollinated. The molecular basis of heterosis is not completely understood (reviewed by Hochholdinger and Hoecker 2007).

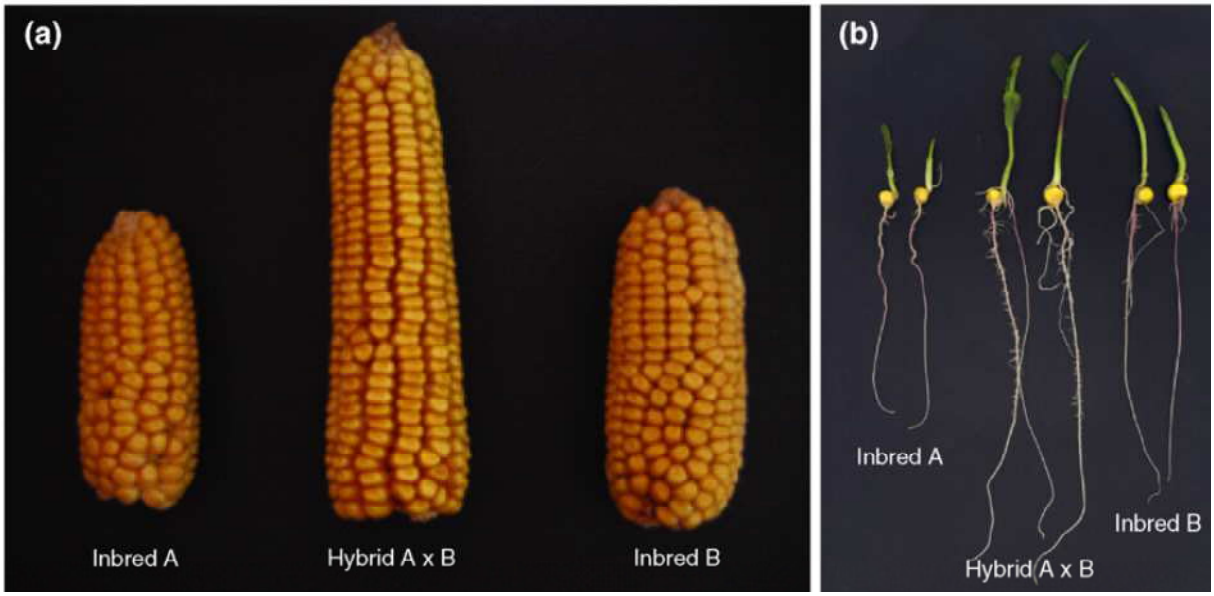

Figure 5. 1– Phenotypic manifestation of heterosis. Heterosis is typically seen in adult traits such as yield or ear size (a) but it already manifests during seedling development (b) (Hochholdinger and Hoecker 2007).

The development of competitive maize hybrids requires the establishment of heterotic patterns, defined as the cross between known genotypes that express a high level of heterosis (Carena and Hallauer, 2001). Crosses among inbred lines from unrelated heterotic groups have better grain yield performance than those crosses among lines in the same group (Moll et al., 1965; Hallauer et al., 1988; Melchinger, 1999). Reid Yellow Dent and Lancaster Sure Crop are two groups of open-pollinated maize cultivars that provide most of the germplasm used to develop early testing inbred lines (evaluation of inbred lines in the first 3 generations) that are used for commercial hybrid seed production. The most exploited heterotic pattern is the cross between Iowa Stiff Stalk Synthetic (BSSS, type Reid) and the Lancaster Sure Crop heterotic groups (Barata and Carena, 2006).The Reid x Lancaster cross is commonly used in hybrid programs in Spain and other areas of Southern Europe (Galarreta and Álbarez 2010). In order to develop new maize hybrids, breeders select better heterotic patterns crossing inbred lines in a heterotic group with tester lines in a different group to evaluate the General Combining Ability between them. Tester lines are representative inbred lines from a known origin that can be used as practical tool in determining heterotic patterns, combining ability and breeding values (Li et al. 2007).

Improved cultivars are a key element among practices used to achieve greater yield, integrated pest management and other properties to increase agricultural sustainability (Kutka 2011). The primary purpose of plant breeding is to develop varieties or hybrids that are efficient in their use of nutrients, give the greatest return of high-quality products per unit area

in relation to cost and ease of production and that, are adapted to the needs of the grower and the consumer. The use of hybrids in maize at the beginning of the 20th century focused on high-yield but new generations of hybrids incorporate new traits for easier pest management, stress tolerance and recently, improved nutrition.

Most of the reports on high carotenoid maize focused on the identification of alleles of key loci that correlate with higher β-carotene content such as *lyce* (Harjes et al. 2008) and *hyd3* (Vallabhaneni et al. 2009) in order to use them in future breeding programs to generate new inbred lines or hybrids with higher carotenoid content. In addition, carotenoid content and heterosis for carotenoid content and composition has been studied in commercial maize hybrids (Egesel et al. 2003; Kljak and Grbeša 2015).

Few reports have been published on the production of hybrids with high carotenoid content by using different approaches: backcross for marker-assisted introgression of an allele (Muthusamy et al. 2014), factorial mating (Menkir et al. 2014) and half-diallel crossing (Senete et al. 2011) (**Figure 5.2**). Marker-assisted introgression by backcross of a β-carotene hydroxylase (BCH) allele corresponding to low capacity of conversion of β-carotene to zeaxanthin, allowed the generation of high β-carotene maize hybrids (Muthusamy et al. 2014). Authors identified 7 inbred lines commonly used to produce commercial hybrids in India (recurrent parents) and 7 inbred lines with high β-carotene content due to a BCH allele provided by CIMMYT-Harvest Plus (donor parents). Two backcross generations and three rounds of self-pollination were required to recover ca: 90% of the recurrent parent genome with the BCH allele of interest from the parents. Thirteen selected improved progenies of the seven inbred lines were used in a breeding program to reconstitute F1 hybrids. Field trials in two different locations in India in 2013 allowed agronomic characterization of the novel hybrids (Muthusamy et al. 2014) (**Figure 5.2**). Assessment of genetic diversity of 38 orange and yellow endosperm maize inbred lines using Amplified Fragment Length Polymorphism (AFLP) markers classified the lines into two groups with varying levels of pro-vitamin A (Adeyemo et al. 2011). Eight inbred lines selected from each AFLP group were divided into two sets each of four inbred lines. The four inbred lines in each set selected from the first AFLP group were used as female parents and crossed with the four inbred lines in another set, selected from the second AFLP group as male parents using a factorial mating scheme. Each inbred line was used as a female parent in one set of crosses and as a male parent in the second set of crosses (Set 1 x Set 2, Set 2 x Set 4, Set 3 x Set 1, and Set 4 x Set 3) to form hybrids (**Figure 5.2**). The resulting 62 hybrids along with duplicate entries of an orange

endosperm commercial hybrid (Oba Super II) were evaluated in 4 locations in Nigeria in 2009 and 2010 cropping seasons (Menkir et al. 2014). In this case, hybrids were generated without previous genomic modification thus accelerating hybrid production. However, an in depth AFPL study was necessary to identify valuable lines in terms of provitamin A content, although traits for good field performance of inbred lines were not considered (Menkir et al. 2014). Twenty-one hybrids were generated from seven inbred lines, selected on the basis of their pro-vitamin A content, following a half-diallel mating design (Senete et al. 2011) (**Figure 5.2**). The F1 seed of each cross was bulked together with the respective reciprocal cross and four locally adapted commercial hybrids were used as experimental checks. Similarly to Menkir et al. 2014, inbred lines used as parents for hybrid production were selected on the basis of carotenoid content rather than good agronomic performance. Thus, traits for good field performance were not assured so they were evaluated in the experiment.

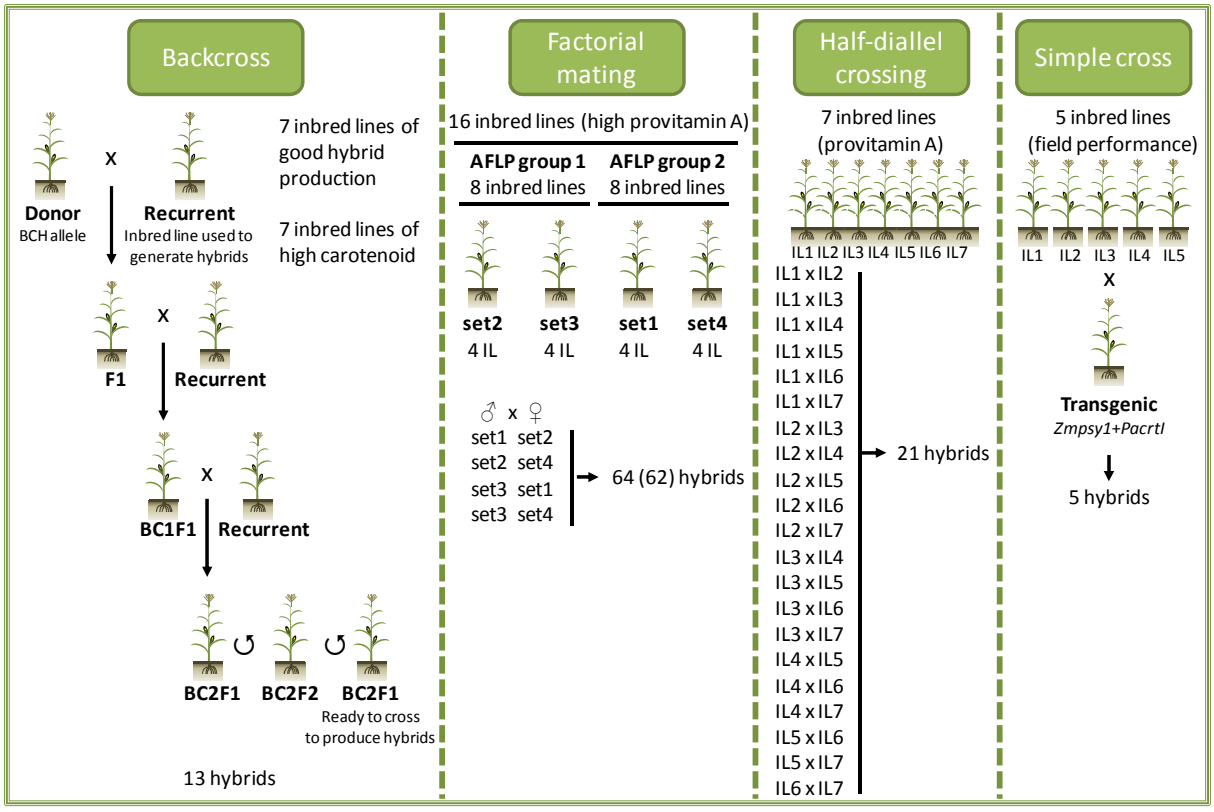

Figure 5. 2 – Schematic representation of different techniques used to produce high carotenoid maize hybrids. Abbreviations: BC, backcross; IL, inbred line, AFLP, Amplified Fragment Length Polymorphism.

A high-carotenoid maize line was generated by the genetic transformation of the elite M37W inbred line with *Zmpsy1* and *PacrtI* (HC) (Zhu et al. 2008). The low field performance and yield of inbred lines make their cultivation economically unattractive. Crosses of parents of diverse origin produce higher grain yields than crosses amongst lines with the same genetic

background (Melchinger & Gumber, 1998) so HC was crossed with five different tester lines (Mo17, B73, EZ6, EZ59 and A619) from different heterotic groups in order to create novel hybrids, with comparable or superior field performance to commercial hybrids, that incorporate the carotenoid-enriched traits conferred by the *Zmpsy1* and *PacrtI* transgenes. Only one growing season is required to generate hybrids by simple cross of a transgenic line with inbred lines from the different heterotic groups. Utilizing the simple cross strategy, we generated 5 hybrids which provided the material for the experiments described in this chapter.

5.3 Materials and methods

5.3.1 Plant material

Five maize tester lines belonging to well-known heterotic groups and commonly used in conventional breeding programs were chosen to evaluate the performance of high carotenoid transgenic maize line (HC) to generate high-yielding hybrids. Specific traits of these lines are listed in **Table 5.1**.

Table 5. 1 – Maize Tester lines used to evaluate the combining ability of HC.

Line	Genotype	Heterotic group	FAO Cycle	Days to Flower	Kernel type
A632	Inbred	Reid	500	87	Dent
B73	Inbred	Reid	700	100	Dent
EZ6	Inbred	OP Orange flint	700	98	Flint
EZ59	Inbred	OP Estarville	500	85	Flint
Mo17	Inbred	Lancaster	700	102	Dent

All lines were provided by Dr. Angel Alvarez, EEAD-CSIC, Zaragoza, Spain

5.3.2 Field trials

In 2013, HC was crossed with the different testers (**Table 5.1**) in experimental field in Lleida (41° 37′ 0″ N, 0° 38′ 0″ E, altitude ~ 167 m). The field trial was under a semiarid climate with low precipitation (38 mm) and high average temperature (23.5°C) in the maize growing period (May to October). The field was irrigated by sprinkler 2-3 times per week, with approximately 600 mm of water per season. Hybrids were generated by collecting HC pollen in standard paper pollinating bags and transferred to the silks of the female parents. To prevent pollen from contaminating the samples a ‘shoot bag’ was kept over the ear until pollination, and the pollinating bag was left over the ear after pollination until harvest. As

maize inbred lines correspond to different FAO cycles, repeat sowing dates were 6th, 14th and 23rd May in order to ensure pollination of all the crosses. Harvest was done in November after physiological maturity which was indicated by a 'black layer', located at the base of the kernels.

In the 2014 growing season, the hybrids obtained the previous season (2013) were evaluated in two different locations in NE Spain (Lleida, 41° 37′ 0″ N, 0° 38′ 0″ E, altitude ~ 167 m; and Sucs, 41° 42′ 7″ N, 0° 24′ 42″ E, altitude ~ 258 m), under similar weather conditions (**Table 5.2**).

Table 5. 2 – Weather conditions during the maize growing season (May-August) 2014. (Source: www.ruralcat.net).

	Month	Maximum T (ºC)	Minimum T (ºC)	Average day T (ºC)	Average precipitation (mm)
Lleida	May	30.5	5.1	17	41.2
	June	34.9	10.9	22.2	27.6
	July	36.5	12	23.2	21.6
	August	36.4	10.6	23.6	35.9
	September	33.2	8.9	21.2	126.9
	October	30.7	5.3	16.5	21
Sucs	May	28.7	2.8	16	22.7
	June	32.4	9.6	21.4	10.4
	July	34.6	9.8	22.4	6
	August	34.6	9.6	22.8	41.2
	September	32	8.1	20.8	118.6
	October	28.5	3.9	16.7	21.4

Both fields were irrigated at 500-600 mm by sprinkler. The Sucs field trial site experienced drought periods because of lack of irrigation on occasion.

In each experiment, 6 maize inbred lines (five testers and HC) and 6 hybrids (the 5 corresponding crosses with HC and one commercial cultivar, Lerma) were evaluated in a random block design with four replicates per location, grouping inbred lines and hybrids independently in order to minimize the effect of hybrids on the growth of the inbred lines. The experimental plot dimensions were 4 m x 0.65 m with 20 plants per row (0.2 m distance between plants in row). Plants were sowed on the 22nd (Lleida) and the 23th (Sucs) of April and harvested in October 2014, after black layer.

5.3.3 Agronomic and morphologic trait assessment of transgenic maize hybrids

Agronomic and morphological traits were measured by harvesting 5 representative plants in 1 m of the field plot per replicate.

Agronomic trait assessment included:

- Flowering date: number of days from sowing when 50% of plants were at the anthesis stage.
- Plant height: distance from stem base to last leaf
- Ear height: distance from stem base to main ear joint
- Yield: kg produced in 1 hectare of cultivated field

$$yield = \frac{grain\ weight\ of\ 5\ plants\ (kg)}{number\ of\ plants\ \times area\ of\ 1\ plant\ (m^2)} \times 10$$

Morphological trait assessment included:

- Ear length: mean distance in mm from base to apex
- Kernel rows per ear
- Grain percentage: weight of total grains of an ear with respect to the full ear weight

$$grain\ percentage = \frac{grain\ weight\ of\ 5\ plants\ (kg)}{ear\ weight\ of\ 5\ plants\ (kg)} \times 100$$

- Conicity, a parameter used to determine ear shape was calculated according the following formula:

$$conicity\ index = \frac{\frac{di - ds}{2}}{\frac{l}{3}} \times 100$$

where *di* is diameter at the base of the ear (mm)

ds is diameter at the apex of the ear (mm)

l is the length of the ear (mm)

5.3.4 Heterosis of transgenic maize hybrids

Heterosis of transgenic maize hybrids versus their corresponding parents was calculated for all the morphological and agronomic parameters described above (days to flower, plant height, ear height, yield, ear length, kernel rows per ear, grain percentage and conicity) according to the following formula:

$$Heterosis = \frac{F1 - PA}{PA},$$

where *F1* is the value of the relevant parameter in F1 offspring (e.g. days, cm, kg/ha, etc.)

PA is the mean value of the parameter of the parents (e.g. days, cm, kg/ha, etc)

5.3.5 Statistical analysis

A general linear model was used to determine statistically significant differences in the agronomic and morphological traits as well as in heterosis for these parameters. Traits were compared by Tukey's mean separation procedure ($p < 0.05$). All the analyses were performed using the JMP Pro (JMP®, Version 11.0.0. SAS Institute Inc., Cary, NC, 2013). Two-factorial analysis of variance (ANOVA) with genotype (G) and location (L) as random factors was applied to the means per location and genotype. Analysis was performed independently for inbred lines and hybrids.

5.4 Results

5.4.1 Development of high carotenoid transgenic maize hybrids

Hybrids were developed by cross-pollination of HC with different tester lines (Mo17, B73, EZ6, EZ59 and A632) from different heterotic groups, in the 2013 growing season. Tester lines and HC fit in different FAO cycles so, in order to assure successful pollination, all parents were sown at three consecutive dates. Resulting hybrid seeds were harvested after black layer. To avoid cross-pollination several precautions were taken, such as keeping a bag over the ear until pollination and the pollinating bags were left over the ear until harvest. In addition, the tassel of female plants was removed to prevent self-pollination. The phenotype of hybrid seeds was clearly different from that of the corresponding parents, as expected. The orange color conferred by the expression of *Zmpsy1* and *PacrtI* from HC, male parent or dent grain morphology due to Mo17, B73 and A632 female parents were the most relevant traits in the hybrids (**Figure 5.3A**).

5.4.2 Evaluation of agronomic traits

In the 2014 growing season, the hybrids obtained in 2013 were evaluated in two different locations in NE Spain (Lleida and Sucs), under similar climatic conditions. Agronomic traits including days to flower, plant height (cm), and ear height (cm) were evaluated in the hybrids and parent inbred lines in order to assess agronomic performance. As expected, different inbred lines and the hybrids derived from their cross with HC exhibited statistically significant differences for all parameters we measured and all parameters were improved in the hybrids compared to the corresponding inbred lines (**Table 5.3**).

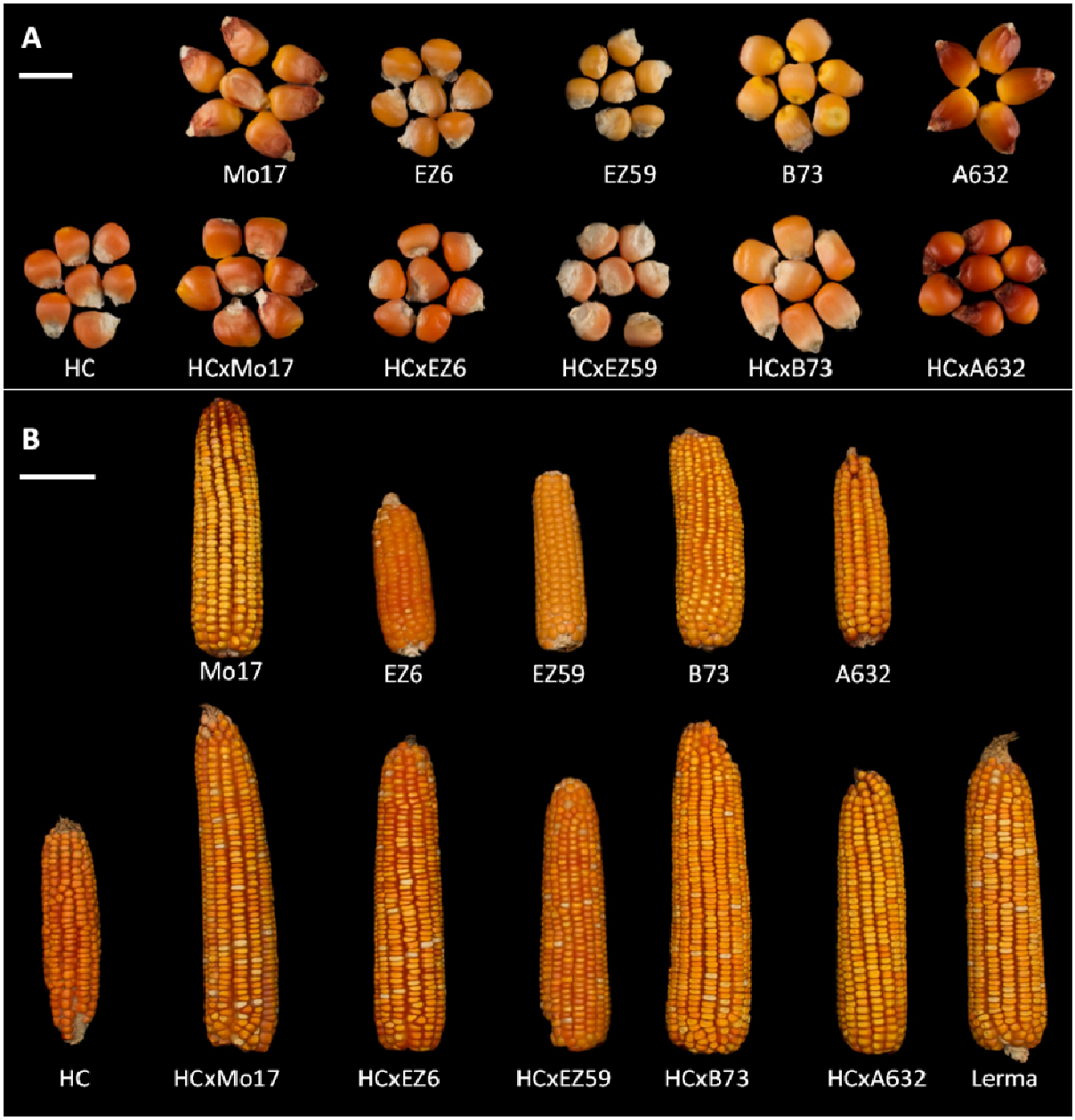

Figure 5. 3 Inbred lines, transgenic hybrids and commercial hybrid phenotypes of (A) seeds and (B) ears. Scale bar: A, 1cm; B, 5cm.

Mean days to flower of inbred lines were in the range 71-86; whereas mean days to flower of hybrids were in the range 76-85. Lerma, a commercial hybrid used as a local check flowered in 71 days, the shortest period observed amongst all the hybrids. Mean days to flower was significantly different amongst genotypes (G) (inbred lines or hybrids) and location (L) (Lleida or Sucs) but not G x L interaction, suggesting that differences in this parameter were due to a genotype effect, influenced by the location even though each genotype performed similarly in each location (**Table 5.3**).

Mean plant and ear height of inbred lines were in the range 91-180 cm and 52-94 cm, respectively, whereas mean plant and ear height of hybrids were in the range 172-220 and 100-122 cm, respectively. Lerma plant height was 143 cm and ear height 60 cm, the lowest height from all the hybrids we evaluated. Mean plant and ear height was significantly different amongst G (inbred lines or hybrids) and L (Lleida or Sucs), suggesting that differences in this parameter were due to a genotype effect, influenced by the location. However, G x L interaction of plant height was not significant, suggesting that each genotype behaved similarly in each location. Ear height of hybrids showed statistically significant differences in the interaction G x L (**Table 5.3**).

5.4.3 Ear morphology

Parameters to determine ear morphology were ear length (cm), number of kernel rows per ear, conicity (ear morphology) and ear grain percentage (weight of total grain of an ear with respect to the weight of the full ear). As expected, different inbred lines and hybrids derived from crosses with HC showed morphological differences. From all the morphological parameters evaluated, ear length was the most increased in the hybrids compared with inbred lines. (**Figure 5.3B; Table 5.3**).

Mean ear length of inbred lines was in the range 10-15 cm with the exception of Mo17 that was 17.6 cm; whereas mean ear length of hybrids was in the range 16-19 cm. Lerma was 14 cm long. Mean ear lenght was significantly different amongst G (inbred lines or hybrids) and L (Lleida or Sucs) but not G x L interaction was found, suggesting that differences in this parameter were due to a genotype effect, influenced by the location even though each genotype performed similarly in each location (**Table 5.3**).

Mean conicity index of inbred lines was in the range 2.8-4.3, whereas mean conicity index of hybrids was in the range 3.8-4.9. Lerma conicity index was 5.4, the highest index observed amongst all the hybrids. Mean conicity index was significantly different amongst G (inbred lines or hybrids) but not amongst L (Lleida or Sucs), suggesting that differences in this parameter were due to a genotype effect (**Table 5.3**).

Table 5. 3 – Results from ANOVA of agronomical and morphological traits of 6 maize inbreed lines and 6 hybrids in 2 sites.

Source of variation	df	Days to flower (days)	Plant height (cm)	Ear height (cm)	Yield (kg/ha)	Ear length (cm)	Kernel rows per ear	Conitcy	Ear grain percentage (%)
Inbred lines									
Genotype									
SS	5	1051.1 (***)	31639.3 (***)	7938.4 (***)	11638493.0 (***)	251.8 (***)	199.6 (***)	9.6 (*)	643.7 (***)
Mo17		78.5 ab	180.0 a	94.4 a	7315.1 a	17.6 a	16.5 a	3.9 a	81.8 a
EZ6		77.6 ab	132.3 b	72.4 bc	4987.5 ab	11.8 cd	11.2 c	3.9 a	81.2 a
A632		82.3 a	135.9 b	60.5 cd	4115.4 ab	11.6 cd	13.2 b	4.3 a	80.5 a
EZ59		70.8 b	91.3 c	51.7 d	2136.5 b	10.6 d	11.7 c	2.8 b	71.5 b
B73		85.1 a	156.9 ab	80.8 b	6608.1 a	13.6 bc	16.1 a	3.6 ab	81.2 a
HC		86.3 a	159.0 ab	74.2 bc	5254.5 ab	15.2 b	12.1 bc	3.4 ab	74.0 b
Location									
SS	1	3045.1 (***)	41378.3 (***)	15326.3 (***)	89617074.0 (**)	151.1 (***)	0.3 (ns)	3.0 (ns)	232.5 (***)
Lleida		71.6 a	173.4 a	91.4 a	6499.1 a	15.3 a	13.6 a	3.9 a	80.7 a
Sucs		88.6 b	110.7 b	53.2 b	3611.3 b	11.5 b	13.4 a	3.4 a	76.0 b
Genotype* Location									
SS	5	164.1 (ns)	2705.9 (ns)	1585.4 (ns)	31560046.0 (ns)	5.8 (ns)	5.7 (ns)	6.9 (ns)	353.3 (***)
Hybrids									
Genotype									
SS	5	1028.3 (***)	31790.0 (***)	20396.8 (***)	217519227.0 (***)	115.4 (***)	54.1 (***)	16.1 (**)	269.8 (***)
HCxMo17		82.8 a	194.6 ab	110.0 ab	11501.3 abc	18.7 ab	13.9 bcd	3.8 c	82.4 b
HCxEZ6		81.8 a	212.3 a	121.9 a	14828.9 a	18.8 a	13.1 cd	3.8 c	81.8 b
HCxA632		80.9 a	182.5 b	98.4 b	10740.4 bc	16.6 b	14.5 abc	4.9 bc	82.7 b
HCxEZ59		75.5 b	172.0 b	100.3 b	9444.3 bc	17.3 ab	12.8 d	4.2 bc	82.5 b
HCxB73		84.6 a	219.8 a	118.8 a	12401.8 ab	17.2 ab	15.1 ab	4.9 ab	84.2 b
Lerma		71.1 b	142.6 c	59.5 c	8165.3 c	14.1 c	15.8 a	5.4 a	88.8 a
Location									
SS	1	3794.6 (***)	55163.5 (***)	32693.9 (***)	79266915.0 (***)	60.2 (***)	3.1 (ns)	0.3 (ns)	23.0 (ns)
Lleida		70.4 a	221.7 a	12.9 a	12483.1 a	18.3 a	14.4 a	4.5 a	83.0 a
Sucs		88.5 b	152.9 b	75.0 b	9877.5 b	16.0 b	13.9 a	4.3 a	84.4 a
Genotype* Location									
SS	5	94.3 (ns)	1583.5 (ns)	3694.3 (**)	33257194.0 (ns)	6.8 (ns)	1.3 (ns)	4.3 (ns)	17.6 (ns)

*, **, ***: significant difference at P<0.05, P<0.01 and P<0.001, respectively. Abbreviations: SS: sum of squares, df: degrees of freedom. Means not sharing the same letter are significantly different.

Mean kernel rows per ear of inbred lines were in the range 11-17, whereas mean kernel rows per ear of hybrids were in the range 13-15. Lerma kernel rows per ear were 16, the highest number of kernel rows per ear observed amongst all the hybrids. Mean kernel rows per ear was significantly different amongst G (inbred lines or hybrids) but neither amongst L (Lleida or Sucs) or the interaction G x L, suggesting that differences in this parameter were due to a genotype effect (**Table 5.3**).

Mean ear grain percentage of inbred lines were in the range 71.5-81.8, whereas mean ear grain percentage of hybrids were in the range 81.8-84.2. Lerma ear grain percentage was 88.8, the highest ear grain percentage observed amongst the hybrids. Mean ear grain percentage was significantly different amongst inbred lines, L (Lleida or Sucs) and G x L, suggesting that the differences in this parameter were due to a genotype effect, influenced by the location and each phenotype performed differently in the different locations. However, mean ear grain percentage was significantly different amongst hybrids but not for L and G x L, suggesting that differences in this parameter were due to a genotype effect (**Table 5.3**).

5.4.4 High-yielding transgenic maize hybrids

Grain yield is the most important parameter in an agronomic evaluation. Mean yield of inbred lines was in the range 2,100-7,300kg/ha; whereas mean yield of hybrids was in the range 9,400-14,800kg/ha. The yield of Lerma was 8,100 kg/ha, the lowest yield observed amongst all the hybrids. Mean yield was significantly different amongst G (inbred lines or hybrids) and L (Lleida or Sucs), suggesting that differences in this parameter were due to a genotype effect, influenced by the location. In addition, mean yield was not significantly different amongst the interaction G x L, suggesting that each genotype performed similarly in each location. The highest yield was measured in HCxEZ6, HCxB73 and HCxMo17 hybrids, which was similar to commercial hybrids grown in the area. Mo17 and B73 inbred lines are widely used in hybrid production because of their high yield potential. EZ6 was also suitable to be crossed with HC because yield reached almost 15,000kg/ha, in the resulting hybrid, ca: 1.8-fold increase compared to Lerma.

5.4.5. Heterosis of transgenic maize hybrids

No statistical difference was found in any of the genotypes in heterosis for flowering date and kernel rows per ear suggesting that these two parameters were not affected by genotype.

Heterosis for conicity and ear height were significantly different by G and they were not affected by L suggesting that these two parameters were very stable. HCxEZ59 and HCxB73 showed the higher value of heterosis for conicity (0.46 and 0.33, respectively) and EZ6xHC, B73xHC, EZ59xHC and A632xHC showed high ear height heterosis (0.77, 0.62, 0.65 and 0.54, respectively). Heterosis for plant height, ear length and ear grain percentage was significantly different by G and E, but no difference in the G x L interaction was measured, suggesting that each genotype performed similarly in the different locations. HCxEZ6, HCxB73, HCxEZ59 and HCxA632 showed the highest values for heterosis for plant height and ear length, whereas HCxEZ59 and HCxB73 were the hybrids most influenced by heterosis for ear grain percentage showing 0.15 and 0.09, heterosis, respectively. Calculation of heterosis for yield revealed that HCxEZ6, and HCxEZ59 showed the highest differences compared with their respective parents (2.33 and 3.06, respectively). In addition, yield heterosis was significantly different by L and G x L, revealing that yield was strongly affected by the location.

Table 5. 4 – Results from ANOVA of heterosis of agronomic and morphological traits of 5 hybrids of inbred line HC crossed with 5 testers in 2 sites.

Source of variation	df	Days to flower	Plant height	Ear height	Yield	Ear length	Kernel rows per ear	Conicity index	Ear grain percentage
Heterosis									
Genotype									
SS	4	0.01 (ns)	0.47 (***)	0.76 (**)	25.59 (***)	0.30 (***)	0.10 (ns)	0.79 (*)	0.04 (*)
HCxMo17		-0.01 a	0.15 b	0.29 b	0.27 c	0.16 b	-0.02 a	0.00 b	0.05 b
HCxEZ6		-0.01 a	0.52 a	0.77 a	2.33ab	0.41 a	0.15 a	0.12b	0.06 b
HCxA632		-0.03 a	0.33 ab	0.54 ab	1.70 b	0.27 ab	0.12 a	0.14b	0.07 b
HCxEZ59		-0.05 a	0.37 a	0.65 a	3.06 a	0.42 a	0.09 a	0.46 a	0.15 a
HCxB73		-0.02 a	0.44 a	0.62 ab	1.57 b	0.24 b	0.09 a	0.33a	0.09 ab
Location									
SS	1	0.04 (*)	0.10 (*)	0.17 (ns)	28.30 (***)	0.35 (***)	0.00 (ns)	0.01 (ns)	0.07 (***)
Lleida		-0.06 a	0.30 a	0.50 a	0.81 a	0.19 a	0.09 a	0.23 a	0.04 a
Sucs		0.01 b	0.42 b	0.65 a	2.76 b	0.41 b	0.09 a	0.19 a	0.13 b
Genotype* Location									
SS	4	0.01 (ns)	0.08 (ns)	0.15 (ns)	9.85 (*)	0.03 (ns)	0.01 (ns)	0.05 (ns)	0.02 (ns)

*, **, ***: significant difference at P<0.05, P<0.01 and P<0.001, respectively. Abbreviations: SS: sum of squares, df: degrees of freedom. Means not sharing the same letter are significantly different.

Relative heterosis of all the parameters was higher for yield (0.27-3.06), followed by ear height (0.29-0.76), plant height (0.15-0.52), ear length (0.16-0.42), conicity (0-0.46), kernel rows per ear (0-0.15), ear grain percentage (0-0.15) and days to flower (0). The higher the heterosis, the better performance of hybrids compared to the corresponding parents. Thus, parameters showing higher heterosis values suggest a stronger influence of the interaction of the parents and they can be increased by choosing different parental genotypes. However, parameters showing lower heterosis values are strictly controlled genetically and they cannot be modified because of the low variability amongst inbred lines.

5.5 Discussion

5.5.1 Genotype of the parental inbred lines had significant influence on agronomic and morphological traits in resulting hybrids demonstrating different field performance depending on the hybrid

In the 2014 growing season, a range of agronomic (days to flower, plant height, and ear height and yield) and morphological (ear length, kernel rows per ear, conicity and ear grain percentage) traits were evaluated in the hybrids and inbred parent lines in order to assess agronomic performance in two different locations (**Table 5.3**). Hybrids and inbred lines were grown in independent plots to assure that the superior field performance of the hybrids did not have a negative influence on the growth of the inbred lines. Thus, statistic analysis of parameters measured in inbred lines and hybrids was performed independently. The performance of the hybrids followed additive genetic effects because plant height, ear height, yield and ear length were superior in the hybrids than in the inbred lines, as reported previously in the literature (Melani and Carena 2005; Galarreta and Álvarez 2010).

Statistical analysis revealed that all agronomic traits were influenced by genotype and that each genotype performed similarly in the different locations with the exception of ear height in the hybrids. B73 and Mo17 are usually used as parents for hybrid production because of their good field performance (Stojaković et al. 2005; Eichten et al. 2011). HCxB73 and HCxMo17 hybrids were taller, had a higher value for ear height and ear length than HCxA632 and HCxEZ59. In contrast, the dent Spanish inbred line EZ6 crossed with HC demonstrated similar performance to HCxB73 and HCxMo17 in both locations, in agreement with the fact that hybrids between flint and dent kernel types commonly result in good field performance

(Ordás 1991). Kernel rows per ear and ear length are the two most common measurements to determine ear morphology (Stojaković et al. 2005). Kernel rows per ear and conicity were the most stable parameters in inbred lines and hybrids because they were only influenced by genotype. Ear length analysis revealed that it was influenced by genotype and that each genotype performed similar in different locations. Differences in grain percentage of inbred lines were due to a genotype effect, influenced by the location, and each genotype performed differently in the different locations. However, mean grain percentage of hybrids was due to genotype effect (**Table 5.3**). Therefore, genetic component of the traits we evaluated in inbred lines and hybrids mostly account for the variation observed (Galarreta and Álvarez 2010).

FAO's cycle classification of a crop estimates the length of growing period of the crop. According to FAO's cycle classification, B73, EZ6 and Mo17 growing cycles are longer than those of A632 and EZ59. However, days to flower (an indication of length of the growing period) in this study revealed that HC, Mo17, EZ6, A632 and B73 needed more days to flower than EZ59, although Mo17 and EZ6 did not differ statistically from EZ59. All hybrids had similar days to flower with the exception of HCxEZ59 which was earlier but similar to the Lerma local check.

5.5.3 Statistical analysis shows that B73xHC, Mo17xHC and EZ6xHC are the highest yielding hybrids

Even though all the parameters described above are important in order to properly characterize field performance of hybrids, the most important parameter is yield. High-yielding hybrids (9,400-14,800kg/ha), comparable with commercial hybrids grown in North East Spain were obtained which means they could be easily adopted by farmers and competitively grown in the area on the basis of agronomic performance. Statistical analysis of yield data suggested that each hybrid or inbred line performed similarly in each location, which is essential to obtain reproducible and reliable field performance. Local checks are commercial cultivars used in the area of the evaluation of new varieties because of their good field performance. It is essential to include local checks in field trials of new hybrids as a reference for their performance in the area of the assessment (Senete et al. 2011). In this study, all hybrids had higher mean yields than the local check Lerma, although only HCxEZ6, and HCxB73 were statistically different from Lerma. However, the yield of the local check Lerma (mean ca: 8,200kg/ha) was lower than expected most likely due to the fact that Lerma had a short phenotype (plant height ca: 140 cm in this study) (Fito, Barcelona, personal

communication) and the superior plant height of HC hybrids (plant height ca: 170-220 cm) allowed them to easily take resources for growth at the expenses of Lerma. Higher yields of HC hybrids were obtained with inbred lines corresponding to longer days to flower (Mo17, B73 and EZ6).. In addition, B73 and Mo17 are usually used as parents for hybrid production because of their high yield (Stojaković et al. 2005; Eichten et al. 2011).

The dent Spanish inbred line EZ6 crossed with HC demonstrated similar yield than HCxB73 and HCxMo17 in both locations, in agreement with hybrids between flint and dent kernel commonly result in good yield (Ordás 1991).

5.5.4 Agronomic performance of hybrids relatively to their corresponding parents resulted in superior heterotic effects in EZ6 and EZ59 hybrids

It is important that heterosis remains stable in different locations to confirm that it is exclusively the result of the interaction of different parent genotypes. In this study, stable heterosis was achieved for all the parameters with exception of yield which suggested that yield is highly influenced by genotype but also by location. Higher heterosis was achieved in hybrids from HC crossed with flint kernel type (EZ6 and EZ59) rather than hybrids from HC crossed with dent kernel type (Mo17, B73 and A632). Even though in all the parameters where heterosis was calculated indicated a positive change in performance of hybrids compared with their corresponding parental, the most impressive result was found in yield (maximum ca: 3 heterosis for yield in HCxEZ59), which confirmed the high variability of this parameter amongst different lines and that could be used to improve new generations of hybrids (Melchinger and Gumber 1998).

5.6 Conclusions

A detailed characterization of agronomic (days to flower, plant height, ear height and yield) and morphological (ear length, kernel rows per ear, conicity and ear grain percentage) traits was performed in inbred lines and hybrids in a pool of plants grown in two different locations in 2014. In addition, calculation of heterosis was performed to compare the performance of the hybrids and their corresponding parents. High heterosis values were obtained for yield, ear height, plant height, ear length and conicity, where two hybrids with flint kernels (EZ6 and EZ59), had the highest values. Even though all parameters are important for a complete characterization, yield is the most relevant in terms of production. In these experiments, high-

yielding maize hybrids were obtained, where the higher yield was achieved in longer flowering dates, HCxEZ63, HCxB73 and HCxMo17 hybrids, which was similar to commercial hybrids grown in the area. EZ6 was shown to be also suitable for HC because yield of the hybrid with HC reached almost 15,000kg/ha, a 1.8-fold increase compared to the commercial hybrid Lerma.

5.7 References

Adeyemo O, Menkir A, Gedil M, Omidiji O (2011) Carotenoid and molecular marker-based diversity assessment in tropical yellow endosperm maize inbred lines. J Food Agric Environ. 9:383–392.

Barata C, Carena MJ (2006) Classification of North Dakota maize inbred lines into heterotic groups based on molecular and testcross data. Euphytica. 151:339-349.

Carena MJ, Hallauer AR (2001) Expression of heterosis in Leaming and Midland Corn Belt populations. J Iowa Acad Sci. 108:73-78.

Egesel CO, Wong JC, Lambert RJ, Rocheford TR (2003) Combining Ability of Maize Inbreds for Carotenoids and Tocopherols. Crop Sci. 43:818–823.

Eichten SR, Foerster JM, de Leon N, Kai Y, Yeh CT, Liu S, Jeddeloh JA, Schenable PS, Kaeppler SM (2011) B73-Mo17 near-isogenic lines demonstrate dispersed structural variation in maize. Plant Physiol. 156:1679–1690.

Galarreta JIR De, Álvarez A (2010) Breeding potential of early-maturing flint maize germplasm adapted to temperate conditions. Spanish J Agric Res. 8:74–81.

Harjes CE, Rocheford TR, Bai L, Brutnell TP, Kandianis CB, Sowinski SG, et al. (2008) Natural genetic variation in lycopene ε-cyclase tapped for maize biofortification. Science. 319:330–333.

Kljak K, Grbeša D (2015) Carotenoid content and antioxidant activity of hexane extracts from selected Croatian corn hybrids. Food Chem. 167:402–408.

Kutka F (2011) Open-pollinated vs. hybrid maize cultivars. Sustainability. 3:1531–1554.

Melani MD, Carena MJ (2005) Alternative maize heterotic patterns for the northern Corn Belt Crop Sci. 45:2186–2194.

Melchinger AE, Gumber RK (1998) Overview of heterosis and heterotic groups in agronomic crops. In: Concepts and breeding of heterosis in crop plants (pp. 29–44). Madison, WI, USA: CCSA Special Publication No. 25.

Menkir A, Gedil M, Tanumihardjo S, Adepoju A, Bossey B (2014) Carotenoid accumulation and agronomic performance of maize hybrids involving parental combinations from different marker-based groups. Food Chem. 148:131–147.

Muthusamy V, Hossain F, Thirunavukkarasu N (2014) Development of β-Carotene Rich Maize Hybrids through Marker-Assisted Introgression of β-carotene hydroxylase Allele. PLoS One. 9:e113583.

O'Hare TJ, Fanning KJ, Martin IF (2015) Zeaxanthin biofortification of sweet-corn and factors affecting zeaxanthin accumulation and colour change. Arch Biochem Biophys. 572:184–187.

Ordás A (1991) Heterosis in Crosses between American and Spanish Populations of Maize. Crop Sci. 31:931-936.

Senete CT, Guimarães PEDO, Paes MCD, Souza JC De (2011) Diallel analysis of maize inbred lines for carotenoids and grain yield. Euphytica. 182:395–404.

Stojaković M, Bekavac G, Vasić M (2005) B73 and related inbred lines in maize breeding. Genetika. 37:245-252.

Vallabhaneni R, Gallagher CE, Licciardello N, Cuttriss AJ, Quinlan RF, Wurtzel ET. (2009) Metabolite sorting of a germplasm collection reveals the hydroxylase3 locus as a new target for maize provitamin A biofortification. Plant Physiol. 151:1635–1645.

Zhu C, Naqvi S, Breitenbach J, Sandmann G, Christou P, Capell T (2008) Combinatorial genetic transformation generates a library of metabolic phenotypes for the carotenoid pathway in maize. Proc Natl Acad Sci U S A. 105:18232–18237.

GENERAL CONCLUSIONS

GENERAL CONCLUSIONS

1. Maize CYP97C19 is a functional ε-hydroxylase which is indispensable for lutein synthesis at the expense of zeinoxanthin in the Arabidopsis *lut1* mutant (lacking lutein).

2. Overexpression of *Zmpsy1* alone or in combination with other carotenogenic genes in maize endosperm resulted in substantial increases in the carotenoid content and the formation of plastoglobuli inside plastids.

3. Higher transcript levels of the endogenous carotenogenic genes *Zmlycb, Zmbch1* and *Zmbch2* as well as the MEP-pathway gene *Zmdxs2* were measured in transgenic lines overexpressing carotenogenic transgenes. This suggested that the carotenoid biosynthetic pathway is regulated in a complex way and that introgressed carotenogenic transgenes influence different steps of the pathway in maize endosperm.

4. Overexpression of the Arabidopsis Orange gene (AtOR) triggers carotenoid accumulation in M37W wild-type maize endosperm without concomitant upregulation of carotenogenic and MEP pathway gene expression, with the exception of *Zmlyce* which correlates with higher zeaxanthin content and *Zmdxs1* which might be responsible for a slight increase of metabolic flux through the carotenoid pathway.

5. In contrast, introgression of AtOR into transgenic maize lines with high carotenoid or high ketocarotenoid content, having different carotenoid profiles in the endosperm did not alter metabolite or transcript levels of carotenogenic, MEP pathway endogenous genes and *pftf* in the resulting hybrids. However, when the pre-existing levels of carotenoids was low in the starting line used to introgress AtOR, ketocarotenoid accumulation increased without concomitant upregulation of carotenogenic and MEP pathway gene expression, with the exception of *Zmdxs1*.

6. RNAi-mediated *Zmbch1* and *Zmbch2* gene silencing in transgenic maize endosperm indicated that these two hydroxylases are key determinants of β-carotene and zeaxanthin accumulation.

7. The more in depth understanding of the mechanisms of carotenoid accumulation in maize endosperm resulting from the work described in this thesis will permit the design and

implementation of more targeted strategies for the creation of plants able to accumulate particular carotenoid profiles for diverse applications.

8. Lower total starch content measured in three high-carotenoid accumulating transgenic maize lines suggested that the accumulation of higher amounts of carotenoids in maize endosperm might occur at the expense of early precursors, also involved in starch biosynthesis. I established that this effect was not due to downregulation of starch-related biosynthetic genes, which suggests that reduction in starch levels is due to alternative mechanisms.

9. Transgenic maize hybrids with field performance similar to, or on occasion, superior to commercial hybrids commonly grown in the area were developed by breeding a high-carotenoid accumulating transgenic line with different inbred lines belonging to well-known heterotic groups. This is the first example of the generation of high-carotenoid transgenic maize hybrids.